



HAL
open science

Nanomaterials as carriers of persistent organic pollutants: risk assessment for the aquatic environment using small invertebrates and model fish

Ignacio Martinez Alvarez

► **To cite this version:**

Ignacio Martinez Alvarez. Nanomaterials as carriers of persistent organic pollutants: risk assessment for the aquatic environment using small invertebrates and model fish. Analytical chemistry. Université de Bordeaux; Universidad del País Vasco. Facultad de ciencias, 2020. English. NNT: 2020BORD0332 . tel-03911547

HAL Id: tel-03911547

<https://theses.hal.science/tel-03911547v1>

Submitted on 23 Dec 2022

HAL is a multi-disciplinary open access archive for the deposit and dissemination of scientific research documents, whether they are published or not. The documents may come from teaching and research institutions in France or abroad, or from public or private research centers.

L'archive ouverte pluridisciplinaire **HAL**, est destinée au dépôt et à la diffusion de documents scientifiques de niveau recherche, publiés ou non, émanant des établissements d'enseignement et de recherche français ou étrangers, des laboratoires publics ou privés.

THÈSE EN COTUTELLE PRÉSENTÉE

POUR OBTENIR LE GRADE DE

DOCTEUR DE

L'UNIVERSITÉ DE BORDEAUX

ET DE L'UNIVERSITÉ DU PAYS BASQUE

ÉCOLE DOCTORALE DES SCIENCES CHIMIQUES (UBX)

ÉCOLE DOCTORALE DE UPV/EHU

SPÉCIALITÉ Chimie analytique et environnementale

Par Ignacio MARTÍNEZ ÁLVAREZ

**Les nanomatériaux comme porteurs des polluants organiques
persistants : évaluation des risques pour l'environnement
aquatique basée sur l'étude d'un petit invertébré et d'un poisson
modèle**

Sous la direction de Hélène BUDZINSKI et de Amaia ORBEA

Soutenue le 22 décembre 2020

Membres du jury :

Mme. FORGET-LERAY, Joelle	Université de Le Havre Normandie	Président
M. GEFFARD, Olivier	IRSTEA-Lyon	Rapporteur
M. COUSIN, Xavier	IFREMER- L'Houmeau	Rapporteur
M. ORTIZ, Maren	Université du Pays Basque	Examineur
Mme. DELLA TORRE, Camilla	Université de Milan	Examineur
M. GONZALEZ, Patrice	Université de Bordeaux	Examineur

Title: Nanomaterials as carriers of persistent organic pollutants: risk assessment for the aquatic environment using small invertebrates and model fish

Abstract: Presence and effects of micro- (< 5mm) and nanomaterials (<100 nm, NM) in the environment are a current issue of concern. Aquatic ecosystems with high pollution pressure already present a cocktail of chemicals, where micro- and NMs can act as sponges for these pollutants due to their high surface to volume ratio and hydrophobic surface. This phenomenon can alter the bioavailability of the pollutants present in the aquatic ecosystem, especially for hydrophobic compounds and, therefore, modulate their toxicity to aquatic organisms. Therefore, in the present Thesis the following objectives were established: (1) To assess the potential bioavailability and toxicity of polystyrene nanoplastics (NPs), and of microplastics (MPs) alone and with sorbed polycyclic aromatic hydrocarbons (PAHs) to brine shrimp larvae and zebrafish; (2) To determine sorption capacity of PAHs to MPs and graphene oxide NMs (GNMs); (3) To assess the potential bioavailability and toxicity of GNMs alone and with sorbed PAHs to zebrafish.

Exposure to pristine MPs did not cause any significant impact on brine shrimp larvae and zebrafish embryo survival, while some treatments containing elevated concentrations (mg/L) of MPs with sorbed benzo(a)pyrene (B(a)P) and B(a)P alone resulted in acute toxicity. In addition, both sizes of MPs were successful vectors of B(a)P to brine shrimp and zebrafish embryos. Results indicated that small MPs (0.5 µm) showed higher maximum sorption capacity for B(a)P than larger MPs (4.5 µm). In the case of a complex and environmentally relevant PAH mixture, as that formed in the water accommodated fraction (WAF) of a crude oil, a relatively limited sorption to 4.5 µm MPs, driven by the hydrophobicity and initial concentration of each PAH, was observed. In adult zebrafish, MPs did not act as PAH vehicle after 21-day exposure to MPs with sorbed PAHs. Only fish exposed to MPs for 21 days presented changes in the transcription level of biotransformation metabolism-related gene *cyp1a* in the liver, along with a significant increase in the prevalence of liver vacuolisation. 21 days of exposure to NPs, but not to MPs, caused oxidative stress in adult zebrafish. Ingestion of NPs was observed in the developing organisms (brine shrimp and zebrafish). In embryos, fluorescent NPs were specially localised in the eyes, yolk sac and tail, showing their capacity to translocate and spread into the embryo body.

For GNMs, graphene oxide (GO) showed a higher sorption capacity for B(a)P than MPs. For the PAH mixture of the WAF, sorption to GO was also higher than to MPs. In embryos exposed to different GNMs alone and with PAHs, no significant mortality was recorded for any treatment. Nevertheless, malformation rate increased significantly in embryos exposed to the highest

concentrations (5 or 10 mg/L) of GO, reduced GO alone and with sorbed B(a)P. According to chemical analysis of adult fish tissues, bioavailability of PAH sorbed to GO for fish was lower than in the case of PAHs alone. Only biochemical responses and genes related to biotransformation metabolism were altered in the liver of fish exposed to B(a)P for 3 days. Transcription level of genes related to oxidative stress were not altered. On the contrary, the gills of fish exposed to GO with sorbed B(a)P and to B(a)P for 3 days and co-exposed to GO and WAF for 21 days showed significantly higher oxidative stress than control fish. A common neurotoxic effect was caused in all fish treated for 21 days. Finally, adult fish exposed to GO presented GO ingestion and liver vacuolisation, but absence of GO translocation to the adult tissue was reported. The present work shows evidences of the capacity of MPs with sorbed PAHs to cause sublethal effects (1) and to carry PAHs (2) in brine shrimp and zebrafish. Finally, GO was greater carrier of PAHs to zebrafish than MPs (3) due to its higher sorption capacity (2), exerting oxidative stress and neurotoxicity as the main sublethal effects in adult zebrafish.

Keywords : Zebrafish; Brine shrimp; Trojan horse effect; Sorption; Benzo(a)pyrene; Nanoplastics; Microplastics; Polycyclic aromatic hydrocarbons ; Graphene oxide nanomaterials.

Titre : Les nanomatériaux comme porteurs des polluants organiques persistants : évaluation des risques pour l'environnement aquatique basée sur l'étude d'un petit invertébré et d'un poisson modèle.

Résumé : La présence et les effets de micro- (<5 mm) et nanomatériaux (<100 nm, NM) dans l'environnement est un sujet d'actualité. Les écosystèmes aquatiques sous forte pression de pollution présentent des mélanges de produits chimiques, dans lesquels les micro- et NMs, en raison de leur rapport surface/volume élevé et de leur surface hydrophobe, peuvent agir comme des éponges pour les polluants. Ce phénomène peut modifier la biodisponibilité de ces derniers et, ainsi, moduler leur toxicité pour les organismes aquatiques. Cette thèse avait donc comme objectifs : (1) d'évaluer la biodisponibilité et la toxicité potentielles de nanoplastiques (NP) et de microplastiques (MP) de polystyrène seuls, et de MP avec des hydrocarbures aromatiques polycycliques (HAP) ad/absorbés pour la larve d'artémie et le poisson zèbre; (2) de déterminer la capacité de sorption des HAP par des MP et NM d'oxyde de graphène (GO); (3) d'évaluer la biodisponibilité et la toxicité potentielles des NM GO seuls et avec des HAP ad/absorbés chez le poisson zèbre.

L'exposition à des MP seuls n'a pas eu d'impact significatif sur la survie pour la larve d'artémie et le poisson zèbre, alors que des concentrations élevées (mg/L) de MP avec du benzo(a)pyrène (B(a)P) ad/absorbé et du B(a)P seul ont entraîné une toxicité aiguë. Les MP se sont révélés des vecteurs de B(a)P chez les organismes en développement. Les résultats ont montré que les MP (0,5 µm) de petite taille présentaient une capacité de sorption du B(a)P plus élevée que les MP de plus grande taille (4,5 µm). Dans le cas d'un mélange complexe de HAP, comme celui obtenu à partir de la solubilisation d'un pétrole brut (WAF), une sorption limitée pour les MP de 4,5 µm, due à l'hydrophobie et à la concentration initiale des HAP, a été observée. Chez le poisson adulte, les HAP n'ont pas été transportés par les MP après une exposition de 21 jours. Seuls les poissons exposés aux MP pendant 21 jours ont présenté des changements au niveau de la transcription du gène *cyp1a* lié au métabolisme de biotransformation dans le foie, ainsi qu'une augmentation significative de la prévalence de la vacuolisation du foie. 21 jours d'exposition aux NP, mais pas aux MP, ont provoqué un stress oxydatif chez les poissons adultes. L'ingestion de NP a été observée chez les organismes en développement. Chez les embryons, les NP ont été internalisés dans les yeux, le sac vitellin et la queue.

GO a montré une plus grande capacité de sorption pour B(a)P que le MP. Pour le mélange de HAP du WAF, la sorption vers le GO était également supérieure à celle des MP. Chez les embryons exposés, le taux de malformation a augmenté de manière significative chez les embryons exposés aux concentrations les plus élevées (5 ou 10 mg/l) de GO, de GO réduit seul et avec du B(a)P ad/absorbé. Selon l'analyse chimique dans les tissus de poisson adulte, la biodisponibilité des HAP avec de GO pour les poissons était plus faible que dans le cas des HAP seuls. Seules les réponses biochimiques et les gènes liés au métabolisme de biotransformation ont été altérés dans le foie des poissons exposés au B(a)P pendant 3 jours. Au contraire, les branchies des poissons exposés au GO avec du B(a)P ad/absorbé et au B(a)P pendant 3 jours et co-exposés au GO et au WAF pendant 21 jours ont montré un stress oxydatif significativement plus élevé que les poissons témoins. Un effet neurotoxique commun a été provoqué chez tous les poissons traités pendant 21 jours. Enfin, les poissons adultes exposés au GO ont présenté une ingestion de GO et une vacuolisation du foie. Le présent travail démontre la capacité des MP avec des HAP ad/absorbés à provoquer des effets sublétaux (1) et à porter des HAP (2) chez l'artémie et le poisson zèbre. Enfin, le GO était plus porteur de HAP pour le poisson zèbre que le MP (3) en raison de sa plus grande capacité de sorption (2), exerçant un stress oxydatif et une neurotoxicité comme principaux effets sublétaux chez le poisson zèbre adulte.

Mots clés : Poisson zèbre; Artémie; Effet cheval de Troie; Ad/absorption; Benzo(a)pyrène; Nanoplastiques; Microplastiques; Hydrocarbures aromatiques polycycliques; Nanomatériau d'oxyde de graphène.

TÍTULO: Los nanomateriales como vehículos de contaminantes orgánicos persistentes: evaluación del riesgo para el ecosistema acuático utilizando un invertebrado pequeño y un pez modelo.

RESUMEN: La presencia y los efectos de micro- (<5 µm) y nanomateriales (100 nm, NM) en el medio ambiente es un tema de preocupación actual. En sistemas acuáticos que presentan un coctel de químicos debido a la alta presión de la contaminación, los micro- y NMs pueden actuar como esponjas para los contaminantes debido a su alto ratio superficie/volumen y a la hidrofobicidad de su superficie. Este fenómeno puede alterar la biodisponibilidad de los contaminantes presentes en los ecosistemas acuáticos, especialmente para los compuestos hidrófobos, y seguidamente, modular su toxicidad para los organismos acuáticos. Por ello, en la presente tesis los siguientes objetivos fueron establecidos: (1) Evaluar la biodisponibilidad y la toxicidad potencial de nanoplasticos de poliestireno (NPs), y de microplásticos (MPs) solos o con hidrocarburos aromáticos policíclicos ad/absorbidos (HAPs) para la larva de *Artemia* y el pez cebra; (2) Determinar la capacidad de ad/absorción de HAPs por los MPs y los NMs de óxido de grafeno (GNMs); (3) Evaluar la biodisponibilidad y toxicidad de GNMs solos o con HAPs ad/absorbidos para el pez cebra.

La exposición a MPs prístinos no causó ningún impacto significativo en la supervivencia de la larva de *Artemia* o del embrión de pez cebra, mientras que algunos tratamientos que contenían elevadas concentraciones (mg/L) de MPs con benzo(a)pireno (B(a)P) ad/absorbido y B(a)P sólo resultaron en toxicidad aguda. Además, ambos tamaños de MPs fueron exitosos vectores de B(a)P en larvas de *Artemia* y embriones de pez cebra. Los resultados indicaron que los MPs pequeños (0.5 µm) mostraron una mayor capacidad máxima de ad/absorción de B(a)P que los MPs grandes (4.5 µm MPs). Para una mezcla compleja y medioambientalmente relevante de HAPs, como es la formada en la fracción acomodada al agua (WAF) de un petróleo crudo, se observó una ad/absorción limitada relativamente a 4.5 µm MPs y que dependió de la hidrofobicidad y la concentración inicial de cada HAP. En adultos de pez cebra, los MPs no actuaron como vehículos de HAP después de 21 días de exposición a MPs con HAPs ad/absorbidos. Solo aquellos peces expuestos a MPs durante 21 días presentaron cambios en los niveles de transcripción del gen *cyp1a* relacionado con el metabolismo de biotransformación en el hígado, junto con un aumento significativo de la prevalencia de la vacuolización del hígado. 21 días de exposición a NPs, pero no a MPs, causó un estrés oxidativo en los adultos de pez cebra. La ingestión de NPs se observó en los organismos en desarrollo (*Artemia* y pez cebra). En embriones, los NPs fluorescentes se localizaron específicamente en los ojos, saco vitelino y cola, mostrando la capacidad de los mismos para ser internalizados y repartidos en el interior del cuerpo del embrión.

Para los GNMs, el óxido de grafeno (GO) presentó una mayor capacidad de ad/absorción de B(a)P que los MPs. Para la mezcla de HAPs del WAF, la ad/absorción a GO fue de nuevo mayor que para los MPs. Para los embriones expuestos a diferentes GNMs solos y con HAPs no se obtuvo una mortalidad significativa. Aun así, el ratio de malformaciones aumento significativamente en embriones expuestos a las concentraciones más altas (5 o 10 mg/L) de GO, GO reducido solo o con B(a)P ad/absorbido. De acuerdo con los ensayos químicos en el tejido de pez adulto, la biodisponibilidad de HAP ad/absorbidos a GO para peces fue menor que en los peces expuestos a HAPs solos. Solo se vieron alteradas las respuestas bioquímicas y los genes relacionados con el metabolismo de biotransformación en hígado de pez expuesto a B(a)P durante 3 días. Los niveles de transcripción no se vieron alterados en genes relacionados con el estrés oxidativo. Al contrario, las branquias de pez expuesto a GO con B(a)P ad/absorbido y a B(a)P durante 3 días y co-expuestos a GO y WAF durante 21 días mostraron un aumento significativo del estrés oxidativo respecto a los peces controles. Un efecto neurotóxico se produjo en todos los peces tratados durante 21 días. Finalmente, los peces adultos expuestos a GO presentaron ingestión del mismo y vacuolización del hígado, aun así, no se observó la internalización de GO en los tejidos. Este trabajo mostro evidencias de la capacidad de los MPs con HAPs ad/absorbido para causar daños subletales (1) y para transportar HAPs (2) en *Artemia* y pez cebra. Finalmente, GO fue un mejor portador de HAPs para pez cebra que los MPs (3) debido a su mayor capacidad de ad/absorción (2), causando estrés oxidativo y neurotoxicidad como los principales daños subletales en adulto de pez cebra.

Palabras clave: Pez cebra; *Artemia*; Caballo de Troya; Ad/absorción; Benzo(a)pireno; Nanoplasticos; Microplasticos; Hidrocarburos aromáticos policíclicos; Nanomateriales de oxido de grafeno.

Dept. of Zoology and Animal Cell Biology

Research Centre for Experimental Marine Biology and Biotechnology PiE and Science
and Technology Faculty, University of the Basque Country

Environnements et Paléoenvironnements Océaniques et Continentaux

UMR 5805 CNRS

Funding

This work has been funded by:

- **University of the Basque Country** through a predoctoral grant in Cotutelle with the University of the Basque Country and the University of Bordeaux (2016-2019).
- **Spanish Ministry of Economy and Competitiveness (MINECO)** through the **NAnoCarrierEra (NACE)** project “Nanomaterials as carriers of persistent organic pollutants in the aquatic environment: development of tools for risk assessment based on alternative methods and model organisms” (CTM2016-81130-R).
- **Basque Government** through a grant to the Consolidated Research Group “Cell Biology in Environmental Toxicology” (IT810-13, 2013-2018 and IT1302-19, 2019-2021).
- **French National Research Agency (ANR)** in the frame of the **Investments for the future Program IdEx Bordeaux** (No.-10-IDEX-03-02).
- **Cluster of Excellence COTE** (ANR-10-LABX 45) through a mobility grant at the University of Bordeaux.
- **AQUIMOB** through a mobility grant for predoctoral students between the University of the Basque Country and the University of Bordeaux.

Acknowledgements

I wish to thank,

- Dr. Amaia Orbea and Prof. H el ene Budzinski my PhD supervisors for giving me the opportunity to perform this research work and for her support and guidance during these years.
- Prof. Miren P. Cajaraville, coordinator of the doctoral program Environmental Contamination and Toxicology, head of Cell Biology in Environmental Toxicology (CBET) research group (UPV/EHU), for accepting and giving the opportunity of joining postdoctoral studies and her team.
- The staff of Driftslaboratoriet Mongstad, Equinor (former Statoil) for supplying the sample of crude oil used in the experiments.
- SGIker (UPV/EHU/ ERDF, EU) for the technical and human support provided by.
- Karyn Le Menach for the help with the chemical analyses and the support with sample preparation and processing.
- Dr. Jos e M. Lacave and to Juli an Garc a for help with the experimental set up and support in sample preparation and processing.

Publications and conference presentations

List of publications

Martínez-Álvarez, I., Cajaraville, M.P., Budzinski, H.; Orbea, A. Screening of the toxicity of polystyrene nano- and microplastics alone and in combination with polycyclic aromatic hydrocarbons using alternative methods (brine shrimp larvae and zebrafish embryos). In preparation

Martínez-Álvarez, I., Le Menach, K., Devier, M.H., Cajaraville, M.P., Orbea, A., Budzinski, H.; 2020. Sorption of benzo(a)pyrene and of a complex mixture of petrogenic PAHs onto polystyrene microplastics. In preparation

Martínez-Álvarez, I., Le Menach, K., Devier, M.H., Cajaraville, M.P., Budzinski, H., Orbea, A. Effects of polystyrene nano- and microplastics and of microplastics with sorbed polycyclic aromatic hydrocarbons in adult zebrafish. In preparation

Martínez-Álvarez, I., Le Menach, K., Devier, M.H., Barbarin, I., Tomovska, R., Cajaraville, M.P., Budzinski, H., Orbea, A. Uptake and effects of graphene family materials alone and in combination with polycyclic aromatic hydrocarbons on zebrafish. Submitted to *Science of the Total Environment*.

Conference presentations

VI Jornadas de investigación de la Facultad de Ciencia y Tecnología. Leioa, 14 March 2018. Martínez-Álvarez, I., Budzinski, H., Cajaraville, M.P., Orbea, A. “Chemical interactions behind toxicological effects: sorption of persistent organic pollutants to plastics and carbon nanomaterials”. Oral presentation (I.M.A.).

VI Jornadas de Investigación de la Facultad de Ciencia y Tecnología. Leioa, 14 March 2018. Lacave, J.M., Martínez-Álvarez, I., Hatfield, J., Nicolussi, G., González-Soto, N., Esteban-Sánchez, A., Duroudier, N., Katsumiti, A., Zaldibar, B., Bilbao, E., Navarro, E., Tomovska, R., Budzinski, H., Orbea, A., Cajaraville, M.P. “Are nanomaterials carriers of other relevant toxic pollutants in the aquatic environment? The NAnoCarrierEra (NACE) project: exploring the “Trojan horse” effect”. Poster.

28th Annual Meeting of the Society of Environmental Toxicology and Chemistry (SETAC Europe). Rome, 13-17 May 2018. Martínez-Álvarez, I., Le Menach, K., Devier, M.H., Cajaraville, M.P., Budzinski, H., Orbea, A. “Characterization of the adsorption/desorption of benzo(a)pyrene to/from polystyrene micro- and nanoplastics for further toxicity assessment”. Poster.

CICTA. Madrid, 27-28 September 2018. Cajaraville, M.P., Martínez-Álvarez, I., Hatfield, J., Nicolussi, G., González-Soto, N., Katsumiti, A., Bilbao, E., Navarro, E., Tomovska, R., Budzinski, H., Orbea, A. “Nanomaterials and microplastics as carriers of persistent organic pollutants in the aquatic environment: development of tools for risk assessment based on alternative methods and model organisms”. Oral Presentation (M.P.C.)

MICRO 2018, Fate and Impact of Microplastics: Knowledge, Actions and Solutions. Lanzarote, 19-23 November 2018. Martínez-Álvarez, I., Le Menach, K., Devier, M.H., Cajaraville, M.P., Budzinski, H., Orbea, A. “Assessment of the Trojan horse effect using PAH-contaminated polystyrene microplastics: sorption studies and responses of adult zebrafish”. Poster.

30th Annual Meeting of the Society of Environmental Toxicology and Chemistry (SETAC Europe). Online meeting, 3-7 May 2020. Martínez-Álvarez, I., Le Menach, K., Devier, M.H., Tomovska, R., Cajaraville, M.P., Budzinski, H., Orbea, A. “Effects of graphene oxide alone and with sorbed PAHs on zebrafish”. Poster.

VII Jornadas de Investigación de la Facultad de Ciencia y Tecnología. Leioa, 29 September 2020. Orbea, A., Bilbao, E., Katsumiti, A., Martínez-Álvarez, I., Estaban, A., González-Soto, N., Prieto, R., Martínez, V., Tomovska, R., Budzinski, H., Cajaraville, M.P. “Environmental impact and risk assessment of nanomaterials and other emerging chemicals”. Poster.

TABLE OF CONTENTS

INTRODUCTION	17
1. Microplastics and nanomaterials in the environment	21
1.1. Microplastics and nanoplastics	21
1.2. Nanomaterials (graphene family)	23
1.3. Sources and predicted/estimated environmental concentrations	26
1.4. Effects in aquatic organisms	29
MPs and NPs	29
Graphene family NMs	32
2. Brine shrimp, a small invertebrate to assess the hazard of microplastics and nanomaterials	35
3. Zebrafish as a model organism to assess the hazard of microplastics and nanomaterials	41
3.1. Effects in developing embryos	41
3.2. Effects in adult organisms	51
STATE OF THE ART, HYPOTHESIS AND OBJECTIVES	73
RESULTS AND DISCUSSION	79
CHAPTER 1. Screening of the toxicity of polystyrene nano- and microplastics alone and in combination with polycyclic aromatic hydrocarbons using alternative methods (brine shrimp larvae and zebrafish embryos)	81
CHAPTER 2. Sorption of benzo(a)pyrene and of a complex mixture of petrogenic PAHs onto polystyrene microplastics	125
CHAPTER 3. Effects of polystyrene nano- and microplastics and of microplastics with sorbed polycyclic aromatic hydrocarbons in adult zebrafish	159
CHAPTER 4. Uptake and effects of graphene oxide nanomaterials alone and in combination with polycyclic aromatic hydrocarbons in zebrafish	195
GENERAL DISCUSSION	255
CONCLUSIONS AND THESIS	277

INTRODUCTION

ABBREVIATIONS

AChE, Acetylcholinesterase

CAT, Catalase

CNMs, Carbon-based NMs

CNTs, Carbon nanotubes

EE2, 17 α -ethynylestradiol

EROD, 7-ethoxyresorufin O-deethylase

GR, glutathione reductase

GSH, glutathione

GST, Glutathione S-transferase

GPx, Glutathione peroxidase

GNMs, Graphene family NMs

GO, Graphene oxide

hpf, Hours post fertilisation

dpf, Days post fertilisation

LC₅₀, Lethal concentration 50

MPs, Microplastics

NPs, Nanoplastics

NMs, Nanomaterials

PAHs, Polycyclic aromatic hydrocarbons

POPs, Persistent organic pollutants

PE, Polyethylene

PET, polyethylene terephthalate

PP, Polypropylene

PVC, Polyvinyl-chloride

PS, Polystyrene

rGO, Reduced graphene oxide

ROS, Reactive oxygen species

SOD, Superoxide dismutase

WWTP, Waste water treatment plant

1. Microplastics and nanomaterials in the environment

1.1. Microplastics and nanoplastics

Plastic as a resistant, easily to handle, versatile and cheap material is being produced since the ~1950s with a progressive increase of its production in the last decades. The global production of plastic increased from 245 to 359 million tons between 2006 and 2018. In 2018, Europa reached 17% of the global plastic production while China was the first producer with a 30% of the total production (Plastic Europa, 2019). Plastic is being largely produced worldwide mainly to its versatility which offers customised solutions to a large quantity of applications. Plastic can be categorised in two groups according to its capacity to be recycled, the former being the thermoplastics and the latter the thermosets. The thermoplastics are the most common in terms of daily uses. The following types of polymers are found within this category: polyethylene (PE), polypropylene (PP), polyvinyl-chloride (PVC), polystyrene (PS), polyethylene terephthalate (PET), expanded polystyrene, polycarbonate and polyamides. The most produced in terms of demand in Europe is PP (19.3% from total demand in 2018), followed by low density PE (17.5%), high density PE (12.2%), PVC (10%), PET (7.7%) and PS (6.4%) (Plastic Europa, 2019). The most produced thermoset plastic is the polyurethane with a 7.9% from total plastic production in Europe. Polyurethane is commonly used in building insulations, pillows and mattresses. The principal applications of the thermoplastics are packaging, building and construction, automotive, electrical and electronics, agriculture, household, leisure and sports.

Due to the long lifespan and wide applications of most plastics, their presence has spread to all ecosystems and tend to accumulate (Eriksen et al., 2014). For instance, marine debris has been identified as a major global problem for the ecosystem (Gregory, 2009; Werner et al., 2016) and a big part of this litter consists on plastic debris. As seen by Compa et al. (2019), 54% of the marine litter found in the Canary Islands was plastic debris. The distribution of the global plastic litter that ends in the aquatic ecosystems is not easy to understand. All over the world, a big part of the plastics waste escapes from recycling or incineration ending up on the water ecosystems. As reported by Jambeck et al. (2015), the highest quantity of plastic available to enter the aquatic ecosystems due to the mismanagement of plastic waste is from China (8.82 million metric tons/year) and the surrounding countries of Asia (Indonesia, Philippines and Vietnam). In the European countries, the quantity of plastic mismanaged is 0.31 million metric tons/year, far below China. The plastic litter accidentally released or mismanaged reaches the aquatic ecosystems, first to the rivers which contribute in a considerable proportion to the plastic litter found in the marine ecosystems (**Fig. 1**, Lebreton et al., 2017). Due to the important river plastic outputs to the sea and the different oceanic currents, the plastic litter is distributed widely in the world (Eriksen et al., 2014). All the plastic that ends in the aquatic ecosystems will be distributed in the different compartments (surface waters, bottom water and sediments) depending on two factors: shape and

Introduction

polymer density. These plastic parameters will interact with the different water characteristics determining their fate in the aquatic ecosystems. As to the composition, PE, PP and PS are the three polymer types most abundantly found in the different environmental compartments (Schwarz et al., 2019). Once plastics reach the aquatic ecosystems, they undergo physical and chemical processes which result in fragmentation or disintegration into smaller plastics. These small plastics are called micro- (MPs) and nanoplastics (NPs).

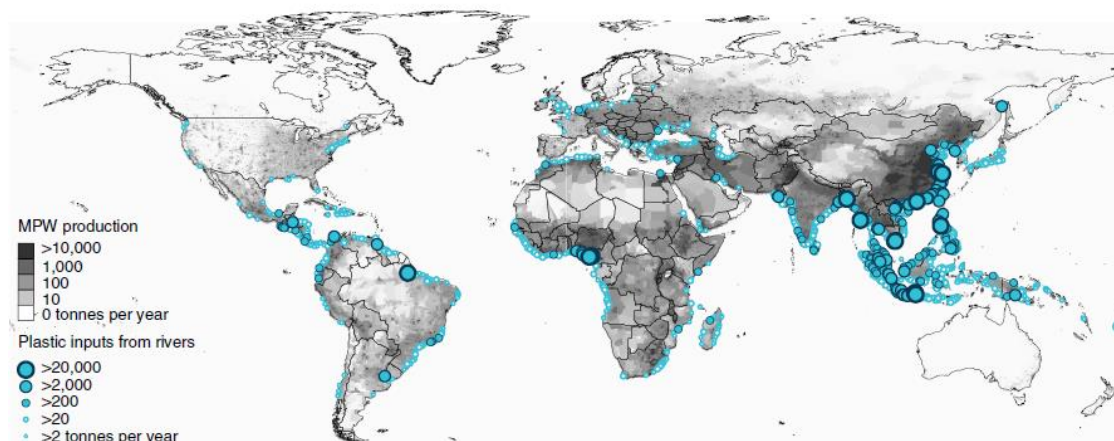


Fig. 1-Mass of plastic inputs from rivers into the oceans in tonnes per year and the mismanaged plastic waste (MPW) production per country (from Lebreton et al., 2017).

MPs are defined as particles with a size below 5 mm. This term was used by Thompson et al. (2004) for the first time. A common and standardised definition of this material is not established yet due to the complexity of these particles (type of polymer composition, shape, source, colour, etc.). In the last years a common effort has been done to establish a better definition to manage and control the pollution produced by these particles. As mentioned by Hartmann et al. (2019), since 2003 several authors have given different definitions for MPs as particles of different size range, but it was not until 2008 during a meeting hosted by the National Oceanic and Atmospheric Administration that the famous definition of MPs as particles under 5 mm was established (Arthur et al., 2008). Nevertheless, Hartman et al. (2019) proposed to define MPs as particles that have at least two dimension between 1 mm and 1 μ m (fibres are included) as an intuitive categorisation. In addition, the plastic particles with a size between 1 to 10 mm will be classified as macroplastics, and those with a size between 1 to 1000 nm as NPs. Other authors agree with this definition and classification as a more easy and logical definition for MPs (Costa et al., 2010).

MPs are classified in two categories depending in their source: primary and secondary plastics. Primary MPs are those manufactured in that size range to fulfil different applications, and secondary MPs are those formed in the environment by degradation of larger plastics. Primary MPs are mainly produced intentionally by abrasion of larger plastics. The main application or

production source of primary MPs are personal care products (Boucher and Friot, 2017). As an example, 43600 tons of microbeads for cosmetic products were produced in Europe and 11% of the total is estimated to be emitted to the North Sea (Gouin et al., 2015). Not only the mentioned applications but the different habits and uses of common products in the daily life liberate MPs to the environment. In addition to the primary MPs, also the MPs generated in the ecosystems (secondary MPs) are the principal source of MPs to the ecosystems due to the huge amount of plastic litter that arrives to the ecosystems every year. Plastics suffer physical and photo degradation weathering, which is easily recognised due to their irregular shapes. Secondary MPs could also be produced accidentally from the use of a product, as for example the production of MPs by pneumatics when driving, the so called tire wear particles. In terms of input of MPs to the ecosystems, the secondary MPs are considered as the principal source of MPs to the oceans (Duis and Coors, 2016; Efimova et al., 2018).

The plastics can also be found in the nano scale. NPs are generated by degradation of MPs in nano scale (nanofragmentation; Enfrin et al., 2020) or intentionally manufactured by polymer synthesis for numerous applications. The three principal applications of NPs are biomedical (Putri et al., 2017), personal care (Hernandez et al., 2017) and laboratory research. NPs are defined as plastic particles that have at least one dimension smaller than 100 nm (Koelmans et al., 2015). There is not an official definition for NPs, the definition previously mentioned is being used from derivation of the nanomaterial (NM) definition (see below). The most commonly manufactured NPs are composed of PS and polymethylmethacrylate due to their easier synthesis than for other polymer types (Shen et al., 2019).

1.2. Nanomaterials (graphene family)

The definition of NM has been a matter of discussion in the scientific community due to the large number of NM types. Some theories even mention that NM should be one of the state of the matter, in addition to the solid, liquid, gas and plasma due to the small size that confers it new hazard properties different to their larger version (Buzea et al., 2007). In 2011, the EU adopted a recommended definition of NM, which is the most commonly used definition. According to the EU COM (2011) definition, a NM is: “*A natural, incidental or manufactured material containing particles, in an unbound state or as an aggregate or as an agglomerate and where, for 50% or more of the particles in the number size distribution, one or more external dimensions is in the size range 1 nm - 100 nm*”. NMs can be classified differently according to their dimensionality, morphology, composition and uniformity or agglomeration state (**Fig. 2**; Buzea et al., 2007). Starting by the dimensionality, NMs can be grouped in to 1D, 2D or 3D materials, where 1D is a material with one dimension inferior to 100 nm, like thin films or a surface coatings, and a 3D is a NM with three dimensions inferior to 100 nm, like membranes with nanopores or the

Introduction

nanoparticles. Taking into account the morphology, two big categories are reported: the high aspect ratio particles (nanowires, nanotubes, nanohelices, nanozigzags, nanopillars, nanobelts) and the low aspect ratio particles (nanospherical, nanopyramids, nanocubes). By composition, the NMs can be classified as single constituent material (compact or hollow) or composites (coated, encapsulated, barcode or mixed). Finally, depending on the agglomeration state or uniformity we can distinguish isometric and inhomogeneous materials, and both can be dispersed or agglomerated. The development of nanotechnology in the two last decades has allowed the incorporation of new materials in consumer products and industrial applications. The list of NM applications is large and varied, such as remediation of waste water (Santhosh et al., 2016; Werkneh and Rene, 2019; Younis et al., 2020), coatings (Wu et al., 2015), paints (Liu et al., 2018), energy conversion and storage (Dang et al., 2016; Wang et al., 2020a), insulating materials (Yang et al., 2018), food contact material (Bratovčić et al., 2015), etc.

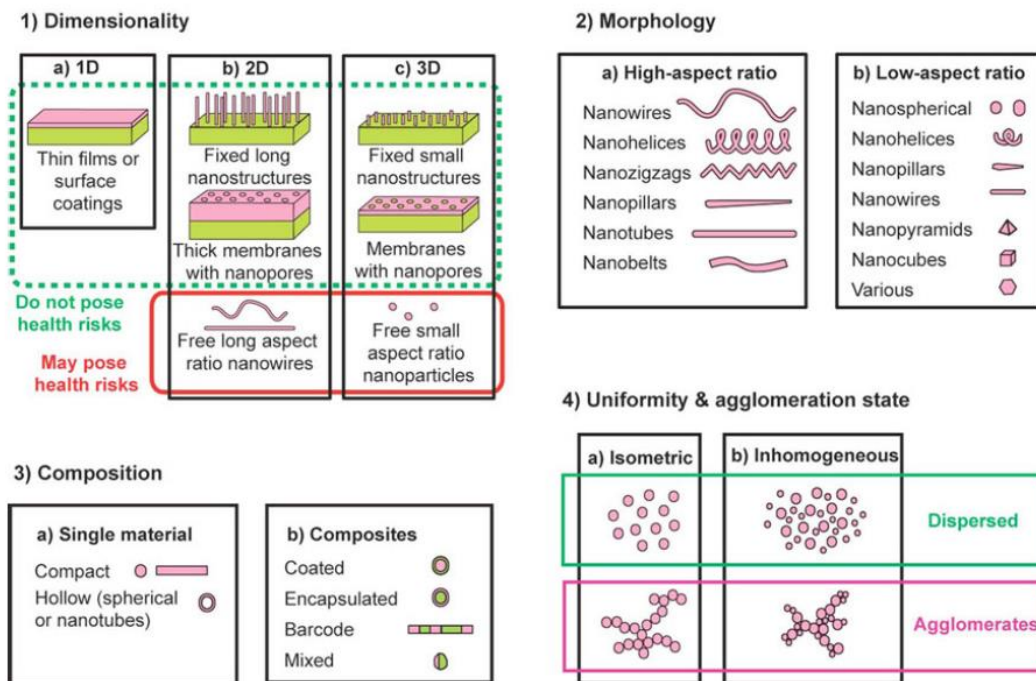


Fig. 2- Classification of nanostructured materials (from Buzea et al., 2007).

Only some elements have the capacity to produce different bonding arrangements with itself producing the so called allotrope. The different crystalline structure that can be formed from a chemical element will display different properties, depending on the characteristics of the chemical element, new and surprising applications can be discovered. One allotrope that has presented a promising future is the carbon allotrope, which presents numerous crystalline structures (**Fig. 3**) and, thus, different properties (large specific surface area, mechanical strength, and remarkable electric and thermal properties) and applications. The number of carbon based NMs (CNMs) has increased in the last years thanks to the various techniques to synthesise

different forms of a single layer of carbon. The principal and original shape is graphite, and the single thin layer of carbon called graphene is obtained from it exfoliation. Graphene was first discovered by Novoselov et al. in 2004, Novoselov and colleagues, who were awarded with the Nobel Prize for ground-breaking experiments with this material and describing its surprising characteristics. Graphene consists in a two-dimensional CNM, formed by a single layer of carbon atoms densely packed into a benzene-ring structure (that does not exist in the free state). After this discovery, many different types of CNMs were described and synthesised, such as carbon nanotubes (CNTs), fullerenes, nanodiamond, graphene oxide (GO) and carbon dots (**Fig. 3**). The graphene characteristics are its high surface area and elevated electronic and thermal properties (Chen et al., 2012a). Graphene has the capacity to be chemically modified (oxidation or reduction) to produce new derivatives such as GO and reduced GO (rGO) (**Fig. 4**) which constitute the graphene family NMs (GNMs).

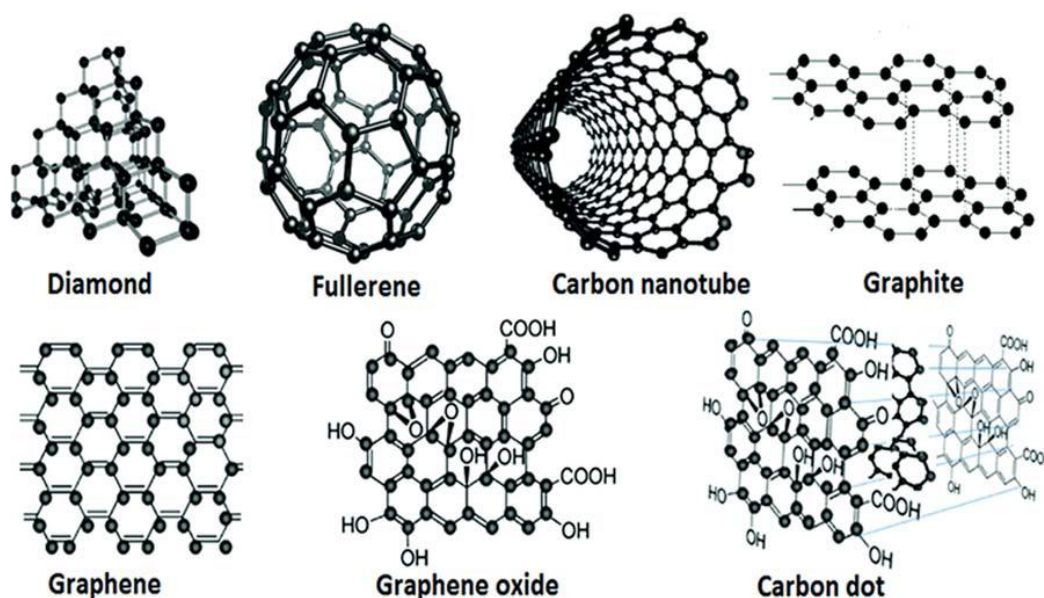


Fig. 3- Different crystalline structures of the carbon allotrope (from Yan et al., 2016).

Introduction

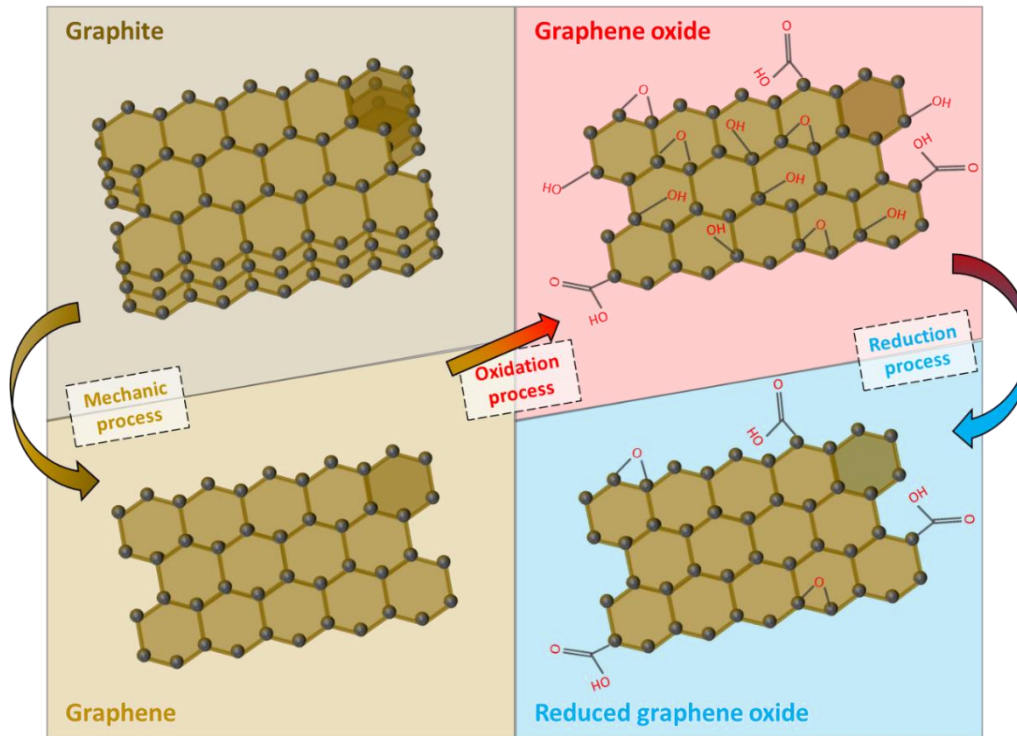


Fig. 4- Different derivatives from graphite (based on Jastrzębska et al., 2012).

The numerous applications that graphene offers are due to the shape adaptability to produce derivatives and new forms that allow new surprising and promising applications. Among them, there are sensors, clean energy devices, antimicrobial products, composite materials, remediation technology and microelectronics (Tiwari et al., 2020; Azizi-Lalabadi et al., 2020). More specifically, graphene is used thanks to its strength and electrical/thermal conductivity in sports equipment, ink and water desalination, and for its strength and energy storage is used for electronic devices and biosensors (Good et al., 2016). One main application that could be a concern in terms of impact in the environment is the use of CNMs for water pollution remediation (Yang et al., 2014; Li et al., 2020b; Younis et al., 2020) and other environmental applications (Mauter and Elimelech, 2008).

1.3. Sources and predicted/estimated environmental concentrations

The sources of MP/NPs and engineered NMs to the environment are different depending on their production. While engineered NMs are intentionally manufactured for a given application, the majority of MPs/NPs are unintentional produced or released by fragmentation of larger plastics, with the exception of some outputs of primary MPs presents as beads in personal care products (Hüffer et al., 2017). The main source of MPs/NPs is the land littering which, in terms of amount, is determined by population density in addition to the plastic waste management that varies among

countries (in less developed countries where plastic is mismanaged) (Jambeck et al., 2015). Other known sources of MPs/NPs, there are postconsumer processes and textiles (fibres) which are discharged to domestic wastewater. Nevertheless, the principal output of MPs is from unlocalised sources, which is dominated by secondary MPs (Duis and Coors, 2016) that are produced in the aquatic ecosystems, mostly in the oceans.

With the improvement of techniques to quantify MPs (10 μm to 5 mm) values of measured concentrations in the marine ecosystems and, in less extent, in freshwater have been calculated (Driedger et al., 2015; Rezania et al., 2018; Bellasi et al., 2020). In addition, some models have been developed in order to estimate the expected concentration and potential impact of MPs in the ecosystems, different environmental compartments of the ecosystems (**Table 1**). MP concentration measurements in WWTPs influent and effluent showed that a noticeable proportion of the MPs that arrived to the water treatment system is retained in the sludge (98.41%; Murphy et al., 2016). Nevertheless, a small percentage passes through the WWTPs and is released via the effluent. Predicted concentrations from effluent of WWTPs are in the concentration range of 0.2 to 66 $\mu\text{g/L}$ (**Table 1**; van Wezel et al., 2015). The predicted total emission of MPs from the mentioned sources to the aquatic ecosystem is 0.0025-0.11 Kg/Km river/year (**Table 1**). The amount of MPs that are released to the aquatic ecosystems is principally due to the sewer overflows and tertiary WWTP effluent (Kawecki and Nowack, 2020). All the MPs that successfully pass through WWTPs are principally released to the rivers. A study in the Rhine River reported 892,777 particles/ Km^2 in 11 locations of the area being the three principal sources: WWTPs, tributaries and weirs (Mani et al., 2015). A huge quantity of the MPs entering the marine ecosystems from rivers (Horton et al., 2017). Models reported that two-thirds of the MPs present in the European rivers flow into the Mediterranean and Black sea through estuaries (Siegfried et al., 2017). As an example, the fibres found in marine ecosystems are principally derived from domestic washing machines that end in the WWTP and, then, in the river, ending up into the sea (Browne et al., 2011). The three polymers most reported in the freshwater ecosystems (rivers, lakes) are PP (24%), PE (24%) and PS (14%), being fibres the most abundant type in terms of shape (59%) (Li et al., 2020a). Measured concentrations of MPs at the sea are widely reported (Andrady, 2011). Floating MPs are estimated to be 6650 buoyant particles/ m^3 and 32-144 particles/Kg of sediment are reported for the deposition zone of the beach (Everaert et al., 2018).

Introduction

Table 1- Predicted environmental concentrations of MPs and CNMs. There are not data available for NPs or GNMs.

	Compartment	Predicted concentration	Reference
MPs	WWTP effluent	0.2-66 µg/L	van Wezel et al. (2016)
	Aquatic ecosystem	0.0025-0.11 Kg/Km/year	Kawecki and Nowack (2020)
	Ocean surface water	6650 buoyant particles/m ³	Everaert et al. (2018)
	Sediment/beach deposition zone	32-144 particles/Kg	
CNTs	Water (surface, fresh and sea)	2. 10 ⁻⁵ -1.82 ng/L	Zhao et al. (2020b)
	Sediment	10 ⁻⁴ -2.66 10 ⁻² mg/Kg	
	Water	0.001-1000 µg/L	De Marchi et al. (2018)
	Surface water	0.23 ng/L	Sun et al. (2014)
WWTP effluent	4 ng/L		
Fullerenes	Natural and urban soil	5.1 ng/Kg/year	Kunhikrishnan et al. (2014)
	Surface water	0.003 ng/L	
	WWTP effluent	4 ng/L	
	Surface water	0.11 ng/L	
	WWTP effluent	1.7 ng/L	
	Natural and urban soil	0.10 ng/Kg/year	Sun et al. (2014)

WWTP: waste water treatment plant; CNTs: carbon nanotubes.

Regarding NPs, the known source is reduced to biomedical applications (Putri et al., 2017) and the rest is unintentionally as they are produced as secondary NPs by the use of 3D printing (Stephens et al., 2013; Rodriguez-Hernandez et al., 2020) and thermal cutting of polystyrene foam (Zhang et al., 2012). Measured concentrations of NPs in the ecosystems are not reported in the literature. Presence of NPs has been detected in aquatic ecosystems (Ter Halle et al., 2017) and quantification methodologies have recently been developed (Schwaferts et al., 2020; Jiemenz-Lamana et al., 2020) but not yet applied successfully. Predictions of NP concentrations in aquatic ecosystems are neither reported in the literature, but some modelling studies of the outputs and retention of these plastics in the ecosystem have been published (Besseling et al., 2017; Koelmans et al., 2017). According to one of the estimations, 2.5% of the total from plastic debris found in the ocean surface layer in 2016 (0.309 million tons) would be NPs, while MPs are the 13.8%

(Koelmans et al., 2017). The other study reported that 100 nm NPs will be retained in the rivers in a high extent with a rate in sediment of 1.5 ng/Kg/day (Besselgin et al., 2017). Nevertheless, NPs are expected to be in the same or higher amount than MPs due to its similar sources and the demonstrated NP production by degradation of MPs in the aquatic ecosystem (Mattson et al., 2015).

Regarding GNMs, prediction models are difficult to obtain, because most of the applications are not being commercialised yet or they are in phase of validation for industrial scale production (Ciriminna et al., 2015; Tiwari et al., 2020). The models require to know the GNM production market and the different sources to the aquatic ecosystems. The current production at global scale for GNMs is growing. A production of 120 tons was reported in 2015 (Kong et al., 2019) and it was expected to grow in the following years. Agriculture and remediation are the intentional sources of CNMs release to the ecosystem; and the unintentional release is from surface run off or WWTPs. Measurements of real environmental concentrations are challenging. First, due to the fact that carbon from CNMs is difficult to be distinguished from natural carbonaceous materials and, second, because the existent techniques to quantify CNMs are not sensible enough to analyse low concentrations, such as those expected in the environment (Goodwin et al., 2018). Therefore, it is important to build prediction models for GNMs as analytical techniques are not still available. Some estimations have been already done for CNTs or fullerenes (**Table 1**; Kunhikrishnan et al., 2014; De Marchi et al., 2018; Zhao et al., 2020b) that could be also valid for GNMs due to their similar surface properties and applications. These models consider the current use of other CNMs because available information is larger than for GNMs. For CNTs, predicted values in the different compartments (surface water, sediments and WWTP effluent, natural and urban soil) are in the range of ng/L. The higher predicted concentration is for the WWTP effluent where 4 ng/L (Sun et al., 2014). Natural and urban soil are expected to receive an input of 5.1 ng/Kg per year and for sediment values of 10^{-4} - $2.66 \cdot 10^{-2}$ mg/Kg are expected. In the case of fullerenes, predicted values are lower than for CNTs in surface water (0.003 ng/L; Kunhikrishnan et al., 2014) and in natural and urban soil (0.10 ng/Kg/ year), mainly due to the lower production (20 t/a) compared to the production of CNTs (380 t/a) (Sun et al., 2014).

1.4. Effects in aquatic organisms

MPs and NPs

One of the main features that make MPs a potential risk for the aquatic organisms is their higher availability compared to that of larger plastics for a wide range of aquatic organisms. Most of the organisms that are present in the aquatic ecosystems are able to ingest MPs, such as invertebrates (Cole et al., 2013; Frias et al., 2014; Rochman et al., 2015; Leslie et al., 2017; Botterell et al., 2019; Prata et al., 2019) and fish (Jabeen et al., 2017; Jovanović, 2017; McNeish et al., 2018;

Introduction

Wang et al., 2020b). The ability of the organisms to ingest and accumulate these small plastics depends principally on their feeding strategy, being the most selective feeders more likely to accumulate less MPs. As observed by Wang et al. (2020b), fish with a carnivore behaviour accumulated less MPs than omnivorous fish. Also, the MP size influences the ingestion by organisms, which is expected to be higher when MP size is similar to the size of the common prey, usually similar to zooplankton for fish. Another process that influences MP accumulation is biomagnification, which occurs through the ingestion of preys that have previously accumulated MPs (Farrell and Nelson, 2013; Saley et al., 2019; Elizalde-Velazquez et al., 2020). Regarding polymers, ingestion depends on their density; those more dense (polyester, PS) that tend to settle will be ingested by benthic organisms, while those less dense (PE, PP) that tend to float will be ingested for organisms living in the surface or in the water column (Erni-Cassola et al., 2019).

Several studies have demonstrated that ingestion of MPs does not produce acute effects in aquatic organisms (Jovanović, 2018; Prata et al., 2019; Wang et al., 2019b, c). One of the main reasons explaining this observation is the fact that MPs are also easily excreted. High rates of plastic elimination have been reported in aquatic organisms (Grigorakis et al., 2017; Jovanović et al., 2018). Nevertheless, ingested MPs can produce changes in food uptake and even affect the weight of aquatic organisms. Small aquatic organisms have shown inhibition of predation and a reduction of nutrient availability as observed in microalgae exposed to MPs (Prata et al., 2019). Intake of large MPs (120-220 μm) was also observed that further produced anorexia to the fish (De Sales-Ribeiro et al., 2020). The effects of MPs in the digestive system of fish were observed in form of dysbiosis, damage and physical blockage and inflammation of the gut and intestine (Lu et al., 2016; Jin et al., 2018; Qiao et al., 2019).

Another common sublethal effect observed in aquatic organisms exposed to MPs is oxidative stress (Paul-Pont et al., 2016; Yu et al., 2018; Qiao et al., 2019; Romano et al., 2020). Oxidative stress reflects an imbalance between generation and elimination of reactive oxygen species (ROS) in the organism. This effect occurs when antioxidant enzymes are not capable to neutralise the excess of ROS production. The most reported antioxidant enzymes to assess effects produced in aquatic organisms are catalase (CAT), superoxide dismutase (SOD), glutathione S-transferase (GST) and glutathione peroxidase (GPx). Increased activity of these enzymes was observed in the liver of crabs after exposure to low concentrations (4 and 400 $\mu\text{g/L}$) of 0.5 μm PS MPs (Yu et al., 2018). Similar increase was also observed in zebrafish exposed to PS MPs (5 and 50 $\mu\text{g/L}$) of the same size (Qiao et al., 2019). These changes in the antioxidant enzyme activities seems to be due to the physical damage produced after ingestion (intestine inflammation), as previously mentioned for fish. Regarding NPs, oxidative stress was observed in the brain of zebrafish embryos (Sökmen et al., 2020). A close relation was observed between MP/NP size decrease and increase of oxidative stress and cell death in adult fish (Sarasamma et al., 2020).

In summary, the main effect of MPs in aquatic organisms is the alteration of organism's systems associated with food intake. Translocation of MPs to the inner tissues has not been demonstrated in aquatic organisms (De Sales-Ribeiro et al., 2020) for particles sizes larger than 5 µm, which would be larger than a regular cell. However, several studies have analysed the translocation of <5 µm MPs and NPs (Rosenkranz et al., 2009; van Pomerene et al., 2017; Pitt et al., 2018a,b; De Sales-Ribeiro et al., 2020) and GNMs in aquatic organisms (Lammel and Navas, 2014; Hu et al., 2017; Katsumiti et al., 2017). MP translocation from water to fish was observed in liver and intestine cells (1-5 µm MPs; De Sales-Ribeiro et al., 2020), for NPs translocation was observed to the eyes of fish embryo (25-50 nm NPs; van Pomerene et al., 2017) and gastrointestinal tract, gallbladder, liver, pancreas, heart, and brain (Pitt et al., 2018a). In the case of GNMs, GO platelets were observed inside mussel hemocytes due to their sharp edges that acted like a blade breaking the cell membrane (Katsumiti et al., 2017), and similar for fish cells where GO was observed in the cytosol (Lammel and Navas, 2014). GO was internalised in the brain of parental and offspring fish, leading to remarkable neurotoxicity in the offspring (Hu et al., 2017). One of the restrictive characteristics that could limit in the internalisation of GO platelets to the tissue is their lateral dimension in the micro range, sometimes larger than 10 µm.

Although NPs present greater ability to cross biological barriers than MPs, the exposure of aquatic organisms to NP cause similar effects as for exposure to MPs. Algae presented inhibited growth and increased ROS production after exposure to 22 and 70 nm NPs concentration higher than 6.5 mg/L (Bhattacharya et al., 2010; Besseling et al., 2014). Hampered larvae motility and induced multiple moulting events are two of the main effects observed in *Artemia franciscana* exposed to 40 nm anionic carboxylated PS particles (Bergami et al., 2016). Another aquatic crustacean, *Daphnia magna*, presented a reduced body size after exposure to 70 nm PS particles along with a lower reproduction rate (Besseling et al., 2014), and *D. magna* immobilisation for high concentrations (1-80 mg/L) of 200 nm PS (Kim et al., 2017). In addition some effects not reported for MPs in aquatic organisms, but that haven been reported for NPs was the alteration of the nervous system. Fish after exposure to NPs presented inhibition of the acetylcholinesterase (AChE) activity (Chen et al., 2017a,b; Sarasamma et al., 2020). AChE is a common biochemical biomarker used to assess neurotransmission activity, which is in charge of the breakdown of acetylcholine, an important neurotransmitter involved on synaptic transmission of nerve impulses. Due to the absence of predicted or measured concentration of NPs in ecosystems, the toxicity studies reported were not performed with environmentally relevant concentrations, only using high concentrations (µg/L-mg/L) known to cause sublethal effects.

Introduction

Graphene family NMs

The study of potential effects provoked by GNMs in aquatic organisms has grown in the last years (Guo and Mei, 2014; Montagner et al., 2017; Dasmahapatra et al., 2019). GNMs are materials, as observed for MPs and NPs, that only exert acute toxicity at elevated concentrations (mg/L) in aquatic organism, and lethality is reported for even higher concentrations that alters normal movement of the exposed organism (materials attachment to the organism body) but are not expected to be found in the ecosystems (Katsumiti et al., 2017; Lv et al., 2018). The *D. magna* exposure to GO presented a LC₅₀ value of 45.4 mg/L after 72 h (Lv et al., 2018). For mussel hemocytes exposed to GO with a LC₅₀ of 49.84 mg/L was reported but, in this case, an increase of cytotoxicity was observed for the exposure to rGO, for which a LC₅₀ of 29.92 mg/L was estimated (Katsumiti et al., 2017). Values of LC₅₀ are not reported for embryo or adult fish exposure to GO, lethality was not observed (Chen et al., 2012b; Hu et al., 2017; Souza et al., 2017)

As previously mentioned, the different derivatives that take part of the GNMs have different characteristics (surface chemistry) that further are involved on the different mechanism that organisms will have to defence against them. Therefore, it should be underlined that each graphene NM can affect different pathways or systems in the aquatic organisms. The principal effect reported of these carbon NMs in organisms is the oxidative stress through generation of ROS (Seabra et al., 2014). This effect has been demonstrated in bacteria (Hu et al., 2010; Gurunathan et al., 2012) and HeLa cells (Gollavelli and Ling, 2012). rGO produced oxidative stress due to the direct contact of the sharp edges in exposed bacteria and it was reported as more toxic than GO to bacteria (Hu et al., 2010). *Chlorella vulgaris* exposed to 0.01-10 mg/L of GO presented oxidative stress, which was observed from the increased ROS levels and SOD activity in algae after exposure (Hu et al., 2015). On the contrary, the green algae *Trebouxia gelatinosa* exposed to GO (1-50 mg/L) did not show oxidative stress but attachment of the material between the cell wall and the plasma membrane was observed (Banchi et al., 2019). Other filter feeder, *D. magna* presented a high ratio of GO ingestion followed by a total excretion, with a consequent oxidative stress (lipid peroxidation and changes in SOD activity; Lv et al., 2018). For zebrafish embryos, oxidative stress was reported after exposure to GO with an excessive generation of ROS, specially detected in embryo eyes (Chen et al., 2016a; Zhang et al., 2017b). For adult fish, oxidative stress was also reported for elevated GO concentrations (20 and 32 mg/L) (Lammel and Navas, 2014; Souza et al., 2017). The source of the oxidative stress was the damage produced in the mitochondria due to the GNMs sharp edges and their reactive surface.

Another factor that can be related to the potential toxicity of MPs/NPs or NMs is the presence of additives during their manufacture (plasticisers, surfactants, etc.). The presence of plasticisers in

MPs collected in aquatic ecosystems has been reported (Ašmonaitė et al., 2018). That makes MPs vectors of other pollutants for aquatic organisms. As an example, the plasticizers present in MPs are known to be endocrine disruptors highly toxic (Talsness et al., 2009) that can alter the estrogenic activity of aquatic organisms when associated with MPs/NPs (Koelmans et al., 2014; Mak et al., 2019; Schrank et al., 2019).

Other pollutants that can interfere in the potential toxicity of MPs/NPs and CNMs are the hydrophobic xenobiotics that can be highly sorbed to them due to their high surface to volume ratio (Apul et al., 2013; Ji et al., 2013; Pei et al., 2013; Wang et al., 2014; Hüffer and Hofmann, 2016; Wang et al., 2018b; Wang et al., 2019a). MPs and NPs have shown a noticeable capacity to sorb persistent organic pollutants (POPs), which is closely related to the particle size, being small particles more prone to sorb pollutants in higher extent than larger particles (Ma et al., 2016; Wang et al., 2019a). For instance, Ma et al. (2016) reported a higher partition coefficient (K_d) value for the sorption of phenanthrene to 50 nm PS MPs (654 L/g) than to 10 μ m PS MPs (16.9 L/g) after 7 days of incubation. The main factors on which the sorption phenomenon depends are MP size and polymer type (glassy state and porosity) (Zuo et al., 2019). The sorption capacity of GNMs for POPs is even higher than for MPs and NPs. Thus, NMs are being proposed for water pollution remediation, due to their impressive capacity to sorb POPs (Younis et al., 2020). Some sponges made of GNMs are being used to remove oil from oil spill scenarios, demonstrating a high capacity to remove oil and better possibility of being recycled and reused than other remediation materials (Niu et al., 2016). In this case, the characteristics that enhance the sorption capacity are the surface chemistry and the potential surface area for sorption that is related with their crystalline structure (Smith and Rodrigues, 2015).

An important number of pollutant types have been found sorbed to MPs in the aquatic ecosystems, especially, polycyclic aromatic hydrocarbons (PAHs) (Frias et al., 2010; Van et al., 2012; Antunes et al., 2013; Karkanorachaki et al., 2018). Data on compounds sorbed in NPs and GNMs collected in the environment are quite difficult to obtain due to the lack of methods to collect those small materials. Nevertheless, due to the increase of nanotechnology market those materials are expected to arrive to the aquatic ecosystem interacting with other pollutants that are already present in the aquatic ecosystem representing a threat for the aquatic organisms.

The potential toxic effects of pollutants transported by micro and nanomaterial to the organisms, a phenomenon known as “Trojan horse effect”, is being a widely studied (Mato et al., 2001; Teuten et al., 2007; Yang and Xing, 2010; Wirnkör et al., 2019). To fully understand the implications of this phenomenon, first the different routes by which materials interact with aquatic organism should be defined (**Fig. 5**). One of the main routes is the ingestion of contaminated particles and release of these compounds from the micro- and NMs in the digestive tract and

Introduction

further absorption by the intestine cells to be metabolised. Some studies reported that after the pH and temperature changes that ingested materials will undergo inside the organism, the sorbed pollutants will be released from the MPs/NPs and CNMs (Wang et al., 2011; Bakir et al., 2014). The bioavailability of PAHs sorbed to CNMs has been demonstrated in crustaceans (Zindler et al., 2016) and fish (Su et al., 2013; Linard et al., 2017). Other ways in which the sorbed pollutants could interact with the organism are via direct contact with the skin of the organism (mucus) or with the organs that are directly exposed to the water column, such as gills (Ma and Lin, 2013). And the last and more complex route is that the micro or NM could translocate from the digestive system to the inner tissues. NMs with sorbed compounds would internalise into the cells (Geppert et al., 2016; Minghetti et al., 2017) where the pollutants could be desorbed and subsequently produce cytotoxicity or genotoxicity to the organism.

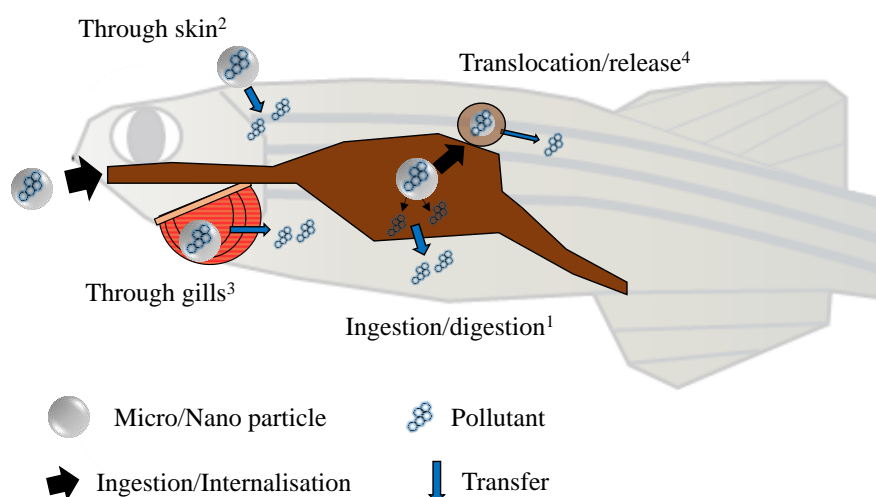


Fig. 5- Illustration of the different routes by which the micro- or NMs with sorbed compounds can be assimilated or transferred to aquatic organisms. (1) By ingestion/digestion where pollutants are released from the micro or NM due to digestive content of the digestive tract (T and pH) and further assimilation by the digestive tissue; (2) By direct contact and diffusion through the skin; (3) By direct contact and diffusion through the gill or respiratory organs; (4) By translocation of the micro- or NM with sorbed compounds to the tissues and further release inside the cells (based on Ma and Lin, 2013).

Three potential situations could occur in the organism exposed to contaminated micro- or NMs: (i) reduction of the pollutant toxicity due to its retention by the material to which is strongly bound; (ii) pollutant released from the material to the organism after crossing organism barriers resulting in an enhancement of the toxicity; (iii) no changes in toxicity because the bioavailability of the pollutant is the same regardless the presence of the material. Most of the studies that address this issue an enhanced toxicity when MPs/NPs were combined with POPs (Batel et al., 2016; Batel et al., 2018; Ašmonaitė et al., 2018; Bussolaro et al., 2019), one work showed no changes in the effects produced by the sorbed compounds (Sleight et al., 2017) and three works presented

a decrease of the toxicity produced by the sorbed compounds to the organism (Karamiet al., 2016; Chen et al., 2017a; Trevisan et al., 2019). For CNMs, most of the works reported less toxicity produced by the sorbed pollutants to the organism (Park et al., 2010; Falconer et al. 2015; Rodd et al., 2019; Yang et al., 2019) and one co-exposure scenario resulted into higher toxicity to the organism than the exposure to pollutants alone (Della Torre et al., 2017). The Trojan horse effect could be expected to occur at less extent for MPs/NPs than for GNMs due to their lower sorption capacity (smaller surface area for sorption and less hydrophobicity). Briefly, the strength of the binding between the sorbent and the sorbate that it is translated into higher sorption capacity plays against bioavailability due to the higher energy required to desorb pollutants from micro- and NMs and to produce the potential toxic effects.

Previous studies have proven that glassy or robbery state of MPs and shape of the NMs are an important parameters for desorption hysteresis (a term referring to a slow desorption kinetic with a thermodynamically irreversible adsorption) been carried out on desorption hysteresis of PAHs from MPs/NPs (Zuo et al., 2019) and carbon NMs (Wang et al., 2011; Wu et al., 2013; Lu et al., 2018) proving). Desorption hysteresis is not expected from graphene, as 2D planar carbon NM, GO has less tendency than graphene for aggregation, a reason explaining why a desorption hysteresis of PAHs is more likely to occur from GO than from graphene. On the contrary, GO with more oxide groups than graphene and consequently with a less polar surface, will have less tendency for desorption hysteresis of PAHs as reported by Wu et al. (2013) and Lu et al. (2018). Nevertheless, many parameters play a role in this phenomenon such as sorbent and sorbate interactions that depends on in the type of sorbate and sorbent, and environmental conditions. Therefore comparisons between MPs and CNMs in terms of sorbed PAH contribution via desorption to aquatic organisms are difficult to establish.

2. Brine shrimp, a small invertebrate to assess the hazard of microplastics and nanomaterials

Brine shrimp is a small crustacean arthropod that belongs to the Artemiidae family commonly found in hypersaline habitats. This organism is a non-selective filter feeder that is distributed in the environment globally due to its tolerance and adaptation to new conditions thanks to its dual reproduction type (ovoviviparous and oviparous). The generation after oviparous reproduction of the called cysts, that are highly resistant to environmental conditions and rich in protein content and amino acids, has made of this organism a commercial food in aquaculture. The brine shrimp is been often used for toxicity assessment in salt water (Johari et al., 2018). Brine shrimp immobilisation test is considered as a suitable model test in toxicity assessment of NMs due to the quick, cheap and reliable results (Libralato, 2014; Rajabi et al.; 2015).

Introduction

The effects caused by MPs to brine shrimp were mostly sublethal and few studies compared with NP exposure. No changes in mortality and growth in brine shrimp larvae exposed to a wide range of concentrations (0.0006 to 5.49 mg/L) of 5 and 10 μm PS MPs for 14-44 days were reported (Wang et al., 2019b; Peixoto et al., 2019). A growth inhibition in brine shrimp larvae exposed to 1 mg/L of 5 μm PS MPs for 7 and 14 days was observed, with an added oxidative stress at 1, 2 and 7 days of exposure reflected by the enhance of ROS levels (Suman et al., 2020). When decreasing the plastic size, 1 mg/L of 50 nm functionalised NPs (cationic amino, PS-NH₂ NPs), caused more effects than MPs, such as inhibition of the nervous system, oxidative stress, genes involved in cell protection and growth inhibition in larvae after 14 days of exposure (Varó et al., 2019). This time the brine shrimp larvae exposed to functionalised NPs presented change at physiological levels (multiple molting) after larvae exposure for 48 h to 50 mg/L of 50 nm PS-NH₂ (Bergami et al., 2016)

Few studies addressed effects of GNMs in brine shrimp (Pretti et al., 2014; Mesarič et al., 2015; Zhu et al., 2017), being oxidative stress was the most reported effect. Exposure to graphene monolayer and nanopowder caused an increase of CAT activity in larvae. This was not seen for graphite due to its thicker structure. In addition, 0.1 mg/L of graphene monolayer increased GPx activity and peroxidation levels in brine shrimp exposed for 48 h. None of the treatments caused mortality at the tested concentrations (0.1, 1 and 10 mg/L) (Pretti et al., 2014). Oxidative stress was also be observed in brine shrimp larvae exposed to GO. In this case, larval mortality was reported after 72 h of exposure from 50 mg/L of GO, which was mainly due to the attachment of GO to the external surface of the brine shrimp along with a swimming inhibition (Mesarič et al., 2015). Again mortality and changes of hatchability and morphology were observed in brine shrimp larvae instar I exposed to elevated concentrations of GO (100-600 mg/L). Oxidative stress was also reported in brine shrimp larvae from the lowest concentration tested (25 mg/L), increase SOD and GPX activities along with a decrease of CAT and GST activities was observed for all the brine shrimp ages tested (instar I, II and III) after 24 h of exposure (Zhu et al., 2017).

For brine shrimp, to the best of our knowledge, there are not studies addressing the Trojan horse effect in this organism of any MPs/NPs or GNMs. Only studies that used brine shrimp exposed to a combination of MPs with sorbed PAHs for diet transfer to fish were found (Batel et a., 2016; Cousin et al., 2020). Analysis of the potential toxicity or any sublethal effect produced by MPs with sorbed PAHs in brine shrimps were not analysed.

Table 2- Summary of studies reporting effects of MPs, NPs and GNMs alone and with other organic pollutants in brine shrimp.

MPs				
Particle concentration and size	Co-contaminant	Endpoints	Main effects	Reference
-1, 10, 10 ² , 10 ³ and 10 ⁴ particles/mL (0.0006, 0.006, 0.055, 0.55, 5.49 mg/L) of 10 µm PS MPs	-non	-Mortality -Uptake and accumulation -Ultrastructure analysis of epithelial cells lining the digestive tract	-No mortality for <i>A. parthenogenetica</i> larvae -No significant impact on growth or development -Ingestion over 24 h and 14 days -Ultrastructural changes on epithelial cells	Wang et al. (2019b)
-1, 25, 50, 75 and 100 mg/L of 5 µm PS MPs	-non	-Mortality -Apoptosis -Uptake and accumulation -ROS levels -Histopathological alterations -Transcriptome	-Growth inhibition at 7 and 14 days of exposure -Enhanced ROS levels at 1, 2, 7 and adult age	Suman et al. (2020)
-0.4, 0.5, 1.6 mg/L of 1-5 µm red fluorescent MPs	-non	-Uptake and accumulation -Mortality -Individual growth	-Ingestion by juvenile and adult individuals of <i>A. franciscana</i> -No mortality or growth inhibition	Peixoto et al. (2019)

-10, 100 and 1000 particles/mL of fluorescently labelled and unlabelled 10 µm PS MPs	-non	-Uptake and accumulation -Food uptake (ingestion rate) -Histopathological alterations	-Decreased ingestion rate at low exposure concentrations over 24 h and 14 days (10 particles/mL) -Increased lipid droplet numbers in epithelia, intestinal epithelial deformation, and disordered cellular arrangement	Wang et al. (2019c)
NPs				
Particle concentration and size	Co-contaminant	Endpoints	Effects	Reference
-5, 25, 50 and 100 mg/L of 40 nm anionic carboxylated NPs (PS-COOH) -5, 25, 50 and 100 mg/L of 50 nm cationic amino NPs (PS-NH ₂)	-non	-Mortality -Locomotor activity -Uptake and accumulation -Moulting alterations	-Hampered larvae motility -Induction of multiple moulting events	Bergami et al. (2016)
-0.006 and 0.6 mg/L of 100 nm fluorescent PS NPs	-non	-Uptake and accumulation -Feeding behaviour in presence or absence of algae	-Ingestion of low concentrations in the presence and in the absence of natural food -Lower ingestion in the presence of food than in starvation treatments	Sendra et al. (2020)

-0.1, 1 and 10 mg/L of 50 nm PS-NH ₂	-non	-Cholinesterase activity -Carboxylesterase activity -Oxidative stress (GST, CAT, malondialdehyde (MDA) activities) -Transcription of selected genes involved in stress response (<i>hsp26</i> , <i>hsp70</i>), metabolism and biosynthesis (<i>cstb</i> , <i>clap</i> and <i>tcp</i>)	-Growth inhibition and development in 48 h nauplii -No effects in juveniles -Neurotoxicity and oxidative stress -Significant upregulation of genes related to cell protection, development and moulting	Varó et al. (2019)
---	------	--	--	--------------------

GNNMs

NM concentration and type	Co-contaminant	Endpoints	Effects	Reference
-0.1, 1, 10 mg/L of pristine graphene monolayer flakes -0.1, 1, 10 mg/L of graphene nano powder -0.1, 1, 10 mg/L of graphite	-non	-Mortality -Oxidative stress (MDA, GPx and CAT activities) -Uptake and accumulation	-No mortality in <i>A. salina</i> larvae exposed to the three treatments -Pristine graphene monolayer significantly increased CAT, GPx activities and lipid peroxidation levels -Graphene nano powder significantly increased CAT activity	Pretti et al. (2014)
-10, 100, 500, 600 and 700 mg/L of GO	-non	-Mortality -Swimming behaviour -Cholinesterase, CAT and GST activities -Uptake and accumulation	-Swimming inhibition -Larva mortality produced by all the tested concentrations at 72 h -Decreased GST activity and increased cholinesterase activity -GO attachment onto the external surface of <i>A. salina</i>	Mesarič et al. (2015)

-25, 50, 100, 200, 400 and 600 mg/L of GO -non	-Hatchability -Mortality rate, swimming inhibition, body length and weight -Oxidative stress (CAT, SOD, GPx, GST and MDA levels) -ROS detection -Uptake and accumulation	-Significant changes in hatchability, mortality and morphological -Increased MDA levels -Increased SOD and GPx activities and decreased CAT and GST activities -Ingestion and distribution in primary body cavity, yolk and intestine	Zhu et al. (2017)
--	--	---	-------------------

CAT: catalase; *clap*: cathepsin L-like protease; *cstb*: cystatin B inhibitor; GO: graphene oxide; GPx: glutathione peroxidase; GST: glutathione S-transferase; *tcp*: chaperonin-containing TCP; *hsp26*: heat-shock protein 26; *hsp70*: heat shock protein 70; MDA: malondialdehyde; PS: polystyrene; PS-COOH: anionic carboxylated; PS-COOH: cationic amino polystyrene; ROS: reactive oxygen species; SOD: superoxide dismutase.

3. Zebrafish as a model organism to assess the hazard of microplastics and nanomaterials

The zebrafish (*Danio rerio*) is a tropical freshwater fish commonly found in South Asia. Zebrafish belongs to the Cyprinidae family (carps and minnows) and takes its common name from the stripes on the sides of its body. This small fish has plenty of characteristics such as ease of breeding, short life cycle, high fecundity, year round spawning, genetic similarities with humans and cheap maintenance that allow it to be an organism of reference.. This fish is being a popular organism model since George Streisinger et al. (1981) described the methods that allow its genetic manipulation. Further description of its whole genome made it a good genetic model to be compared with mammals (Howe et al., 2013). Zebrafish is recommended in many fields as organism of reference, such as molecular biology, developmental biology, cancer research, neurobiology and genetic research. Regarding MPs and NPs or CNMs, zebrafish is already being used as a suitable model organism (Haque et al., 2019; Bhagat et al., 2020) due to the transparency of embryos (standardisation of developmental studies (OECD TG236. (2013)), genetic similarities to humans and availability to test pollutants via multiple routes of exposure.

3.1. Effects in developing embryos

Effects provoked by MPs and NPs in zebrafish embryo development are summarized in **Table 2**. Exposure of zebrafish embryos to all the tested MP or NP concentration reported in the literature did not cause mortality (van Pomeran et al., 2017; Pitt et al., 2018a; Cormier et al., 2019; Sökmen et al.; 2020). Although MPs/NPs are inert materials, they were able to provoke some sublethal effects in zebrafish embryo development. Mainly reported effects include oxidative stress and alterations of immune and nervous systems. Embryos exposed to 1 mg/L of 5 and 50 µm PS MPs for 7 days presented a significant decrease of CAT activity and glutathione (GSH) content. In addition, disruption of the glycolipid and energy metabolism was observed (Wan et al., 2019). Oxidative stress was also detected in zebrafish embryos exposed to smaller MPs, 1 mg/L of 0.5 µm PS MP, with an increase of SOD activity and a significant decrease of the cell stress through reduced cyclooxygenase activity (Parenti et al., 2019). At molecular level, embryos exposed to 1 mg/L of 1 µm PS MPs for 96 h presented up-regulation of *cat* and *interleukin 1 beta (il1b)* associated with inhibition of the locomotor activity of the larvae (Qiang and Cheng, 2019). 500 µg/L of 4.64-17.6 µm low-density PE MPs caused an increase of *cat* and *caspase 9* mRNA levels after 10 days of exposure indicating an impact on antioxidant system and defence against apoptosis (Karami et al., 2017). For the smallest NPs tested in embryos oxidative DNA damage and apoptosis were also observed after injection of 3 nL of 1% stock of 20 nm PS NPs (Sökmen et al., 2020). 50 nm PS NPs were able to cross the chorion of developing zebrafish showing alteration of swimming behaviour and decrease of heart rate at the end of the exposure (120 hpf)

Introduction

to 1 and 1 mg/L (Pitt et al., 2018a). The offspring of adult zebrafish treated with 1 mg of 42 nm NPs via diet presented bradycardia and oxidative stress (reduction of glutathione reductase (GR) and thiols levels), without changes in locomotor activity. Treatment of adults lead to maternal transfer of NPs to the offspring via accumulation in the eggs of exposed females (Pitt et al., 2018b). Up-regulation of transcription levels of immune genes (*il1 β* , *irg11*, *socs3a* and *ccl20a*) of zebrafish embryos after exposure to 25 nm PS NPs (10 mg/L) was reported, in addition to inflammatory response in the skin and intestine cells (Brun et al., 2018).

When MPs were combined with other pollutants, a reduction of the toxic effects of the pollutant alone was observed in zebrafish embryos (Chen et al., 2017a; Sleight et al., 2017). In embryos exposed to a combination of 400 mg/L of 200-250 μ m plasticised PVC and 0.5 mg/L of phenanthrene or 1 μ g/L of 17 α -ethynylestradiol (EE2), no remarkable changes in biotransformation metabolism related genes nor increase of the compound bioavailability was observed (Sleight et al., 2017). The embryo hypoactivity caused by 2 μ g/L of EE2 alone was reduced in presence of 1 mg/L of 45 μ m PS MPs. On the contrary, 50 nm NPs alone and combined with EE2 altered the nervous and antioxidant systems of the embryos, AChE activity was inhibited and GSH content increased (Chen et al., 2017a). Particle size plays an important role determining the mechanisms of toxicity of contaminated MPs and NPs, likely due to their different ability to cross biological barriers. MPs (11-13 μ m PE) spiked with benzo(a)pyrene (B(a)P) (16.87 μ g/g MPs) provoked an increase of biotransformation metabolism (7-ethoxyresorufin O-deethylase (EROD) activity and *cytochrome P450 1A (cyp1a)* transcription levels), indicating the successfully transfer of B(a)P via MPs to the embryo (Cormier et al., 2019). 44 nm PS NPs (10 mg/L) combined with PAHs from a sediment extract provoked a dysfunction of the mitochondria. The reported effect was no longer observed when embryos were exposed to the corresponding environmental PAH mixture (5073 ng/mL) alone while a coupling efficiency and impaired brain vascularity were reported (Trevisan et al., 2019).

The toxicity of GNMs has also been studied in zebrafish embryos (**Table 2**). GO concentrations higher than 50 mg/L caused hatching delay (Chen et al., 2012b; Chen et al., 2016b) is an effect that has not been reported previously in zebrafish embryos exposed to MPs/NPs. In addition, in 96 hpf zebrafish embryos exposed to 100 mg/L increased heart rate and increased incidence of pericardial/yolk sac edema was also reported, along with ROS induction and lipid peroxidation (Chen et al., 2016b). Prevalence of yolk sac edema and pericardial edema was also significantly higher in zebrafish embryos exposed to GO concentrations higher than 5 mg/L, along with a decrease of heart beat rate and reduction of movement frequency (d'Amora et al., 2017). Again, significant increase in embryo malformation rate accompanied by protein carbonylation and excessive generation of ROS, especially the superoxide radical, was observed after exposure to GO, in this case at lower concentration (0.01 mg/L) (Zhang et al., 2017b). As previously

mentioned, oxidative stress is a common response in zebrafish embryos exposed to GO, being the main reason explaining the damage observed in the mitochondria, which is closely related with GO translocation to the embryo tissues (Ren et al., 2016; Hu et al., 2017; Zou et al., 2018). A disorder in proteins involved in mitochondrial function was observed after an increase of oxidoreductase activity in zebrafish embryos (7 dpf) exposed to 100 µg/L of GO (Zou et al., 2018). Again, mitochondrial damage, and an increase of apoptosis were reported in zebrafish embryos exposed to low concentrations of GO (0.01, 0.1 and 1 µg/L). In addition, translocation of GO from water to the diencephalon, intestine and tail of zebrafish embryos was observed (Ren et al., 2016). Translocation of GO was detected in the brain of the offspring of adults exposed to GO, affecting offspring immune and nervous systems (decreased AChE activity) (Hu et al., 2017). Regarding rGO, few works have been done in zebrafish embryos (Liu et al., 2014; Zhang et al., 2017a). rGO increased hatching time and decreased larval length at higher extent than GO, while GO was the only form that affected heart beat rate of zebrafish embryos exposed at a range of concentrations from 5 to 100 mg/L (Liu et al., 2014). However, exposure of zebrafish embryos to 100 mg/L of rGO quantum dots did change heart beat rate maybe due to their smaller size and higher bioavailability than regular rGO. In addition, up-regulation of transcription levels of biotransformation metabolism related genes (*cyp1a*, *cytochrome P450 1c1*) was observed in embryos exposed to 100 mg/L of rGO quantum dots (Zhang et al., 2017a).

Only one study addressing the potential toxicity provoked by GNMs as vector of organic pollutants was reported in the literature (Yang et al., 2019). Two concentration of GO (0.1 and 1 mg/L) were used in combination with bisphenol A (50 and 500 µg/L) to assess the role of GO as a vector of bisphenol A to zebrafish embryos. Results showed that, in all the cases, GO reduced or alleviated the effects produced by bisphenol A (embryo malformation, elevated levels of vitellogenin and estrogen) along with a reduction of bisphenol A bioavailability (Yang et al., 2019). Other carbon NMs with similar properties, such as CNTs and fullerenes have been used to investigate this phenomenon in zebrafish embryos (Park et al., 2011; Falconer et al., 2015; Della Torre et al., 2017). 72 hpf embryos co-exposed to an increased concentration of fullerenes (15 to 100 mg/L) and a fixed concentration of EE2 (1 µg/L) presented a reduction of EE2 bioavailability after 96 h. In this case, fullerenes acted as inhibitors of EE2 toxicity for developing embryos (Park et al., 2011). Also, an increase in the concentration of multiwalled CNTs combined with phenanthrene (10 mg/L) reduced the mortality caused by phenanthrene alone to 24 hpf zebrafish embryos (Falconer et al., 2015). On the contrary, amorphous carbon nanomaterials (carbon nanopowder) in addition to the carcinogenic B(a)P was able to induce B(a)P toxicity in zebrafish embryos. Apoptotic and necrotic cells and decrease of oxidative stress were the main responses of zebrafish embryo exposed to 50 mg/L of carbon nanopowder combined with 20 µg/L of B(a)P (Della Torre et al., 2017).

Table 2- Summary of studies reporting effects of MPs, NPs and GNMs alone and with other organic pollutants in zebrafish embryos.

MPs				
Particle concentration and size	Co-contaminant	Endpoints	Main effects	Reference
-1 mg/L of 45 µm PS MPs	-2 and 20 µg/L of EE2 (co-exposure)	-Locomotor system -Transcription levels of <i>gfap</i> , <i>a1-tubulin</i> , <i>zfrho</i> and <i>zfbblue</i> -CAT, GPx, GSH, AChE -Bioconcentration of EE2	-Hypoactivity alleviated by co-exposure with EE2	Chen et al. (2017a)
-1 mg/L of 0.5 µm PS MPs	-non	-Uptake and distribution of PS MPs -Cellular stress (glycoprotein and cyclooxygenase activities) -Oxidative stress (GST, CAT, GPx, SOD, ROS production) -Swimming behaviour	-Significant decrease in cyclooxygenase activity -Induction of SOD -Accumulation in the gut and in the intestine	Parenti et al. (2019)
-10, 100 and 1000 µg/L of 1 µm fluorescent PS MPs	-non	-Locomotor system -Hatching -Transcription levels of oxidative stress related genes (<i>illb</i> , <i>cat</i> , <i>sod</i>)	-Inhibition of larval locomotion -Upregulation of <i>illb</i> and <i>cat</i>	Qiang and Cheng (2019)
-100 and 1000 µg/L of 5 and 50 µm PS MPs	-non	-Uptake and accumulation -Composition of microbiome -Transcription of glycolysis and lipid metabolism related genes -Biomarkers of oxidative stress (GSH, SOD and CAT)	-Significant decrease of CAT activity and GSH content -Disturbed glycolipid and energy metabolism	Wan et al. (2019)

10 and 100 mg/L of 11-13 µm PE MPs	-16.87 µg of B(a)P/g of PE -0.08 µg of oxybenzone/g of PE -70.22 µg of perfluorooctane sulfonate/g of PE (co-exposure)	-Hatching, mortality -Biotransformation metabolism -Larval behaviour	-B(a)P spiked PE MPs increase of EROD activity significantly and upregulated <i>cyp1a</i>	Cormier et al. (2019)
-5, 50 and 500 µg/L of 4.64-17.6 µm low-density PE MPs	-non	-Transcription levels of <i>casp9</i> , <i>casp3a</i> and <i>cat</i>	-Minimal impact on biomarker responses -Accumulation in the intestine	Karami et al. (2017)
-5 10 ⁶ of 1 and 5 µm of undisclosed composition fluorescent MPs -1.2 10 ⁶ of 10 and 20 µm fluorescent PE MPs	-1 µM B(a)P (252 µg/L) (sorbed pollutant)	-Malformations -Fluorescent imaging of B(a)P transfer by MPs to embryos	-B(a)P from spiked MPs did not induce morphological effects	Batel et al. (2018)
-400 mg/L of 200-250 µm plasticised PVC	-0.5 mg/L of phenanthrene -1 µg/L of EE2 (sorbed pollutant)	-Transcription levels of <i>cyp1a</i> , <i>vtg</i> and β - <i>actin</i>	-No increased bioavailability of spiked pollutants -No remarkable changes in gene transcription	Sleight et al. (2017)

NPs

Particle concentration and size	Co-contaminant	Endpoints	Effects	Reference
-10 mg/L of 25 nm PS NPs	-non	-Immune response of skins cells and the intestine -Transcription of immune response related genes (<i>illβ</i> , <i>tnfa</i> , <i>irg1l</i> , <i>socs3a</i> , <i>ccl20a</i>)	-Induction of pro-inflammatory responses in the skin and intestine cells -Accumulation of PS NPs in the intestine and in the cavity of the neuromast	Brun et al. (2018)
-1 mg/L of 50 nm fluorescent or non fluorescent NPs	-2 and 20 µg/L of EE2 (co-exposure)	-Locomotor system -Transcription levels of <i>gfap</i> , <i>α1-tubulin</i> , <i>zfrho</i> and <i>zfbblue</i> -CAT, GPx, GSH -AChE -Bioconcentration -Uptake of NPs	-Inhibition of larval locomotion -Presence of oxidative stress and neurotoxicity by NPs	Chen et al. (2017a)
-0.1, 1 and 10 mg/L of 50 nm fluorescent PS NPs	-non	-Mortality and malformations -Mitochondrial bioenergetics (oxygen consumption rate) -Heart rate -Uptake and distribution -Swimming behaviour	-No mortality and deformities -No changes in mitochondrial bioenergetics -Decrease of the heart rate -Swimming hypoactivity -NPs crossed the chorion of developing embryos	Pitt et al. (2018a)
-1 mg of 42 nm PS NPs/g fish injection	-non	-Survival and developmental delays in F1 embryos exposed cross-generationally -Heart rate -Oxidative stress biomarkers (CAT, GPx, GR, redox state and thiol levels) -Uptake and accumulation	-NPs maternally transferred to the offspring via accumulation in the eggs of exposed females -Bradycardia -Reduction of GR and thiols levels -No effects in locomotor activity	Pitt et al. (2018b)

-3 nL injection of 1% stock (30 ng) of 20 nm PS NPs	-non	-Hatching and survival rate -ROS production -Apoptosis	-Oxidative DNA damage in the brain -Brain apoptosis	Sökmen et al. (2020)
-10 and 100 mg/L of 44 nm PS NPs	-5073 ng/mL of an environmental PAH (36 PAHs) mixture from a sediment extract (sorbed pollutant)	-Malformation rate -PAH bioaccumulation -Mitochondrial bioenergetics -Heart rate -EROD activity	-Mitochondrial dysfunction by NPs and NPs combined with PAHs -Inhibition of cardiotoxicity and impaired brain vascularity by NP-PAH -Cardiotoxicity, bioaccumulation and impaired brain vasculature by PAHs alone	Trevisan et al. (2019)
-25 and 50 mg/L of 25 or 50 nm PS NPs -5 mg/L of 250 and 700 nm PS NPs	-non	-Malformation and mortality rate -Eye size	-Accumulation of PS NPs in intestine, epidermis and eye	van Pomeran et al. (2017)
GNMs				
NM concentration and type	Contaminant	Endpoints	Effects	Reference
-3.4, 7.6, 12.5, 25 and 50 mg/L of GO	-non	-Hatching and malformations -Cell death (apoptosis)	-Hatching delay -No apoptosis	Chen et al. (2012b)
-0.01, 0.1, 1, 10 and 100 mg/L of GO	-non	-Hatching and malformation rate -Locomotor activity -Heart rate -ROS production -Uptake and localisation -DNA methylation -Cell death (apoptosis)	-Hatching delay -Mobility reduction -ROS induction in eye, heart and tail. -Lipid peroxidation -Apoptosis in eye, heart and tail	Chen et al. (2016b)

-5, 10, 50 and 100 mg/L of GO	-non	<ul style="list-style-type: none"> -Malformation rate -Locomotor activity -Heart rate 	<ul style="list-style-type: none"> -Yolk sac edema and pericardial edema -Reduction of movement frequency -Decrease of heart beat rate 	d'Amora et al. (2017)
-0.01, 0.1 and 1 µg/L of GO	-non	<ul style="list-style-type: none"> -Hatching and malformation -Transcription levels of genes: <i>claudina</i>, <i>claudink</i>, <i>claudin5a</i> and <i>claudin5b</i> -Immunoperoxidase detection -Melatonin assay -AChE -ROS production and β-galactosidase levels -Metabolome -Uptake and localisation of GO 	<ul style="list-style-type: none"> -Significant downregulation of <i>claudin5a</i> -Translocation of GO to the brain -Decrease of AChE activity -Increase of β-galactosidase levels -Decreases in carbohydrate and fatty acid metabolism 	Hu et al. (2017)
40-80 mg/L of GO Nafion GO	-non	<ul style="list-style-type: none"> -Hatching, malformation and mortality rate -mRNA levels of immune system related genes: <i>HO-1</i>, <i>iNOS</i> and <i>β-actin2</i> 	<ul style="list-style-type: none"> -No sublethal effects or mortality -Increase of <i>HO-1</i> and <i>iNOS</i> mRNA levels 	Pecoraro et al. (2018)
-0.01, 0.1 and 1 µg/L of GO	-non	<ul style="list-style-type: none"> -Malformation and mortality rate -ROS production and β-galactosidase levels -Cell death (apoptosis) 	<ul style="list-style-type: none"> -GO translocation to the diencephalon, intestine and tail -Mitochondrial damage -Increase of β-galactosidase levels -Disturbance of locomotor activity -<i>Caspase 8</i>-associated apoptosis 	Ren et al. (2016)

-5, 10, 50 and 100 mg/L of GO	-non	<ul style="list-style-type: none"> -Hatching, malformation, length and mortality rate -Heart rate -Locomotor activity -Transcription levels of <i>gap43</i>, <i>gfap</i>, <i>nestin</i>, <i>neurogenin 1</i>, <i>dat</i> and <i>syn2</i> -AChE activity -Neuronal ultrastructure 	<ul style="list-style-type: none"> -Altered locomotion -Cardiac and dopaminergic alterations -Neuronal gene transcription and morphology modifications 	Soares et al. (2017)
-0.1 and 1 mg/L of GO	-50 and 500 µg/L of bisphenol A (co-exposure)	<ul style="list-style-type: none"> -Uptake and accumulation -Hatching and malformation rate -Bioaccumulation of bisphenol A -Transcription levels of endocrine disruption related genes estrogen receptor α -Biomarkers of endocrine disruption: estradiol, testosterone and vitellogenin levels 	<ul style="list-style-type: none"> -Significantly lower malformation rate of embryos co-exposed to GO and bisphenol A than in embryos exposed to bisphenol A alone -Less bioaccumulation of bisphenol A in embryos co-exposed to GO than in embryos exposed to bisphenol A alone -Alteration of biomarkers of endocrine disruption in co-exposed embryos alleviated in presence of GO 	Yang et al. (2019)
-0.001, 0.01, 0.1, 1, 10 and 100 mg/L of GO	-non	<ul style="list-style-type: none"> -Hatching, malformation and mortality rate -Heart rate -ROS generation -Skeletal and cardiac development 	<ul style="list-style-type: none"> -Increase of mortality and malformation -Protein carbonylation and excessive generation of ROS, especially superoxide radical 	Zhang et al. (2017b)
-1, 10 and 100 µg/L of GO	-non	<ul style="list-style-type: none"> -Malformation and mortality at 7 days post fertilisation -Protein abundance of cytoskeleton/muscle system -Mitochondrial function -GSH content and oxidoreductase activity -Cardiac muscle contraction and calcium handling 	<ul style="list-style-type: none"> -Increase of mortality and malformation rate -Downregulating proteins involved in actin filaments and the cytoskeleton (<i>krt8</i>, <i>vim</i> and <i>lmna</i>) -Induction of oxidative stress -Reduction of GSH content -Mitochondrial disorders 	Zou et al. (2018)

-1, 5, 10 and 50, 100 mg/L of GO and rGO	-non	-Hatching rate, larval length, mortality and malformations -Spontaneous movement -Heart rate	-Not effects on morphology, malformation or mortality -GO increased heart rate -rGO delayed hatching -rGO reduced larval length	Liu et al. (2014)
-25, 50 and 100 mg/L of quantum dots of rGO	-non	-Heart beat rate -Gene transcription levels of <i>βactin</i> , <i>cyp1a</i> , <i>cyp1c</i> and <i>cyp7a1</i>	-Reduction of heart beats -Significant upregulation of <i>cyp1a</i> and <i>cyp1c</i>	Zhang et al. (2017a)

AChE: acetylcholinesterase; *α1-tubulin*: alpha 1-tubulin; B(a)P: benzo(a)pyrene; *casp3a*: caspase 3; *casp9*: caspase 9 ; CAT: catalase; *ccl20a*: chemokine (C-C motif) ligand 20a; *cyp1a*: cytochrome P450 1a; *cyp1a1*: cytochrome P450 1a1; *cyp7a1*: cytochrome P450 7a1; *cyp1c*: cytochrome P450 1c; *dat*: dopamine transporter; EE2: 17 α-ethynylestradiol; EROD: 7-ethoxyresorufin O-deethylase; GO: graphene oxide; *gap43*: growth associated protein 43; *gfap*: glial fibrillary acidic protein; GPx: glutathione peroxidase; GR: glutathione reductase; GSH: glutathione; GST: glutathione S-transferase; *HO-1*: heme oxygenase 1 ; *il1β*: interleukin-1beta; *iNOS*: inducible nitric oxide synthase; *irg1l*: immunoresponsive gene 1, like; *krt8*: keratin 8 ; *lmna*: lamin A; PAHs: polycyclic aromatic hydrocarbons; PS: polystyrene; PVC: polyvinyl-chloride; rGO: reduced graphene oxide; ROS: reactive oxygen species; *socs3a*: suppressor of cytokine signaling 3a; SOD: superoxide dismutase; *syn2*: synapsin IIa; *tnf-α*: tumour necrosis factor-α; *vim*: vimentin; *vtg*: vitellogenin; *zblue*: opsin 1; *zrho*: rhodopsin.

3.2. Effects in adult organisms

Table 3 summarises the effects reported for MPs, NPs and GNMs to adult zebrafish. A common effect in zebrafish exposed to MPs, regardless their size, was digestive system alteration at molecular or tissue level (Jin et al., 2018; Lei et al., 2018; Qiao et al., 2019; Limonta et al., 2019; Zhao et al., 2020a; Gu et al., 2020). A considerable amount (0.001–10.0 mg/L) of different polymers (polyamide, PE, PVC, PP and PS) of the same size (70 µm) was used for exposure of adult zebrafish for 10 days. Differences in histopathology alterations among different polymers were not observed. Only a common induction of enterocyte damage was observed in exposed fish (Lei et al., 2018). 200 µm and 5 µm PS MPs caused dysfunction of intestinal immune cells and an increase of pathogenic bacteria appeared in zebrafish exposed for 21 days (Gu et al., 2020). 5 µm MPs size also led to a decrease of hepatic biochemical indicators (isocitrate dehydrogenase levels, α -ketoglutaric acid levels and *peroxisome proliferator activated receptor- γ*) that were translated in to a decrease in the body weight of fish exposed for 21 days (Zhao et al., 2020). In zebrafish exposed to 100 and 1000 µg/L of 0.5 and 50 µm PS MPs for 14 days, only small MPs caused a significant increase of protein levels (IL1 α , IL1 β and IFN), with a consequent dysbiosis and gut inflammation (Jin et al., 2018). Alteration of the transcription of genes related to immunity and metabolic pathways in the liver was reported in zebrafish exposed to a mixture of virgin high-density PE and PS (25-90 µm). In addition, loss of tissue integrity in gills and in the gastrointestinal tract and increase of fish activity during light photoperiod was observed (Limonta et al., 2019). Only one study reported clear signs of oxidative stress (increase of CAT and SOD activity) in zebrafish exposed for 21 days to 50 and 500 µg/L of 5 µm MPs (Qiao et al., 2019). Other oxidative stress biomarkers, such as diamine oxidase and D-lactate levels, decreased and increased, respectively, at both exposure concentrations in zebrafish. Also, inflammation and alteration of gut microbiome has been reported (Qiao et al., 2019).

Few studies assessed the potential Trojan horse effect produced by MPs or NPs in combination with POPs to adult zebrafish (Batel et al., 2016; Batel et al., 2018; Chen et al., 2017b; Rainieri et al., 2018). Potential transfer of a mix of polychlorinated biphenyls, polybrominated diphenyl ethers, polyfluorinated compounds and methylmercury (77.9 ng/g food) by 125-250 µm low-density PE MPs to zebrafish after 21 days of exposure was investigated to determine changes in the biotransformation metabolism of the liver and brain and in the normal histology of both organs. In summary, a significant upregulation of *cytochrome P4501A1 (cyp1a1)* in the brain of fish exposed to pollutants alone compared to co-exposed fish was reported, indicating the inhibition of the pollutant effects by MPs. On the contrary, an up-regulation of *peroxiredoxin 1*, *gstp1*, *neurogenin 1* and *cyp1a1* in the liver of co-exposed fish and of fish exposed to pollutants alone were reported compared to control ones. Also, the liver of fish co-exposed presented a

Introduction

greater vacuolisation than those exposed to MPs or to pollutants alone (220 ng/g) (Rainieri et al., 2018).

Zebrafish exposed to a combination of MPs of two sizes (1-5 µm and 10-20 µm) incubated in a B(a)P concentration of 252 µg/L did not show changes in liver EROD activity, suggesting that B(a)P associated to MPs was not able to exert its proven capacity to induce EROD activity (Batel et al., 2016). Nevertheless, exposure of adult zebrafish to PE MPs (10^6 particles/L) of two size ranges (1-5 µm and 10-20 µm) with sorbed B(a)P (252 µg/L) led to transport of B(a)P to the organism via the re-solution into the exposure media or via direct contact with the gills (Batel et al., 2018). After exposure to 50 nm NPs, the brain of zebrafish exposed to 1 mg/L for 1-3 days presented a reduction of AChE activity, while this effect was alleviated in the brain of zebrafish co-exposed to NPs and bisphenol A (1 µg/L). Bisphenol A combined with NPs worked as an inhibitor of both treatments toxicity alone to zebrafish since the bisphenol A alone produced the same reduction of AChE activity in exposed zebrafish. On the contrary, the co-exposure scenario provoked effects that were not reported for the exposure to NPs and bisphenol A alone, such as significantly upregulation of genes related to the central nervous system: *dopamine*, *α1-tubulin* and *manf* (Chen et al., 2017b).

As for zebrafish embryos, oxidative stress is a common effect in adult zebrafish exposed to GO (Chen et al., 2016a; Souza et al., 2017; Fernandes et al., 2018; Souza et al., 2019). Exposure for 48 h to 5 and 50 mg/L of graphene modulated the antioxidant system through an increase of GSH levels in the brain and intestine, and an increased GST activity in the intestine and gills of exposed fish. Tissues of fish exposed to graphene presented pathologies such as ganglionic proliferation, increased microglia and moderate oedema in brain, closely related to an immune response (Fernandes et al., 2018). 20 mg/L of GO induced CAT activity, SOD activity and lipid peroxidation, and reduced GPx activity in gills after 48 h of exposure (Souza et al., 2019). 10 and 20 mg/L of GO caused a significant increase of ROS production and apoptotic cells in gills of zebrafish exposed for 24 h. The oxidative stress resulted in necrosis of liver and gill, liver vacuolisation and gill aneurism, indicating the noticeable impact of GO at tissue level (Souza et al., 2017). Exposure to GO (1, 5 and 10 mg/L) produced a short-term response (1-4 days) of oxidative stress biomarkers with a reduction of GSH levels and induction of CAT and SOD activities. For all the tested concentrations, biomolecular response of immune system were increased and liver and intestine tissue presented a significant vacuolisation (Chen et al., 2016a). For low GO concentrations (0.01, 0.1, 1 µg/L), the previous reported oxidative stress in zebrafish was not observed, but internalisation of GO from water to the brain was detected with a downregulation of immune related genes (Hu et al., 2017).

Introduction

As for embryos, to the best of our knowledge, there are not studies addressing the potential Trojan horse effect produced by GNMs in adult zebrafish. Even for other CNMs, only one study was found in the literature (Park et al., 2010). Exposure to fullerenes (666 mg/L) combined with EE2 (1 µg/L) for 5 days reduced the bioavailability of EE2 to adult male zebrafish while the selected biomarker of endocrine disruption (upregulation of vitellogenin genes) were no longer high activated in the co-exposure scenario (Park et al., 2010).

Table 3- Summary of studies reporting effects of MPs, NPs and GNMs alone and with other organic pollutants in adult zebrafish.

MPs				
Particle concentration and size	Co-contaminant	Endpoints	Main effects	Reference
-500 µg/L of 5 µm and 200 µm PS MPs	-non	-Histopathological alterations -Cytokine analysis -Intestinal microbiota -Uptake and accumulation	-Dysfunction of intestinal immune cells -Increased abundance of pathogenic bacteria	Gu et al. (2020)
-100 and 1000 µg/L of 0.5 µm and 50 µm PS MPs	-non	-Mucus secretion -Gut microbiota -mRNA and protein levels of several cytokines in the gut (<i>IL1a</i> , <i>IL1b</i> and <i>IFN</i>)	-0.5 µm MPs increased mRNA levels of <i>IL1a</i> , <i>IL1b</i> and <i>IFN</i> -Dysbiosis and gut inflammation for both sizes	Jin et al. (2018)
-50 and 500 µg/L of 5 µm PS MPs	-non	-MP accumulation and histopathological alterations -CAT, SOD, diamine oxidase and D-lactate activities -Gut metabolome content and microbiome	-CAT and SOD induction -Increased D-lactate and reduced diamine oxidase levels -Induced inflammation and oxidative stress in the gut -Significant alterations in the metabolome and microbiome of the gut -Accumulation of MPs in the gut	Qiao et al. (2019)
-20 and 100 µg/L of 5 µm PS MPs	-non	-Body length and weight -Hepatic biochemical indicators (glucose, triglyceride, total cholesterol, α-ketoglutaric acid, pyruvate, and isocitrate dehydrogenase) -Hepatic transcriptome	-Decreased body weight -Decreased glucose, pyruvic acid, α-ketoglutaric acid, and isocitrate dehydrogenase activities	Zhao et al. (2020a)

-0.001, 0.01, 0.1, 1 and 10 mg/L of 70 µm PA, PE, PVC, PP and PS MPs	-non	-Histopathological alterations of the intestine	-Enterocyte damage -No differences among polymers	Lei et al. (2018)
-100 and 1000 µg/L of 25-90 µm of virgin high-density PE and PS mix	-non	-Behaviour -Liver transcriptome -Gill and gastrointestinal tract histopathology alterations	-Alteration of the transcription of genes related to immunity and metabolic pathways in the liver -Loss of tissue integrity in gills and gastrointestinal tract -Increased fish activity during light photoperiod	Limonta et al. (2019)
-1.2 10 ⁶ of 1 and 5 µm undisclosed composition MPs -1.2 10 ⁶ of 10 and 20 µm PE MPs	-1 µM B(a)P (252 µg/L) (sorbed pollutant)	-Uptake and transfer via diet of MPs spiked with B(a)P -EROD activity in liver	-No significant induction of EROD in liver -Higher transfer of B(a)P by small MPs	Batel et al. (2016)
-5 10 ⁶ of 1 and 5 µm undisclosed composition fluorescent MPs -1.2 10 ⁶ of 10 and 20 µm fluorescent PE MPs	-1 µM B(a)P (252 µg/L) (sorbed pollutant)	-EROD activity gills -Localisation of MPs	-CYP1A induction via exposure to B(a)P-spiked MPs in gill -Presence of MPs adhered between gill filaments	Batel et al. (2018)

-4% (8 mg/g food) of 125-250 µm low-density PE MPs -2% (4 mg/ g food) of 125-250 µm low-density PE MPs for co-exposure	-Mix of PCBs, PBDEs, PFCs and methylmercury: 77.9 ng/g food (co-exposure)	-Histopathological alterations -Bioaccumulation -Transcription levels of biotransformation metabolism related genes in liver and brain: <i>chrna1, cypl1a1, esr2, gstp1, ngn1</i> and <i>prdx1</i>	-Greater liver vacuolisation in fish co-exposed than in fish exposed to MPs or pollutants alone -Significant up-regulation of <i>prdx1, gstp1, chrna1, ngn1</i> and <i>cypl1a1</i> in liver of co-exposed and pollutant alone exposed fish -Significant up-regulation of <i>cypl1a1</i> in brain of fish exposed to pollutants alone than co-exposure	Rainieri et al. (2018)
---	---	--	---	------------------------

NPs

Particle concentration and size	Co-contaminant	Endpoints	Main effects	Reference
-1 mg/L of 50 nm PS NPs	-1 µg/L of bisphenol A (co-exposure)	-Transcription levels of <i>mbp</i> and <i>α1-tubulin</i> , and the mRNA expression of <i>manf</i> in the fish head -Dopamine content -AChE activity	-Co-exposure produced significant upregulation of <i>mbp, α1-tubulin</i> and <i>manf</i> -NPs inhibited AChE activity but not when co-exposed with bisphenol A	Chen et al. (2017b)
-500 µg/L of 100 nm PS NPs	-non	-Histopathological alterations -Cytokine quantification by enzyme-linked immunosorbent assay (ELISA) -Intestinal microbiota -Uptake and accumulation	-Higher effect of NPs than of MPs on secretory cells and on the transcription of genes related to phagocyte-produced ROS	Gu et al. (2020)
-1 mg of 42 nm PS NPs/g fish	-non	-Antioxidant enzymes -Mitochondrial function parameters -Uptake and accumulation	-No significantly effects on reproductive success -Reduced GR activity in brain, muscle, and testes -Not effects in mitochondrial function in heart or gonads	Pitt et al. (2018b)

-0.5 and 1.5 mg/L of 70 nm PS NPs	-non	-Oxidative stress -AChE activity in brain -Energetic metabolism	-Disturbance of lipid and energy metabolism -Increased ROS and decreased ATP levels in muscle -Decreased AChE, dopamine, melatonin, aminobutyric acid, serotonin, vasopressin, kisspeptin, and oxytocin levels	Sarasamma et al. (2020)
GNMs				
NM concentration and type	Co-contaminant	Endpoints	Main effects	Reference
-5 and 50 mg/L of graphene	-non	-Biochemical responses of glutamate cysteine ligase, GSH and GST in gills, intestine, muscle and brain - <i>gclc</i> and <i>nrf2</i> transcription levels -Histopathological alterations in gills, intestine, muscle and brain	-Increased GSH levels in the brain, and induced GST activity in the intestine and brain -Histopathological damage in brain and gills -Not increased transcription levels of related genes	Fernandes et al. (2018)
-1, 5, 10 and 50 mg/L of GO	-non	-Liver, gill and intestine histopathology -Oxidative stress in liver - <i>TNF-α</i> , <i>IL-1β</i> and <i>IL-6</i> mRNA levels in spleen	-Liver and intestine vacuolisation -Induced CAT and SOD activities and malondialdehyde levels in liver, and reduced the GSH levels -Immunotoxicity: increased transcription levels of <i>IL-1β</i> and <i>IL-6</i> in the spleen	Chen et al. (2016a)
-0.01, 0.1 and 1 μ g/L of GO	-non	-Immunoperoxidase detection in brain -Melatonin levels -AChE activity -ROS production - <i>claudina</i> , <i>claudink</i> , <i>claudin5a</i> and <i>claudin5b</i> transcription levels	-Significant downregulation of <i>claudin5a</i> -Translocation of GO to the brain.	Hu et al. (2017)

-2, 10 and 20 mg/L of GO	-non	-ROS generation -Cell death (apoptosis) -Histopathological alteration of gills and liver	-Increased ROS generation -Gill cells apoptosis -Aneurism and necrosis of gill tissue -Vacuolisation and necrosis of liver tissue	Souza et al. (2017)
-2, 10 and 20 mg/L of GO	-non	-Oxidative stress in gills (SOD, CAT, GPx) -Lipid peroxidation (TBAR production)	-Induced CAT and SOD activities, and reduced GPx activity -2 mg/L of GO produced increase in lipid peroxidation	Souza et al. (2019)

AChE: acetylcholinesterase; *α1-tubulin*: *alpha 1-tubulin*; B(a)P: benzo(a)pyrene; CAT: catalase; *chrna1*: *cholinergic receptor nicotinic alpha 1*; *cyp1a1*: *cytochrome P450 1a1*; EROD: 7-ethoxyresorufin O-deethylase; *esr2*: *estrogen receptor-beta*; *gclc*: *glutamate cysteine ligase catalytic subunit*; GO: graphene oxide; GPx: glutathione peroxidase; GR: glutathione reductase; GSH: glutathione; GST: glutathione S-transferase; *gstp1*: *glutathione S-transferase pi 1*; *IL-1β*: *interleukin-1beta*; *IL-6*: *Interleukin 6*; *IFN*: *interferón*; *manf*: *mesencephalic astrocyte-derived neurotrophic factor*; *mbp*: *myelin basic protein*; *ngn1*: *neurogenin 1*; *nrf2*: *nuclear transcription factor [erythroid-derived 2]-like 2*; PA: polyamide; PBDEs: polybrominated diphenyl ethers; PCBs: polychlorinated biphenyls; PE: polyethylene; PFCs: perfluorinated compounds; PP: polypropylene; *prdx1*: *peroxiredoxin 1*; PS: polystyrene; PVC: polyvinyl-chloride; ROS: reactive oxygen species; SOD: superoxide dismutase; *TNF-α*: *tumor necrosis factor-α*.

REFERENCES

1. Andrady, A.L., 2011. Microplastics in the marine environment. *Mar. Pollut. Bull.* 62, 1596-1605.
2. Antunes, J.C., Frias, J.G.L., Micaelo, A.C., Sobras, P., 2013. Resin pellets from beaches of the Portuguese coast and adsorbed persistent organic pollutants. *Estuar. Coast. Shelf Sci.* 130, 62-69.
3. Apul, O.G., Wang, Q., Zhou, Y., Karanfil, T., 2013. Adsorption of aromatic organic contaminants by graphene nanosheets: Comparison with carbon nanotubes and activated carbon. *Water Res.* 47, 1648-1654.
4. Arthur, C., Baker, J., Bamford, H., (Eds.) 2009. Proceedings of the international research workshop on the occurrence, effects and fate of microplastic marine debris, Sept 9–11, 2008. NOAA technical memorandum NOS-OR&R-30.
5. Ašmonaitė, G., Larsson, K., Undeland, I., Sturve, J., Carney Almroth, B., 2018. Size matters: ingestion of relatively large microplastics contaminated with environmental pollutants posed little risk for fish health and fillet quality. *Environ. Sci. Technol.* 52, 14381-14391.
6. Azizi-Lalabadi, M., Hashemi, H., Feng, J., Jafari, S.M., 2020. Carbon nanomaterials against pathogens; the antimicrobial activity of carbon nanotubes, graphene/graphene oxide, fullerenes, and their nanocomposites. *Adv. Colloid Interfaces Sci.* 284, 102250.
7. Bakir, A., Rowland, S.J., Thompson, R.C., 2014. Enhanced desorption of persistent organic pollutants from microplastics under simulated physiological conditions. *Environ. Pollut.* 185, 16-23.
8. Barnes, D. K. A., Galgani, F., Thompson, R. C., Barlaz, M., 2009. Accumulation and fragmentation of plastic debris in global environments. *Philos. Trans. Royal Soc. B* 364, 1985-1998.
9. Batel, A., Borchert, F., Reinwald, H., Erdinger, L., Braunbeck, T., 2018. Microplastic accumulation patterns and transfer of benzo[a]pyrene to adult zebrafish (*Danio rerio*) gills and zebrafish embryos. *Environ. Pollut.* 235, 918-930.
10. Batel, A., Linti, F., Scherer, M., Erdinger, L., Braunbeck, T., 2016. Transfer of benzo[a]pyrene from microplastics to *Artemia* nauplii and further to zebrafish via a trophic food web experiment: CYP1A induction and visual tracking of persistent organic pollutants. *Environ. Toxicol. Chem.* 35, 1656-1666.
11. Bellasi, A., Binda, G., Pozzi, A., Galafassi, S., Volta, P., Bettinetti, R., 2020. Microplastic contamination in freshwater environments: a review, focusing on interactions with sediments and benthic organisms. *Environments* 7, 30.
12. Bessling, E., Quik, J.T.K., Sun, M., Koelmans, A.A., 2017. Fate of nano- and microplastic in freshwater systems: A modelling study. *Environ. Pollut.* 220, 540-548.
13. Bergami, E., Bocci, E., Vannuccini, M.L., Monopoli, M., Salvati, A., Dawson, K.A., Corsi, I., 2016. Nano-sized polystyrene affects feeding, behaviour and physiology of brine shrimp *Artemia Franciscana* larvae. *Ecotoxicol. Environ. Saf.* 123, 18-25.
14. Bessling, E., Wang, B., Lüring, M., Koelmans, A.A., 2014. Nanoplastic affects growth of *S. obliquus* and reproduction of *D. magna*. *Environ. Sci. Technol.* 48, 12336-12343.
15. Bhagat, J., Zang, L., Nishimura, N., Shimada, Y., 2020. Zebrafish: An emerging model to study microplastic and nanoplastics toxicity. *Sci. Total Environ.* 728, 138707.
16. Bhattacharya, P., Lin, S., Turner, J.P., Ke, P.C., 2010. Physical adsorption of charged plastic nanoparticles affects algal photosynthesis. *J. Phys. Chem. C* 114, 16556-16561.

Introduction

17. Botterell, Z.L.R., Beaumont, N., Dorrington, T., Steinke, M., Thompson, R.C., Lindeque, P.K., 2019. Bioavailability and effects of microplastics on marine zooplankton: A review. *Environ. Pollut.* 245, 98-110.
18. Boucher, J., Friot, D., 2017. Primary microplastics in the oceans: a global evaluation of sources. In: Lundin, C.G., de Sousa, J.M., (Eds.), IUCN, Gland, Switzerland, pp. 1-43.
19. Bratovčić, A., Odošajić, S., Čatić, I., Šestan, 2015. Application of polymer nanocomposite materials in food packaging, *Croat. J. Food Sci. Technol.* 7, 86-94.
20. Browne, M.A., Crump, P., Niven, S.J., Teuten, E., Tonkin, A., Galloway, T., Thompson, R., 2011. Accumulation of microplastic on shorelines worldwide: sources and sinks. *Environ. Sci. Technol.* 45, 9175-9179.
21. Brun, N.R., Koch, B.E.V., Varela, M., Peijnenburg, W.J.G.M., Spink, H.P., Vijver, M.G., 2018. Nanoparticles induce dermal and intestinal innate immune system responses in zebrafish embryos. *Environ. Sci. Nano* 5, 904.
22. Burns, E.E., Boxall, A.B.A., 2018. Microplastic in the aquatic environment: evidence for or against adverse impacts and major knowledge gaps. *Environ. Toxicol. Chem.* 37, 2776-2796.
23. Buzea, C., Pacheco, I.I., Robbie, K., 2007. Nanomaterials and nanoparticles: sources and toxicity. *Biointerphases* 2, MR17-71.
24. Carbery, M., O'Connor, W., Thavamani, P., 2018. Trophic transfer of microplastics mixture and mixed contaminants in the marine food web and implications for human health. *Environ. Int.* 115, 400-409.
25. Chen, L., Hernandez, Y., Feng, X., Müllen, K., 2012a. From nanographene and graphene nanoribbons to graphene sheets: chemical synthesis. *Angew. Chem. Int. Ed.* 51, 7640-7654.
26. Chen, L., Hu, P., Zhang, L., Huang, S., Luo, L., Huang, C., 2012b. Toxicity of graphene oxide and multi-walled carbon nanotubes against human cells and zebrafish. *Sci. China Chem.* 55, 2209-2216.
27. Chen, M., Yin, J., Liang, Y., Yuan, S., Wang, F., Song, M., Wang, H., 2016a. Oxidative stress and immunotoxicity induced by graphene oxide in zebrafish. *Aquat. Toxicol.* 174, 54-60.
28. Chen, Q.Q., Gundlach, M., Yang, S.Y., Jiang, J., Velki, M., Yin, D.Q., Hollert, H., 2017a. Quantitative investigation of the mechanisms of microplastics and nanoplastics toward zebrafish larvae locomotor activity. *Sci. Total Environ.* 584, 1022-1031.
29. Chen, Y., Hu, X., Sun, J., Zhou, Q., 2016b. Specific nanotoxicity of graphene oxide during zebrafish embryogenesis. *Nanotoxicology* 10, 42-52.
30. Ciriminna, R., Zhang, N., Yang, M., Meneguzzo, F., Xu, Y., Pagliaro, M., 2016. Commercialization of graphene-based technologies: a critical insight. *Chem. Comm.* 51, 7090-7095.
31. Cole, M., Lindeque, P., Fileman, E., Halsband, C., Goodhead, R., Moger, J., Galloway, T.S., 2013. Microplastic ingestion by zooplankton. *Environ. Sci. Technol.* 47, 6646-6655.
32. Compa, M., March, D., Deudero, S., 2019. Spatio-temporal monitoring of coastal floating marine debris in the Balearic Islands from sea-cleaning boats. *Mar. Pollut. Bull.* 141, 205-214.
33. Cormier, B., Batel, A., Cachot, J., Bégout, M.-L., Braunbeck, T., Cousin, X., Keiter, S.H., 2019. Multi-laboratory hazard assessment of contaminated microplastic particles by means of enhanced fish embryo test with the zebrafish (*Danio rerio*). *Front. Environ. Sci.* 7, 135.

34. Costa, M.F., Ivar do Sul, J.A., Silva-Cavalcanti J.S., Araújo, M.C.B, Spengler, A., Tourinho, P.S., 2010. On the importance of size of plastic fragments and pellets on the strandline: a snapshot of a Brazilian beach. *Environ. Monit. Assess.* 168, 299-304.
35. Cousin, X., Batel A., Bringer, A., Hess, S., Bégout, M., Braunbeck, T., 2020. Microplastics and sorbed contaminants – Trophic exposure in fish sensitive early life stages. *Mar. Environ. Res.* 161, 105126.
36. D' Amora, M., Camisasca, A., Lettieri, S., Giordani, S., 2017. Toxicity assessment of carbon nanomaterials in zebrafish during development. *Nanomaterials* 7, 414.
37. Dang, Z-M., Zheng, M-S., Zha, J-W., 2016. 1D/2D carbon nanomaterial-polymer dielectric composites with high permittivity for power energy storage applications. *Small* 12, 1688-1701.
38. Dasmahapatra, A.K., Dasari, T.P.S., Tchounwou, P.B., 2019. Graphene-based nanomaterials toxicity in fish. *Rev. Environ. Contam. Toxicol.* 247, 1-58.
39. Della Torre, C., Parolini, M., Del Giacco, L., Ghilardi, A., Ascagni, M., Santo, N., Maggioni, D., Magni, S., Madaschi, L., Prosperi, L., La Porta, C., Binelli, A., 2017. Adsorption of B(a)P on carbon nanopowder affects accumulation and toxicity in zebrafish (*Danio rerio*) embryos. *Environ. Sci. Nano.* 4, 1132-1146.
40. De Marchi, L., Pretti, C., Gabriel, B., Marques, P.A.A.P., Freitas, R., Neto, V., 2018. An overview of graphene materials: Properties, applications and toxicity on aquatic environments. *Sci. Total Environ.* 631-632, 1440-1456.
41. De Sales-Ribeiro, C., Brito-Casillas, Y., Fernández, A., Caballero, M.J., 2020. An end to the controversy over the microscopic detection and effects of pristine microplastics in fish organs. *Sci. Rep.* 10, 12434.
42. Driedger, A.G.J., Dürr, H.H., Mitchell, K., Van Cappellen, P., 2015. Plastic debris in the Laurentian Great Lakes: A review. *J. Great Lake R.* 41, 9.19.
43. Duis, K., Coors, A., 2016. Microplastic in the aquatic and terrestrial environment: sources (with a specific focus on personal care products), fate and effects. *Environ. Sci. Eur.* 28, 2.
44. Efimova, I., Bagaeva, M., Bagaev, A., Kileso, A., Chubarenko, I.P., 2018. Secondary microplastics generation in the sea swash zone with coarse bottom sediments: laboratory experiments. *Front. Mar. Sci.* 5, 313.
45. Elizalde-Velázquez, A., Carcano, A.M., Crago, J., Green, M.J., Shah, S.A., Cañas-Carell, J.E., 2020. Translocation, trophic transfer, accumulation and depuration of polystyrene microplastics in *Daphnia magna* and *Pimephales promelas*. *Environ. Pollut.* 259, 113937.
46. Enfrin, M., Lee, J., Gibert, Y., Basheer, F., Kong, L., Dumée, L.F., 2020. Release of hazardous nanoplastic contaminants due to microplastics fragmentation under shear stress forces. *J. Hazard. Mater.* 384, 121393.
47. Eriksen, M., Lebreton, L.C.M., Carson, H.S., Thiel, M., Moore, C.J., Borerro, J.C., Galgani, F., Ryan, P.G., Reisser, J., 2014. Plastic pollution in the world's oceans: more than 5 trillion plastic pieces weighing over 250,000 tons afloat at sea. *PLoS ONE* 9, e111913.
48. Erni-Cassola, G., Zadjelovic, V., Gibson, M.I., Christie-Oleza, J.A., 2019. Distribution of plastic polymer types in the marine environment; A meta-analysis. *J. Hazard. Mat.* 369, 691-698.
49. EU COM, Commission Recommendation of 18 October 2011 on the definition of nanomaterial Text with EEA relevance OJ L 275, 20.10.2011, p. 38–40 (EN). (<http://data.europa.eu/eli/reco/2011/696/oj>) (accessed Oct 12, 2020)

Introduction

50. Everaert, G., Van Cauwenberghe, L., De Rijcke, M., Koelmans, A.A., Mees, J., Vandegehuchte, M., Janssen, C.R., 2018. Risk assessment of microplastics in the ocean: Modelling approach and first conclusions. *Environ. Pollut.* 242, 1930-1938.
51. Falconer, J.L., Jones, C.F., Lu, S., Grainger, D.W., 2015. Carbon nanomaterials rescue phenanthrene toxicity in zebrafish embryo cultures. *Environ. Sci. Nano* 2, 645-652.
52. Farrell, P., Nelson, K., 2013. Trophic level transfer of microplastic: *Mytilus edulis* (L.) to *Carcinus maenas* (L.) *Environ. Pollut.* 177, 1-3.
53. Fernandes, A.L., Nascimento, J.P., Santos, A.P., Furtado, C.A., Romano, L.A., Eduardo da Rosa, C., Monserrat, J.M., Ventura-Lima, J., 2018. Assessment of the effects of graphene exposure in *Danio rerio*: A molecular, biochemical and histological approach to investigating mechanisms of toxicity. *Chemosphere* 210, 458-466.
54. Frias, J.P.G.L., Otero, V., Sobral, P., 2014. Evidence of microplastics in samples of zooplankton from Portuguese coastal waters. *Mar. Environ. Res.* 95, 89-95.
55. Geppert, M., Sigg, L., Schirmer, K., 2016. A novel two-compartment barrier model for investigating nanoparticle transport in fish intestinal epithelial cells. *Environ. Sci. Nano* 3, 388-395.
56. Gollavelli, G., Ling, Y.C., 2012. Multi-functional graphene as an *in vitro* and *in vivo* imaging probe. *Biomaterials* 33, 2532-2545.
57. Good, K.D., Bergman, L.E., Klara, S.S., Leitch, M.E., VanBriesen, J.M., 2016. Implication of engineered nanomaterials in drinking water sources. *J. Am. Water Works Assoc.* 108, E1-E17.
58. Goodwin, D.G., Adeleye, A.S., Sung, L., Ho, K.T., Burgess, R.M., Petersen, E.J., 2018. Detection and quantification of graphene-family nanomaterials in the environment. *Environ. Sci. Technol.* 52, 4491-4513.
59. Gouin, T., Avalos, J., Brunning, I., Brzuska, K., de Graaf, J., Kaumanns, J., Koning, T., Meyberg, M., Rettinger, K., Schlatter, H., Thomas, J., van Welie, R., Wolf, T., 2015. Use of micro-plastic beads in cosmetic products in Europe and their estimated emission to the North Sea environment. *SOFW-Journal* 141, 3-2015.
60. Gregory, M.R., 2009. Environmental implications of plastic debris in marine settings entanglement, ingestion, smothering, hangers-on, hitchhiking and alien invasions. *Philos. Trans. R. Soc. B: Biol. Sci.* 364, 2013-2025.
61. Grigorakis, S., Mason, S.A., Drouillard, K.G., 2017. Determination of the gut retention of plastic microbeads and microfibers in goldfish (*Carassius auratus*). *Chemosphere* 169, 233-238.
62. Gu, W., Liu, S., Chen, L., Liu, Y., Gu, C., Ren, H.Q., Wu, B., 2020. Single-cell RNA sequencing reveals size-dependent effects of polystyrene microplastics on immune and secretory cell populations from zebrafish intestines. *Environ. Sci. Technol.* 54, 3417-3427.
63. Gurunathan, S., Woong Han, J., Abdal Daye, A., Eppakayala, V., Kim, J., 2012. Oxidative stress-mediated antibacterial activity of graphene oxide and reduced graphene oxide in *Pseudomonas aeruginosa*. *Int. J. Nanomed.* 7, 5901-5914.
64. Guo, X., Mei, N., 2014. Assessment of the toxic potential of graphene family nanomaterials. *J. Food Drug Anal.* 22, 105-115.
65. Haque, E., Nurunnabi, M., Liongue, C. Ward, A.C., 2019. Chapter 10: Biocompatibility assessment of nanomaterials using zebra fish as a model. In: Nurunnabi, M., McCarthy, J. (Eds.), *Micro and Nano Technologies, Biomedical Applications of Graphene and 2D Nanomaterials*, Elsevier, Amsterdam, pp. 217-234.

66. Hartmann, N.B., Hüffer, T., Thompson, R.C., Hassellöv, M., Verschoor, A., Daugaard, A.E., Rist, S., Karlsson, T., Brennholt, N., Cole, M., Herrling, M.P., Hess, M.C., Ivelva, N.P., Lusher, A.L., Magner, W. 2019. Are we speaking the same language? Recommendations for a definition and categorization framework for plastic debris. *Environ. Sci. Technol.* 53, 1039-1047.
67. Hernandez, L.M., Yousefi, N., Tufenkji, N., 2017. Are there nanoplastics in your personal care products? *Environ. Sci. Technol. Lett.* 4, 280-285.
68. Horton, A.A., Walton, A., Spurgeon, D.J., Lahive, E., Svendsen, C., 2017. Microplastics in freshwater and terrestrial environments: Evaluating the current understanding to identify the knowledge gaps and future research priorities. *Sci. Total Environ.* 586, 127-141.
69. Howe, K., Clark, M.D., Torroja, C.F., Torrance, J., Berthelot, C., Muffato, M., Collins, J.E., Humphray, S., McLaren, K., et al., 2013. The zebrafish reference genome sequence and its relationship to the human genome. *Nature* 496, 498-503.
70. Hu, X., Ouyang, S., Mu, L., An, J., Zhou, Q., 2015. Effects of graphene oxide and oxidized carbon nanotubes on the cellular division, microstructure, uptake, oxidative stress, and metabolic profiles. *Environ. Sci. Technol.* 49, 10825-10833.
71. Hu, X., Wei, Z., Mu, L., 2017. Graphene oxide nanosheets at trace concentrations elicit neurotoxicity in the offspring of zebrafish. *Carbon* 117, 182-191.
72. Hu, W., Peng, C., Luo, W., Li, X., Li, D., Huang, Q., Fan, C., 2010. Graphene-based antibacterial paper. *ACS Nano* 4, 4317-23.
73. Hüffer T., Hofmann T., 2016. Sorption of non-polar organic compounds by micro-sized plastic particles in aqueous solution. *Environ. Pollut.* 214, 194-201.
74. Hüffer, T., Praetorius, A., Wagner, S., von der Kammer, F., Hofmann, T., 2017. Microplastic exposure assessment in aquatic environments: learning from similarities and differences to engineered nanoparticles. *Environ. Sci. Technol.* 51, 2499-2507.
75. Jabeen, K., Su, L., Li, J., Yang, D., Tong, C., Mu, J., Shi, H., 2017. Microplastics and mesoplastics in fish from coastal and fresh waters of China. *Environ. Pollut.* 221, 141-149.
76. Jambeck, J.R., Geyer, R., Wilcox, C., Siegler, T.R., Perryman, M., Andrady, A., Narayan, R., Law, K.L., 2015. Plastic waste inputs from land into the ocean. *Science* 347, 768-771.
77. Jastrzębska, A.M., Kurtyez, P., Olszyna, A.R., 2012. Recent advances in graphene family materials toxicity investigations. *J. Nanopart. Res.* 14, 1320.
78. Jiménez-Lamana, J., Marigliano, L., Allouche, J., Grassl, B., Szpunar, J., Reynaud, S., 2020. A novel strategy for the detection and quantification of nanoplastics by single particle inductively coupled plasma mass spectrometry (ICP-MS). *Anal. Chem.* 92, 11664-11672.
79. Ji, L., Chen, W., Xu, Z., Zheng, S., Zhu, D., 2013. Graphene nanosheets and graphite oxide as promising adsorbents for removal of organic contaminants from aqueous solution. *J. Environ. Qual.* 42, 191-198.
80. Jin, Y., Xia, J., Pan, Z., Yang, J., Wang, W., Fu, Z., 2018. Polystyrene microplastics induce microbiota dysbiosis and inflammation in the gut of adult zebrafish. *Environ. Pollut.* 235, 322-329.
81. Johari, S.A., Rasmussen, K., Gulumian, M., Ghazi-Khansari, M., Tetarazako, N., Kashiwada, S., Asghari, S., Park, J-W., Yu, I.J., 2018. Introducing a new standardized nanomaterial environmental toxicity screening testing procedure, ISO/TS 20787: aquatic toxicity assessment of manufactured nanomaterials in saltwater Lakes using *Artemia sp. nauplii*. *Toxicol. Mech. Methods* 29, 95-109.

Introduction

82. Jovanović, B., 2017. Ingestion of microplastics by fish and its potential consequences from a physical perspective. *Integr. Environ. Assess. Manag.* 13, 510-515.
83. Jovanović, B., Gökda, K., Güven, O., Emre, Y. & Whitley, E. M., 2018. Virgin microplastics are not causing imminent harm to fish after dietary exposure. *Mar. Pollut. Bull.* 130, 123-131.
84. Karami, A, Groman, D.B., Wilson, S.P., Ismail, P., Neela, V.K., 2017. Biomarker responses in zebrafish (*Danio rerio*) larvae exposed to pristine low-density polyethylene fragments. *Environ. Pollut.* 223, 466-475.
85. Karkanorachaki, K., Kiparissis, S., Kalogerakis, G.C., Yiantzi, E., Psillakis, E., Kalogerakis, N., 2018. Plastic pellets, meso- and microplastics on the coastline of Northern Crete: Distribution and organic pollution. *Mar. Pollut. Bull.* 133, 578-589.
86. Katsumiti, A., Tomovska, R., Cajaraville, M.P., 2017. Intracellular localization and toxicity of graphene oxide and reduced graphene oxide nanoplatelets to mussel hemocytes *in vitro*. *Aquat. Toxicol.* 188, 138-147.
87. Kawecki, D., Nowack, B., 2020. A proxy-based approach to predict spatially resolved emissions of macro and microplastic to the environment. *Sci. Total Environ.* 748, 141137.
88. Kim, D., Chae, Y., An, Y.J., 2017. Mixture toxicity of nickel and microplastics with different functional groups on *Daphnia magna*. *Environ. Sci. Technol.* 51, 12852-12858.
89. Koelmans, A.A., Besseling, E., Foekema, E.M., 2014. Leaching of plastic additives to marine organisms. *Environ. Pollut.* 187, 49-54.
90. Koelmans, A.A., Besseling, E., Shim, W.J., 2015. Nanoplastics in the aquatic environment. In: Bergmann, M., Gutow, L., Klages, M. (Eds.), *Marine Anthropogenic Litter*. Springer, Berlin, pp. 329-344.
91. Koelmans, A.A., Kooi, M., Law, K.L., van Sebille, E., 2017. All is not lost: deriving a top-down mass budget of plastic at sea. *Environ. Res. Lett.* 12, 114028.
92. Kong, W., Kum, H., Bae, S., Shim, J., Kim, H., Kong, L., Meng, Y., Wang, K., Kim, C., Kim, J., 2019. Path towards graphene commercialization from lab to market. *Nat. Nanotechnol.* 14, 927-938.
93. Kunhikrishnan, A., Shon, H.K., Bolan, N.S., El Saliby, I., Vigneswaran, S., 2015. Sources, distribution, environmental fate, and ecological effects of nanomaterials in wastewater streams. *Crit. Rev. Environ. Sci. Technol.* 45, 277-318.
94. Lammel, T., Navas, J.M., 2014. Graphene nanoplatelets spontaneously translocate into the cytosol and physically interact with cellular organelles in the fish cell line PLHC-1. *Aquat. Toxicol.* 150, 55-65.
95. Lebreton, L.C.M., van der Zwet, J., Damsteeg, J., Slat, B., Andrady, A., Riesser, J., 2017. River plastic emissions to the world's oceans. *Nat. Commun.* 8, 15611.
96. Lei, L., Wu, S., Lu, S., Liu, M., Song, Y., Fu, Z., Shi, H., Raley-Susman, K.M., He, D., 2018. Microplastic particles cause intestinal damage and other adverse effects in zebrafish *Danio rerio* and nematode *Caenorhabditis elegans*. *Sci. Total Environ.* 619-620, 1-8.
97. Leslie, H.A., Brandsma, S.H., van Velzen, M.J.M., Vethaak, A.D., 2017. Microplastics en route: Field measurements in the Dutch river delta and Amsterdam canals, wastewater treatment plants, North Sea sediments and biota. *Environ. Int.* 101, 133-142.
98. Li, C., Busquets, R., Campos, L.C., 2020. Assessment of microplastics in freshwater systems: A review. *Sci. Total Environ.* 707, 135578.
99. Li, F., Chen, J., Hu, X., He, F., Bean, E., Tsang, D.C.W., Ok, Y.S., Gao, B., 2020b. Applications of carbonaceous adsorbents in the remediation of polycyclic aromatic hydrocarbon-contaminated sediments: A review. *J. Clean. Prod.* 255, 120263.

100. Libralato, G., 2014. The case of *Artemia spp.* in nanoecotoxicology. *Mar. Environ. Res.* 101, 38-43.
101. Limonta, G., Mancina, A., Benkhalqui, A., Bertolucci, C., Abelli, L., Fossi, M.C., Panti, C., 2019. Microplastics induce transcriptional changes, immune response and behavioural alterations in adult zebrafish. *Sci. Rep.* 9, 15775.
102. Linard, E.N., Apul, O.G., Karanfil, T., van den Hurk, P., Klaine, S.J., 2017. Bioavailability carbon nanomaterial-adsorbed polycyclic aromatic hydrocarbons to *Pimephales promelas*: influence of adsorbate molecular size and configuration. *Environ. Sci. Technol.* 51, 9288-9296.
103. Liu, S., Chevali, V.S., Xu, Z., Hui, D., Wang, H., 2018. A review of extending performance of epoxy resin using carbon nanomaterials. *Compos. Part B-Eng.* 136, 197-214.
104. Liu, X.T., Mu, X.Y., Wu, X.L., Meng, L.X., Guan, W.B., Ma, Y.Q., Sun, H., Wang, C.J., Li, X.F., 2014. Toxicity of multi-walled carbon nanotubes, graphene oxide, and reduced graphene oxide to zebrafish embryos. *Biomed. Environ. Sci.* 27, 676-683.
105. Lu, L., Wang, J., Chen, B., 2018. Adsorption and desorption of phthalic acid esters on graphene oxide and reduced graphene oxide as affected by humic acid. *Environ. Pollut.* 232, 505-513.
106. Lu, Y., Zhang, Y., Deng, Y., Jiang, W., Zhao, Y., Geng, J., Ding, L., Ren, H., 2016. Uptake and accumulation of polystyrene microplastics in zebrafish (*Danio rerio*) and toxic effects in liver. *Environ. Sci. Technol.* 50, 4054-4060.
107. Luis, L.G., Ferreira, P., Fonte, E., Oliveira, M., Guilhermino, L., 2015. Does the presence of microplastics influence the acute toxicity of chromium(VI) to early juveniles of the common goby (*Pomatoschistus microps*)? A study with juveniles from two wild estuarine populations. *Aquat. Toxicol.* 164, 163-174.
108. Lv, X., Yang, Y., Tao, Y., Jiang, Y., Chen, B., Zhu, X., Cai, Z., Li, B., 2018. A mechanism study of toxicity of graphene oxide to *Daphnia magna*: direct link between bioaccumulation and oxidative stress. *Environ. Pollut.* 234, 953-959.
109. Ma, Y., Huang, A., Cao, S., Sun, F., Wang, L., Guo, H., Ji, R., 2016. Effects of nanoplastics and microplastics on toxicity, bioaccumulation, and environmental fate of phenanthrene in fresh water. *Environ. Pollut.* 219, 166-173.
110. Mak, C.W., Yeung, K.C-F., Chan, K.M., 2019. Acute toxicity of polyethylene microplastic on adult zebrafish. *Ecotoxicol. Environ. Saf.* 182, 109442.
111. Ma, S., Lin, D., 2013. The biophysicochemical interactions at the interfaces between nanoparticles and aquatic organisms: adsorption and internalization. *Environ. Sci. Process. Impacts* 15, 145-160.
112. Ma, Y., Huang, A., Cao, S., Sun, F., Wang, L., Guo, H., Ji, R., 2016. Effects of nanoplastics and microplastics on toxicity, bioaccumulation, and environmental fate of phenanthrene in fresh water. *Environ. Pollut.* 219, 166-173.
113. Mani, T., Hauk, A., Walter, U., Burkhardt-Holm, P., 2015. Microplastics profile along the Rhine River. *Sci. Rep.* 5, 17988.
114. Mato, Y., Isobe, T., Takada, H., Kanehiro, H., Ohtake, C., Kaminuma, T., 2001. Plastic resin pellets as a transport medium for toxic chemicals in the marine environment. *Environ. Sci. Technol.* 35, 318-324.
115. Mattsson, K., Hansson, L.A., Cedervall, T., 2015. Nano-plastics in the aquatic environment. *Environ. Sci. Process. Impacts* 17, 1712-1721.
116. Mauter, M.S., Elimelech, M., 2008. Environmental applications of carbon-based nanomaterials. *Environ. Sci. Technol.* 42, 5843-5859.

Introduction

117. McNeish, R.E., Kim, L.H., Barrett, H.A., Mason, S.A., Kelly, J.J., Hoellein, T.J., 2018. Microplastic in riverine fish is connected to species traits. *Sci. Rep.* 8, 11639.
118. Mesarič, T., Gambardella, C., Milivojević, T., Faimali, M., Drobne, D., Falugi, C., Makovec, D., Jemec, A., Sepčić, K., 2015. High surface adsorption properties of carbon-based nanomaterials are responsible for mortality swimming inhibition and biochemical responses in *Artemia salina* larvae. *Aquat. Toxicol.* 163, 121-9.
119. Minghetti, M., Drieschner, C., Bramaz, N., Schug, H., Schirmer, K., 2017. A fish intestinal epithelial barrier model established from the rainbow trout (*Oncorhynchus mykiss*) cell line, RTgutGC. *Cell. Biol. Toxicol.* 33, 539-555.
120. Montagner, A., Bosi, S., Tenori, E., Bidussi, M., Alshatwi, A.A., Tretiach, M., Prato, M., Syrgiannis, Z., 2017. Ecotoxicological effects of graphene-based materials. *2D Mater.* 4, 012001.
121. Murphy, F., Ewins, C., Carbonnier, F., Quinn, B., 2016. Wastewater treatment works (WwTW) as a source of microplastics in the aquatic environment. *Environ. Sci. Technol.* 50, 5800-5808.
122. Niu, Z., Liu, L., Zhang, L., Chen, X., 2014. Porous graphene materials for water remediation. *Small* 17, 3434-3441.
123. Novoselov, K.S., Geim, A.K., Morozov, S.V., Jiang, D., Zhang, Y., Dubonos, S.V., Grigorieva, I.V., Firsov, A.A., 2004. Electric field effect in atomically thin carbon films. *Science* 306, 666-669.
124. OECD TG236. 2013. OECD guidelines for the testing of chemicals. Section 2: Effects on biotic systems Test No. 236: Fish embryo acute toxicity (FET) test. Organization for Economic Cooperation and Development, Paris, France, 22 pp.
125. Oliveira, M., Ribeiro, A., Hylland, K., Gulhermino, L., 2013. Single and combined effects of microplastics and pyrene on juveniles (0+ group) of the common goby *Pomatoschistus microps* (Teleostei, Gobiidae). *Ecol. Indic.* 34, 641-647.
126. Parenti, C.C., Ghilardi, A., Della Torre, C., Magni, S., Del Giacco, L., Binelli, A., 2019. Evaluation of the infiltration of polystyrene nanobeads in zebrafish embryo tissues after short-term exposure and the related biochemical and behavioural effects. *Environ. Pollut.* 254, 112947.
127. Park, J.W., Henry, T.B., Meen, F.M., Compton, R.N., Sayler, G.S., 2010. No bioavailability of 17 α -ethinylestradiol when associated with nC60 aggregates during dietary exposure in adult male zebrafish (*Danio rerio*). *Chemosphere* 81, 1227-1232.
128. Park, J.W., Henry, T.B., Ard, S., Menn, F.M., Compton, R.N., Sayler, G.S., 2011. The association between nC(60) and 17 alpha-ethinylestradiol (EE2) decreases EE2 bioavailability in zebrafish and alters nanoaggregate characteristics. *Nanotoxicology* 5, 406-416.
129. Paul-Pont, I., Lacroix, C., Gonzalez, C.F., Hégaret, H., Lambert, C., Le Goïc, N., Frère, L., Cassone, A-L., Sussarellu, R., Fabioux, C., Guyomarch, J., Albentosa, M., Huvet, A., Soudant, P., 2016. Exposure of marine mussels *Mytilus* spp. to polystyrene microplastics: Toxicity and influence on fluoranthene bioaccumulation. *Environ. Pollut.* 216, 724-737.
130. Pecoraro, R., D'Angelo, D., Filice, S., Scalese, S., Capparucci, F., Marino, F., Iaria, C., Guerriero, G., Tibullo, D., Scalisi, E.M., Salvaggio, A., Nicotera, I., Brundo, M.V., 2018. Toxicity evaluation of graphene oxide and titania loaded nafion membranes in zebrafish. *Front. Physiol.* 8, 1039.
131. Pei, Z., Li, L., Sun, L., Zhang, S., Shan, X., Yang, S., Wen, B., 2013. Adsorption characteristics of 1,2,4-trichlorobenzene, 2,4,6-trichlorophenol, 2-naphthol and naphthalene on graphene and graphene oxide. *Carbon* 51, 156-163.

132. Peixoto, D., Amorim, J., Pinheiro, C., Oliva-Teles, L., Varó, I., Rocha, R.M., Vieira, M.N., 2019. Uptake and effects of different concentrations of spherical polymer microplastics on *Artemia franciscana*. *Ecotoxicol. Environ. Saf.* 176, 211-218.
133. Pitt, J.A., Kozal, J.S., Jayasundara, N., Massarsky, A., Trevisan, R., Geitner, N., Wiesner, M., Levin, E.D., Di Giulio, R.T. 2018a. Uptake, tissue distribution, and toxicity of polystyrene nanoparticles in developing zebrafish (*Danio rerio*). *Aquat. Toxicol.* 194, 185-194
134. Pitt, J.A., Trevisan, R., Massarsky, A., Kozal, J.S., Levin, E.D., Di Giulio, R.T., 2018b. Maternal transfer of nanoplastics to offspring in zebrafish (*Danio rerio*): A case study with nanopolystyrene. *Sci. Total Environ.* 643, 324-334.
135. Plastics Europe. Plastics – the Facts 2019: An analysis of European plastics production, demand and waste data. Plastics Europe, 2019 (<https://www.plasticseurope.org/en/resources/publications/1804-plastics-facts-2019>) (accessed Jan 14, 2020).
136. Prata, J.C., da Costa, J.P., Lopes, I., Duarte, A.C., Rocha-Santos, T., 2019. Effects of microplastics on microalgae populations: A critical review. *Sci. Total Environ.* 665, 400-405.
137. Pretti, C., Oliva, M., Di Pietro, R., Monni, G., Cevasco, G., Chiellini, F., Pomelli, C., Chiappe, C., 2014. Ecotoxicity of pristine graphene to marine organisms *Ecotoxicol. Environ. Saf.* 101, 138-45.
138. Putri, A.D., Murti, B.T., Sabela, M., Kanchi, S. and Bisetty, K., 2017. Nanopolymer chitosan in cancer and Alzheimer biomedical application. In: Ahmed, S., Ikram, S., (Eds.), Chitosan: Derivatives, composites and applications. Scrivener Publishing LLC, Beverly, pp. 311-359.
139. Qiang, L., Cheng, J., 2019. Exposure to microplastics decreases swimming competence in larval zebrafish (*Danio rerio*). *Ecotoxicol. Environ. Saf.* 176, 226-233.
140. Qiao, R., Sheng, C., Lu, Y., Zhang, Y., Ren, H., Lemos, B., 2019. Microplastics induce intestinal inflammation, oxidative stress, and disorders of metabolome and microbiome in zebrafish. *Sci. Total. Environ.* 662, 246-253.
141. Rajabi, S., Ramazani, A., Hamidi, M., Naji, T., 2015. *Artemia salina* as a model organism in toxicity assessment of nanoparticles. *DARU J. Pharm. Sci.* 23, 20.
142. Ren, C., Hu, X., Li, X., Zhou, Q., 2016. Ultra-trace graphene oxide in a water environment triggers Parkinson's disease-like symptoms and metabolic disturbance in zebrafish larvae. *Biomaterials* 93, 83-94.
143. Rainieri, S., Conlledo, N., Larse, B.K., Granby, K., Barranco, A., 2018. Combined effects of microplastics and chemical contaminants on the organ toxicity of zebrafish (*Danio rerio*). *Environ. Res.* 162, 135-143.
144. Rezania, S., Park, J., Md Din, M.F., Taib, S.M., Talaiekhosani, A., Yadav, K.Y., Kamyab, H., 2018. Microplastic pollution in different aquatic environments and biota: A review of recent studies. *Mar. Pollut. Bull.* 133, 191-208.
145. Rochman, C.M., Tahir, A., Williams, S.L., Baxa, D.V., Lam, R., Miller, J.T., Teh, F., Werorilangi, S., Teh, S.J., 2015. Anthropogenic debris in seafood: Plastic debris and fibres from textiles in fish and bivalves sold for human consumption. *Sci. Rep.* 5, 14340.
146. Rodriguez-Hernandez, A.G., Chiodoni, A., Bocchini, S., Vazquez-Duhalt, R., 2020. 3D printer waste, a new source of nanoplastic pollutants. *Environ. Pollut.* 267, 115609.
147. Romano, N., Renukdas, N., Fischer, H., Shrivastava, J., Baruah, K., Egnew, N., Sinha, A.K., 2020. Differential modulation of oxidative stress, antioxidant defence, histomorphology, ion-regulation and growth marker gene expression in goldfish

Introduction

- (*Carassius auratus*) following exposure to different dose of virgin microplastics. *Comp. Biochem. Physiol.* 238C, 108862.
148. Rosenkranz, P., Chaudhry, Q., Stone, V., Fernandez, T.F., 2009. A comparison of nanoparticle and fine particle uptake by *Daphnia magna*. *Environ. Toxicol. Chem.* 28, 2142-2149.
 149. Saley, A.M., Smart, A.C., Bezerra, M.F., Brunham, T.L.U., Capece, L.R., Lima, L.F.O., Carsh, A.C., Williams, S.L., Morgan, S.G., 2019. Microplastic accumulation and biomagnification in a coastal marine reserve situated in a sparsely populated area. *Mar. Pollut. Bull.* 146, 54-59.
 150. Santhosh, C., Velmurugan, V., Jacob, G., Jeong, S.K., Grace, A.N., Bhatnagar, A., 2016. Role of nanomaterials in water treatment applications: A review. *Chem. Eng. J.* 306, 1116-1137.
 151. Sarasamma, S., Audira, G., Siregar, P., Malhotra, N., Lai, Y.-H., Liang, S.-T., Chen, J.-R., Chen, K.H.-C., Hsiao, C.-D., 2020. Nanoplastics cause neurobehavioral impairments, reproductive and oxidative damages, and biomarker responses in zebrafish: throwing up alarms of wide spread health risk of exposure. *Int. J. Mol. Sci.* 21, 1410.
 152. Schirmer, K., 2014. Chapter 6: Mechanisms of nanotoxicity. In: Lead, J.R., Valsami-Jones, E. (Eds.), *Frontiers of Nanoscience: Nanoscience and the Environment*, Elsevier, Amsterdam, 195-221.
 153. Schwaferts, C., Sogne, V., Welz, R., Meier, F., Klein, T., Niessner, R., Elsner, M., Ivleva, N.P., 2020. Nanoplastic analysis by online coupling of Raman microscopy and field-flow fractionation enabled by optical tweezers. *Anal. Chem.* 92, 5813-5820.
 154. Schwarz, A.E., Ligthart, T.N., Boukris, E., van Harmelen, T., 2019. Sources, transport, and accumulation of different types of plastic litter in aquatic environments: A review study. *Mar. Pollut. Bull.* 143, 92-100.
 155. Seabra, A.B., Paula, A.J., de Lima, R., Alves, O.L., Durán, N., 2014. Nanotoxicity of graphene and graphene oxide. *Chem. Res. Toxicol.* 27, 159-168.
 156. Sendra, M., Sparaventi, E., Blasco, J., Moreno-Garrido, I., Araujo, C.V.M., 2020. Ingestion and bioaccumulation of polystyrene nanoplastics and their effects on the microalgal feeding of *Artemia franciscana*. *Ecotoxicol. Environ. Saf.* 268, 115769.
 157. Shen, M., Zhang, Y., Zhu, Y., Song, B., Zeng, G., Hu, D., Wen, X., Ren, Z., 2019. Recent advances in toxicological research of nanoplastics in the environment: A review. *Environ. Pollut.* 252, 511-521.
 158. Siegfried, M., Koelmans, A.A., Besseling, E., Kroeze, C., 2017. Export of microplastics from land to sea. A modelling approach. *Water Res.* 127, 249-257.
 159. Sleight, V.A., Bakir, A., Thompson, R.C., Henry, T.B., 2017. Assessment of micropalstic-sorbed contaminant bioavailability through analysis of biomarker gene expression in larval zebrafish. *Mar. Pollut. Bull.* 116, 291-297.
 160. Smith, S.C., Rodrigues, D.F., 2015. Carbon-based nanomaterials for removal of chemical and biological contaminants from water: A review of mechanisms and applications. *Carbon* 91, 122-143.
 161. Soares, J., Pereira, T., Costa, K., Maraschin, T., Basso, N., Bogo, M., 2017. Developmental neurotoxic effects of graphene oxide exposure in zebrafish larvae (*Danio rerio*). *Colloids Surf. B: Biointerfaces* 157, 335-346.
 162. Sökmen, T.Ö., Sulukan, E., Türkoğlu, M., Baran, A., Özkaraca, M., Ceyhun, S.B.J.N., 2020. Polystyrene nanoplastics (20 nm) are able to bioaccumulate and cause oxidative DNA damages in the brain tissue of zebrafish embryo (*Danio rerio*). *Neurotoxicology* 77, 51-59.

163. Souza, J.P., Baretta, J.F., Santos, F., Paino, I.M.M., Zucolotto, V., 2017. Toxicological effects of graphene oxide on adult zebrafish (*Danio rerio*). *Aquat. Toxicol.* 186, 11-18.
164. Souza, J.P., Mansano, A.S., Venturini, F.P., Santos, F., Zucolotto, V., 2019. Antioxidant metabolism of zebrafish after sub-lethal exposure to graphene oxide and recovery. *Fish. Physiol. Biochem.* 45, 1289-1297.
165. Stephens, B., Azimi, P., El Orch, Z., Ramos, T., 2013. Ultrafine particle emissions from desktop 3D printers. *Atmos. Environ.* 79, 334-339.
166. Streisinger, G., Walker, C., Dower, N., Knauber, D., Singer, F., 1981. Production of clones of homozygous diploid zebra fish (*Brachydanio rerio*). *Nature* 291, 293-296.
167. Su, Y., Yan, X., Pu, Y., Xiao, F., Wang, D., Yang, M., 2013. Risks of single-walled carbon nanotubes acting as contaminants-carriers: potential release of phenanthrene in Japanese Medaka (*Oryzias latipes*). *Environ. Sci. Technol.* 47, 4704-4710.
168. Suman, T.Y., Jia, P-P., Li, W-G., Junaid, M., Xin, G-Y., Wang, Y., Pei, D-S., 2020. Acute and chronic effects of polystyrene microplastics on brine shrimp: First evidence highlighting the molecular through transcriptome analysis. *J. Hazard. Mater.* 400, 12322.
169. Sun, T.Y., Gottschalk, F., Hungerbühler, K., Nowack, B., 2014. Comprehensive probabilistic modelling of environmental emissions of engineered nanomaterials. *Environ. Pollut.* 185, 69-76.
170. Talsness, C.E., Andrade, A.J.M., Kuriyama, S.N., Taylor, J.A., vom Saal, F. S., 2009. Components of plastic: Experimental studies in animals and relevance for human health. *Philos. Trans. R. Soc. B* 364, 2079-2096.
171. Ter Halle, A., Jeanneau, L., Martignac, M., Jarde, E., Pedrono, B., Brach, L., Gigault, J., 2017. Nanoplastic in the North Atlantic Subtropical Gyre. *Environ. Sci. Technol.* 51, 13689-13697.
172. Teuten, E.L., Rowland, S.J., Galloway, T.S., Thompson, R.C., 2007. Potential for plastics to transport hydrophobic contaminants. *Environ. Sci. Technol.* 41, 7759-7764.
173. Thompson, R.C., Olsen, Y., Mitchell, R.P., Davis, A., Rowland, S.J., John, A.W. G., McGonigle, D., Russell, A.E., 2004. Lost at sea: where is all the plastic? *Science*, 304, 838.
174. Tiwari, S.K., Sahoo, S., Wang, N., Huczko, A., 2020. Graphene research and their outputs: Status and prospect. *J. Sci. Adv. Mater. Dev.* 5, 10-29.
175. Trevisan, R., Voy, C., Chen, S., Di Giulio, R.T., 2019. Nanoplastics decrease the toxicity of a complex PAH mixture but impair mitochondrial energy production in developing zebrafish. *Environ. Sci. Technol.* 53, 8405-8415.
176. Van, A., Rochman, C.M., Flores, E.M., Hill, K.L., Vargas, E., Vargas, S.A., Hoh, E., 2012. Persistent organic pollutants in plastic marine debris found on beaches in San Diego, California. *Chemosphere* 86, 258-263.
177. van Pomeren, M., Brun, N.R., Peijnenburg, W.J.G.M., Vijver, M.G., 2017. Exploring uptake and biodistribution of polystyrene (nano)particles in zebrafish embryos at different developmental stages. *Aquat. Ecotoxicol.* 190, 40-45.
178. van Wezel, A., Caris, I., Kools, S.A.E, 2016. Release of primary microplastics from consumer products to wastewater in the Netherlands. *Environ. Toxicol. Chem.* 35, 1627-1631.
179. Varó, I., Perini, A., Torreblanca, A., Garcia, Y., Begami, E., Vannuccini, M.L., Corsi, I., 2019. Time-dependent effects of polystyrene nanoparticles in brine shrimp *Artemia franciscana* at physiological, biochemical and molecular levels. *Sci. Total Environ.* 675, 570-580.

Introduction

180. Wan, Z., Wang, C., Zhou, J., Shen, M., Wang, X., Fu, Z., Jin, Y., 2019. Effects of polystyrene microplastics on the composition of the microbiome and metabolism in larval zebrafish. *Chemosphere* 217, 646-658.
181. Wang, H., Liang, X., Wang, J., Jiao, S., Xue, D., 2020a. Multifunctional inorganic nanomaterials for energy applications. *Nanoscale* 12, 14-42.
182. Wang, J., Chen, Z., Chen, B., 2014. Adsorption of polycyclic aromatic hydrocarbons by graphene and graphene oxide nanosheets. *Environ. Sci. Technol.* 48, 4817-4825.
183. Wang, J., Liu, X., Liu, G., Zhang, Z., Wu, H., Cui, B., Bai, J., Zhang, W., 2019a. Size effect of polystyrene microplastics on sorption of phenanthrene and nitrobenzene. *Ecotoxicol. Environ. Saf.* 173, 331-338.
184. Wang, S., Zhang, C., Pan, Z., Sun, D., Zhou, A., Xie, S., Wang, J., Zou, J., 2020b. Microplastics in wild freshwater fish of different feeding habits from Beijiang and Pearl River Delta regions, south China. *Chemosphere* 258, 127345.
185. Wang, W., Wang, J., 2018b. Different partition of polycyclic aromatic hydrocarbons on environmental particulates in freshwater: Microplastics in comparison to natural sediment. *Ecotoxicol. Environ. Saf.* 147, 648-655.
186. Wang, Y., Zhang, D., Zhang, M., Jingli, M., Ding, G., Mao, Z., Cao, Y., Jin, F., Cong, Y., Wang, L., Zhang, W., Wang, J., 2019b. Effects of ingested polystyrene microplastics on brine shrimp, *Artemia parthenogenetica*. *Environ. Pollut.* 244, 514-722.
187. Wang, Y., Zheng, M., Zhang, M., Ding, G., Sun, J., Du, M., Liu, Q., Cong, Y., Jin, F., Zhang, W., Wang J., 2019c. The uptake and elimination of polystyrene microplastics by the brine shrimp, *Artemia parthenogenetica*, and its impact on its feeding behaviour and intestinal histology. *Chemosphere* 234, 123-131.
188. Wang, Z., Zhao, J., Song, L., Mashayekhi, H., Chefetz, B., Xing, B., 2011. Adsorption and desorption of phenanthrene on carbon nanotubes in simulated gastrointestinal fluids. *Environ. Sci. Technol.* 45, 6018-6024.
189. Werkenh, A.A., Rene, E.R., 2019. Applications of nanotechnology and biotechnology for sustainable water and wastewater treatment. In: Bui, X.T., Chiemchaisri, C., Fujioka, T., Varjani, S. (Eds.), *Water and Wastewater Treatment Technologies. Energy, Environment, and Sustainability*. Springer, Singapore, pp. 405-430.
190. Werner, S., Budziak, A., van Franeker, J., Galgani, F., Hanke, G., Maes, T., Matiddi, M., Nilsson, P., Oosterbaan, L., Priestland, E., Thompson, R., Veiga, J. and Vlachogianni, T., 2016. Harm caused by marine litter. MSFD GES TG Marine Litter - Thematic Report; JRC Technical report; EUR 28317 EN.
191. Wirnkor, V.A., Ebere, E.C., Ngozi, V.E., Oharley, N.K., 2019. Microplastic-toxic chemical interaction: a review study on quantified levels, mechanism and implication. *SN Appl. Sci.* 1, 1400.
192. Wu, W., Jiang, C., Roy, V.A.L., 2015. Recent progress in magnetic iron oxide–semiconductor composite nanomaterials as promising photocatalysts. *Nanoscale* 7, 38-58
193. Wu, W., Jiang, W., Zhang, W., Lin, D., Yang, K., 2013. Influence of functional groups on desorption of organic compounds from carbon nanotubes into water: insight into desorption hysteresis. *Environ. Sci. Technol.* 47, 8373-8382.
194. Yan, Q., Gozin, M., Zhao, F., Cohen, A., Pang, S., 2016. Highly energetic compositions based on functionalized carbon nanomaterials. *Nanoscale* 8, 4799-4851.
195. Yang, B., Zhang, M., Lu, Z., Luo, J.J., Song, S., Zhang, Q., 2018. From Poly(*p*-phenylene terephthalamide) broken paper: high-performance aramid nanofibers and their

- application in electrical insulating nanomaterials with enhanced properties. *ACS Sustainable Chem. Eng.* 6, 8954-8963.
196. Yang, K., Wang, J., Chen, B., 2014. Facile fabrication of stable monolayer and few-layer graphene nanosheets as superior sorbents for persistent aromatic pollutant management in water. *J. Mater. Chem.* 2, 18219.
 197. Yang, K., Xing, B., 2010. Adsorption of organic compounds by carbon nanomaterials in aqueous phase: Polanyi theory and its application. *Chem. Rev.* 110, 5989-6008.
 198. Yang, J., Zhong, W., Chen, P., Zhang, Y., Sun, B., Liu, M., Zhu, Y., Zhu, L., 2019. Graphene oxide mitigates endocrine disruption effects of bisphenol A on zebrafish at an early development stage. *Sci. Total Environ.* 697, 134158.
 199. Younis, S.A., Maitlo, H.A., Lee, J., Kim, K-H., 2020. Nanotechnology-based sorption and membrane technologies for the treatment of petroleum-based pollutants in natural ecosystems and wastewater streams. *Adv. Colloid Interface Sci.* 275, 102701.
 200. Yu, P., Liu, Z., Wu, D., Chen, M., Lv, W., Zhao, Y., 2018. Accumulation of polystyrene microplastics in juvenile *Eriocheir sinensis* and oxidative stress effects in the liver. *Aquat. Toxicol.* 200, 28-36.
 201. Zhang, H., Kuo, Y.-Y., Gerecke, A.C., Wang, J., 2012. Co-release of hexabromocyclododecane (HBCD) and nano-and microparticles from thermal cutting of polystyrene foams. *Environ. Sci. Technol.* 46, 10990-10996.
 202. Zhang, J.-H., Sun, T., Niu, A., Tang, Y.-M., Deng, S., Luo, W., Xu, Q., Wei, D., Pei, D.-S., 2017a. Perturbation effect of reduced graphene oxide quantum dots (rGOQDs) on aryl hydrocarbon receptor (AhR) pathway in zebrafish. *Biomaterials* 133, 49-59.
 203. Zhang, X., Zhou, Q., Zou, W., Hu, X., 2017b. Molecular mechanisms of developmental toxicity induced by graphene oxide at predicted environmental concentrations. *Environ. Sci. Technol.* 51, 7861-7871.
 204. Zhao, Y., Bao, Z., Wan, Z., Fu, Z., Yuanxiang, J., 2020a. Polystyrene microplastic exposure disturbs hepatic glycolipid metabolism at the physiological, biochemical, and transcriptomic levels in adult zebrafish. *Sci. Total Environ.* 710, 136279.
 205. Zhao, J., Lin, M., Wang, Z., Cao, X., Xing, B., 2020b. Engineered nanomaterials in the environment: Are they safe? *Crit. Rev. Environ. Sci. Technol.*
 206. Zhu, S., Luo, F., Chen, W., Zhu, B., Wang, G., 2017. Toxicity evaluation of graphene oxide on cysts and three larval stages of *Artemia salina*. *Sci. Total Environ.* 595, 101-109.
 207. Ziccardi, L.M., Edgington, A., Hentz, K., Kulacki, K.J., Kane, D.S., 2016. Microplastics as vectors for bioaccumulation of hydrophobic organic chemicals in the marine environment: a state-of-the-science review. *Environ. Toxicol. Chem.* 35, 1667-1676.
 208. Zindler, F., Glomstad, B., Altin, D., Liu, J., Jenssen, B.M., Booth, A.M., 2016. Phenanthrene bioavailability and toxicity to *Daphnia magna* in the presence of carbon nanotubes with different physicochemical properties. *Environ. Sci. Technol.* 50, 12446-12454.
 209. Zou, W., Zhou, Q., Zhang, X., Mu, L., Hu, X., 2018. Characterization of the effects of trace concentrations of graphene oxide on zebrafish larvae through proteomic and standard methods. *Ecotoxicol. Environ. Saf.* 159, 221-231.
 210. Zuo, L-Z., Li, H-X., Lin, L., Sun, Y-X., Diao, Z-H., Liu, S., Zhang, Z-Y., Xu, X-R., 2019. Sorption and desorption of phenanthrene on biodegradable poly(butylene adipate co-terephthalate) microplastics. *Chemosphere* 215, 25-32.

STATE OF THE ART, HYPOTHESIS AND OBJECTIVES

STATE OF THE ART

The noticeable increase in the entrance of micro- and nanomaterials (NMs) in the environment due to their use in consumer products and industrial applications forecast a threat for the aquatic ecosystems. The size of these materials and their capacity to sorb pollutants due to their higher surface to volume ratio than that of larger materials make them available for a wide range of organisms and a potential source of toxicity. The small materials are able to cross biological barriers and internalise and spread in the organism's body. Once these materials arrive to the aquatic ecosystems, they can modulate the bioavailability and further toxicity for aquatic organisms of other pollutants already present in the water column (especially hydrophobic organic pollutants). The lack of consensus about the role and toxicity of micro- and NMs as vectors of pollutants requires further studies. Several aspects must be taken into account: (I) the type of interaction between sorbate pollutant and sorbent material, (II) the magnitude of the sorption phenomenon, (III) the uptake and accumulation of the micro and NMs alone and in combination with pollutants and (IV) the modulation of toxicity upon micro and NMs in combination with pollutants.

Polycyclic aromatic hydrocarbons (PAHs) are hydrophobic organic pollutants known for their carcinogenic potential to living organisms. PAHs are widely present in the aquatic ecosystems derived principally from industrial activities, and accidental releases, such as oil spills. NMs are used in remediation of water pollution (oil spills, removal of pollutants arriving to WWTPs), activity that could be a relevant source of NMs contaminated with PAHs to the aquatic ecosystems.

In order to gain knowledge in the previously mentioned aspects, brine shrimp as a salt water organism commonly used for toxicity assessment of pollutants, and zebrafish, as a model organism, widely used in toxicology are considered as suitable test organisms. Acute toxicity evaluation in developmental stage of brine shrimp and zebrafish help to assess and to rank the toxicity of micro and NMs alone and in combination with PAHs, toxicity experiments with developing organisms give fast and relevant responses. The complexity of this phenomena makes necessary to select markers of exposure to confirm the successful transfer of PAHs by micro and NMs to the organism. The use of markers of the induction of biotransformation metabolism can be useful to elucidate the role of micro- and NMs as carriers of PAHs that are pollutant well known to be metabolised efficiently by the biotransformation metabolism of aquatic organisms. Also, markers of toxicity at molecular and biochemical level are required such as oxidative stress and cell cycle regulation. As a more complex effect, the different potential alterations in the tissue of organs help to understand impact at long term, such as in gills (as most exposed organ to pollutants present in the water column) and in liver a well-known organ of xenobiotic detoxification.

State of the art, hypothesis and objectives

The data that will be obtained from the previously mentioned analyses will provide useful information for environmental risk assessment of these upcoming micro and NMs in the market that will end up in the aquatic ecosystems.

HYPOTESIS

Micro- and nanomaterials sorb persistent organic pollutants, including polycyclic aromatic hydrocarbons, being able to act as carriers (Trojan horse effect) for aquatic species, such as crustaceans and fish, and potentially modulate their availability and toxicity. The sorption capacity of micro- and nanomaterials is determined by the size and surface properties of the materials and the chemical nature of the pollutants.

OBJECTIVES

In order to prove this hypothesis true, the following specific objectives were addressed:







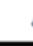


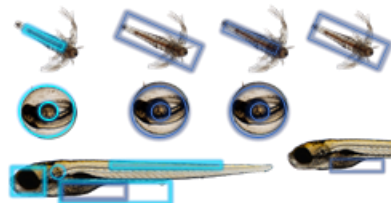
1. To assess the developmental toxicity of “pristine” polystyrene (PS) plastic particles of different sizes (50 nm, 0.5 μm and 4.5 μm) and of dissolved benzo(a)pyrene (B(a)P) on brine shrimp larvae and zebrafish embryos.
2. To assess the toxicity of microplastics (MPs) (0.5 and 4.5 μm) with sorbed B(a)P; and the availability of nanoplastics (NPs) and MPs with sorbed B(a)P to brine shrimp larvae and zebrafish embryos.
3. To assess the sorption capacity of two different sized PS MPs (4.5 and 0.5 μm) for a model pyrolytic polycyclic aromatic hydrocarbon (PAH) of high molecular weight such as B(a)P.
4. To assess the sorption capacity of 4.5 μm PS MPs for PAHs present in the water accommodated fraction (WAF) of a naphthenic North Sea (NNS) crude oil, as an environmentally relevant mixture of petrogenic PAHs of low molecular weight.
5. To assess the sublethal toxicity of 50 nm PS NPs and 4.5 μm PS MPs alone and with sorbed B(a)P, as a model pyrolytic PAH, or with sorbed petrogenic PAHs from an environmentally relevant mixture such as the WAF of a NNS crude oil.
6. To assess the potential transfer and bioaccumulation of PAH from 4.5 μm PS MPs to adult zebrafish.
7. To assess the sorption capacity of graphene oxide nanomaterials (GO NMs) for a model pyrolytic PAH such as B(a)P and for an environmentally relevant mixture of petrogenic PAHs from the WAF of a NNS crude oil.
8. To assess the uptake and potential acute toxicity of GO NMs alone or in combination with PAHs to zebrafish embryos.

State of the art, hypothesis and objectives

9. To evaluate the sublethal toxicity of GO alone and in combination with PAHs to adult zebrafish.

RESULTS AND DISCUSSION

CHAPTER 1. Screening of the toxicity of polystyrene nano- and microplastics alone and in combination with polycyclic aromatic hydrocarbons using alternative methods (brine shrimp larvae and zebrafish embryos)

		size						
		+				-		
		4.5 μ m	0.5 μ m	50 nm	50 nm	4.5 μ m	0.5 μ m	B(a)P
		MPs	MPs	NPs	FL-NPs	MPs-B(a)P	MPs-B(a)P	B(a)P
								
	Toxicity	✗	✗	✗	✗	✗	✓	✓
	Ingestion	✓	?		✓	✓	✓	✓
	Toxicity	✗	✗	✗	✗	✓	✗	✓
	Ingestion	?	?		✓	✓	✓	✓
	Localisation							

ABBREVIATIONS

B(a)P, Benzo(a)pyrene

CAT, Catalase

DMSO, Dimethylsulfoxide

EC₅₀, Effective concentration 50

EE2, 17 α -ethynylestradiol

EROD, 7-ethoxyresorufin O-deethylase activity

GC/MS, Gas chromatography and mass spectrometry

GSH, Glutathione

hpf, Hours post fertilisation

hph, Hours post hatch

LC₅₀, Lethal concentration 50

MPs, Microplastics

NPs, Nanoplastics

PAHs, Polycyclic aromatic hydrocarbons

PCBs, Polychlorinated biphenyls

PE, Polyethylene

PET, Polyethylene terephthalate

POPs, Persistent organic pollutants

PP, Polypropylene

PS, Polystyrene

PUR, Polyurethane

PVC, Polyvinyl chloride

SPME, Solid phase microextraction

ABSTRACT

The presence of nano- (NPs) and microplastics (MPs) in aquatic ecosystems and the effects that these particles can cause to wildlife is nowadays an issue of great concern. Moreover, their capacity to sorb hydrophobic pollutants represents an additional threat to aquatic organisms. Polycyclic aromatic hydrocarbons (PAHs) are persistent and toxic compounds for aquatic organisms that can readily sorb to plastic particles due to their chemical nature. Thus, NPs and MPs could bind PAHs at higher concentrations than those found dissolved in the water column and act as carriers into organisms (Trojan horse effect). This study aims to assess the potential bioavailability and acute toxicity of NPs and of MPs alone and with sorbed benzo(a)pyrene (B(a)P), as a model pyrolytic PAH. The embryo/larval stages of two organisms, brine shrimps and zebrafish, were used to screen toxicity as alternative animal models to the use of adult organisms. Spherical polystyrene (PS) particles of 50 nm, 0.5 μm and 4.5 μm at a concentration ranging from 0 to 50.1 mg/L were employed. To prepare contaminated MPs, particles were incubated for 24 h in 0.1 mg/L of B(a)P and filtered. Exposure to pristine plastics did not cause any significant impact on brine shrimp survival, while some treatments of MPs with sorbed B(a)P and all tested concentrations of B(a)P alone (0.1-10 mg/L) resulted acutely toxic. For zebrafish embryos, 4.5 μm MPs with sorbed B(a)P and B(a)P alone resulted the most toxic treatments, provoking a significant increase of embryo malformation at 50.1 mg MP/L and 5 and 10 mg B(a)P/L, respectively. Ingestion of NPs was observed by 24-48 hours of exposure in the two tested organisms at concentration from 0.069 mg/L to 6.87 mg/L. In brine shrimps, NPs were observed over the body surface and within the digestive tract, associated with faeces. In zebrafish, NPs were localised in the eyes, yolk sac and tail at 72 hours post fertilisation (hpf), showing their capacity to translocate and spread into the zebrafish embryo body, potentially hampering its development. MP ingestion was only demonstrated for 4.5 μm particles in brine shrimp. MP ingestion was not observed in zebrafish embryos, but when exposed to both sizes of MPs-B(a)P, B(a)P was capable to pass through the chorion and appeared in the yolk sac of the embryo. Noticeable presence of B(a)P was also observed in brine shrimp larvae exposed to 0.5 μm MPs-B(a)P. In conclusion, 4.5 μm and 0.5 μm PS MPs were successful vectors of B(a)P to brine shrimp and zebrafish embryos and the MP size played a significant role in explaining the toxicity of MPs with sorbed B(a)P. Once ingestion has been demonstrated, studies at other levels, such as long term analysis and consequences at physiological or behavioural level, are required.

Key words: polystyrene nanoplastics and microplastics, benzo(a)pyrene, zebrafish embryos, brine shrimp larvae, Trojan horse effect.

INTRODUCTION

Presence of nano- (NPs) and microplastics (MPs) in aquatic ecosystems is reported worldwide (Avio et al., 2017), even in remote places such as Antarctic marine system (Waller et al., 2017). NPs (one dimension <100 nm) and MPs (<5 mm) arrive to remote places due to their durability and widespread use in populated areas. The sources of NPs and MPs are numerous (Wu et al., 2019), being less heavy NPs and MPs more prone to arrive to aquatic ecosystems. The polymer types mostly present in aquatic ecosystems include polyethylene (PE), polypropylene (PP), polystyrene (PS), polyvinyl chloride (PVC), polyurethane (PUR) and polyethylene terephthalate (PET). PS has an intermediate density (1.05 g/cm^3) among the previously mentioned polymers (higher density than PP and PE and lower density than PUR, PET or PVC) and close to water density ($1-1.03 \text{ g/cm}^3$ depending on salinity). This makes PS MPs to behave differently in waters of different salinity and, thus, to become bioavailable for populations from surface water to bottom waters or sediments (Erni-Cassola et al., 2019).

Several studies have already reported harmful effects of NPs and MPs on aquatic biota (Kögel et al., 2020). As reviewed for 28 taxonomic orders of zooplankton, MPs provoke negative effects on feeding behaviour, growth, development and life span of some arthropods and fish larvae, being MP size and density the main characteristics controlling their bioavailability (Botterell et al., 2019). Among aquatic organisms commercialised for human consumption, a high prevalence of filter feeders containing plastic debris in their digestive system has been reported (Rochman et al., 2015). Non-selective filter feeders, such as brine shrimp which has been proposed as a suitable biological model in nanoecotoxicology due to its cost-effectiveness (Libralato, 2014), showed ingestion and elimination of NPs and MPs (Bergami et al., 2016; Wang et al., 2019b), impairing food uptake. However, lethal effects of MPs were not reported in brine shrimps (Gambardella et al., 2017; Bergami et al., 2016; Wang et al., 2019a,b). No significant mortality was observed in organisms exposed up to 100 mg/L of 0.05 , 0.1 or $10 \text{ }\mu\text{m}$ - PS MPs for 24 or 48 h.

Organisms, such as fish, that occupy a high position in the trophic chain also ingest and accumulate MPs (Vendelet al., 2017; Jovanović, 2017), being early life stages especially sensitive for NP and MP impact (Barria et al., 2020). Zebrafish embryos have been widely used to test the toxicity of dissolved chemicals and nanomaterials (Lammer et al., 2009; Haque and Ward, 2018). More recently, zebrafish embryos have been also utilised to test toxicological effects of NPs and MPs (Qiang and Cheng, 2019; Chen et al., 2017a; Karami et al., 2017; Brun et al., 2018; Pitt et al., 2018). As shown for brine shrimp larvae, sub-lethal effects, such as changes in locomotor activity, heart beat rate, oxidative stress and nervous system, were caused by 0.025 , 0.05 , 0.1 or $45 \text{ }\mu\text{m}$ PS MPs/NPs ($0.1-10 \text{ mg/L}$) on zebrafish embryos of 120 hours post fertilisation (hpf) (Chen et al., 2017a; Brun et al., 2018; Pitt et al., 2018), and motility reduction was observed after

Results and discussion

exposure to PS MPs of 1 μm (0.01-1 mg/L) (Qiang and Cheng, 2019). In addition to the expected increase of NP and MP concentration into aquatic ecosystems due to up-growing plastic industry (Plastic EU, 2018), another concern has more recently raised regarding plastic pollution. It has been already proven that plastics sorb other pollutants (Mato et al., 2001; Teutan et al., 2007; **Chapter 2**), especially persistent organic pollutants (POPs), featured by a high hydrophobicity and resistance to degradation (persistence) in the ecosystems. Most POPs are well known toxic compounds to aquatic organisms and many of them display carcinogenic properties (Santana et al., 2018). These is the case of the ubiquitous polycyclic aromatic hydrocarbons (PAHs; Collier et al., 2013).

It has been seen that, apart from polymer type, particle size is a key factor driving the sorption capacity of the plastics; overall, the smaller the size of the plastics, the higher the sorption capacity (Ma et al., 2016; **Chapter 2**). Pollutants sorbed to NPs and MPs can be released inside organisms after assimilation (Hartmann et al., 2017). This phenomenon is called “Trojan horse effect” and it was first reported by Limbach et al. (2007) to describe the release of metal ions from metal nanoparticles, which produced enhanced oxidative stress to cells compared to the soluble form of the metal. Currently, this concept is also applied to plastic pollution to address the hazard of contaminated NPs and MPs for aquatic organisms (Rodrigues et al., 2019).

Few studies have addressed the potential Trojan horse effect produced by PS NPs/MPs combined with POPs in non-selective filter feeders (Ma et al., 2016; Lin et al., 2019). The potential transfer of C¹⁴ phenanthrene (0.05-1.2 mg/L) in co-exposure with two different sized PS particles (50 nm NPs and 10 μm MPs; 2.5-14.5 mg/L and 2.5-50 mg/L, respectively) was evaluated in *D. magna*. Results showed that co-exposure for 2, 7 and 14 days with NP provoked higher C¹⁴ phenanthrene bioaccumulation than co-exposure with MPs, due to the higher adsorption capacity of NPs for phenanthrene (Ma et al., 2016). *D. magna* was also co-exposed to 100 nm PS NPs (0.01-75 mg/L) and polychlorinated biphenyls (PCBs, 0.640 mg/L). The increase in the PS NP concentration combined with a fixed concentration of PCBs increased mortality of *D. magna*, indicating that NPs enhanced the PCB toxicity toward *D. magna* (Lin et al., 2019).

Fish larvae, including zebrafish embryos (Sleight et al., 2017; Chen et al., 2017a; Pannetier et al., 2019; Trevisan et al., 2019), have been also studied to evaluate potential Trojan horse effect of PS NPs/MPs for POPs. Pannetier et al. (2019) assessed the potential transport of B(a)P into medaka embryos using MPs collected from beaches. A mixture with 1% of <600 μm MPs (PP, PE and PS) coated with B(a)P (250 μg of B(a)P/g of MPs) caused high mortality (81%) of medaka embryos after 48 h of exposure, as well as an increase of 7-ethoxyresorufin-O-deethylase activity (EROD). Smaller size MPs (200-250 μm , 400 mg/L) were also analysed for the capacity to transport 17 α -ethynylestradiol (EE2, 0.001-1 μg /L) and phenanthrene (0.1-0.5 mg/L) into

zebrafish embryos (Sleight et al., 2017). A decrease of EE2 and phenanthrene bioavailability, indicated by gene expression in zebrafish in embryos, was due to the sedimentation of MPs. When MPs and NPs are compared for potential transfer of compounds to zebrafish embryos, a higher EE2 bioaccumulation was observed in zebrafish co-exposed to 50 nm NPs (1 mg/L) and EE2 (2 and 20 µg/L) than in those co-exposed to 45 µm PS MPs (1 mg/L), which resulted in an enhanced larval hypoactivity. This change in larval activity was not observed in embryos exposed to EE2 alone, indicating the capacity of NPs to enhance toxicity when combined with (Chen et al., 2017a). 44 nm PS NPs (10 mg/L) alone and combined with PAHs from a sediment extraction provoked a dysfunction of the mitochondrial function. The reported mitochondrial dysfunction was no longer observed in the embryos exposed to the corresponding PAH mixture alone (5073 ng/mL) while cardiotoxicity and impaired brain vascularity were observed (Trevisan et al., 2019).

The aim of the present study was to test the toxicity of PS NPs and MPs and their potential role as “Trojan horses” for B(a)P, as a model PAH, using two aquatic alternative models: brine shrimp larvae and zebrafish embryos. Therefore, the specific objectives were (1) to assess the developmental toxicity of “pristine” PS plastic particles of different sizes (50 nm, 0.5 µm and 4.5 µm) and of dissolved B(a)P on brine shrimp larvae and zebrafish embryos; (2) to assess the toxicity of MPs (0.5 and 4.5 µm) with sorbed B(a)P; and (3) to evaluate the availability of NPs and MPs with sorbed B(a)P to brine shrimp larvae and zebrafish embryos.

MATERIALS AND METHODS

Chemicals and plastic particles. Benzo(a)pyrene (B(a)P, C₂₀H₁₂, purity ≥ 96%) and dimethylsulfoxide (DMSO, purity ≥ 96%) were purchased from Sigma-Aldrich (St. Louis, MO, USA). Polystyrene NPs (50 nm) and MPs (0.5 µm and 4.5 µm) in aqueous suspensions were purchased from Polysciences, Inc. (Warrington, PA, USA). Fluorescent Fluoresbrite® carboxylate 50 nm NPs (excitation/emission wavelength of 360/407 nm) were also purchased from Polysciences. The concentration of the commercial stocks was 2.5% (3.64 10¹⁴ particles/mL for 50 nm fluorescent and non fluorescent PS NPs, 3.64 10¹¹ particles/mL for 0.5 µm PS MPs and 4.99 10⁸ particles/mL for 4.5 µm PS MPs).

Preparation and analysis of exposure media. Preparation and analysis of B(a)P exposure media. B(a)P concentrations used for toxicity assays were 0.1, 0.5 and 1 mg/L B(a)P in 0.01% DMSO and 5 and 10 mg/L B(a)P in 0.1% DMSO. An initial stock solution of 10 g/L (50 mg of B(a)P in 5 mL pure DMSO) was prepared and used to prepare other two stock solutions of 5 and 1 g/L of B(a)P in 100% DMSO. These stock and intermediate solutions were stored at -20 °C in closed glass vials. All the stock solutions, intermediates solutions and final dilutions were dispersed for 10 min in an ultrasounds bath (VWR, Thorofare, EEUU) before being used. Each stock solution was diluted 1:1000 in the exposure medium required for each experiment (MilliQ

Results and discussion

water for chemical analysis of B(a)P concentration, embryo water for zebrafish embryo toxicity test or salt water for brine shrimp immobilisation test) in order to obtain the three highest B(a)P exposure concentrations (10, 5 and 1 mg/L B(a)P) in 0.1% (v/v) DMSO. 0.5 and 0.1 mg/L B(a)P were prepared in 0.01% DMSO by diluting the previous ones 1:10 in exposure media.

B(a)P solutions at the concentrations used for toxicity tests were prepared in MilliQ water in order to analyse the actual exposure concentrations. Immediately after being prepared, an aliquot from each concentration was collected and diluted with MilliQ water up to 1 µg/L in 10 mL glass vials. Quantification was performed by gas chromatography and mass spectrometry (GC/MS) after solid phase microextraction (SPME). SPME consisted in a heating process at 40 °C with 35 min stirring period at 250 rpm of the polydimethylsiloxane (PDMS) fiber (Supelco, Sigma-Aldrich, South Africa). The fibre (100 µm) was thermally desorbed into the GC/MS system (Agilent GC 7890A/Agilent MSD 5975C, Agilent Technology, California) for 10 min at 280 °C. In order to assess whether there was any B(a)P loss during experimental exposures, 2 mL of each concentration were placed in duplicate in a 24-well microplate. The microplate was maintained under photoperiod simulating the test conditions (12 h light/12 h dark, 20 °C). Aliquots were taken at 24, 48 and 120 h, diluted up to 1 µg/L and processed as described before.

Preparation of the plastic containing exposure media. **Table 1** shows the exposure concentrations for PS NPs and MPs of the three sizes in terms of number of particles and in terms of PS mass used in the toxicity assays with brine shrimp larvae and zebrafish embryos. Concentrations were selected to be equivalent in terms of mass for the three particle sizes. To prepare MPs with sorbed B(a)P for brine shrimp assays, 1 mg of 0.5 µm or 4.5 µm MPs were incubated in 20 mL of 100 µg/L B(a)P (0.01% DMSO) prepared in MilliQ water into glass bottles. In the case of zebrafish experiments, 3.675 mg of 0.5 µm or 4.5 µm MPs were incubated in 73.5 mL of 100 µg/L B(a)P (0.01% DMSO) prepared in MilliQ water into glass bottles. The incubation volume used for MPs contamination with B(a)P depended on amount of MPs required for the assays, always keeping the MPs concentration used on sorption experiments (50 mg/L; **Chapter 2**). MP suspensions were wrapped with aluminium and shaken at 300 rpm for 24 h at 20 °C. Then, samples were filtered through a polyethersulfone filter (0.45 µm filter pore, SARSTEDT AG & Co., Nümbrecht, Germany) and washed two times with 10 mL of MilliQ water. MPs were recovered from the filter using 20 mL of salt water or 70 mL of embryo water. These MPs-B(a)P suspensions were diluted with the corresponding medium to prepare the five exposure concentration (**Table 1**). The recovery of 4.5 µm MPs after filtration was measured using a Coulter Counter (Z-counter, Beckman Coulter, Brea, USA) (**Fig. S1**).

Table 1- Relationship between the plastic concentrations in terms of mass and in terms of number of particles for the three sizes used.

50 nm NPs		0.5 μm MPs		4.5 μm MPs	
particles/mL	mg/L	particles/mL	mg/L	particles/mL	mg/L
10^6	0.000069				
10^7	0.00069	$5 \cdot 10^3$	0.00034		
		10^4	0.00069		
				$5 \cdot 10^2$	0.025
10^9	0.069	10^6	0.069	10^3	0.050
10^{10}	0.687	10^7	0.687	10^4	0.501
10^{11}	6.87	10^8	6.87	10^5	5.01
				10^6	50.1

Acute toxicity assays. Brine shrimp cultures and immobilisation test. 1 g of brine shrimp cysts (*Artemia Koral GmbH, Nürnberg, Germany*) were incubated in plastic bottles provided with a tap and with vigorous aeration in a temperature-controlled room at 26 °C under continuous illumination in 30‰ salt water prepared from commercial salt (*Sera, Heinsberg, Germany*). After 24 h, the aeration was removed and the culture was allowed to settle for some minutes in order to separate three differentiated phases: the upper part containing the empty floating cyst capsules, the intermediate part containing the hatched larvae and the bottom part containing the non-hatched cysts. Hatched larvae were harvested with a glass pipette, avoiding collecting unhatched cysts, and transferred to a freshly prepared salt medium where larvae were maintained for 24 or 48 h before starting the toxicity tests.

At 24 or 48 hours post hatch (hph), cultures were moved for some hours to a temperature-controlled room at 20 °C to acclimate individuals for the toxicity assays, which were performed following a procedure based on the standardised OECD TG 202 (2004) for *Daphnia magna*, using immobilisation as a criterion for acute toxicity. The experiments were run in covered 24-well polystyrene microplates at 20 ± 1 °C with a photoperiod of 12 h light/12 h dark. Five brine shrimps were placed in each well with 2 mL of exposure medium and 6 wells were used per concentration (30 individuals per experimental group and 30 individuals as controls). The selection of the individuals was made under a stereoscopic microscope (*Nikon smz800, Kanagawa, Japan*) paying attention to the morphology corresponding to the 24 hph and 48 hph stages. After 24 and 48 h of exposure, the amount of immobilised larvae was recorded. A larva was considered as immobilised when it was not able to move after shaking the plate. The toxicity of 0.01, 0.05 and 0.1% DMSO was tested in parallel.

Zebrafish maintenance, egg production and embryo toxicity test. The zebrafish (wild type AB Tübingen) stock was maintained in a temperature-controlled room at 28 °C with a 14 h light/10 h

Results and discussion

dark cycle in 100 L tanks provided with mechanic and biological filters following standard protocols for zebrafish culture. Conditioned water (600 μ S/cm and 7-7.5 pH) was prepared from deionised water and commercial salt. Fish were fed twice per day with Vipagran baby (Sera) and brine shrimp nauplii of 24 hpf, cultured as described above. Breeding female fish were selected and maintained separately in fish breeding nets inside the same tanks, in order to avoid continuous spawning.

The day before the assay, one female and two male zebrafish were placed separately in a breeding tramp previously located in a 2 L tank containing conditioned water. Fish were left overnight and, just before the light switched on, the separation was removed. The fertilised eggs were collected in a Petri dish with the help of a Pasteur pipette. The eggs selected as viable under a stereoscopic microscope (Nikon smz800, Kanagawa, Japan) were transferred to the exposure microplates.

The toxicity tests were carried out in covered 24-well polystyrene microplates placing one embryo per well in 2 mL of test solution made in embryo water (600-800 μ S/cm, 6.5-6.8 pH) (Brand et al., 2002) following the OECD guideline TG236 (2013). In each microplate two different concentrations were tested (10 embryos per concentration). Four control embryos were placed in embryo water in the remaining wells. For each compound three replicates were prepared, resulting in 30 embryos exposed to each concentration and 36 control embryos. Embryos were exposed up to 120 hpf. The test was considered as valid only when the survival of the control group of each replicate was $\geq 90\%$. The toxicity of 0.01, 0.05 and 0.1% DMSO was tested in parallel. Daily and up to the end of the test, embryos were examined to determine survival rate (as the percentage of alive embryos at 120 hpf), hatching time (as the time that embryos need to hatch) and malformation prevalence (as the percentage of malformed embryos over surviving embryos at 120 h). Normal embryo morphology and malformations were based on Fako and Furgeson (2009). Developmental abnormalities scored as malformations were spinal cord flexure, caudal fin alteration, tail malformation, pericardial edema, yolk sac edema, eye abnormality and stunted body. Malformations were recorded and photographed under a stereoscopic microscope (Nikon AZ100, Kanagawa, Japan).

Analysis of bioavailability of plastic particles and B(a)P. Presence of plastic particles in the zebrafish chorion and inside the brine shrimp larvae were examined under the stereoscopic microscope and a confocal microscope (Olympus Fluoview FV500, Tokyo, Japan), respectively. The analysis of fluorescence emitted by accumulated B(a)P in brine shrimp larvae and zebrafish embryos exposed to B(a)P was analysed at the end of the toxicity assays using a Cytation 5 microplate reader (Biotek Instruments Inc., Winooski, USA) provided with a blue filter (360/460 nm excitation/emission wavelength). For imaging, brine shrimp larvae were anaesthetised with 2% (v/v) chloroform in salt water and zebrafish embryos were anaesthetised with 200 mg/L benzocaine

prepared in embryo water. The accumulation of fluorescent NPs (50 nm) and of 0.5 and 4.5 μm MPs with sorbed B(a)P in brine shrimp and zebrafish was examined under a confocal microscope provided with a blue filter (330-385/400 nm excitation/emission wavelength). Same particle concentrations used for toxicity tests was employed. Micrographs were taken after 24 and 48 h of exposure for brine shrimp of both ages and every 24 h for zebrafish embryos. Individuals were washed and anesthetised as described above before observation at the microscope.

Statistical analyses. Data on survival and prevalence of malformations in zebrafish embryos were analysed by binominal logistic regression (Lacave et al., 2017; Orbea et al., 2017). Odd ratios were calculated in order to estimate and to compare the risk associated with the exposure to the MPs alone and with sorbed B(a)P. EC_{50} and LC_{50} values and confidences intervals (CI) at 95% were calculated using a Probit model with a confidence interval of 95% to 5%. For binominal logistic regression and Probit model, R package (R Foundation for Statistical Computing, Vienna, Austria) was used. Hatching time of zebrafish embryos was analysed by one-way ANOVA followed by the Tukey post-hoc test ($p < 0.05$) using the GraphPad Prism version 5.00 for Windows (GraphPad Software, La Jolla, California, USA).

RESULTS

Analysis of the B(a)P exposure media. Values of measured B(a)P along time in the polystyrene microplates for the five exposure concentrations are shown in **Table 2**. B(a)P concentration measured at 0 h was always lower (29%-63%) than the nominal B(a)P concentration. B(a)P concentration kept constant during the first 24 h, with the exception of 5 mg/L of B(a)P, whose concentration dropped to 1.173 ± 0.505 mg/L. At 48 h, the B(a)P concentrations dropped in all cases, except for 10 mg/L B(a)P, which remained quite stable until 120 h. At this time, the lowest B(a)P concentration (0.1 mg/L) presented the highest relative loss (up to 48.3% of initially measured concentration in the aqueous phase). Intermediate concentration showed similar or even higher values than those measured at 48 h.

Toxicity assays in brine shrimp larvae. Effect on survival of the exposure to NPs and MPs alone and with sorbed B(a)P for 24 h and 48 h of 24 hph and 48 hph brine shrimp larvae is shown in **Table 3**. Larvae exposed to pristine NPs and MPs did not show any significant difference on survival compared to controls at any exposure concentration or time. Survival rate of exposed larvae ranged from 75% in the most impacting treatment (exposure of 48 hph larvae for 48 h to 50.1 mg/L of 0.5 μm MPs) to 100%. Exposure of 24 hph larvae to 0.00034 mg/L, 0.00069 mg/L and 6.87 mg/L of 0.5 μm MPs-B(a)P for 48 h caused a significant decrease on survival rate compared to control larvae. 48 hph larvae exposed to 0.00034 mg/L of 0.5 μm MPs-B(a)P for 48 h also showed a significant reduction on survival compared to control larvae. B(a)P alone resulted

Results and discussion

the most toxic treatment, except for 24 hph brine shrimp larvae exposed for 24 h, that did not show any detrimental effect. However, exposure for 48 h to all B(a)P concentrations provoked a significant reduction on survival compared to control larvae, declining up to 59.4% in larvae exposed to the highest concentration. In the case of 48 hph larvae, exposure to any B(a)P concentration for 24 or 48 h provoked 100% mortality. Exposure of brine shrimp larvae of 24 hph or 48 hph up to 0.1% DMSO for 24 h or 48 h did not provoke any acute toxic effect (**Table S1**).

Table 2– Values of measured B(a)P concentration (mg/L) along time in the polystyrene microplates for the five exposure concentrations. Percentage of recovered B(a)P compared to that measured at time 0 is indicated in brackets. Values are given as mean \pm S.D. of duplicates.

Nominal concentration	Measured concentration			
	0 h	24 h	48 h	120 h
0.1	0.029 \pm 0.005	0.029 \pm 0.006 (100%)	0.022 \pm 0.002 (75.9%)	0.014 \pm 0.001 (48.3%)
0.5	0.315 \pm 0.142	0.432 \pm 0.084 (137.1%)	0.2578 \pm 0.011 (81.8%)	0.282 \pm 0.012 (89.5%)
1	0.496 \pm 0.111	0.503 \pm 0.006 (101.4%)	0.301 \pm 0.001 (60.7%)	0.265 \pm 0.025 (53.4%)
5	1.496 \pm 0.707	1.173 \pm 0.505 (78.4%)	0.738 \pm 0.299 (49.3%)	1.118 \pm 0.053 (74.7%)
10	4.922 \pm 1.995	5.023 \pm 0.397 (102.1%)	4.927 \pm 0.283 (100.1%)	5.269 \pm 1.095 (107%)

In the case of brine shrimp larvae of 24 hph exposed for 48 h to 0.5 μ m MPs-B(a)P, estimated LC₅₀ value was 4.75 \pm 1.03 mg/L (95% CI: 2.7-6.81). For the other treatments with plastics, LC₅₀ values were always higher than the highest tested concentration. For B(a)P alone, calculated LC₅₀ values for brine shrimp larvae of 24 hph were also higher than the highest tested concentration (nominal concentration 10 mg B(a)P/L, measured initial concentration 4.92 mg/L), while for brine shrimp larvae of 48 hph LC₅₀ values of 0.004 \pm 0.197 mg B(a)P/L (95% CI: -0.390-0.397) and 0.002 \pm 0.119 mg B(a)P/L (95% CI: -0.236-0.240) for 24 h and 48 h of exposure, respectively, were calculated.

Comparison between exposure treatments revealed some significant effects of the sorbed B(a)P and of the plastic particle size in the survival rate of brine shrimp larvae. Regarding the effect of the sorbed B(a)P, exposure of 24 hph larvae to 0.00069 mg/L and 6.87 mg/L of 0.5 μ m MPs-B(a)P for 48 h caused a significant decrease of survival compared to the exposure to 0.5 μ m MPs alone (**Table 3**, **Table S2**). Similarly, exposure of 48 hph larvae to 0.00034 mg/L, 0.687 and 6.87 mg/L of 0.5 μ m MPs-B(a)P for 48 h caused a significant decrease of survival compared to the exposure to 0.5 μ m MPs alone.

Table 3- Effects on survival (%) of the exposure to the NPs and MPs alone and in combination with B(a)P for 24 h and 48 h of 24 hph and 48 hph brine shrimp larvae. Asterisks indicate statistically significant differences ($p < 0.05$) compared to the control group according to the binomial logistic regression. Dollars indicate statistically significant differences ($p < 0.05$) compared to the exposure to MPs of the same size without B(a)P at the same exposure concentration. Hashes indicate statistically significant differences ($p < 0.05$) between 0.5 μm MPs-B(a)P and 4.5 μm MPs-B(a)P at the same exposure concentration. The values of the corresponding odd ratios and confidence intervals are given in **Table S2**.

	Concentration (mg/L)	24 hph larvae		48 hph larvae	
		24 h	48 h	24 h	48 h
50 nm NPs	0	100.0	96.8	93.8	100.0
	0.000069	93.3	90.0	100.0	100.0
	0.00069	97.0	97.0	96.8	93.3
	0.069	96.9	96.9	93.3	100.0
	0.687	96.7	90.0	100.0	100.0
	6.87	93.1	89.7	100.0	93.3
0.5 μm MPs	0	96.8	93.5	100.0	100.0
	0.00034	93.5	96.8	100.0	96.8
	0.00069	93.3	93.3	100.0	100.0
	0.069	96.8	87.1	100.0	91.2
	0.687	90.9	87.9	100.0	97.0
	6.87	97.1	94.3	100.0	96.9
4.5 μm MPs	0	100.0	96.8	100.0	93.3
	0.0251	100.0	96.8	100.0	96.8
	0.0501	96.8	93.5	100.0	80.0
	0.501	100.0	93.3	96.9	93.8
	5.01	96.7	93.3	96.7	87.1
	50.1	100.0	96.7	100.0	75.0
0.5 μm MPs-B(a)P	0	96.7	86.7	100.0	80.0
	0.00034	93.3	80.0*	93.3	53.3*\$
	0.00069	100.0	60.0*\$	100.0	60.0
	0.069	96.7	83.3	100.0	56.7
	0.687	100.0	73.3	100.0	56.7\$#
	6.87	93.3	36.7*\$#	100.0	60.0\$#
4.5 μm MPs-B(a)P	0	96.7	76.7	93.3	80.0
	0.0251	90.0	60.0\$	96.7	90.0
	0.0501	100.0	83.3	100.0	86.7
	0.501	86.7	56.7	100.0	90.0
	5.01	90.0	70.0\$	100.0	70.0
	50.1	100.0	63.3\$	93.3	90.0
B(a)P	0	97.2	91.7	93.3	80.0
	0.1	100.0	65.6*	0.0	0.0
	0.5	94.3	51.4*	0.0	0.0
	1	97.0	57.6*	0.0	0.0
	5	87.9	45.5*	0.0	0.0
	10	90.6	59.4*	0.0	0.0

Results and discussion

Significant differences were observed on survival rate of 24 hph larvae exposed for 48 h to 0.025 mg/L, 0.501 mg/L and 50.1 mg/L of 4.5 μm MPs-B(a)P compared to larvae exposed to same concentration of 4.5 μm MPs. Regarding the effect of the particle size, in the case of MPs with sorbed B(a)P, small MPs (0.5 μm) caused stronger effect than larger MPs (4.5 μm), being the difference statistically significant in the case of 24 hph larvae exposed to 6.87 mg/L of 0.5 μm MPs-B(a)P and for 48 hph brine shrimp larvae exposed to 6.87 and 0.687 mg/L of 0.5 MPs-B(a)P for 48 h.

Toxicity assays in zebrafish embryos. Results of the developmental parameters of zebrafish embryos are presented in **Tables 4** and **S3**. Exposure to PS NP and MPs alone or in combination with B(a)P did not provoke any significant effect on zebrafish embryo survival at 120 hpf or in hatching time. Only the exposure of embryos to 50.1 mg/L of 4.5 μm MPs-B(a)P caused a significant increase (up to 56.7%) of malformed embryos at 120 hpf. A similar prevalence of malformed embryos was recorded after exposure to 5 mg/L (50%) and 10 mg/L (58.6%) of B(a)P alone. Exposure to B(a)P caused a concentration-dependent increase of malformation prevalence. Previous toxicity assays with different DMSO concentrations showed that the DMSO concentration present in the B(a)P exposure was not deleterious for zebrafish embryo (**Table S4**). The EC_{50} values estimated for malformation prevalence at 120 hpf of embryos exposed to NPs and MPs alone and to 0.5 μm MPs-B(a)P were always above the highest exposure concentration. EC_{50} values calculated for embryo exposed to 4.5 μm MPs-B(a)P and to B(a)P alone were 45.57 ± 9.12 mg/L (95% CI: 27.34-63.81) and 3.55 ± 0.68 mg/L (95% CI: 2.183-4.915), respectively.

The prevalence of individual malformations is also shown in **Table 4** and **Fig. 1** illustrates some of the malformations found. Spinal cord flexure was the most prevalent malformation found in embryos exposed to all the treatments (**Fig. 1B, 1C, 1D**). Those exposed to 4.5 μm MPs-B(a)P (**Fig. 1D**) and to B(a)P presented the highest prevalence, with values of 36.7% and 44.8%, respectively. High prevalence of pericardial edema was observed in embryos exposed to the highest concentration of B(a)P alone (**Fig. 1E**) or to 4.5 μm MPs-B(a)P (50.1 mg/L) with a 24.1% and 30% of this malformation, respectively (**Fig. 1D**). Yolk sac edema (**Fig. 1C**) was observed only in two or one individual per concentration and treatment such as in embryo exposed to 5.1 and 50.1 mg/L of 4.5 μm MPs-B(a)P (3.3% and 6.7%, respectively), and to 1 and 5 mg/L of B(a)P (3.8% and 3.4%, respectively) (**Fig. 1D, 1F**). Only one case of eye abnormality was observed in one embryo exposed to 0.687 mg/L of 0.5 μm MPs.

Table 4- Results of the developmental parameters (% of surviving embryos at 120 h, hatching time and % of malformed embryos at 120 h) of zebrafish embryos exposed to NPs and MPs alone and in combination with B(a)P. Asterisks indicate statistically significant differences ($p < 0.05$) compared to the control group according to the binomial logistic regression. Dollars indicate statistically significant differences ($p < 0.05$) compared to the exposure to MPs of the same size without B(a)P at the same exposure concentration. The values of the corresponding odd ratios and confidence intervals are given in **Table S4**.

	Exposure conc.(mg/L)	Surv. (%)	Hatching time (h)	Malform. (%)	Type of malform. (%)			
					SC	PE	YE	EA
50 nm NPs	0	97.2	72	11.4	11.4	0	0	0
	0.000069	96.7	72	20.7	20.7	0	0	0
	0.00069	100	72	6.7	6.7	0	0	0
	0.069	93.3	72	7.1	3.6	3.6	0	0
	0.687	96.7	72	10.3	10.3	0	0	0
	6.87	90	72	3.7	3.7	0	0	0
0.5 μ m MPs	0	94.4	72	8.8	8.8	0	0	0
	0.00034	93.3	72	10.7	10.7	0	0	0
	0.00069	90	71.1 \pm 4.6	11.1	11.1	0	0	0
	0.069	96.7	72	17.2	17.2	0	0	0
	0.687	96.7	72	20.7	20.7	3.5	3.5	3.5
	6.87	93.3	72	21.4	14.3	10.7	0	0
4.5 μ m MPs	0	94.4	71.3 \pm 4.1	2.9	2.9	0	0	0
	0.0251	96.7	72	10.3	6.9	3.4	0	0
	0.0501	100	72	16.7	10	6.7	0	0
	0.501	93.3	70.3 \pm 6.3	7.1	7.1	0	0	0
	5.01	100	72	16.7	13.3	3.3	0	0
	50.1	100	70.4 \pm 6.1	20	16.6	6.7	0	0
0.5 μ m MPs-B(a)P	0	94.4	58.6 \pm 12.1	16.7	13.9	2.8	0	0
	0.00034	93.3	55.7 \pm 11.4	16.7	10	6.7	0	0
	0.00069	90	54.2 \pm 10.7	26.7	26.7	6.6	3.3	0
	0.069	96.7	57.1 \pm 11.9	16.7	13.3	3.3	0	0
	0.687	96.7	55.4 \pm 11.3	16.7	10	6.7	0	0
	6.87	93.3	56.6 \pm 12.0	10	6.7	6.7	0	0
4.5 μ m MPs-B(a)P	0	100	71.3 \pm 4	11.1	11.1	0	0	0
	0.0251	100	72	16.7	16.7	0	0	0
	0.0501	100	72.0	16.7	16.7	3.3	0	0
	0.501	100	70.4 \pm 6.1	13.3	10	3.3	0	0
	5.01	100	72	26.7	20	10	3.3	0
	50.1	100	70.4 \pm 6.1	56.7* $\$$	36.7	30	6.7	0
B(a)P	0	97.2	67.2 \pm 9.7	11.6	8.6	2.9	0	0
	0.1	96.7	69.5 \pm 8.3	13.8	13.8	0	0	0
	0.5	86.7	69.6 \pm 7.8	24.1	23.1	7.7	0	0
	1	86.7	69.2 \pm 7.8	26.9	23.1	7.7	3.8	0
	5	96.7	70.3 \pm 6.2	50*	27.5	20.6	3.4	0
	10	96.7	70.3 \pm 6.2	58.6*	44.8	24.1	0	0

Conc. = concentration; EA: eye abnormality; Malform. = malformation; PE= pericardial edema; SC= spinal cord flexure; Surv. = survival; YE= yolk sac edema.

Results and discussion

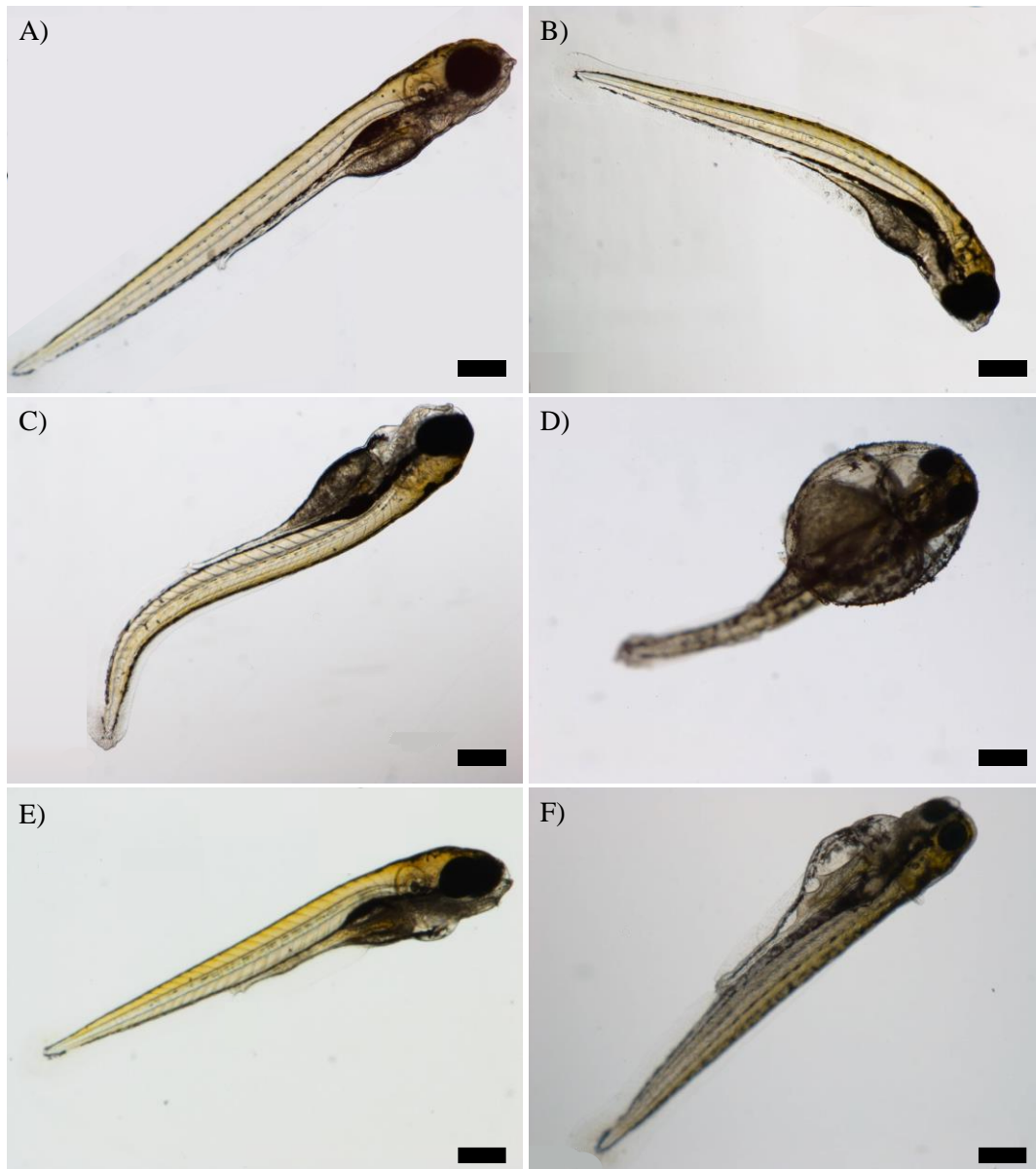


Fig. 1- Micrographs of different malformations found in exposed embryos at 120 hpf. A) unexposed control embryo showing normal morphology; B) embryo exposed to 0.687 mg/L of 0.5 μm MPs showing spinal cord flexure; C) embryo exposed to 0.069 mg/L of 0.5 μm MPs-B(a)P showing pericardial edema and spinal cord flexure; D) embryo exposed to 50.1 mg/L of 4.5 μm MPs-B(a)P showing multiple malformations such as pericardial edema, yolk sac edema and spinal cord flexure; E) embryo exposed to 10 mg/L of B(a)P showing pericardial edema; F) embryo exposed to 1 mg/L of B(a)P showing yolk sac edema. Scale bars: 100 μm .

Bioavailability of plastic particles and B(a)P. Brine shrimp larvae. In order to assess the bioavailability of NPs, brine shrimp larvae were exposed to fluorescent 50 nm NPs (**Fig. 2**). Unexposed brine shrimp did not show any fluorescence signal at any larval stage or exposure time of (**Fig. 2A, 2B**). Fluorescence was detected by confocal microscopy mainly along the digestive tract, in the faeces (**Fig. 2C, 2E, 2F**) and in the labrum (**Fig. 2D**) at two NP concentrations (0.687 and 6.87 mg/L) and in brine shrimps of both stages (24 hpf and 48 hpf).

Ingestion of 4.5 μm MPs was observed in brine shrimp larvae of 24 hph exposed for 48 h to 50.1 mg/L, MPs were found in the digestive tract (**Fig. 3A, 3B**). No evidence of MPs internalisation into the tissues was found. 4.5 μm MPs were also found in 48 hph brine shrimp faeces (**Fig. 3C**) after 24 h of exposure. Due to their small size, 0.5 μm MPs were not identified under the light microscope.

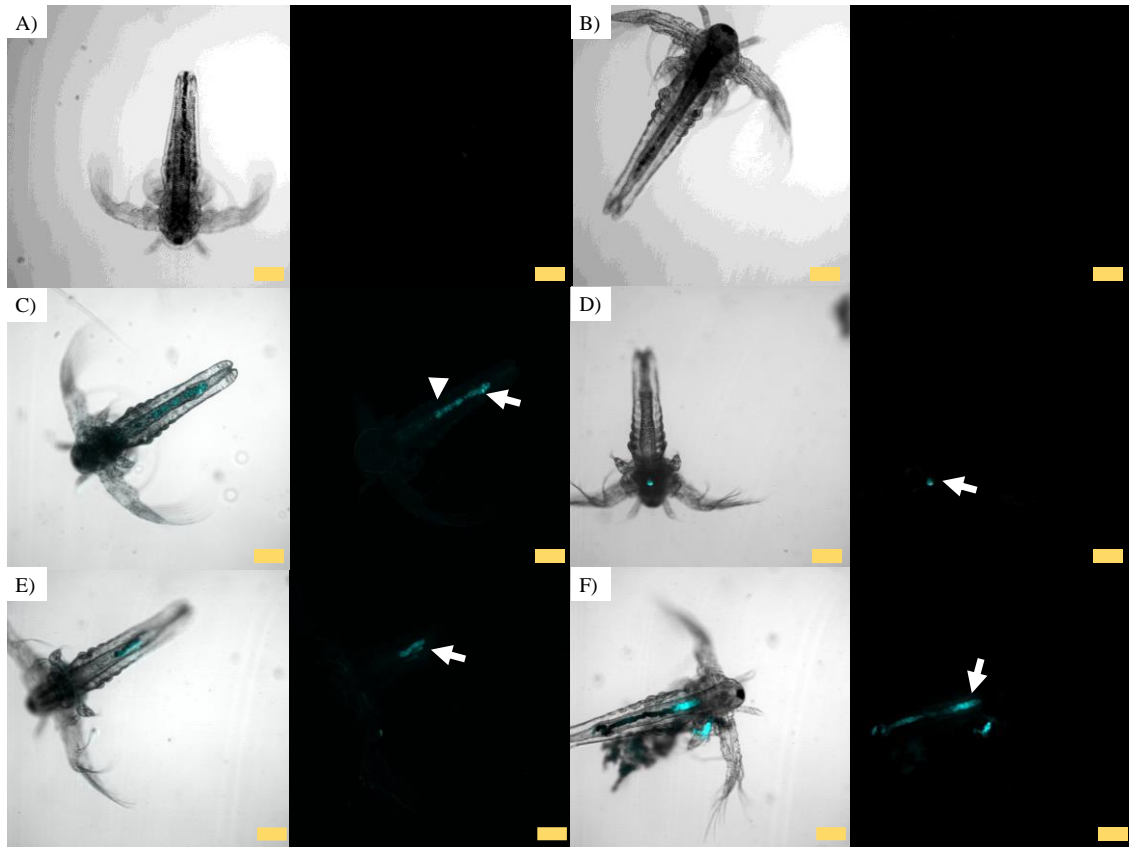


Fig. 2- Confocal micrographs of brine shrimp larvae at different stages of development. A) unexposed control larva at 48 hph; B) unexposed control larva at 72 hph; C) 24 hph larva exposed to 6.87 mg/L of fluorescent NPs for 24 hours showing fluorescence along the digestive tract (arrowhead) and in the faeces (white arrow); D) 24 hph larva exposed to 6.87 mg/L of fluorescent NPs for 48 h showing fluorescence in the labrum (white arrow); E) 48 hph larva exposed to 0.687 mg/L of NPs for 24 hours showing fluorescence inside the digestive tract (arrowhead); F) 48 hph larva exposed to 6.87 mg/L of NPs for 24 h showing fluorescence inside the digestive tract (arrowhead). Scale bars: 100 μm .

Results and discussion

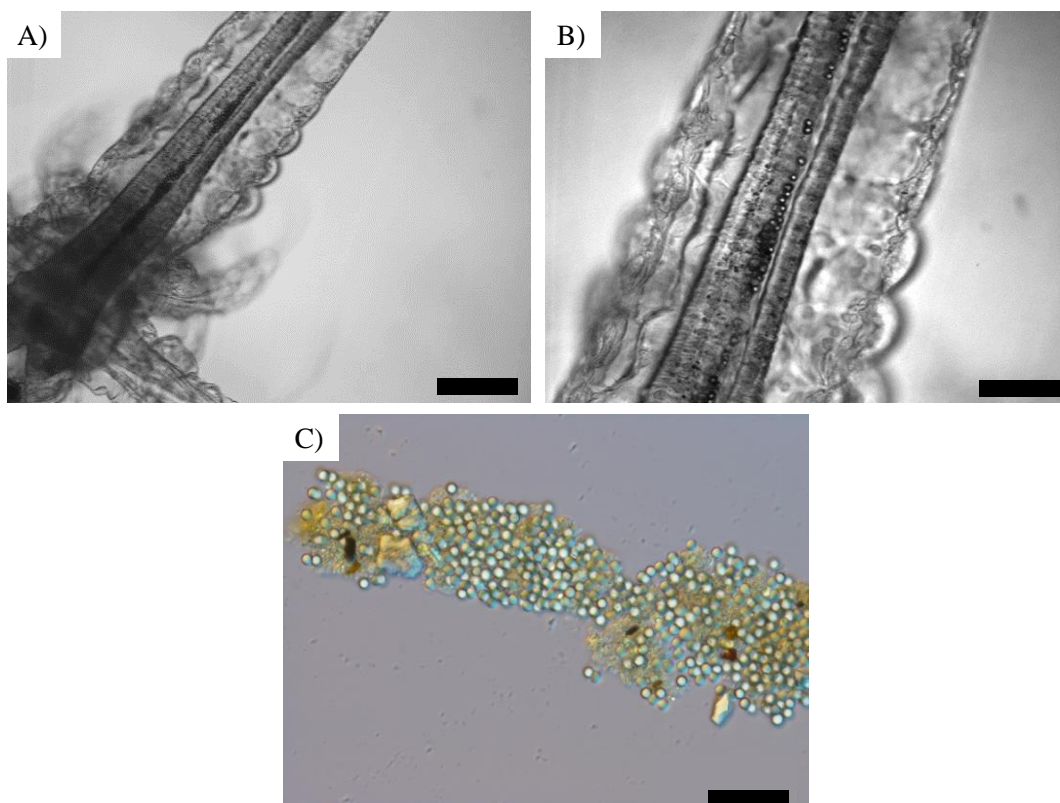


Fig. 3- Micrographs of brine shrimp larvae exposed to plastic particles. A) 24 hph larva exposed to 50.1 mg/L of 4.5 μm MPs for 48 h viewed under a stereoscopic microscope; B) 4.5 μm MPs in the digestive tract of the larva shown in (A) at higher magnification; C) and faeces of brine shrimp larvae exposed to 50.1 mg/L of 4.5 μm MPs. Scale bars: 100 μm (A), 50 μm (B) and 25 μm (C).

Micrographs of brine shrimp larvae exposed to 0.5 and 4.5 μm MPs with sorbed B(a)P are shown in **Fig. 4**. Unexposed brine shrimp larvae did not show fluorescence at any developmental stage (**Fig. 4A, 4B, 4C**). At early stages, 24 hph larvae exposed to 6.87 mg/L of 0.5 μm MPs-B(a)P for 24 h showed fluorescence all over the body and inside the digestive tract (**Fig. 4D**). 24 hph larvae exposed to 0.00069 mg/L (the second lowest concentration) also presented fluorescence (**Fig. 4E**). In brine shrimps of 48 hph, fluorescence inside the digestive tract was again observed after exposure to concentrations between 0.00069 mg/L and 6.87 mg/L of 0.5 μm MPs-B(a)P for 24 h (**Fig. 4F**). After 48 h of exposure, brine shrimp larvae did not present fluorescence at any exposure concentration (**Fig. 4G**). With the increased size of MPs with sorbed PAHs, no fluorescence signal was detected in 24 hph brine shrimp larvae exposed to any exposure concentration of 4.5 μm MPs-B(a)P for 24 h (**Fig. 4H**), but after 48 h of exposure to 50.1 mg/L fluorescence was observed all over and inside (digestive tract) the brine shrimp body (**Fig. 4I**). As it can be seen in the micrograph of the same larvae taken at higher magnification (**Fig. 4J**), the digestive tract is full of 4.5 μm MPs that can be seen individually.

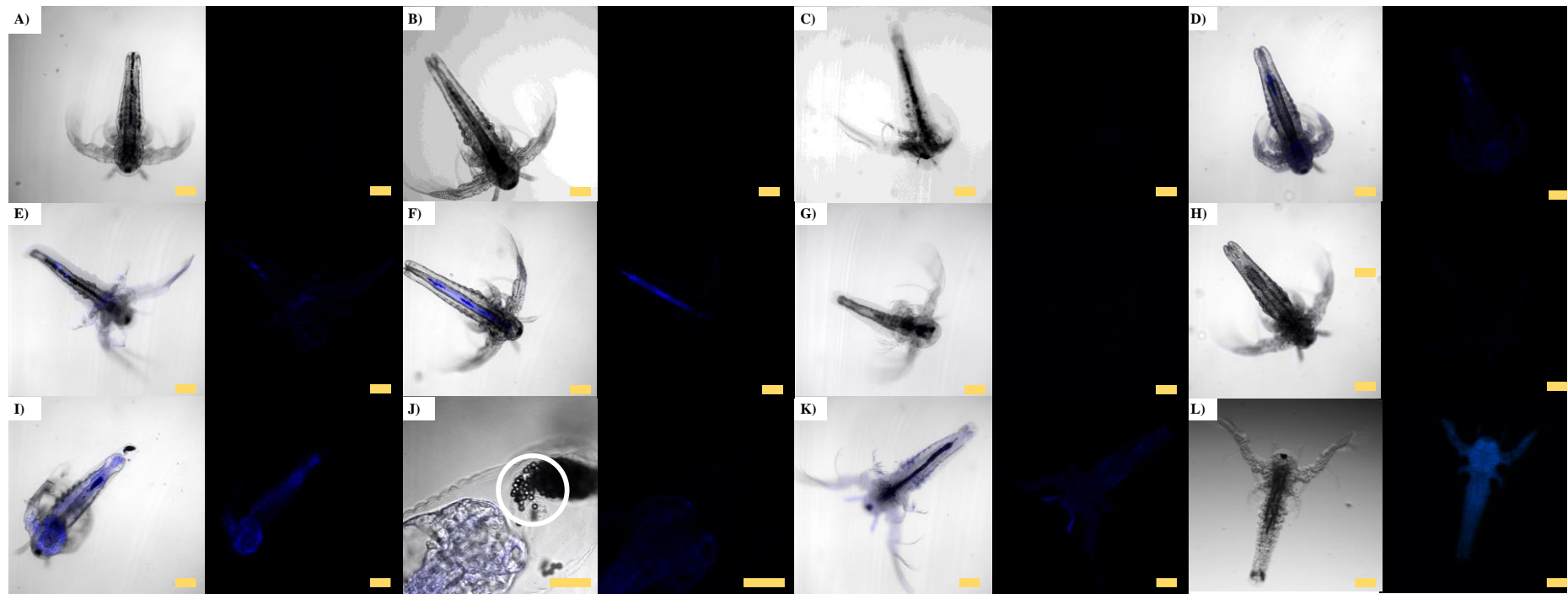


Fig. 4- Confocal micrographs of brine shrimp larvae at different stages of development exposed to MPs-B(a)P. A) unexposed control larva at 48 hph; B) unexposed control larva at 72 hph; C) unexposed control larva at 96 hph; D) 24 hph larva exposed for 24 h to 6.87 mg/L of 0.5 μm MPs-B(a)P; E) 24 hph larva exposed for 48 h to 0.00069 mg/L of 0.5 μm MPs-B(a)P; F) 48 hph larva exposed for 24 h to 6.87 mg/L of 0.5 μm MPs-B(a)P; G) 48 hph larva exposed for 48 h to 0.687 mg/L of 0.5 μm MPs-B(a)P; H) 24 hph larva exposed for 24 h to 50.1 mg/L of 4.5 μm MPs-B(a)P; I) 24 hph larva exposed for 48 h to 50.1 mg/L of 4.5 μm MPs-B(a)P; J) 4.5 μm MPs-B(a)P (white circle) excreted from the digestive tract of a 24 hph larva exposed for 48 h observed at higher magnification; K) 48 hph larvae exposed for 48 h to 5.01 mg/L of 4.5 μm MPs-B(a)P; L) 48 hph larvae exposed for 48 h to 0.1 mg/L of B(a)P. Scale bars: 100 μm (A-I, K, L) and 25 μm (J).

Results and discussion

The fluorescence indicating the presence of B(a)P appears in the surface and inside of larvae, but no fluorescence was observed on the surface of the 4.5 μm MPs-B(a)P ingested. At longer exposure time, brine shrimp larvae exposed to 4.5 μm MPs-B(a)P presented fluorescence on the surface of the body at exposure concentrations above 5.01 mg/L (**Fig. 4K**). As previously mentioned, B(a)P emits fluorescence which is clearly observed in 48 hpf brine shrimp larvae exposed to dissolved B(a)P for 48 h (100 $\mu\text{g/L}$; **Fig. 4L**).

Zebrafish embryos. Fluorescent 50 nm NPs were found distributed in different organs of the embryo: eye, tail and yolk sac (**Fig. 5**). For early stages, zebrafish embryos of 24 hpf showed fluorescence on the chorion surface and in the yolk sac (**Fig. 5B**) only at the highest exposure concentration (6.87 mg/L). At 48 hpf, fluorescence appeared in embryos exposed to 0.687 mg/L (**Fig. 5D**) and was increased in embryos exposed to 6.87 mg/L (**Fig. 5E**). The lowest exposure concentration at which fluorescence was detected in 72 hpf embryo was 0.069 mg/L (**Fig. 5G**). Hatched embryos of 72 hpf showed fluorescence in the yolk sac (**Fig. 5H**), in discrete areas near the yolk sac and along the tail (**Fig. 5I**) and within the eyes (**Fig. 5J**). At the end of exposure (120 h), fluorescence remained as shown for 72 hpf exposed embryos and also appeared in embryos exposed to lower concentration (0.069 mg/L, **Fig. 5L**). Unexposed zebrafish embryos did not show fluorescence at any stage (**Fig. 5A, 5C, 5F, 5K**).

48 hpf embryos exposed to 6.9 mg/L of 50 nm NPs or 0.5 μm MPs did not show perceptible plastic particles over surface of the chorion, allowing to observe the embryo development (**Fig. 6B, 6C**), while 48 hpf embryos exposed to comparable concentration of 4.5 μm MPs (5.01 mg/L) presented a full coverage of the chorion surface (**Fig. 6D**). This full coverage resulted in a rare case of a 120 hpf unhatched embryo exposed to 5.01 mg/L of 4.5 μm MPs-B(a)P that was still alive at the end of the experiment (**Fig. 6E**). Zebrafish embryos exposed to MPs with sorbed B(a)P were also observed under the confocal microscope (**Figs. 7 and 8**). Unexposed embryos did not show fluorescence at any time (**Fig. 7A, 7D, 7H, 7K**). 24 and 48 hpf zebrafish embryos exposed to 0.5 μm MPs-B(a)P showed fluorescence on the chorion surface at exposure concentrations of 0.687 mg/L (**Fig. 7B, 7C, 7E**) and of 6.87 mg/L. Only at the highest exposure concentration of 0.5 μm MPs-B(a)P, fluorescence was detected in the yolk sac of 24 and 48 hpf zebrafish embryos (**Fig. 7C, 7F, 7G**). For the highest concentration of 0.5 μm MPs with sorbed B(a)P, the fluorescence continued to be present in 72 hpf hatched embryo exposed to 6.87 mg/L (**Fig. 7I**) with an intense fluorescence in the yolk sac. In 96 hpf embryos, similar localisation of fluorescence was observed at 0.687 mg/L of 0.5 μm MPs-B(a)P (**Fig. 7J**). In addition, fluorescence signal around the embryo eye was observed. At the end of the exposure, fluorescence was detected in 120 hpf embryo exposed above 0.069 mg/L of 0.5 μm MPs-B(a)P (**Fig. 7L**).

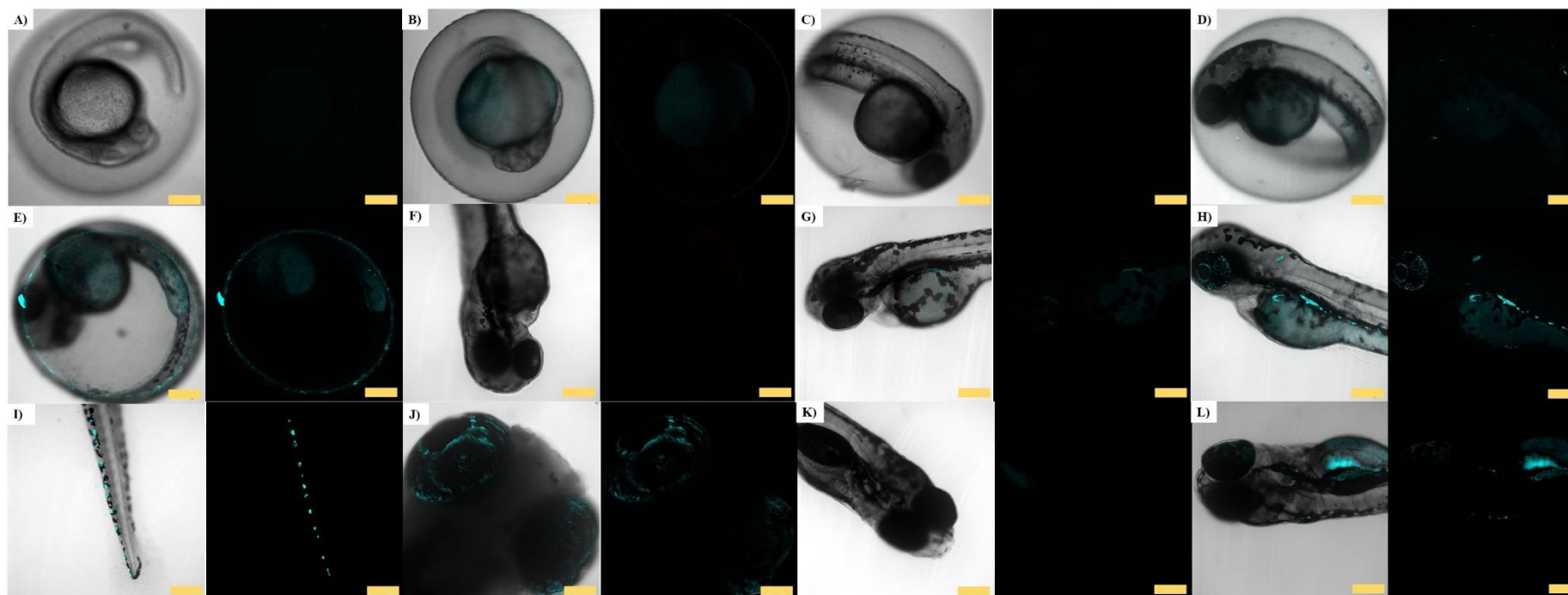


Fig. 5- Confocal micrograph stacks of zebrafish embryos exposed to fluorescent 50 nm NPs. A) unexposed control embryo at 24 hpf; B) 24 hpf embryo exposed to 6.87 mg/L NPs; C) unexposed control embryo at 48 hpf; D) 48 hpf embryo exposed to 0.687 mg/L NPs; E) 48 hpf embryo exposed to 6.87 mg/L NPs; F) unexposed control embryo at 72 hpf; G) 72 hpf embryo exposed to 0.069 mg/L NPs; H) 96 hpf embryo exposed to 6.87 mg/L NPs; I) 96 hpf embryo exposed to 6.87 mg/L; J) 96 hpf embryo exposed to 6.87 mg/L; K) unexposed control embryo at 120 hpf; L) 120 hpf embryo exposed to 0.069 mg/L. Scale bars: 100 μm (A-I, K, L) and 25 μm (J).

Results and discussion

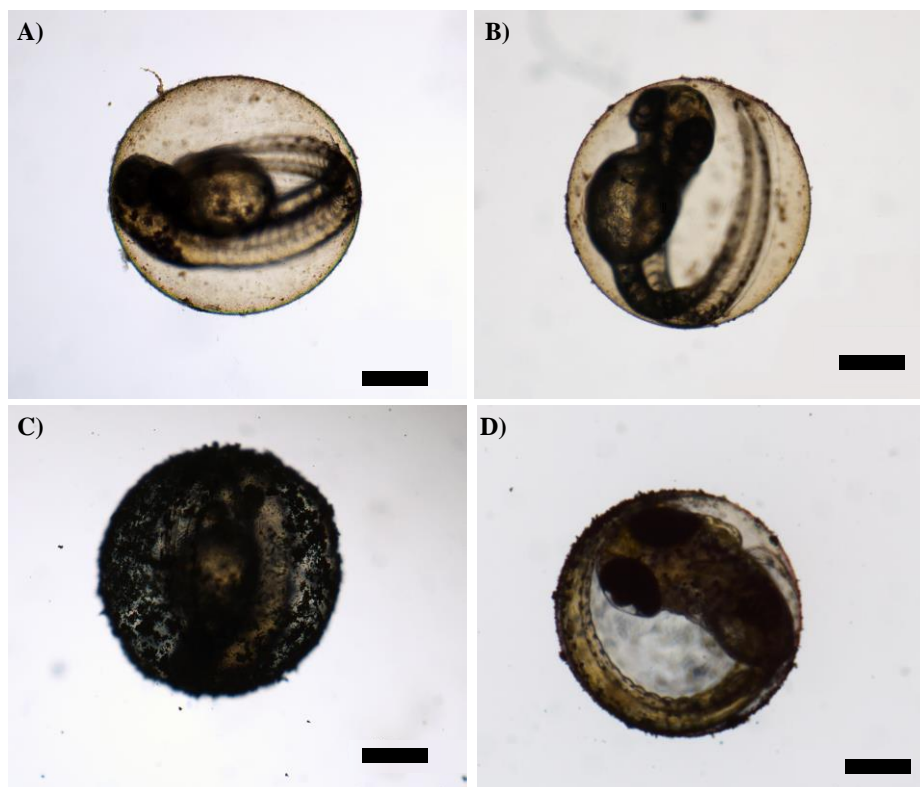


Fig. 6– Micrographs of zebrafish embryos exposed to similar masses of plastics of different sizes. A) embryo exposed to 6.87 mg/L of 50 nm NPs at 48 hpf; B) 48 hpf embryo exposed to 6.87 mg/L of 0.5 μm MPs; C) 48 hpf embryo exposed to 5.01 mg/L of 4.5 μm MPs; D) non hatched 120 hpf alive embryo exposed to 5.01 mg/L of 4.5 μm MPs-B(a)P. Scale bars: 100 μm .

Fluorescence due to the exposure to 4.5 μm MPs-B(a)P (**Fig. 8**) was first detected in 24 hpf embryos exposed at concentrations higher than 5.01 mg/L (**Figs. 8A-B**). At 5.01 mg/L fluorescence was only detected over the embryo chorion (**Fig 8A**) and, at the highest exposure concentration, it was also detected in the yolk sac (**Fig. 8B**). Same localisation of the fluorescence was observed in 48 hpf embryos exposed to 5.01 mg/L (**Fig. 8C**) and in embryos exposed to 50.1 mg/L (**Fig. 8D**) a more intense fluorescence was observed compared to 24 hpf embryo exposed to the same concentration. 72 hpf zebrafish embryos exposed to 4.5 μm MPs-B(a)P (**Fig. 8E-F**) showed fluorescence in the yolk sac at exposure concentrations above 0.501 mg/L. Similar signal in the yolk sac was observed in 96 hpf zebrafish embryos exposed to 5.01 and 50.1 mg/L of 4.5 μm MPs-B(a)P (**Fig. 8G-H**). 120 hpf embryos presented fluorescence at exposure concentrations higher than 0.501 mg/L of 4.5 μm MPs-B(a)P (**Fig. 8I**) and up to 5.01 mg/L (**Fig. 8J**). As it can be seen, the fluorescence intensity was higher for zebrafish embryos exposed to 0.5 μm MPs-B(a)P (**Fig 7**) than to 4.5 μm MPs-B(a)P (**Fig. 8**). 120 hpf zebrafish embryo exposed to different B(a)P concentration (0.1 and 0.5 mg/L, **Fig 8K, 8L**) presented fluorescence with a similar intensity than embryos exposed to MPs contaminated with B(a)P.

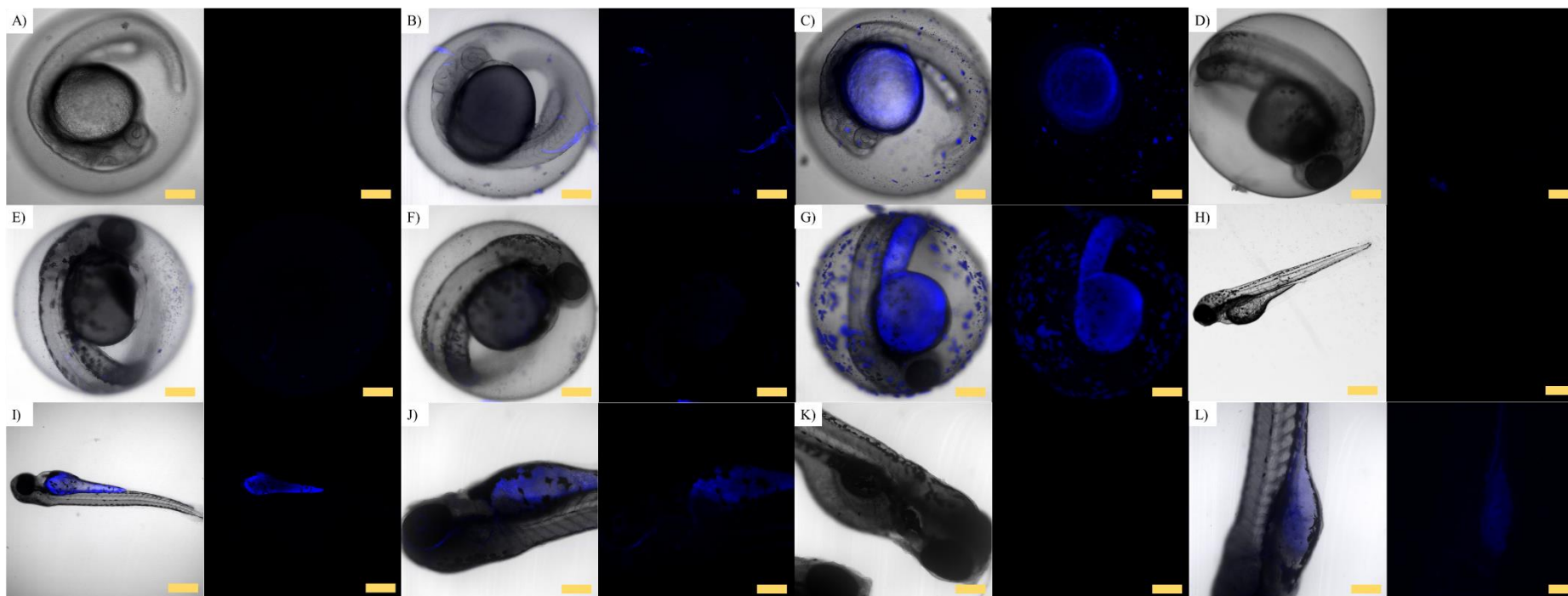


Fig. 7- Confocal micrograph stacks of zebrafish embryos at different stages of development exposed to 0.5 μm MPs-B(a)P. A) 24 hpf unexposed control embryo; B) 24 hpf embryo exposed to 0.687 mg/L; C) 24 hpf embryo exposed to 6.87 mg/L; D) 48 hpf unexposed control embryo; E) 48 hpf embryo exposed to 0.687 mg/L; F) 48 hpf embryo exposed to 0.687 mg/L; G) 48 hpf embryo exposed to 6.87 mg/L; H) 72 hpf unexposed control embryo; I) 72 hpf embryo exposed to 6.87 mg/L; J) 96 hpf embryo exposed to 0.687 mg/L; K) 120 hpf unexposed control embryo; L) 120 hpf embryo exposed to 0.069 mg/L. Scale bars: 250 μm (H,I) and 100 μm (A-G,J-L).

Results and discussion

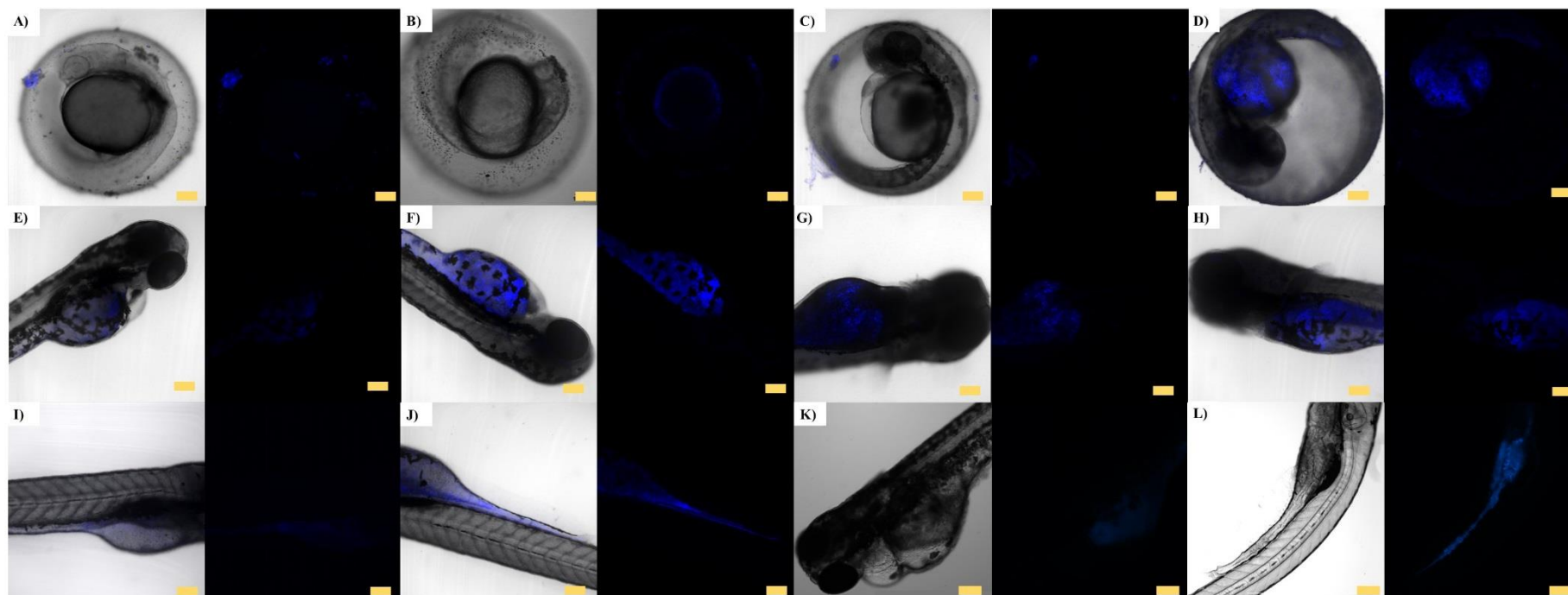


Fig. 8- Micrograph stacks obtained by confocal microscopy of zebrafish embryos at different stages of development exposed to 4.5 μm MPs-B(a)P. A) 24 hpf embryo exposed to 5.01 mg/L; B) 24 hpf embryo exposed to 50.1 mg/L; C) 48 hpf embryo exposed to 5.01 mg/L; D) 48 hpf embryo exposed to 50.1 mg/L; E) 72 hpf embryo exposed to 0.501 mg/L; F) 72 hpf embryo exposed to 5.01 mg/L; G) 96 hpf embryo exposed to 5.01 mg/L; H) 96 hpf embryo exposed to 50.1 mg/L; I) 120 hpf embryo exposed to 0.501 mg/L; J) 120 hpf embryo exposed to 5.01 mg/L. In addition, micrograph of zebrafish embryos exposed to the B(a)P concentration used for MPs incubation and a higher one: K) 120 hpf embryo exposed to 0.1 mg/L of B(a)P; L) 120 hpf embryo exposed to 0.5 mg/L of B(a)P. Scale bars: 200 μm .

DISCUSSION

In the present study, we aimed to assess the potential toxicity of polystyrene NPs and MPs on brine shrimp larvae and zebrafish embryo development, as alternative model organisms, and whether these microplastics can act as carriers of PAHs. Three plastic sizes were used in order to investigate the effect of this parameter on their toxicity and bioavailability. Previous studies that tested the toxicity of NPs and MPs in different species of brine shrimps reported no significant effects on survival (Bergami et al., 2016; Gambardella et al., 2017; Peixoto et al., 2019; Wang et al., 2019b; Suman et al., 2020). In *Artemia parthenogenetica*, acute effects were not observed after 14 days of exposure to low concentrations of 10 µm PS MPs (1-1000 particles/mL or 0.55-550 µg/L). However, alterations at cell level, such as abnormal ultrastructure of intestinal epithelial cells and appearance of autophagosomes that could affect the energetic system were described (Wang et al., 2019b). Similar results were obtained in *Artemia franciscana*. Exposure to 0.1 µm PS MPs did not caused toxicity with a LC₅₀ value higher than the highest tested concentration (100 mg/L) (Gambardella, 2017). For smaller plastics, such as functionalised PS NPs (40 nm PS-COOH and PS-NH₂), toxicity tests were performed in *A. franciscana* larvae and no effect was recorded on mortality, even for the highest exposure concentration (100 mg/L, Bergami et al., 2016). In the present study, LC₅₀ values higher than the highest tested concentrations, 50.1 mg/L for 4.5 µm MPs and 6.9 mg/L for 0.5 µm MPs and 50 nm NPs, were estimated in agreement with the previously mentioned results reported in the literature.

Survival rate, hatching time and malformation prevalence in zebrafish embryos exposed to the different sized MPs and to NPs did not show any significant change compared to control values. Lethal effects in zebrafish embryos are neither reported in the literature, and sublethal effects are not always reported (Karami et al., 2017; Brun et al., 2018; Lei et al., 2018; Qiang and Cheng, 2019; Kurchaba et al., 2020). Brun et al. (2018) investigated the potential toxicity of PS NPs (25 nm) on the immune system of the skin and intestine of zebrafish embryos after injection of 1 nL of 1 mg NPs/L at 30 hpf. NP injection did not provoke significant changes on survival or hatching rate of 54 hpf zebrafish embryos, but upregulation of immune system related genes (*interleukin1β* and *chemokine (C-C motif) ligand 20a*) in 54 hpf exposed embryos compared to control embryos was observed. Karami et al. (2017) exposed zebrafish embryos to a mixture of low-density PE fragments (5-500 µg/L) of different sizes (<17.6 µm). No effect was observed after 10 days of exposure for the assessed genes (*casp8*, *casp3a*, *sod1*, *gstp1* and *cat*), while a significant down-regulation of *cat*, *casp3a* and *casp9* after 20 days of exposure that resulted in minimal impact on the organisms was reported. Nevertheless, effects on swimming mobility of zebrafish embryos after exposure to 1 mg/L of 1 µm PS MPs were observed without significant changes on hatching rate compared to controls (Qiang and Cheng, 2019). In addition, up-regulation of oxidative stress

Results and discussion

related genes (*interleukin1 β* and *catalase*) in embryos exposed to 1 mg/L of PS MPs was observed. Thus, overall, NPs and MPs are reported as non acutely toxic materials.

NPs and non-contaminated MPs did not cause acute toxic effects, but when early life stages of brine shrimp were exposed to MPs with sorbed B(a)P, significant effects on survival were observed. 0.5 μm MPs-B(a)P were toxic for 24 hpf brine shrimp larvae after 48 h of exposure with a LC_{50} value of 4.75 mg/L. To the best of our knowledge, effects from MPs associated with POPs to brine shrimp larvae have not been previously reported. In *D. magna*, another aquatic branchiopod commonly used for aquatic toxicity assessment, higher lethality was recorded in individuals co-exposed for 48 h to PS NPs (100 nm) and PCBs (0.64 mg/L) than in those exposed to PCBs alone. However, the combined toxicity to *D. magna* depended on the relative concentration of NPs and PCBs, being PCBs less toxic when combined with low concentration of NPs (< 1 mg/L), while higher concentration of NPs enhanced the lethality (Lin et al., 2019). When PS MP size increased up to 1 μm (3.10^5 particles/mL or 0.038 mg/L), and MPs were combined with previously known toxic concentrations of the insecticides dimethoate and deltamethrin, Trojan horse effect was not observed for water borne exposure of *D. magna* in any of the studied endpoints, such as survival and mobility alterations (Horton et al., 2018). After been internalised, the amount of B(a)P sorbed to the MPs could be released to the brine shrimp digestive system increasing the toxicity (Bakir et al., 2014). Significant differences were found between the exposure of brine shrimp larvae to similar concentration of 4.5 μm MPs-B(a)P (5.01 mg/L) and to 0.5 μm MPs-B(a)P (6.87 mg/L), showing that the risk of death increased with the decrease of contaminated MP size. Thus, results from literature and from the present study suggest that in the case of contaminated MPs, size plays a critical role in toxicity being smaller size MPs more toxic for aquatic organisms than higher size MPs when combined with other toxic pollutants. This seems to be due to the higher surface/volume ratio of smaller particles that confers them higher capacity to carry B(a)P (**Chapter 2**).

Previous studies have addressed the potential toxicity of MPs combined with organic compounds on zebrafish development (Chen et al., 2017a; Sleight et al., 2017; Cormier et al., 2019). In 3 hpf zebrafish embryos, co-exposure for 48 h and 72 h to 45 μm PS MPs or 50 nm PS NPs with EE2 (2 $\mu\text{g/L}$ and 20 $\mu\text{g/L}$) produced an increase of toxicity when the highest EE2 concentration was combined with MPs or NPs. Embryos co-exposed to the high concentration showed an induction of catalase (CAT) activity and glutathione (GSH) content compared to control embryos. High concentration of EE2 combined with MPs were, in terms of oxidative stress, more toxic than high concentration of EE2 combined with NPs, showing that bioavailability of EE2 was higher in presence of MPs than of NPs (Chen et al., 2017a). Another studied where zebrafish embryos were co-exposed to larger MPs, 200–250 μm PVC MPs, with EE2 or phenanthrene reported that co-exposure reduced the bioavailability of the organic compounds to zebrafish resulting in non toxic

effect of the tested treatments in zebrafish embryos (Sleight et al., 2017). Intermediate MP size (11-13 μm PE, 100 mg/L) spiked with PAHs (16.87 $\mu\text{g/B(a)P}$) provoked an increase of biotransformation metabolism (7-ethoxyresorufin O-deethylase (EROD) activity and *cytochrome P450 1A* (*cyp1a*) transcription levels), indicating the successful transfer of B(a)P via MPs to the embryos. Even if the transfer of B(a)P via MPs to zebrafish was observed, the PAH concentration selected were not enough to produced deleterious effects in zebrafish embryos (Cormier et al., 2019). MP size seems to change PAH bioavailability and toxicity in zebrafish embryos, being 4.5 μm MPs more likely to affect zebrafish through a potential higher transfer of B(a)P than 0.5 μm MPs. Only exposure to 4.5 μm MPs with sorbed B(a)P caused toxicity to 120 hpf embryos ($\text{EC}_{50}=45.57\pm 9.12$ mg/L or $9.1 \cdot 10^6$ particles/mL) while significant effects were not recorded at the highest tested concentration of 0.5 μm MPs-B(a)P ($\text{EC}_{50} > 6.87$ mg/L or 10^8 particles/mL). The types of malformations observed in 120 hpf zebrafish embryos exposed to 4.5 μm MPs-B(a)P were similar to those provoked by B(a)P exposure. 30% of the embryos exposed to 52.5 mg/L of 4.5 μm MPs-B(a)P presented pericardial edema. As previously mentioned, a common effect of PAHs from crude oil in zebrafish embryos is the cardiotoxicity. An observed increase in the percentage of pericardial edema in zebrafish embryos exposed to PAHs from crude oil is a common effect provoked by organic compounds from crude oil (Incardona et al., 2013; Meador and Nahgang, 2019).

B(a)P is a well-known toxic compound for aquatic organisms (Baird et al., 2005; Sánchez-Bayo, 2006; Ikenaka et al., 2013). In this study, estimated LC_{50} value for 48 hph brine shrimp larvae exposed for 24 and 48 h were 0.004 ± 0.197 mg/L and 0.002 ± 0.119 mg/L, respectively, and EC_{50} value, based on malformation appearance, for zebrafish embryo exposed for 120 h was 3.55 ± 0.68 mg/L. Brine shrimp presented an increased sensitivity along the developmental stages (24 hph to 96 hph) when exposed to B(a)P. This increased sensitivity is due to the progressive loss of energy reservoirs present in the first developmental stages and the lack of feeding during the assay. The reported LC_{50} values for 48 hph brine shrimp larvae exposed to B(a)P are similar to those reported for *D. magna*. Exposure of *D. magna* for 48 h to 1-32 $\mu\text{g/L}$ B(a)P without feeding resulted in a LC_{50} value of 4.7 $\mu\text{g/L}$ (Ikenaka et al., 2013). PAHs, together with other organic compounds, such as PCBs, are amongst the most toxic compounds to planktonic crustaceans (branchiopod, copepod and ostracod), primarily due to the higher toxicity and more persistence of their metabolites than of the parent compounds (Sánchez-Bayo, 2006). The observed mortality in early stages of brine shrimps at low B(a)P exposure concentration shows the sensitivity of this organism for PAH exposure, being a suitable model for toxicity evaluation of these compounds.

Zebrafish embryo was less sensitive to B(a)P exposure than brine shrimp larvae. Nevertheless, B(a)P has also been proven to be a toxic PAH for zebrafish embryo development (Weigt et al., 2011; Sogbanmu et al., 2016; Knecht et al., 2017; McCarrick et al., 2019). Knecht et al. 2017

Results and discussion

observed a non-significant increase of mortality rate and malformation prevalence in 120 hpf zebrafish embryos exposed to 0.1 and 1 mg/L of B(a)P (1% DMSO), but the alteration of the swimming behaviour resulted into hyperactivity of embryos exposed to B(a)P. Furthermore, an increasing in B(a)P concentration up to 2.5 mg/L caused mortality in 72 hpf zebrafish embryos, with a LC_{50} value of 1.285 mg/L and a EC_{50} for malformations of 0.131 mg/L (Weigt et al., 2011). Higher B(a)P concentration (50 μ m = 12.6 mg/L) provoked 40-50% of malformed embryos (72 hpf) without further changes in their heart rate, but oxidative damage to DNA was observed in 72 hpf zebrafish embryos exposed to lower B(a)P concentration (1 μ M = 0.25 mg/L) (Sogbanmu et al., 2016). Exposure to 1 μ M B(a)P also caused genotoxicity in 96 hpf embryos (Mc Carrick et al., 2019). The lower sensitivity observed by brine shrimps exposed to B(a)P than in zebrafish embryos was due to the efficiency of aquatic vertebrates, even at first stages of development, for detoxification of organic compounds compared to invertebrates (Honda and Suzuki, 2020).

Previous works reported the use of B(a)P concentrations ranging from 0.2 to 25.2 mg/L for developmental and sublethal toxicity in zebrafish embryos (Weigt et al., 2011; Knecht et al., 2017). The low solubility of B(a)P in water (1.64 μ g/L; May et al., 1983) makes difficult to reach acute concentration for organisms (Costa et al., 2011; Zhao et al., 2013), which are usually above solubility point even using DMSO as vehicle. Due to this low solubility, B(a)P in water tends to aggregate leading to analytical errors. Analytical results reported by Costa et al. (2011) and Zhao et al. (2013) showed that none of the B(a)P solutions reached the expected nominal concentration. Four nominal B(a)P concentrations (10, 20, 50 and 100 μ g/L) were prepared by Costa et al. (2011) for waterborne exposure of Nile tilapia obtaining actual B(a)P exposure concentrations of 0.34, 0.69, 12.19, and 25.70 μ g/L, respectively. In addition, B(a)P has been proven as a hydrophobic compound that tends to be sorbed on the plastic material used for biological test, especially to uncoated PS microplates (Chlebowski et al., 2016; Fischer et al., 2018). According to Fischer et al. (2018), working with PAHs that have partition coefficient ($\log K_{ow}$) higher than 6, such as B(a)P, should be carefully monitored, especially for not very concentrated tests, due to predicted losses higher than 80% from initial concentration as result of adsorption to PS microplates. Chlebowski et al. (2016) also reported high sorption of different PAHs (fluoranthene, pyrene, chrysene and B(a)P) at the highest exposure concentration used (0.32 μ M each PAH studied). In the case of B(a)P, 48% from the total (80.64 μ g/L = 0.32 μ M) remained in the water, 39% was sorbed onto the walls and 13% assimilated by the zebrafish embryos. Our results showed that B(a)P concentration decreased when the test media were placed into the PS microplate wells, likely due to both, degradation and sorption to the microplate walls, being the percentage loss higher for the lowest concentrations.

Confocal micrographs showed an abundant presence of 50 nm fluorescent NPs and 4.5 µm MPs within the brine shrimp digestive tract. For 0.5 µm MPs this distribution was not observed due to their smaller size that make them not distinguishable at light microscopy level if they are not fluorescently labelled. Nevertheless, taken into account that 50 nm NPs and 4.5 µm MPs are ingested, assimilation of 0.5 µm MPs is also expected to occur. Localisation of plastic particles in the digestive tract of brine shrimp has been reported for NPs and MPs of different sizes (Wang et al., 2019a, Bergami et al., 2016). For smaller plastics, such as 40 nm anionic carboxylated (PS-COOH) and 50 nm cationic amino (PS-NH₂) fluorescent PS NPs, ingestion by *A. franciscana* was observed by fluorescence detection for concentrations ranging from 5 to 100 mg/L, although fluorescence was only detected on the surface of the faeces of brine shrimp (Bergami et al., 2016). Ingestion was observed for a concentration ranging from 1 to 1000 particles/mL of 10 µm PS MPs by *A. parthenogenetica* (<24 h old) over 24 h (Wang et al., 2019a). As previously highlighted, it is evident that MPs and NPs are ingested by brine shrimps but signs of internalisation into the tissues have not been reported yet. The ingestion of NPs and MPs by zooplanktonic species such as brine shrimp, that are consumed by numerous organisms in higher levels of the trophic chain, is a potential risk for plastic transfer and accumulation in the food web, even between different zooplanktonic organisms (Setälä et al., 2014; Peixoto et al., 2019) in aquatic ecosystems.

In the case of zebrafish, NPs spread through the body and accumulated in specific organs (eye, yolk sac and tail) even in early development stages mainly due to the large pores size of the embryo chorion (0.6-0.7 µm) (Duan et al., 2020). By confocal microscopy, fluorescence was detected in several optical sections observed indicating internalisation of NPs in the eye. Lacave et al. (2016) reported the presence of 27 nm SiO₂ fluorescent nanoparticles into embryo eyes at 120 hpf. 25 and 50 nm PS NPs studied by van Pomerene et al. (2017) were specifically internalised in the eye between 72 and 120 hpf, but for PS NPs of larger size (200 nm) internalisation of NPs in the eye of the embryo was not observed. Presence of nanoparticles in the yolk sac is usually reported for zebrafish embryos (Lacave et al., 2016; Pitt et al., 2018). Zebrafish embryos exposed to 51 nm fluorescent PS NPs presented a fluorescence increase due to a higher internalisation of NPs with the increase of larval age, this fluorescence was located in the surface of the chorion (48 hpf) and in the head (Pitt et al., 2018). A different organ accumulation of NPs, like pancreas and liver, was observed in 120 hpf zebrafish embryo. In this study, a notorious increase of fluorescence was observed near the tail and the yolk sac in form of irregular deposits. As seen by Evensen et al. (2019), an injection of fluorescent PS NPs (100 nm) in the cardinal vein produced an accumulation of NPs on macrophages with similar structure and distribution to those found in our study. A similar distribution for fluorescent PS NPs was observed, but localised inside macrophages, at neuromast level (Brun et al., 2018). NPs can be a potential source of damage to

Results and discussion

nervous and digestive systems due to the reported accessibility to different organs. As mentioned in literature, the presence of NPs in eyes and brain lead to, for example, locomotor alterations (Chen et al., 2017a). Thus, further studies on long term effects in juveniles and adults after an acute exposure event at embryo stage is of high interest. However, ingestion or internalisation of MPs or contaminated MPs was not observed directly in zebrafish embryos in the present study even when B(a)P fluorescent was observed all over the zebrafish embryo exposed to contaminated MPs from early stages. B(a)P emits fluorescence in the visible spectrum (excitation/emission wavelength of 297/405 nm, Rivera-Figueroa et al., 2004) due to its aromatic structure (five benzene rings). This fluorescent could be detected due to the desorption of the B(a)P from MPs after ingestion by the embryo or by direct contact with the skin of the embryo.

Regarding MPs of both sizes sorbed with B(a)P, results for brine shrimp and zebrafish exposure showed a successful transport of B(a)P from MPs to the organisms in a wide concentration range for exposure to 0.5 μm (0.00069 to 6.9 mg/L) and 4.5 μm contaminated MPs (0.501 to 50.1 mg/L). For brine shrimp exposure, results of the exposure to 0.5 μm MPs-B(a)P differ from results of the exposure to 4.5 μm MPs-B(a)P, since in the case of 0.5 μm MPs-B(a)P fluorescence was only detected in the digestive tract and in the faeces while for 4.5 μm MPs-B(a)P fluorescence was only observed all over the body and in the digestive tract. As shown by Batel et al. (2016), 1-5 μm and 10-20 μm PE MPs with sorbed B(a)P released the B(a)P all over the body of brine shrimps and B(a)P was transferred from brine shrimps to adult zebrafish via diet. Due to the capacity of brine shrimps to filter a large amounts of water, exposure to MPs with sorbed B(a)P can lead to increased exposure to B(a)P compared to other organisms that are more selective in terms of feeding, representing a risk to these organisms. B(a)P fluorescence was observed on the surface of the chorion and at the yolk sac of zebrafish embryo in the present study. A successful transport of B(a)P into embryos by MPs of both sizes was observed even through the chorion wall, proving the risk of MPs as vector of other compounds. However, it is not possible to say whether the transport of B(a)P has taken place by desorption of B(a)P from MPs in the exposure media or was desorbed after ingestion, which could not be demonstrated in embryos.

In summary, NPs and MPs alone did not cause acute effects in zebrafish embryos and brine shrimp larvae, even with the reported ingestion of these materials by both organisms. However, toxicity increased when MPs (4.5 μm and 0.5 μm) were contaminated with B(a)P and exposure to MPs-B(a)P resulted into B(a)P accumulation in brine shrimp larvae and zebrafish embryos. The MP size played a significant role in explaining the toxicity of MPs with sorbed B(a)P, implying a potential risk for brine shrimps when MP size decreased due to the increase of surface to volume ratio that results into a higher B(a)P sorbed for potential transfer. Thus, polystyrene MPs of different size are likely to act as vectors of PAHs in the aquatic environment modulating their bioavailability and provoking toxic effects in organism that play important roles in the

ecosystems. Still a lot of work has to be done especially for standardisation of MP experiments and also for the use of relevant MPs concentrations in order to provide information of higher quality to evaluate the threat posed for NP and MP contamination. Further studies should be performed to increase the scarce available information. Once ingestion has been demonstrated, studies at other levels, such as long term analysis and consequences at physiological or behavioural level, are required.

REFERENCES

1. Avio, C.G., Gorbi, S., Regoli, F., 2017. Plastics and microplastics in the oceans: From emerging pollutants to emerged threat. *Mar. Environ. Res.* 128, 2-11.
2. Baird, W.M., Hooven, L.A., Mahadevan, B., 2005. Carcinogenic polycyclic aromatic hydrocarbons-DNA adducts and mechanism of action. *Environ. Mol. Mutagen.* 45, 106-114.
3. Bakir, A., Rowland, S.J., Thompson, R.C., 2014. Enhanced desorption of persistent organic pollutants from microplastics under simulated physiological conditions. *Environ. Pollut.* 185, 16-23.
4. Barria, C., Brandts, I., Tort, L., Oliveira, M., Teles, M., 2020. Effect of nanoplastics on fish health and performance: A review. *Mar. Pollut. Bull.* 151, 110791.
5. Bergami, E., Bocci, E., Vannuccini, M.L., Monopoli, M., Salvati, A., Dawson, K.A., Corsi, I., 2016. Nano-sized polystyrene affects feeding, behaviour and physiology of brine shrimp *Artemia franciscana* larvae. *Ecotoxicol. Environ. Saf.* 123, 8-25.
6. Botterell, Z.L.R., Beaumont, N., Dorrington, T., Steinke, M., Thompson, R.C., Lindeque, P.K., 2019. Bioavailability and effects of microplastics on marine zooplankton: A review. *Environ. Pollut.* 245, 98-110.
7. Brand, M., Granato, M., Nüsslein-Volhard, C., 2002. Chapter 1: Keeping and raising zebrafish. In: Nusslein-Volhard C., Dahm, R (Eds), *Zebrafish: A practical approach*, Oxford University Press, New York, pp. 7-37.
8. Brun, N.R., Koch, B.E.V., Varela, M., Pejinenburg, J.G.M., Spaink, H.P., Vijver, M.G., 2018. Nanoparticles induce dermal and intestinal innate immune system responses in zebrafish embryos. *Environ. Sci. Nano* 5, 904-916.
9. Chen, Q., Gundlach, M., Yang, S., Jiang, J., Velki, M., Yin, D., Hollert, H., 2017a. Quantitative investigation of the mechanisms of microplastics and nanoplastics toward zebrafish larvae locomotor activity. *Sci. Total Environ.* 584-585, 1022-1031.
10. Chlebowski, A.C., Tanguay, R.L., Simonich, S.L.M., 2016. Quantitation and prediction of sorptive losses during toxicity testing of polycyclic aromatic hydrocarbon (PAH) and nitrated PAH (NPAH) using polystyrene 96-well plates. *Neurotoxicol. Teratol.* 57, 30-38.
11. Collier, T.K., Anulacion, B.F., Arkoosh, M.R., Dietrich, J.P., Incardona, J.P., Johnson, L.L., Ylitalo, G.M., Myers, M.S., 2013. Effects on fish of polycyclic aromatic hydrocarbons (PAHs) and naphthenic acid exposures. In: Tierney K.B., Farrell A.P., Brauner C.J. (Eds), *Organic chemical toxicology of fishes*. Academic Press. Pp 195-255.
12. Cormier, B., Batel, A., Cachot, J., Bégout, M.-L., Braunbeck, T., Cousin, X., Keiter, S.H., 2019. Multi-laboratory hazard assessment of contaminated microplastic particles by means of enhanced fish embryo test with the zebrafish (*Danio rerio*). *Front. Environ. Sci.* 7, 135.
13. Costa, J., Ferreira, M., Rey-Salgueiro, L., Reis-Henriques, M.A., 2011. Comparison of the waterborne and dietary routes of exposure on the effects of benzo(a)pyrene on

Results and discussion

- biotransformation pathways in Nile tilapia (*Oreochromis niloticus*). *Chemosphere* 84, 1452-1460.
14. Duan, Z., Duan, X., Zhao, S., Wang, X., Wang, J., Liu, Y., Peng, Y., Gong, Z., Wang, L., 2020. Barrier function of zebrafish embryonic chorions against microplastics and nanoplastics and its impact on embryo development. *J. Hazard. Mater.* 395, 122621.
 15. Erni-Cassola, G., Zadjelovic, V., Gibson, M.I., Christie-Oleza, J.A., 2019. Distribution of plastic polymer types in the marine environment: A meta-analysis. *J. Hazard. Mater.* 369, 691-698.
 16. Evensen, L., Johansen, P.L., Koster, G., Zhu, K., Herfindal, L., Speth, M., Fenaroli, F., Hildahl, J., Bagherifam, S., Tulotta, C., Prasmickaite, L., Maelandsmo, G.M., Snaar-Jagalska, E., Griffiths, G., 2016. Zebrafish as a model system for characterization of nanoparticles against cancer. *Nanoscale* 8, 862-877.
 17. Fako, V.E., Furgeson, D.Y., 2009. Zebrafish as a correlative and predictive model for assessing biomaterial nanotoxicity. *Adv. Drug Deliv. Rev.* 61, 478-486.
 18. Fischer, F.C., Cirpka, O.A., Goss, K., Henneberger, L., Escher, B.I., 2018. Application of experimental polystyrene partition constants and diffusion coefficients to predict the sorption of neutral organic chemicals to multiwell plates in *in vivo* and *in vitro* bioassays. *Environ. Sci. Technol.* 52, 13511-13522.
 19. Gambardella, C., Morgana, S., Ferrando, S., Bramini, M., Piazza, V., Costa, E., Garaventa, F., Faimali, M., 2017. Effects of polystyrene microbeads in marine planktonic crustaceans. *Ecotoxicol. Environ. Saf.* 145, 250-257.
 20. Hartmann, N.B., Rista, S., Bodin, J., Jensen, L.H.S., Schmidt, S.N., Mayer, P., Meibom, A., Baun, A., 2017. Microplastics as vectors for environmental contaminants: exploring sorption, desorption, and transfer to biota. *Integr. Environ. Assess. Manag.* 13, 488-493.
 21. Haque, E., Ward, A.C., 2018. Zebrafish as a model to evaluate nanoparticle toxicity. *Nanomaterials* 8, 561.
 22. Honda, M., Suzuki, N., 2020. Toxicity of polycyclic aromatic hydrocarbons for aquatic animals. *Environ. Res. Public Health* 17, 1363.
 23. Horton, A.A., Vijver, M.G., Lahive, E., Spurgeon, D.J., Svendsen, C., Heutink, R., van Bodegom, P.M., Baas, J., 2018. Acute toxicity of organic pesticides to *Daphnia magna* is unchanged by co-exposure to polystyrene microplastics. *Ecotoxicol. Environ. Saf.* 166, 26-34.
 24. Ikenaka, Y., Sakamoto, M., Nagata, T., Takahashi, H., Miyabara, Y., Hanazato, T., Ishizuka, M., Isobe, T., Kim, J., Chang, K., 2013. Effects of polycyclic aromatic hydrocarbons (PAHs) on an aquatic ecosystem: acute toxicity and community-level toxic impact tests of benzo[a]pyrene using lake zooplankton community. *J. Toxicol. Sci.* 38, 131-136.
 25. Incardona, J.P., Swarts, T.L., Edmunds, R.C., Linbo, T.L., Aquilina-Beck, A., Sloan, C.A., Gardner, L.D., Block, B.A., Scholz, N.L., 2013. Exxon Valdez to Deepwater Horizon: Comparable toxicity of both crude oils to fish early life stages. *Aquat. Toxicol.* 142-143, 303-316.
 26. Jovanović, B., 2017. Ingestion of microplastics by fish and its potential consequences from a physical perspective. *Integrated Environmental Assessment and Management* 13, 510-515.
 27. Karami, A., Groman, D.B., Wilson, S.P., Ismail, P., Neela, V.K., 2017. Biomarker responses in zebrafish (*Danio rerio*) larvae exposed to pristine low-density polyethylene fragments. *Environ. Pollut.* 223, 466-475.
 28. Knecht, A.L., Truong, L., Simonich, M.T., Tanguay, R.L., 2017. Developmental benzo(a)pyrene (B[a]P) exposure impacts larval behavior and impairs adult learning in zebrafish. *Neurotoxicol. Teratol.* 59, 27-34.

29. Kögel, T., BJORoy, Ø., Toto, B., Bienfait, A.M., Sanden, M., 2020. Micro- and nanoplastic toxicity on aquatic life: Determining factors. *Sci. Total Environ.* 709, 136050.
30. Kurchaba, N., Cassone, B.J., Northam, C., Ardelli, B.F., LeMoine, C.M.R., 2020. Effects of MP polyethylene microparticles on microbiome and inflammatory response of larval zebrafish. *Toxics* 8, 55.
31. Lacave, J.M., Retuerto, A., Vicario-Parés, U., Gilliland, D., Oron, M., Cajaraville, M.P., Orbea, A., 2016. Effects of metal-bearing nanoparticles (Ag, Au, CdS, ZnO, SiO₂) on developing zebrafish embryos. *Nanotechnology* 27, 325102-325116.
32. Lacave, J.M., Fanjul, A., Bilbao, E., Gutiérrez, N., Barrio, I., Arostegui, I., Cajaraville, M.P., Orbea, A., 2017. Acute toxicity, bioaccumulation and effects of dietary transfer of silver from brine shrimp exposed to PVP/PEI-coated silver nanoparticles to zebrafish. *Comp. Biochem. Physiol. C Toxicol. Pharmacol.* 199, 69-80.
33. Lammer, E., Carr, G.J., Wendler, K., Rawlings, J.M., Belanger, S.E., Braunbeck, Th., 2009. Is the fish embryo toxicity test (FET) with the zebrafish (*Danio rerio*) a potential alternative for the fish acute toxicity test? *Comp. Biochem. Physiol.* 149C, 196-209.
34. Lei, L., Wu, S., Lu, S., Liu, M., Song, Y., Fu, Z., Shi, H., Raley-Susman, K.M., He, D., 2018. Microplastic particles cause intestinal damage and other adverse effects in zebrafish *Danio rerio* and nematode *Caenorhabditis elegans*. *Sci. Total Environ.* 619-620, 1-8.
35. Libralato, G., 2014. The case of *Artemia spp.* in nanoecotoxicology. *Mar. Environ. Res.* 101, 38-43.
36. Limbach, L.K., Wick, P., Manser, P., Grass, R.N., Bruinink, A., Stark, W.J., 2007. Exposure of engineered nanoparticles to human lung epithelial cells: influence of chemical composition and catalytic activity on oxidative stress. *Environ. Sci. Technol.* 41, 4158-4163.
37. Lin, W., Jiang, R., Xiong, Y., Wu, J., Xu, J., Zheng, J., Zhu, F., Ouyang, G., 2019. Quantification of the combined toxic effect of polychlorinated biphenyls and nano-sized polystyrene on *Daphnia magna*. *J. Hazard. Mater.* 364, 531-536.
38. Ma, Y., Huang, A., Cao, S., Sun, F., Wang, L., Guo, H., Ji, R., 2016. Effects of nanoplastics and microplastics on toxicity, bioaccumulation, and environmental fate of phenanthrene in fresh water. *Environ. Pollut.* 219, 166-173.
39. Mato, Y., Isobe, T., Takada, H., Kanehiro, H., Ohtake, C., Kaminuma, T., 2001. Plastic resin pellets as a transport medium for toxic chemicals in the marine environment. *Environ. Sci. Technol.* 35, 318-324.
40. May, W.E., Wasik, S.P., Miller, M.M., Tewari, Y.B., Brown-Thomas, J.M., Goldberg, R.N., 1983. Solution thermodynamics of some slightly soluble hydrocarbons in water. *J. Chem. Eng. Data* 28, 197-200.
41. McCarrick, S., Cunha, V., Zapletal, Vondráček, J., Dreij, K., 2019. *In vitro* and *in vivo* genotoxicity of oxygenated polycyclic aromatic hydrocarbons. *Environ. Pollut.* 246, 678-687.
42. Meador, J.P., Nahrgang, J., 2019. Characterizing crude oil toxicity to early-life stage fish based on a complex mixture: are we making unsupported assumptions? *Environ. Sci. Technol.* 53, 11080-11092.
43. OECD TG202. 2004. OECD Guidelines for the testing of chemicals. Section 2: Effects on biotic systems. Test No. 202: *Daphnia sp.* acute immobilization test. Organization for Economic Cooperation and Development, Paris, France. 12 pp.
44. OECD TG236. 2013. OECD guidelines for the testing of chemicals. Section 2: Effects on biotic systems Test No. 236: Fish embryo acute toxicity (FET) test. Organization for Economic Cooperation and Development, Paris, France, 22 pp.

Results and discussion

45. Orbea, A., González-Soto, N., Lacave, J.M., Barrio, I., Cajaraville, M.P., 2017. Developmental and reproductive toxicity of PVP/PEI-coated silver nanoparticles to zebrafish. *Comp. Biochem. Physiol.* 199C, 69-80.
46. Pannatier, P., Morin, B., Clérandeau, C., Laurent, J., Chapelle, C., Cachot, J., 2019. Toxicity assessment of pollutants sorbed on environmental microplastics collected on beaches: Part II- adverse effects on Japanese Medaka early life stage. *Environ. Pollut.* 248, 1098-1107.
47. Peixoto, D., Amorim, J., Pinheiro, C., Oliva-Teles, L., Varó, I., Rocha, R.M., Vieira, M.N., 2019. Uptake and effects of different concentrations of spherical polymer microparticles on *Artemia franciscana*. *Ecotoxicol. Environ. Saf.* 176, 211-218.
48. Pitt, J.A., Kozal, J.S., Jayasundara, N., Massarsky, A., Trevisan, R., Geitner, N., Wiesner, M., Levin, E.D., Di Giulio, R.T., 2018. Uptake, tissue distribution, and toxicity of polystyrene nanoparticles in developing zebrafish (*Danio rerio*). *Aquat. Toxicol.* 194, 185-194.
49. Plastics Europe. Plastics – the Facts 2018: An analysis of European plastics production, demand and waste data. Plastics Europe, 2018 (<https://www.plasticseurope.org/en/resources/publications/619-plastics-facts-2018>) (accessed Jan 14, 2020).
50. Rivera-Figueroa, A.M., Ramazan, K.A., Finlayson-Pitts, B.J., 2004. Fluorescence, absorption, and excitation spectra of polycyclic aromatic hydrocarbons as a tool for quantitative analysis. *J. Chem. Educ.* 81, 242-245.
51. Rochman, C.M., Tahir, A., Williams, S.L., Baxa, D.V., Lam, R., Miller, J.T., Teh, F., Werorilangi, S., Teh, S.J., 2015. Anthropogenic debris in seafood: Plastic debris and fibers from textiles in fish and bivalves sold for human consumption. *Sci. Rep.* 5, 14340.
52. Qiang, L., Cheng, J., 2019. Exposure to microplastics decreases swimming competence in larval zebrafish (*Danio rerio*). *Ecotoxicol. Environ. Saf.* 176, 226-233.
53. R Core Team (2013). R: A language and environment for statistical computing. R Foundation for Statistical Computing, Vienna, Austria. URL <http://www.R-project.org/>.
54. Rodrigues, J.P., Duarte, A.C., Santos-Echeandía, Rocha-Santos, T., 2019. Significance of interactions between microplastics and POPs in the marine environment: A critical overview. *Trends Anal. Chem.* 111, 252-260.
55. Sánchez-Bayó, F., 2006. Comparative acute toxicity of organic pollutants and reference values for crustaceans. I. Branchiopoda, Copepoda and Ostracoda. *Environ. Pollut.* 139, 385-420.
56. Santana, M.S., Sandrini-Neto, L., Neto, F.F., Ribeiro, C.A.O., Di Domenico, M., Prodocimo, M.M., 2018. Biomarker responses in fish exposed to polycyclic aromatic hydrocarbons (PAHs): Systematic review and meta-analysis. *Environ. Pollut.* 242, 449-461.
57. Setälä, O., Fleming-Lehtinen, V., Lehtiniemi, M., 2014. Ingestion and transfer of microplastics in the planktonic food web. *Environ. Pollut.* 185, 77-83.
58. Sleight, V.A., Bakir, A., Thompson, R.C., Henry, T.B., 2017. Assessment of micropalstic-sorbed contaminant bioavailability through analysis of biomarker gene expression in larval zebrafish. *Mar. Pollut. Bull.* 116, 291-297.
59. Sogbanmu, T.O., Nagy, E., Philips, D.H., Arlt, V.M., Otitolaju, A.A., Bury, N.R., 2016. Lagos lagoon sediment organic extracts and polycyclic aromatic hydrocarbons induce embryotoxic, teratogenic and genotoxic effects in *Danio rerio* (zebrafish) embryos. *Environ. Sci. Pollut. Res.* 23, 14489-14501.
60. Suman, T.Y, Jia, P-P., Li, W-G., Junaid, W., Xin, G-Y., Wang, Y., Pei, D-S., 2020. Acute and chronic effects of polystyrene microplastics on brine shrimp: First evidence highlighting the molecular mechanism through transcriptome analysis. *J. Hazard. Mater.* 400, 123220.

61. Teuten, E.L., Rowland, S.J., Galloway, T.S., Thompson, R.C., 2007. Potential for plastics to transport hydrophobic contaminants. *Environ. Sci. Technol.* 41, 7759-7764.
62. van Pomeran, M., Brun, N.R., Peijnenburg, W.J.G.M., Vijver, M.G., 2017. Exploring uptake and biodistribution of polystyrene (nano)particles in zebrafish embryos at different developmental stages. *Aquat. Ecotoxicol.* 190, 40-45.
63. Vendel, A.L., Bessa, F., Alves, V.E.N., Amorim, A.L.A., Patrício, J., Palma, A.R.T., 2017. Widespread microplastic ingestion by fish assemblages in tropical estuaries subjected to anthropogenic pressures. *Mar. Pollut. Bull.* 117, 448-455.
64. Waller, C.L., Griffiths, H.J., Waluda, C. M., Thorpe, S.E., Loaiza, I., Moerno, B., Pacherres, C.O., Hughes, K.A., 2017. Microplastics in the Antarctic marine system: An emerging area of research. *Sci. Total Environ.* 598, 220-227.
65. Wang, Y., Zheng, M., Zhang, M., Ding, G., Sun, J., Du, M., Liu, Q., Cong, Y., Jin, F., Zhang, W., Wang J., 2019a. The uptake and elimination of polystyrene microplastics by the brine shrimp, *Artemia parthenogenetica*, and its impact on its feeding behaviour and intestinal histology. *Chemosphere* 234, 123-131.
66. Wang, Y., Zhang, D., Zhang, M., Jingli, M., Ding, G., Mao, Z., Cao, Y., Jin, F., Cong, Y., Wang, L., Zhang, W., Wang, J., 2019b. Effects of ingested polystyrene microplastics on brine shrimp, *Artemia parthenogenetica*. *Environ. Pollut.* 244, 514-722.
67. Weigt, S., Huebler, N., Strecker, R., Braunbeck, T., Broschard, T.H., 2011. Zebrafish (*Danio rerio*) embryos as a model for testing proteratogens. *Toxicology* 281, 25-36.
68. Wu, P., Huang, J., Zheng, Y., Yang, Y., Zhang, Y., He, F., Chen, H., Quan, G., Yan, J., Li, T., Gao, B., 2019. Environmental occurrences, fate, and impacts of microplastics. *Ecotoxicol. Environ. Saf.* 184, 109612.
69. Zhao, Y., Luo, K., Fan, Z., Huang, C., Hu, J., 2013. Modulation of benzo[a]pyrene-induced toxic effects in japanese medaka (*Oryzias latipes*) by 2,2',4,4'-tetrabromodiphenyl ether. *Environ. Sci. Technol.* 47, 13068-13076.

SUPPORTING INFORMATION

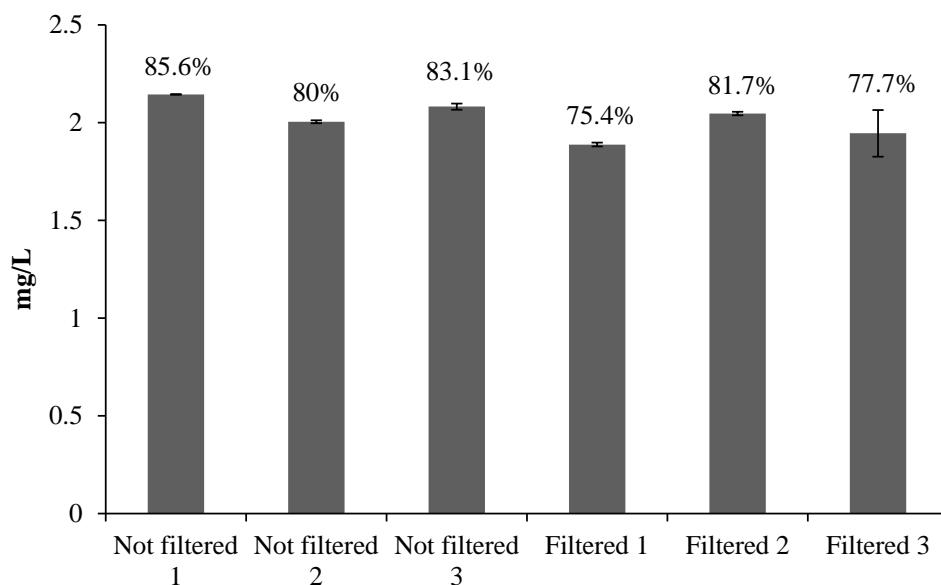


Fig. S1- Measured concentration from a nominal concentration of 2.51 mg/L or 5.10^4 particles/mL of 4.5 μm MPs using a cell counter before and after filtration using a polyethersulfone filter (0.45 μm filter pore). Bars represent the mean of 3 instrumental replicates with their corresponding standard deviation. The percentage of MP measured from the nominal concentration is given above each bar.

Table S1- Effect on survival (%) of the exposure of 24 hph and 48 hph brine shrimp larvae to DMSO for 24 h and 48 h.

Concentration (v/v)	24 hph		48 hph	
	24 h	48 h	24 h	48 h
0	100	97	100	97
0.01%	97	93	97	93
0.10%	100	93	100	100

Results and discussion

Table S2- Odd ratio values indicating the risk of death (immobilisation) for brine shrimp larvae exposed to MPs alone or in combination with B(a)P.

Treatment test		Treatment for comparison	Conc. (mg/L)	Odd ratio	Confidence interval (5%, 95%)	p value
0.5 µm MPs-B(a)P	24 hph 48 h	Control	0.00034	1.94 10 ⁵⁴	7.83 10 ⁵⁰ - 4.78 10 ⁵⁷	0
			0.00069	1.94 10 ⁵⁴	7.83 10 ⁵⁰ - 2.71 10 ²⁷¹	0
	48 hph 48 h	Control	6.87	1.422	1.179 - 1.715	0.000
B(a)P	24 hph 48 h	Control	0.00034	1.94 10 ⁵⁴	7.83 10 ⁵⁰ - 2.72 10 ²⁷¹	0
			0.1	2.82 10 ⁸	25.257 - 3.16 10 ¹⁵	0.008
			0.5	196	7.939 - 4838.811	0.000
			1	10.706	2.148 - 53.348	0.001
			5	1.741	1.263 - 2.399	0.000
0.5 µm MPs-B(a)P	24 hph 48 h	0.5 µm MPs	0.00069	9.333	1.866 - 46.683	0.001
			6.87	24.182	4.808 - 121.625	0.000
	48 hph 48 h	0.5 µm MPs	0.00034	25.375	3.050-211.104	0.000
			0.687	22.176	2.661-184.798	0.000
			6.87	19.333	2.313-161.565	0.000
4.5 µm MPs-B(a)P	24 hph 48 h	4.5 µm MPs	0.025	19.333	2.313 - 161.565	0.000
			0.501	10.706	2.148 - 53.348	0.001
			50.1	16.789	2.001 - 140.898	0.001
4.5 µm MPs-B(a)P	24 hph 48 h	0.5 µm MPs-B(a)P	5.01, 6.87	0.706	0.539 - 0.924	0.009
			48 hph 48 h	0.5 µm MPs-B(a)P	0.501, 0.687	0.617
	48 hph 48 h	0.5 µm MPs-B(a)P	5.01, 6.87	0.639	0.450 - 0.906	0.006

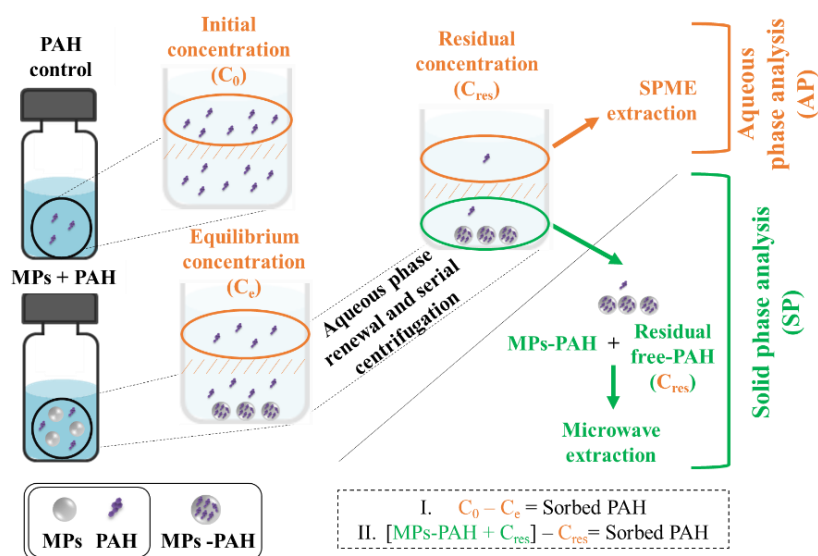
Table S3- Odd ratio values indicating the risk of malformation in 120 hpf zebrafish embryos exposed to 4.5 μm MPs alone or in combination with B(a)P or to B(a)P alone.

Treatment test	Treatment for comparison	Conc. (mg/L)	Odd ratio	Confidence interval (5%, 95%)	p value
4.5 μm MPs-B(a)P	Control	50.1	1.045	1.019 - 1.072	0.0001
B(a)P	Control	5	1.373	1.081 - 1.744	0.0063
		10	1.239	1.098 - 1.397	0.0002
4.5 μm MPs-B(a)P	4.5 μm MPs	50.1	5.71	1.82 - 20.66	0.0000

Table S4. Effects of 120 h DMSO exposure on developmental parameters of zebrafish embryos.

Concentration (% v/v)	% survival	hatching time (h)	% malformed embryos
0.0	100	70.0	8.3
0.01	100	68.7	10.0
0.1	100	69.3	13.3

CHAPTER 2. Sorption of benzo(a)pyrene and of a complex mixture of petrogenic PAHs onto polystyrene microplastics



ABBREVIATIONS

AP, Aqueous phase

B(a)P, Benzo(a)pyrene

CAT, Catalase

DDT, 1,1'-(2,2,2-trichloroethane-1,1-diyl)bis(4-chlorobenzene)

DMSO, Dimethyl sulfoxide

GC/MS, Gas chromatography- mass spectrometry

L.Q., Limit of quantification

MLOQ, Method limit of quantification

MPs, Microplastics

n.d., Not detected

NPs, Nanoplastics

NNS, Naphthenic North Sea

PAHs, Polycyclic aromatic hydrocarbons

PE, Polyethylene

PP, Polypropylene

POPs, Persistent organic pollutants

PS, Polystyrene

SP, Solid phase

SPME; Solid phase micro extraction

WAF, Water accommodated fraction

ABSTRACT

Microplastics (MPs) largely occur in aquatic ecosystems due to degradation of larger plastics or release from MP-containing products. Due to the hydrophobic nature and large specific surface of MPs, other contaminants, such as polycyclic aromatic hydrocarbons (PAHs), can potentially sorb onto MPs. Several studies have addressed the potential impact of MPs as vectors of PAHs for aquatic organisms, therefore the role of MPs as sorbents of these compounds should be carefully investigated. The present study aimed to determine sorption capacity of benzo(a)pyrene (B(a)P), as a model pyrolytic PAH, to polystyrene MPs of different sizes (4.5 and 0.5 μm). In addition, sorption of PAHs present in the water accommodated fraction (WAF) of a naphthenic North Sea crude oil to 4.5 μm MPs was also studied, as model of a complex mixture of petrogenic PAHs that could appear in oil-polluted environments. Results indicated that 0.5 μm MPs showed higher maximum sorption capacity (Q_{max}) for B(a)P (145-242.89 $\mu\text{g/g}$) than 4.5 μm MPs (30.50-67.65 $\mu\text{g/g}$). From the WAF mixture, naphthalene was sorbed at a higher extent than the other PAHs to 4.5 μm MPs, but with weak binding interactions ($K_f=69.25$ L/g; $1/n=0.46$) according to the analysis of the aqueous phase, whereas phenanthrene showed stronger binding interactions ($K_f=0.24$ L/g; $1/n=0.98$) based on analysis of the solid phase. Sorption of PAHs of the complex WAF mixture to 4.5 μm MPs was relatively limited and driven by the hydrophobicity and initial concentration of each PAH. Overall, results indicate that sorption estimations based solely on the analysis of the aqueous phase could overestimate the capacity of MPs to carry PAHs. Therefore, controlled laboratory assays assessing the “Trojan Horse effect” of MPs for aquatic organisms should consider these findings in order to design accurate and relevant experimental procedures.

Keywords: Microplastics, polystyrene, sorption, benzo(a)pyrene, competition.

INTRODUCTION

The wide spread use of plastic in consumer products due to their resistance and durability to degradation has become an issue of concern in the last years. The production of plastics has increased worldwide from 230 million tons in 2005 to 359 million tons in 2018 (Plastic Europe, 2019) leading to a rise of the amount of plastic waste entering in aquatic ecosystems mostly by rivers ending into the oceans (Lebreton et al., 2017). Plastic can be degraded in the environment by physical and chemical processes producing small plastics known as secondary microplastics (MPs, <5 mm). Plastic is also manufactured to produce small size particles (primary MPs) that are incorporated into personal care products and used in industrial applications such as abrasives (Boucher et al., 2017). Discharge of these primary MPs during manufacture and use also contributes to the input of small plastic items to the aquatic ecosystems. MPs are reported worldwide in the aquatic ecosystems (Chae and An, 2017) at concentrations ranging from 0.002 to 102000 items/m³ for marine ecosystems (Shahul et al., 2018). The most frequent polymers reported in aquatic ecosystems are polyethylene (PE), polypropylene (PP) and polystyrene (PS) (Duis and Coors, 2016; Li et al., 2020).

Due to their hydrophobic nature and large specific surface, MPs can sorb persistent organic pollutants (POPs) present in the environment, thus modulating their bioavailability and hazard. Mato et al. (2001) showed for the first time remarkable capacity of plastic resin pellets as a transport medium for POPs in the environment. Afterwards, controlled laboratory experiments investigated the sorption of polycyclic aromatic hydrocarbons (PAHs) to MPs of different composition (Hüffer and Hoffman, 2016; Ma et al., 2016; Wang and Wang, 2018b), as relevant POPs widely distributed on aquatic ecosystems. These experiments show that the properties (density, porosity) of the polymer play an important role in the PAH sorption process and that PS could play an important role as carrier of POPs. It has also been proven that a larger surface to volume ratio of MPs can lead to a higher sorption of pollutants present in the water column (Ma et al., 2016; Li et al., 2019; Wang et al., 2019).

Diverse methodologies have been applied to assess sorption of POPs onto MPs. Extraction is an especially sensitive step, due to the potentially damaging effect of the solvents used for extraction on the MPs. For instance, the use of methanol and dichloromethane combined with fluid extraction resulted in a complete dissolution of the MPs (Fuller and Gautman, 2016). A summary of different analytical procedures has been compiled by Rios Mendoza et al. (2016) who showed that gas chromatography-mass spectrometry (GC/MS) is the most suitable analytical technique and that a great variety of solvents and extraction techniques are available. Few studies have undertaken the direct analysis of the PAHs sorbed to MPs (solid phase, SP) due to the aforementioned fragility of MPs (Teuten et al., 2007; Bakir et al., 2012). Most studies estimate

Results and discussion

the sorption of PAHs only measuring the difference in the concentration of the aqueous phase (AP) after MP incubation (Fries and Zarfl, 2012; Ma et al., 2016; Wang and Wang, 2018b; Lin et al., 2019; Wang et al., 2019). However, in order to properly assess the sorption of POPs to MPs in controlled experiments, a methodology that takes into account both phases (Teuten et al., 2007) is required.

PAHs are included in the EPA priority pollutant list because of their ubiquitous distribution in the environment and because some members of this chemical class such as benzo(a)pyrene (B(a)P) are prominent and strong carcinogens (Akcha et al., 2003). B(a)P is widely used in ecotoxicological assays as model carcinogenic compound, but in the real environment pollutants do not appear isolated but form complex mixtures and interacting with each other. The oil derived PAHs are also reported as a threat for aquatic organisms (Perrichon et al., 2016), especially the most water soluble PAHs (naphthalene and phenanthrene) that appear at elevated concentrations in water after spills of many types of oils (Kappell et al., 2014), being therefore the most likely to be present in plastic particles in the environment at places with high pollution pressure (Foshtomi et al., 2019). PAHs behave differently individually or in mixture towards MPs (Khan et al., 2007; Bakir et al., 2012). The hydrophobicity, solubility of each compound, initial concentration and presence of co-solutes seem to be relevant factors to take into account for sorption of PAH mixtures to a sorbent (Lamichhane et al., 2016).

The MP ability to act as carriers of POPs can lead to a phenomenon known as “Trojan Horse effect” (Koelmans et al., 2013; Bakir et al., 2015). MPs with sorbed POPs are susceptible of being ingested by aquatic organisms where those compounds can be released provoking toxic effects. The large majority of the studies addressing the “Trojan Horse effect” in aquatic organisms are performed using PS microspheres as model MPs (Shen et al., 2019; Strungaru et al., 2019). This is partly explained by the availability of well-characterised and homogeneous particles of a wide range of sizes, especially of small size (few microns), and characteristics (i.e. fluorescent, functionalised) manufactured by commercial providers. Therefore, we consider important an analysis of the PAH sorption to PS MPs small than 10 μm , which are studied at lesser extent than larger MPs (Fred-Ahmadu et al., 2020). These small particles are more easily uptaken by a wide range of aquatic organisms. The small size of these particles make them available for the planktonic species that play a key role in the food chain as the lowest trophic level (Carbery et al., 2018).

The aims of the present work were: (I) to assess the sorption capacity of two different sized PS MPs (4.5 and 0.5 μm) for a model pyrolytic PAH of high molecular weight such as benzo(a)pyrene (B(a)P); (II) to assess the sorption capacity of 4.5 μm PS MPs for PAHs present in the WAF of a naphthenic North Sea (NNS) crude oil, as an environmentally relevant mixture

of petrogenic PAHs of low molecular weight. To accomplish these objectives, the two phases of the sorption process were considered: AP where the free or dissolved PAHs are present, and SP or MPs, where sorbed PAHs are measured. Modelling of sorption isotherms was applied to estimate the different sorption coefficients in order to compare with previous studies. Ultimately, this work aimed to provide the basis for the design of ecotoxicological studies in order to assess the Trojan horse effect of MPs for aquatic organisms.

MATERIALS AND METHODS

Materials and chemicals. Aqueous suspensions (2.5% solids, w/v) of PS microspheres of 4.5 and 0.5 μm in diameter were purchased from Polysciences, Inc. (Warrington, USA). According to the information provided by the manufacturer, particles were monodispersed (coefficient of variance < 10%) and inert. Particles presented a glass transition temperature of 95 °C, density: 1.05 g/cm³, refractive index at 589 nm of 1.59.

B(a)P (purity $\geq 96\%$), its internal standard (B(a)P d₁₂), other 18 deuterated PAHs and dimethyl sulfoxide (DMSO, purity $\geq 96\%$) were purchased from Sigma-Aldrich (St. Louis, USA). Unless otherwise specified, other solvents such as methanol (HPLC grade) and isooctane (HPLC grade), and reagents were also purchased from Sigma-Aldrich. The NNS crude oil was provided by Driftslaboratoriet Mongstad, Equinor (former Statoil).

Conditioned water, used to emulate the sorption process of PAHs to MPs in a real medium for freshwater fish, such as zebrafish, commonly used in ecotoxicology, was prepared from deionised water and commercial salt (SERA, Heinsberg, Germany). The initial pH and conductivity were adjusted to 7-7.5 and 600 $\mu\text{S}/\text{cm}$, respectively.

Preparation of PAH solutions. Stocks of 1, 0.1 and 0.01 g/L B(a)P were prepared in 100% DMSO from an initial concentration of 10 g/L. Solutions of 100, 10 and 1 $\mu\text{g}/\text{L}$ (0.01% DMSO (v/v) used in the sorption experiments were prepared in deionised water. These concentrations were selected based on previous studies assessing the potential toxicity of MPs combined with PAHs (Batel et al., 2016). Considering GC/MS analyses, solutions of B(a)P d₁₂ were prepared in ethanol (2 $\mu\text{g}/\text{g}$) for solid phase micro extraction (SPME) or in isooctane for direct injection (2 $\mu\text{g}/\text{g}$). WAF was prepared following Singer et al. (2000). A small glass bottle was filled with 130 mL of conditioned water and 0.65 g of NNS oil. The bottle was wrapped with aluminium foil and placed in a magnetic stirrer (IKA®-Werke GmbH & Co. KG, Staufen, Germany) at 800 rpm, without vortexing, and 21 °C. After 40 h, the AP (100% WAF) was collected, avoiding taking oil droplets, and stored at -20 °C in a glass bottle until chemical analysis. Dilutions were made in conditioned water to obtain 50% and 25% WAF solutions (v/v) for sorption experiments. Solutions of the 18 deuterated PAHs were prepared in ethanol (initial stock solution at 2 $\mu\text{g}/\text{g}$ and

Results and discussion

diluted ones) for SPME/GC/MS analyses and in isooctane (initial stock solution at 8 µg/g and diluted ones) for direct injections.

Sorption experiments. 50 mg/L of MPs of 4.5 and 0.5 µm were incubated (in triplicate) for 24 h in capped aluminium-wrapped glass vials containing 10 mL of 100, 10 or 1 µg/L B(a)P or 100, 50 and 25% NNS oil WAF. All materials used in this study were made of glass in order to avoid loss of PAHs due to sorption to other plastic surfaces. Incubation time was also selected according to the literature (Teuten et al., 2007; Batel et al., 2016; Wang and Wang, 2018a). Sorption equilibrium was expected to be reached in the first day of incubation although it might depend on the polymer, MP size, as well as on studied PAHs (Teuten et al., 2007; Wang and Wang, 2018a). Elevated concentrations (400 mg/L) of several types of polymers (100-250 µm PE, PS, PP and PVC) reached sorption equilibrium for phenanthrene (100 µg/L) between 24 h and 48 h of incubation (Teuten et al., 2007; Wang and Wang, 2018a). Thus, shorter time of equilibrium could be expected for smaller MPs. PAH solutions without MPs (SP) were processed in parallel to monitor potential (PAH loss due to degradation, sorption onto the vial walls or to other factors during the experimental procedure). Vials were maintained in an orbital shaker (M1000 VWR, Thorofare, USA) at 300 rpm and 21±1°C in darkness. After incubation, samples were centrifuged (Hettich Universal 32R centrifuge, Tuttlingen, Germany) at 3000 g and 4 min for 4.5 µm MPs, and 5423 g and 45 min for 0.5 µm MPs, according to manufacturer's instructions. The supernatants were removed, the pellets were washed and resuspended in deionised water and centrifuged again in the same conditions. This step was repeated three times. The supernatants from the first (CE1, free PAHs) and 4th (CE4, residual free PAHs) centrifugations were placed in new vials, while supernatants from the 2th and 3th centrifugations were discarded. All fractions were weighted for mass balance calculation. Then, CE1 samples were diluted up to 1 µg/L according to nominal concentration with deionised water in 10 mL glass SPME vials. SPME consisted in a heating process at 40 °C with 35 min stirring period at 250 rpm of the polydimethylsiloxane (100 µm PDMS) fibre (Supelco, Sigma-Aldrich, South Africa). After extraction, the fibre was thermally desorbed into the GC/MS system (Agilent GC 7890A/Agilent MSD 5975C, Agilent Technology, California) for 10 min at 280 °C. The CE4 samples and the pellets containing the MPs were frozen and freeze dried (Fisher Bioblock Scientific, Illkirch, France) and, then, resuspended in methanol (**Fig. S1**). PAHs were extracted from MPs by two serial extraction steps of 10 min each by a microwave extraction system (Start E, Milestone, Leutkirch, Germany) in a temperature curve up to 70 °C (5 min at 900 W and 5 min at 500 W). Methanol was evaporated with argon gas flux and the extracts were resuspended in isooctane and further injected in pulsed splitless injection mode into the GC/MS system. A blank analysis was carried out to ensure the absence of contamination prior and during analysis. The quality

assurance and controls (extraction efficiency, limits of quantification and control charts) that were carried out are reported on the Supporting Information (**Fig. S2, Table S1-Table S3**).

Sorption models. Using the information obtained through the analysis of the AP and of the SP, MP sorption capacity was calculated using two approaches. Values of sorption were expressed as Q_e , which is the sorption concentration of the PAH to MPs at equilibrium and it was calculated as follows for the AP (equation 1):

$$Q_e = \frac{(C_0 - C_e)V}{M} \quad (1)$$

where C_e ($\mu\text{g/L}$) is the equilibrium concentration in the AP, C_0 ($\mu\text{g/L}$) is the average PAH concentration of the control sample after centrifugation, V (L) is the medium volume and M (g) is the plastic mass.

For the SP, equation 2 was used to calculate Q_e values:

$$Q_e = \frac{M_{ext} - C_{res}V_{res}}{M} \quad (2)$$

where M_{ext} (μg) is the extracted PAH mass, C_{res} (μg) is the residual PAH mass remaining in the AP, V_{res} is the volume of the residual PAH fraction that remained after last supernatant removal and M (g) is the plastic mass. In order to evaluate the sorption capacity of the MPs of the different sizes for PAHs, the linear, Langmuir and Freundlich sorption isotherm models were applied (**Table 1**; Yang and Xing, 2010; Wang and Wang, 2018b). A linear adaptation of Langmuir and Freundlich models was used for graphic representation and parameter acquisition.

Table 1. Equations describing the different sorption models and their linear adaptation for graphic representation.

Model	Equation	Graphic representation of equation
Linear model	$Q_e = K_d \cdot C_e$	$Q_e = K_d \cdot C_e$
Langmuir model	$Q_e = Q_{max} \cdot b \cdot C_e / (1 + b \cdot C_e)$	$1/Q_e = 1/Q_{max} + 1/(b \cdot Q_{max}) \cdot 1/C_e$
Freundlich model	$Q_e = K_f \cdot C_e^{1/n}$	$\text{Log } Q_e = \text{log } K_f + 1/n \cdot \text{log } C_e$

Q_e ($\mu\text{g/g}$): sorption concentration of PAHs to MPs at equilibrium; C_e ($\mu\text{g/L}$): equilibrium solution phase concentration of PAHs; K_d : partition coefficient of PAH between plastic (MPs) and aqueous phase at equilibrium (L/g); Q_{max} : maximum amount of the PAH per weight unit of MPs ($\mu\text{g/g}$); b : Langmuir constant related to the affinity of binding sites (L/ μg); K_f : sorption capacity (L/g); $1/n$: degree of dependence of sorption at equilibrium.

RESULTS AND DISCUSSION

Sorption of B(a)P to MPs of different sizes. In the experiments with 4.5 μm MPs, the measured B(a)P mass in initial incubation solutions was lower (68-43%) than the nominal mass (**Table 2**). Similar values were obtained in the experiment with 0.5 μm MPs (54-48%). B(a)P is a highly hydrophobic PAH (water solubility: 1.62 $\mu\text{g/L}$; ChemIDplus, 2020). Therefore, in laboratory experiments, DMSO is commonly used as vehicle to increase B(a)P solubility up to 10-50 mg/mL (Keith and Walters, 1991). Nevertheless, transfer of B(a)P from DMSO to a water phase provokes aggregation and precipitation for concentrations higher than its water solubility. Despite these limitations, the selected concentrations allow to contaminate MPs in a short time (Wang and Wang et al., 2018a), which is further needed to perform experiments to assess the potential “Trojan Horse effect” produced by MPs with sorbed PAHs.

B(a)P mass in the control samples varied depending on centrifugation conditions, which, in turn, depended on MP size. Thus, B(a)P controls run for the MPs of the two sizes resulted in different recovery values. For 0.5 μm MPs, the increased centrifugation speed and time resulted in a B(a)P recovery of $\approx 60-90\%$, while for 4.5 μm MPs almost 100% was recovered. The amount of B(a)P mass in the AP after centrifugation of MPs-B(a)P samples was also lower for 0.5 μm MPs (48.92 ± 1.63 ng) than for 4.5 μm MPs (533.85 ± 58.82 ng) for the highest incubation concentration. The residual mass in the AP (CE4) was less than 20% of the B(a)P control mass and, therefore, almost no interference for SP analysis was assumed. 0.5 μm MP samples showed higher difference (13-20.5%) than 4.5 MPs (0-0.55%) between residual and control samples. Sorbed B(a)P mass measured in SP was higher for 0.5 μm MPs (133.01 ± 35.49 , 17.93 ± 2.15 and 2.50 ± 0.53 ng) than for 4.5 μm MPs (28.11 ± 17.32 , 6.36 ± 1.42 and 0.94 ± 0.05 ng) at the three sorption concentrations used. Thus, using both AP and SP approaches, results show that, for the same plastic mass; 0.5 μm MPs are able to sorb a higher amount of B(a)P than 4.5 μm MPs. Previous studies have also proved that a decrease in MP size increases the capacity of sorption of POPs. Batel et al. (2016) analysed the AP after filtration and found that 1-5 μm fluorescent PS MPs showed higher B(a)P sorption capacity than 10-20 μm PS MPs. A MP size decrease of 4-10 times resulted in a decrease of 4 times of the total mass of B(a)P found in the AP. In our study, a 10 times decrease of size of PS MPs decreased 10-fold the B(a)P measured mass in the AP.

Table 2. B(a)P mass (in ng) in the different measured fractions.

	Nominal sorption mass	Initial measured mass		Mass in the aqueous phase (AP, CE1)	Residual mass (AP, CE4)	Sorbed mass (SP)	
	1000	681.00±61.27	B(a)P control	665.25 (98%)	-	-	
			MPs-B(a)P	533.85±58.82	0.30±0.22	28.11±17.32	
	4.5 µm	100	52.90±2.39	B(a)P control	50.18 (95%)	-	-
				MPs-B(a)P	28.73±12.17	0.16±0.10	6.36±1.42
	10	4.34±0.38	B(a)P control	4.33 (100%)	-	-	
			MPs-B(a)P	2.44±0.43	<L.Q.	0.94±0.05	
	Blank	n.d.		n.d.			
	1000	546.19±34.04	B(a)P control	316.71 (58%)	-	-	
			MPs-B(a)P	48.92±1.63	6.33±1.08	133.01±35.49	
	0.5 µm	100	50.76±7.31	B(a)P control	34.70 (68%)	-	-
				MPs-B(a)P	5.11±0.30	0.99±0.48	17.93±2.15
	10	4.84±0.68	B(a)P control	4.43 (92%)	-	-	
			MPs-B(a)P	0.39±0.04	0.08(*)	2.50±0.53	
			Blank	n.d.		n.d.	

L.Q.: limit of quantification (see Table S1); n.d.: not detected; -: not analysed; (): recovery percentage from initial mass; *: value obtained from 1 replicate because the other replicates showed values below L.Q. or not detectable.

The percentage of described B(a)P by analysing one phase (AP) or the two phases (AP and SP) for both MP sizes is shown in **Fig. 1**. Most studies estimate the amount of the sorbed compounds based on the difference of concentration in the initial incubation solution and in the AP after SP separation by filtration (Fries and Zarfl, 2012; Ma et al., 2016; Wang and Wang, 2018b; Lin et al., 2019; Wang et al., 2019). Our results for both MP sizes show that the percentage of B(a)P measured in the SP is markedly lower than the percentage estimated from the measurement of the AP (**Fig. 1**). According to the data obtained only with the analysis of the AP, the 4.5 µm MPs would have sorbed 43% of the B(a)P versus the 13% of B(a)P measured from SP, in the case of MP incubation in the intermediate B(a)P concentration (10 µg/L). For 0.5 µm MPs the differences in terms of percentage are higher, ranging from 91% of B(a)P sorbed based on the analysis of the AP versus 56% of B(a)P sorbed based on the analysis of the SP, for the lowest initial B(a)P concentration (1 µg/L). As shown by our results and by Teuten et al. (2007) a methodology that includes the analysis of the two phases is the most accurate method for an aqueous-solid sorption phenomenon. These authors evaluated the sorption capacity of polyvinyl chloride, PP and PE

Results and discussion

(200-250 μm) for phenanthrene in seawater. The analysis of the AP and the SP allowed to explain between 74% (PP) and 85% (PE) of phenanthrene, which is similar to the results obtained in the present study for B(a)P.

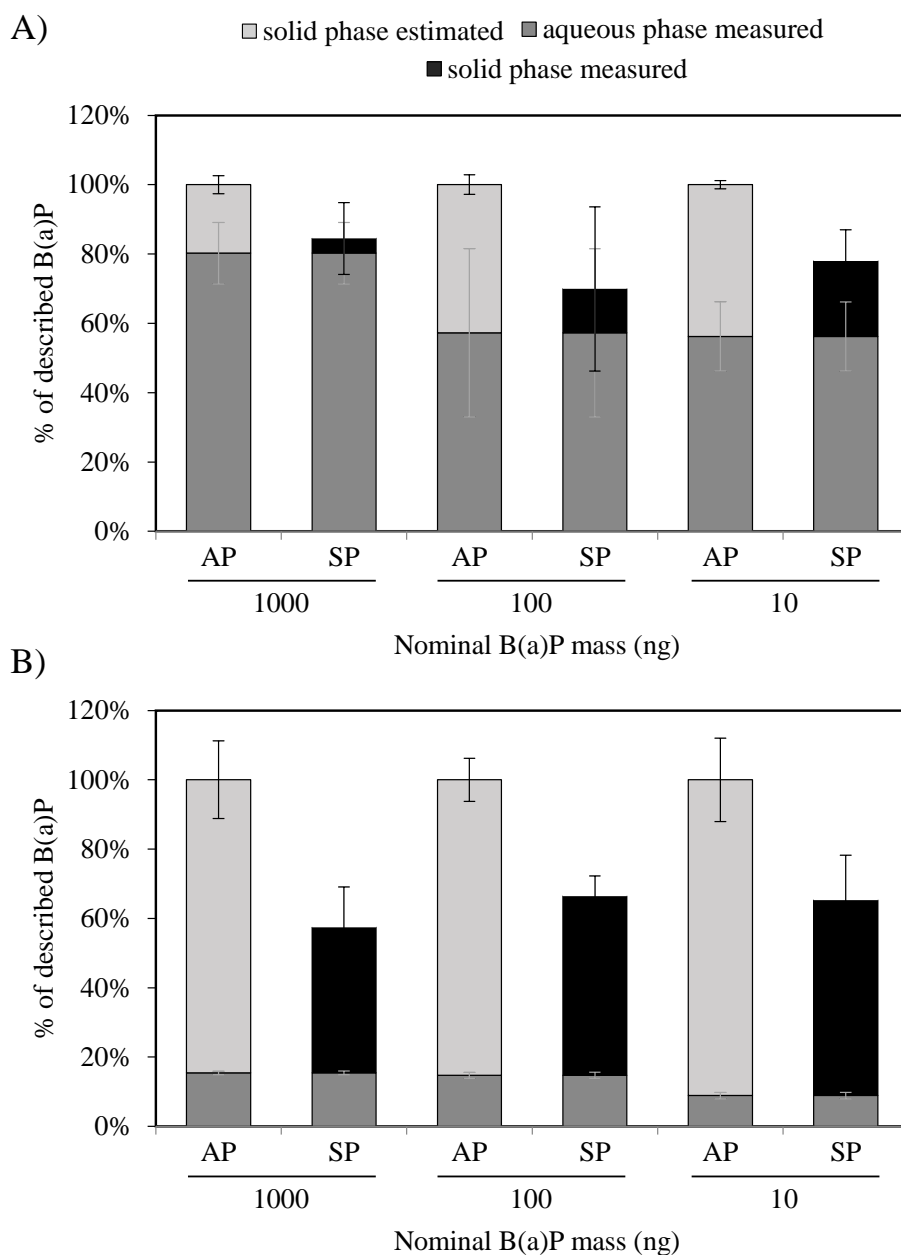


Fig. 1. Percentage of described B(a)P mass for A) 4.5 μm MPs and for B) 0.5 μm MPs according to measurements done in the aqueous phase (AP) or in aqueous and in solid phases (SP).

The percentage of sorbed B(a)P increases with the decrease of initial B(a)P mass for both MP sizes (Table 2, Fig. 1). Wang and Wang (2018b) observed a decrease of the sorption efficiency of phenanthrene to 200-250 μm PS MPs from 55.9 to 32.7% when the initial concentration was increased (0-100 $\mu\text{g/L}$). On the other hand, the percentage of B(a)P sorbed measured is lower than

the expected value for 0.5 μm MPs with a difference of 20% to 40%, and for 4.5 μm MPs with 10% to 25% in the three analysed concentrations. That seems to be related to the total surface area, smaller MPs display larger total surface area than larger MPs at the same MP concentration. A higher surface means more sorption sites, that are potential points of PAH adsorption interactions (hydrophobic and π - π binding interaction) onto the MPs. These adsorption interactions are more labile than absorption interaction, due to the porosity of the material, that could account in higher extent for sorbed B(a)P in larger particles (White and Pignatello, 1999; Lin et al., 2019). Thus, higher B(a)P desorption could be expected from the small MPs (Fred-Ahmadu et al., 2020) during centrifugation and cleaning steps.

WAF characterisation and sorption of PAHs from crude oil WAF to 4.5 μm MPs. WAF produced from the NNS oil presented low PAH concentration (ΣPAHs = 300.94 $\mu\text{g/L}$; **Table S4**) as expected for a low energy WAF (Singer et al., 2000; Perrichon et al., 2016; Katsumiti et al., 2019). Low energy WAFs (24 h at 21 $^{\circ}\text{C}$) produced from Arabian Light crude oil (BAL 110) and Erika heavy fuel oil (HFO, no. 2) resulted in similar PAH concentrations, 6.16-170.81 $\mu\text{g/L}$ and 26.10- 257.03 $\mu\text{g/L}$, respectively (Perrichon et al., 2016). Naphthalene (292 $\mu\text{g/L}$) followed by fluorene and phenanthrene (4.438 and 3.095 $\mu\text{g/L}$, respectively) were the most abundant PAHs. From the 18 PAHs analysed, only 8 PAHs (the least heavy and hydrophobic ones) were detected in the three WAF dilutions. Thus, the WAF produced from the NNS oil was mostly composed of volatile compounds; the most hydrophobic and potentially toxic compounds were not present or below detection limits.

The naphthalene, fluorene and phenanthrene masses for the different fractions are shown in **Table 3**. Only PAHs that appeared in concentrations above quantification limits in the AP and in the SP after the sorption to MPs were analysed. Measurements in the AP of control samples indicated good recoveries, above 75% in most cases, except for phenanthrene in 25% and 100% WAF. PAH masses were reduced in the AP for MPs-PAH samples compared to control PAH samples for the three studied PAHs. Naphthalene showed the highest decrease in the AP of 100% WAF, from 1895.97 ng to 1617.94 \pm 123.06 ng. Fluorene and phenanthrene followed with a mass change from 31.03 ng to 19.21 \pm 2.87 ng and from 13.56 ng to 11.74 \pm 0.90 ng, respectively. Usually, PAH hydrophobicity ($\log K_{ow}$) is the main factor explaining sorption of PAHs to MPs (Hüffer and Hofmann, 2016; Wang and Wang, 2018). According to this, we expected that phenanthrene ($\log K_{ow}$ = 4.46) would be sorbed at the highest extent, followed by fluorene ($\log K_{ow}$ = 4.18) and naphthalene ($\log K_{ow}$ = 3.30). Nevertheless, in a complex PAH mixture, other factors could be more relevant and should be taken into account to understand sorption behavior to MPs.

Results and discussion

Table 3. PAH mass (in ng) for the different fractions measured.

	WAF dilution	Initial measured mass		Mass in the aqueous phase (AP, CE1)	Residual mass (AP, CE4)	Sorbed mass (SP)
Naphthalene	100%	2316.55±241.11	Napht control	1895.97 (82%)	-	-
			MPs-Napht	1617.94±123.06	10.51±3.00	0.58±0.39
	50%	928.39±25.45	Napht control	851.09 (92%)	-	-
			MPs-Napht	618.84±41.70	3.49±1.82	0.13±0.06
	25%	428.59±11.57	Napht control	326.93 (76%)	-	-
			MPs-Napht	258.89±15.52#	2.22±0.47#	0.12±0.03#
		Blank	n.d.			0.08
Fluorene	100%	35.13±1.23	Fluo control	31.03 (88%)	-	-
			MPs-Fluo	19.21±2.87	0.21±0.09	0.13±0.07
	50%	15.83±0.65	Fluo control	13.99 (88%)	-	-
			MPs-Fluo	12.32±0.67	<L.Q.	0.07*
	25%	7.91±0.35	Fluo control	8.36 (106%)	-	-
			MPs-Fluo	5.08±0.012#	<L.Q.	0.05#
		Blank	n.d.			n.d.
Phenanthrene	100%	24.50±1.68	Phe control	13.56 (55%)	-	-
			MPs-Phe	11.74±0.90	0.17±0.06	0.43±0.10
	50%	11.16±0.26	Phe control	9.29 (83%)	-	-
			MPs-Phe	8.19±0.39	<L.Q.	0.25±0.07
	25%	5.68±0.06	Phe control	3.93 (69%)	-	-
			MPs-Phe	3.38±0.03#	<L.Q.	0.24±0.05#
		Blank	n.d.			0.17

L.Q.: limit of quantification (see Table S1); n.d.: not detected; -: not analysed; (:): recovery percentage from initial mass; #: value obtained from 2 data; *: value obtained from 1 replicate because the other replicates showed values below L.Q. or not detectable.

One of these factors is the co-solute phenomenon, as competition among PAHs in the mixture could occur. According to Wang and Wang (2018a), the increase in pyrene concentration (0-20 µg/L) reduces the sorption (K_d) of phenanthrene to PS MPs. In addition, the different ranges of concentrations among PAHs present in the NNS oil WAF (naphthalene was 100 times more concentrated than the other two PAHs) could change the sorption affinity of the different solutes

to the sorbent, prioritising competition for those present at a higher concentration. A favourable sorption scenario has been reported for those PAHs that are present at higher initial concentrations and that show a higher affinity for the polymer surface (Bakir et al., 2012; Koelmans et al., 2013; Lamichhane et al., 2016).

After serial centrifugation and AP renewal, the residual mass (CE4) for naphthalene, phenanthrene and fluorene was under quantification limits or less than 10% of the control sample, indicating almost no interference for the extraction method of the SP. According to the analysis in the SP (**Table 3**), naphthalene (0.12-0.58 ng) was the most abundant PAH in the 4.5 μm MPs, followed by phenanthrene (0.24-0.43 ng) and finally fluorene (0.05-0.13 ng). Those values were close to quantification limits and similar to the values obtained in the blank samples (0.08 ng for naphthalene, 0.17 ng for phenanthrene and not detected for fluorene). For naphthalene and fluorene, measured sorbed mass was lower than the residual free mass suggesting that no sorption occurred to 4.5 μm MPs.

The percentages of described mass of naphthalene, phenanthrene and fluorene sorbed to 4.5 μm MPs are shown in **Fig. 2**. Based on the analysis of the AP, differences in the initial PAH concentration did not influence the PAH sorption efficiency, as was seen for B(a)P sorbed to 4.5 μm MPs. Nevertheless, noticeable differences were recorded among compounds. Phenanthrene is more hydrophobic than naphthalene or fluorene and, as a result, it would bind to MPs more strongly than fluorene and naphthalene. However, the higher concentration of naphthalene favours its sorption to MPs, outcompeting to the other PAHs. According to the AP analysis in 100% WAF, naphthalene mass sorbed was 278.03 ng versus 11.82 ng and 1.82 ng for fluorene and phenanthrene, respectively. Comparing data for AP and SP analyses, the highly sorbed naphthalene could be desorbed due to cleaning and renewal of the medium. Only the compounds more strongly bound to the MPs such as phenanthrene would remain after the process and would then be recovered in the SP analysis.

Results and discussion

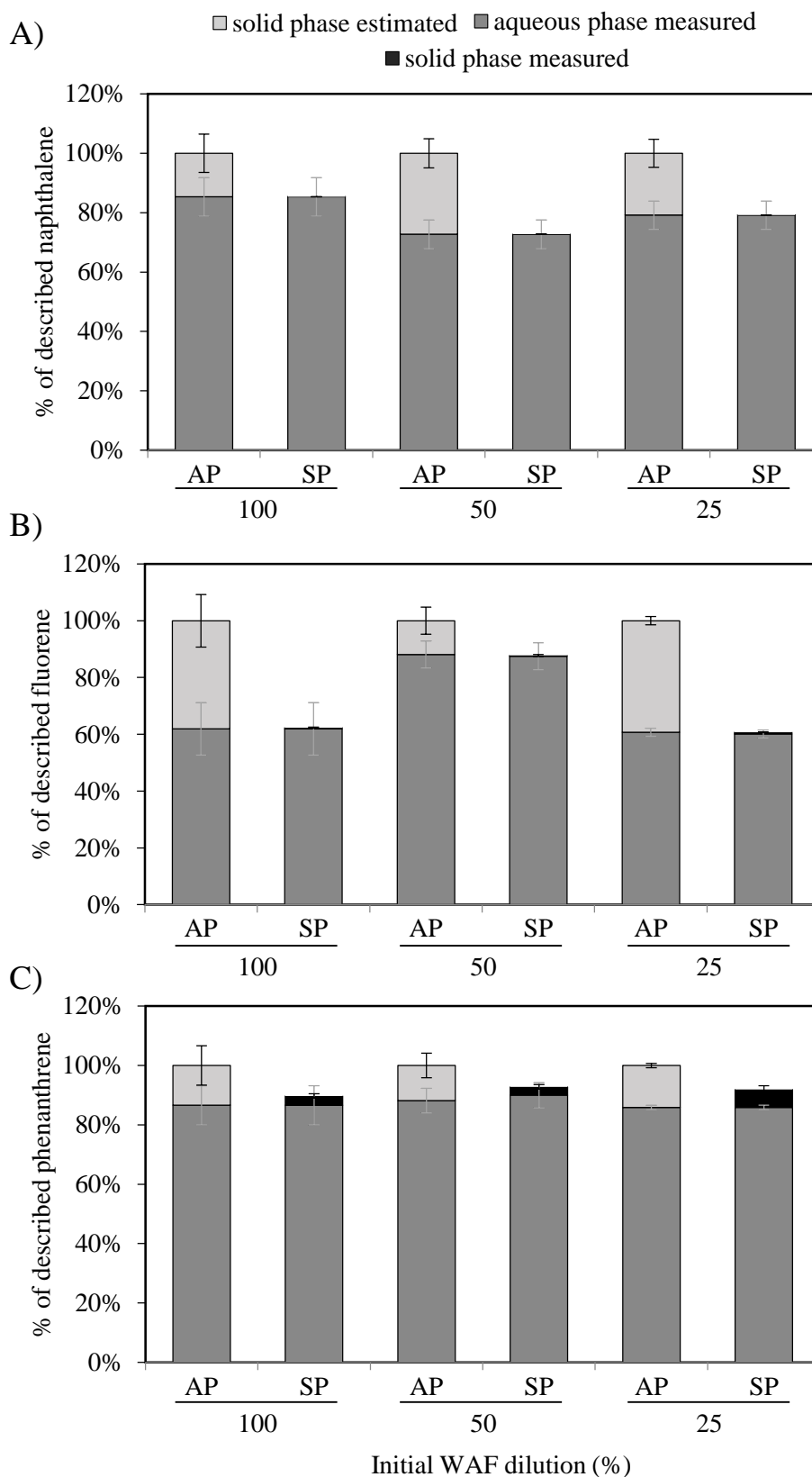


Fig. 2. Percentage of described PAH mass for A) naphthalene, B) fluorene and phenanthrene C) to 4.5 μm MPs according to measurements done in the aqueous phase (AP) or in aqueous and in solid phases (SP).

Sorption models. In order to analyse the interaction strength and mechanisms of B(a)P sorption to PS MPs, sorption isotherm models were applied from Q_e depending on the analysed phase and the corresponding C_e values (**Fig. S3**). The corresponding constants and parameters obtained for each model are presented in **Table 4**. The three models showed linearity, with linear regression coefficients (R^2) ranging from 0.71 to 1.00 for the two MP sizes and the two phases analysed. The models fitted better for 0.5 μm MPs than for 4.5 μm MPs and for the AP than for the SP analysis. Only in the case of 4.5 μm MPs, the SP data fitted better than that of the AP analysis ($R^2 = 0.91$ vs 0.76 for Langmuir model and 0.93 vs 0.88 for Freundlich model). According to the linear model, the partition coefficient (K_d) of B(a)P was higher for 0.5 μm MPs than for 4.5 μm MPs with the following order: AP 0.5 μm > SP 0.5 μm > AP 4.5 μm > SP 4.5 μm . Liu et al. (2016) reported K_d values ranging from 38.02 to 177.82 L/g for the sorption of B(a)P to 70 nm PS MPs after 30 days of incubation. Herein, for B(a)P, K_d ranged from 1.13 to 5.14 L/g in the case of 4.5 μm MPs and from 53.57 to 108.43 L/g in the case of 0.5 μm MPs, lower than those reported by Liu et al. (2016), possibly due to the higher MP size. Ma et al. (2016) reported a higher K_d value for the sorption of phenanthrene to 50 nm PS MPs (654 L/g) than to 10 μm PS MPs (16.9 L/g) after 7 days of incubation.

Table 4. Estimated parameters for the Linear, Langmuir and Freundlich models explaining the sorption of B(a)P to MPs of different sizes, according to data obtained from the aqueous phase (AP) or solid phase (SP).

MPs	Linear model		Langmuir model			Freundlich model			
	K_d	R^2	Q_{\max}	b	R^2	K_f	1/n	R^2	N
4.5 μm AP	5.14	0.74	67.65	0.28	0.76	14.66	0.76	0.88	9
4.5 μm SP	1.13	0.71	30.50	0.31	0.91	5.77	0.61	0.93	9
0.5 μm AP	108.43	0.99	242.89	0.86	0.98	125.84	0.87	1.00	9
0.5 μm SP	53.57	0.95	145.00	0.86	0.95	68.60	0.83	0.99	9

K_d = partition coefficient of B(a)P between MPs and the aqueous phase at equilibrium (L/g); Q_{\max} = maximum amount of the B(a)P per weight unit of MPs ($\mu\text{g/g}$); b= Langmuir constant related to the affinity of binding sites (L/ μg); K_f = sorption capacity (L/g); 1/n= degree of dependence of sorption at equilibrium; R^2 : linear regression coefficient; N: number of samples.

Wang and Wang (2018b) also analysed sorption of phenanthrene to 200-250 μm PS MPs and estimated a partition coefficient of 1.861 L/g. Thus, our results agree with previously published

Results and discussion

data regarding PAH partition coefficient and MP size: the higher the MP size the lower the partition coefficient.

Results of the Langmuir model based on the analysis of the AP indicated that 0.5 μm MPs showed a higher maximum sorption capacity (Q_{max}) for B(a)P than 4.5 μm MPs: Q_{max} of 242.89 $\mu\text{g/g}$ and 67.65 $\mu\text{g/g}$ for 0.5 μm MPs and 4.5 μm MPs, respectively. Wang and Wang (2018a) reported a Q_{max} value of 127 $\mu\text{g/g}$ using a range of pyrene concentrations from 0 to 100 $\mu\text{g/L}$ to assess sorption to 100-150 μm PS MPs (200 mg/L) after 48 h of incubation. This value was similar to the value we calculated for 4.5 μm MPs and lower than the value for 0.5 μm MPs, likely due to the higher concentration of PS MPs used and the lower hydrophobicity of pyrene ($\log K_{\text{ow}} = 4.88$) in comparison to B(a)P ($\log K_{\text{ow}} = 6.35$). The b independent coefficient indicates the sorption nature between the sorbate and the sorbent, being unfavourable if $b > 1$, linear if $b = 1$, favourable if $0 < b < 1$ or irreversible if $b = 0$ (Zhan et al., 2016). The b independent coefficient showed values of 0.86 L/ μg for 0.5 μm MPs and 0.28-0.31 L/ μg for 4.5 MPs (**Table 4**), indicating a more favourable sorption of B(a)P for 0.5 μm MPs than for 4.5 μm MPs.

For MPs of both sizes, the Freundlich model fitted better than the Langmuir model. The Freundlich model describes the formation of a sorbate monolayer assuming that the adsorption occurs on a homogenous surface and there are no interferences between different sorbates (Yang and Xing, 2010). In agreement with previous data, the affinity of the sorbate to the sorbent (K_f) was higher for 0.5 μm MPs than for 4.5 μm MPs, being 125.84 and 14.66 L/g respectively, based on the analysis of the AP. Liu et al. (2016) reported a non-linear sorption tendency of B(a)P to 70 nm PS nanoparticles with a K_f value of 33884.41 L/g. In the present study, 10 times smaller MPs resulted in almost 10-fold increase of K_f value according to the analysis of the AP and 13-fold increase of K_f value according to the analysis of the SP. The coefficient “1/n” allows to know whether the adsorption is cooperative ($1/n < 1$; Bakir et al., 2014; Hüffer and Hofmann, 2016). Results indicate that cooperation was also higher for 0.5 μm MPs ($1/n = 0.87$ for AP analysis and $1/n = 0.83$ for SP analysis) than for 4.5 μm MPs ($1/n = 0.76$ for AP analysis and $1/n = 0.61$ for SP analysis). $1/n$ values close to 1 seem to be related to sorption by partitioning into the PS MPs rather than to adsorption onto the polymer surface. In the study by Wang et al. (2019) sorption of phenanthrene to PS MPs of 50 nm-170 μm ranged from 100 to 80 $\mu\text{g/L}$, the cooperation was up to 0.79 for 170 μm PS MPs and 0.95 for 50 nm MPs, indicating that cooperation increased with the MP size. Higher B(a)P sorption capacity and sorption affinity for 0.5 μm MPs than for 4.5 μm MPs was confirmed.

Isotherms for the three PAHs analysed in the NNS crude oil WAF and 4.5 μm MPs experiments were non-linear (**Fig. S4**) for both analysed phases. Values of the linear regression coefficients (R^2) for Freundlich model ranged from 0.16 to 0.51 (**Table 5**). This non-linearity suggests PAH

binding onto the surface of the MPs and no correlation between initial PAH concentration and amount of PAHs sorbed to MPs (similar sorption values for the three WAF dilutions used). PAHs that are poorly bound to the sorbent can also be lost during the sample processing. Despite of the non-linear tendency shown by the models, average affinity values (K_f) were calculated. Naphthalene showed the highest K_f value (69.25 L/g), followed by fluorene (10.82 L/g) and finally phenanthrene (3.28 L/g) according to the analysis of the AP (**Table 5**). But opposite to K_f values, $1/n$ coefficients showed a higher sorption cooperation for fluorene (0.70) and phenanthrene (0.63), with similar octanol/water partition coefficients, than for naphthalene (0.46). Few authors have addressed the sorption of naphthalene to MPs. Hüffer and Hofmann (2016) reported that naphthalene was the compound that sorbed less to different polymers, only followed by benzene. Karapanagioti et al. (2010) observed that naphthalene was the first PAH (before pyrene and phenanthrene) to reach sorption equilibrium to PE and PP pellets. In addition, naphthalene is a small PAH that tends to interact with MPs by “hole-filling” (Khan et al., 2007). Naphthalene can outcompete with heavier PAHs for adsorption to the material surface.

Table 5. Estimated parameters of Freundlich model for WAF PAH sorption to 4.5 μm MPs, according to data obtained from the aqueous phase (AP) or solid phase (SP).

PAH	$\log K_{ow}$		K_f	$1/n$	R^2	N
Naphthalene	3.36	AP	69.25 \pm 32.68	0.46	0.36	8
		SP	-	-	-	-
Fluorene	4.18	AP	10.82 \pm 7.85	0.70	0.16	8
		SP	0.12 \pm 0.02	-0.29	0.48	3
Phenanthrene	4.46	AP	3.28 \pm 1.22	0.63	0.51	8
		SP	0.24 \pm 0.16	0.98	0.32	7

K_f = sorption capacity of MPs for PAHs (L/g); $1/n$ = degree of dependence of sorption at equilibrium; R^2 : linear regression coefficient; N: number of samples.

Naphthalene sorption to MPs could not be assessed in the SP because higher naphthalene concentration was found in the residual fraction than in the SP. From the analysis of the SP, phenanthrene showed higher K_f (0.24 L/g) and $1/n$ coefficients (0.98) than fluorene ($K_f = 0.12$ L/g; $1/n = -0.29$). Phenanthrene is one of the most studied PAHs regarding sorption to MPs (Bakir et al., 2014; Ma et al., 2016; Liu et al., 2016; Wang et al., 2018b). Bakir et al. (2014) assessed PE MPs (200-250 μm) for 1,1'-(2,2,2-trichloroethane-1,1-diy)bis(4-chlorobenzene) (DDT) and phenanthrene sorption affinity at the same range of concentrations (0.2-6.1 $\mu\text{g/L}$). They reported more affinity for the most hydrophobic compound (DDT), with K_f values of 794.3 L/g and 79.43 L/g for DDT and phenanthrene, respectively. Fries and Zarfl (2012) showed that sorption values to PE MPs were lower for fluorene than for phenanthrene, with K_d values of 8 L/Kg and 19 L/Kg,

Results and discussion

respectively, reinforcing the idea that sorption was closely related with the log K_{ow} of the analysed PAHs.

In conclusion, the present study shows that a methodology for the assessment of PAH sorption to MPs based on the analysis of both, aqueous and solid phases, provides information that helps to understand the interaction and mechanisms of sorption of PAHs to MPs of different sizes. Results show that the estimated amount of sorbed compounds to MPs is usually overestimated if based only on the analysis of the aqueous phase. 0.5 μm MPs were found to sorb higher amounts of B(a)P than 4.5 μm MPs indicating that size is a key parameter influencing the role of MPs as carriers of organic pollutants. At complex environmental conditions, as those that can reflect the PAH mixture present in a naphthenic crude oil WAF, PAH sorption to 4.5 μm MPs is mainly driven by PAH hydrophobicity and initial PAH concentration. Moreover, competition among PAHs for binding sites of MPs results in complex interactions between PAHs and MPs. Further studies with MPs of different sizes and other organic pollutants at environmentally relevant conditions would help to characterise the risk posed by MPs as vectors of pollutants for aquatic ecosystems.

REFERENCES

1. Akcha, F., Burgeot, T., Narbonne, J.-F. and Garrigues, P., 2003. Metabolic Activation of PAHs: Role of DNA Adduct Formation in Induced Carcinogenesis. In: Weeks, J.M.; O'Hare, S., Rattner, B.A., Douben, P.E.T. (Eds.), PAHs: An Ecotoxicological Perspective, John Wiley & Sons Ltd., England, pp 65-80.
2. Bakir, A., Rowland, S.J., Thompson, R.C., 2012. Competitive sorption of persistent organic pollutants onto microplastics in the marine environment. *Mar. Pollut. Bull.* 64, 2782-2789.
3. Bakir, A., Rowland, S.J., Thompson, R.C., 2014. Enhanced desorption of persistent organic pollutants from microplastics under simulated physiological conditions. *Environ. Pollut.* 185, 16-23.
4. Batel, A., Linti, F., Scherer, M., Erdinger, L., Braunbeck, T., 2016. Transfer of benzo[a]pyrene from microplastics to artemia nauplii and further to zebrafish via a trophic food web experiment: *cyp1a* induction and visual tracking of persistent organic pollutants. *Environ. Toxicol. Chem.* 35, 1656-1666.
5. Boucher, J., Friot, D., 2017. Primary microplastics in the oceans: a global evaluation of sources. IUCN, Gland, Switzerland.
6. Carbery, M., O'Connor, W., Thavami, P., 2018. Trophic transfer of microplastics and mixed contaminants in the marine food web and implications for human health. *Environ. Int.* 115, 400-409.
7. Chae, Y., An, Y., 2017. Effects of micro- and nanoplastics on aquatic ecosystems: Current research trends and perspectives. *Mar. Pollut. Bull.* 124, 624-632.
8. ChemIDplus by SRC, Inc. [http://chem.sis.nlm.nih.gov/chemidplus/name/benzo\(a\)pyrene](http://chem.sis.nlm.nih.gov/chemidplus/name/benzo(a)pyrene) (accessed Jan 20, 2020).

9. Duis, K., Coors, A., 2016. Microplastics in the aquatic and terrestrial environment: sources (with a specific focus on personal care products), fate and effects. *Environ. Sci. Eur.* 28, 1-25.
10. Foshtomi, M.Y., Oryan, S., Taheri, M., Bastami, K.D., Zahed, M.A., 2019. Composition and abundance of microplastics in surface sediments and their interaction with sedimentary heavy metals, PAHs and TPH (total petroleum hydrocarbons). *Mar. Pollut. Bull.* 149, 110655.
11. Fred-Ahmadu, O.H., Bhagwat, G., Oluyoye, I., Benson, N.U., Ayejuyo, O.O., Palanisami, T., 2020. Interaction of chemical contaminants with microplastics: Principles and perspectives. *Sci. Total Environ.* 706, 135978.
12. Fries, E., Zarfl, C., 2012. Sorption of polycyclic aromatic hydrocarbons (PAHs) to low and high density polyethylene (PE). *Environ. Sci. Pollut. Res.* 19, 1296–1304.
13. Fuller, S., Gautam, A., 2016. A procedure for measuring microplastics using pressurized fluid extraction. *Environ. Sci. Technol.* 50, 5774-5780.
14. Hüffer, T., Hofmann, T., 2016. Sorption of non-polar organic compounds by micro-sized plastic particles in aqueous solution. *Environ. Pollut.* 214, 194-201.
15. Kappell, A.D., Wei, Y., Newton, R.J., Van Nostrand, J.D., Zhou, J., McLellan, S.L., Hirstova, K.R., 2014. The polycyclic aromatic hydrocarbon degradation potential of Gulf of Mexico native coastal microbial communities after the Deepwater Horizon oil spill. *Front. Microbiol.* 5, 205
16. Karapanagioti, H., Ogata, Y., Takada, H., 2010. Eroded plastic pellets as monitoring tools for polycyclic aromatic hydrocarbons (PAH): laboratory and field studies. *Global NEST J.* 12, 327-334.
17. Katsumiti, A., Nicolussi, G., Bilbao, D., Prieto, A.; Etxebarria, N., Cajaraville, M.P., 2019. *In vitro* toxicity testing in hemocytes of the marine mussel *Mytilus galloprovincialis* (L.) to uncover mechanisms of action of the water accommodated fraction (WAF) of a naphthenic North Sea crude oil without and with dispersant. *Sci. Total Environ.* 670, 1084-1094.
18. Keith, L.H., Walters, D.B., 1991. National Toxicology program's chemical solubility database. In: Walters D.B; Keith, L.H, (Eds.); Lewis Publishers: Chelsea.
19. Khan, E., Khaodhir, S., Rotwiron, P., 2007. Polycyclic aromatic hydrocarbon removal from water by natural fiber sorption. *Water Environ. Res.* 79, 901-911.
20. Koelmans, A.A., Besseling, E., Wegner, A., Foekema, E.M., 2013. Plastic as a carrier of POPs to aquatic organisms: A Model Analysis. *Environ. Sci. Technol.* 47, 7812-7820.
21. Lamichhane, S., Bal Krishna, K.C., Sarukkalige, R., 2016. Polycyclic aromatic hydrocarbons (PAHs) removal by sorption: A review. *Chemosphere* 148, 336-353.
22. Lebreton, L.C.M., Zwet, J., Damsteeg, J., Slat, B., Andrady, A., Reisser, J., 2017. River plastic emissions to the world's oceans. *Nat. Commun.* 8, 15611.
23. Li, C., Busquets, R., Campos, L.C., 2020. Assessment of microplastics in freshwater systems: A review. *Sci. Total Environ.* 707, 133578.
24. Li, Y., Li, M., Li, Z., Yang, L., Liu, X., 2019. Effects of particle size and solution chemistry on Triclosan sorption on polystyrene microplastic. *Chemosphere* 231, 308-314.
25. Lin, W., Jiang, R., Wu, J., Wei, S., Yin, L., Xiao, X., Hu, S., Shen, Y., Ouyang, G., 2019. Sorption properties of hydrophobic organic chemicals to micro-sized polystyrene particles. *Sci. Total Environ.* 690, 565-572.
26. Liu, L., Fokkink, R., Koelmans, A.A., 2016. Sorption of polycyclic aromatic hydrocarbons to polystyrene nanoplastic. *Environ. Toxicol. Chem.* 35, 1650-1655.
27. Ma, Y., Huang, A., Cao, S., Sun, F., Wang, L., Guo, H., Ji, R., 2016. Effects of nanoplastics and microplastics on toxicity, bioaccumulation, and environmental fate of phenanthrene in fresh water. *Environ. Pollut.* 219, 166-173.

Results and discussion

28. Mato, Y., Isobe, T., Takada, H., Kanehiro, H., Ohtake, C., Kaminuma, T., 2001. Plastic resin pellets as a transport medium for toxic chemicals in the marine environment. *Environ. Sci. Technol.* 35, 318-324.
29. Perrichon, P., Le Menach, K., Akcha, F., Cachot, J., Budzinski, H., Bustamante, P., 2016. Toxicity assessment of water-accommodated fractions from two different oils using a zebrafish (*Danio rerio*) embryo-larval bioassay with a multilevel approach. *Sci. Total Environ.* 568, 952-966.
30. Plastics Europe. Plastics – the Facts 2019: An analysis of European plastics production, demand and waste data. *Plastics Europe*, 2019 (<https://www.plasticseurope.org/en/resources/publications/619-plastics-facts-2018>) (accessed Oct 15, 2019).
31. Rios Mendoza, L.M., Taniguchi, S., Karapanagioti, H.K., 2016. Advanced analytical techniques for assessing the chemical compounds related to microplastics. In: *Comprehensive Analytical Chemistry, Characterization and Analysis of Microplastics*; Duarte, A. C., (Eds.), Elsevier: Amsterdam, pp 209-240.
32. Shahul Hamid, F., Bhatti, M.S., Anuar, N., Anuar, N., Mohan, P., Periathamby, A., 2018. Worldwide distribution and abundance of microplastic: How dire is the situation? *Waste Manag. Res.* 36, 873-897.
33. Shen, M., Zhang, Y., Zhu, Y., Song, B., Zeng, G., Hu, D., Wen, X., Ren, X., 2019. Recent advances in toxicological research of nanoplastics in the environment: A review. *Environ. Pollut.* 252, 511-521.
34. Singer, M.M., Aurand, D., Bragin, G.E., Clark, J.R., Coelho, G.M., Sowby, M.L., Tjeerdema, R.S., 2000. Standardization of the preparation and quantitation of water-accommodated fractions of petroleum for toxicity testing. *Mar. Pollut. Bull.* 40, 1007-1016.
35. Strungaru, S., Jije, R., Nicoara, M., Plavan, G., Faggio, C., 2019. Micro- (nano) plastics in freshwater ecosystems: Abundance, toxicological impac and quantification methodology. *Trends Anal. Chem.* 110, 116-128.
36. Teuten, E.L., Rowland, S.J., Galloway, T.S., Thompson, R.C., 2007. Potential for plastics to transport hydrophobic contaminants. *Environ. Sci. Technol.* 41, 7759-7764.
37. Wang, J., Liu, X., Liu, G., Zhang, Z., Wu, H., Cui, B., Bai, J., Zhang, W., 2019. Size effect of polystyrene microplastics on sorption of phenanthrene and nitrobenzene. *Ecotoxicol. Environ. Saf.* 173, 331-338.
38. Wang, W., Wang, J., 2018a. Comparative evaluation of sorption kinetics and isotherms of pyrene onto microplastics. *Chemosphere* 193, 567-573.
39. Wang, W., Wang, J., 2018b. Different partition of polycyclic aromatic hydrocarbons on environmental particulates in freshwater: Microplastics in comparison to natural sediment. *Ecotoxicol. Environ. Saf.* 147, 648-655.
40. White, J.C., Pignatello, J.J., 1999. Influence of bisolute competition on the desorption kinetics of polycyclic aromatic hydrocarbons in soil. *Environ. Sci. Technol.* 33, 4292-4298.
41. Yang, K., Xing, B., 2010. Adsorption of organic compounds by carbon nanomaterials in aqueous phase: Polanyi theory and its application. *Chem. Rev.* 110, 5989-6008.
42. Zhan, Z., Wang, J., Peng, J., Xie, Q., Huang, Y., Gao, Y., 2016. Sorption of 3,3',4,4'-tetrachlorobiphenyl by microplastics: A case study of polypropylene. *Mar. Pollut. Bull.* 210, 559-563.

SUPPORTING INFORMATION

MPs fragility. Preliminary experiments done with dichloromethane as solvent used for microwave assisted extraction resulted in damage (**Fig. S1**) or melting the plastic which could provoke interferences with the GC/MS system and ultimately damage the injection system and GC column.

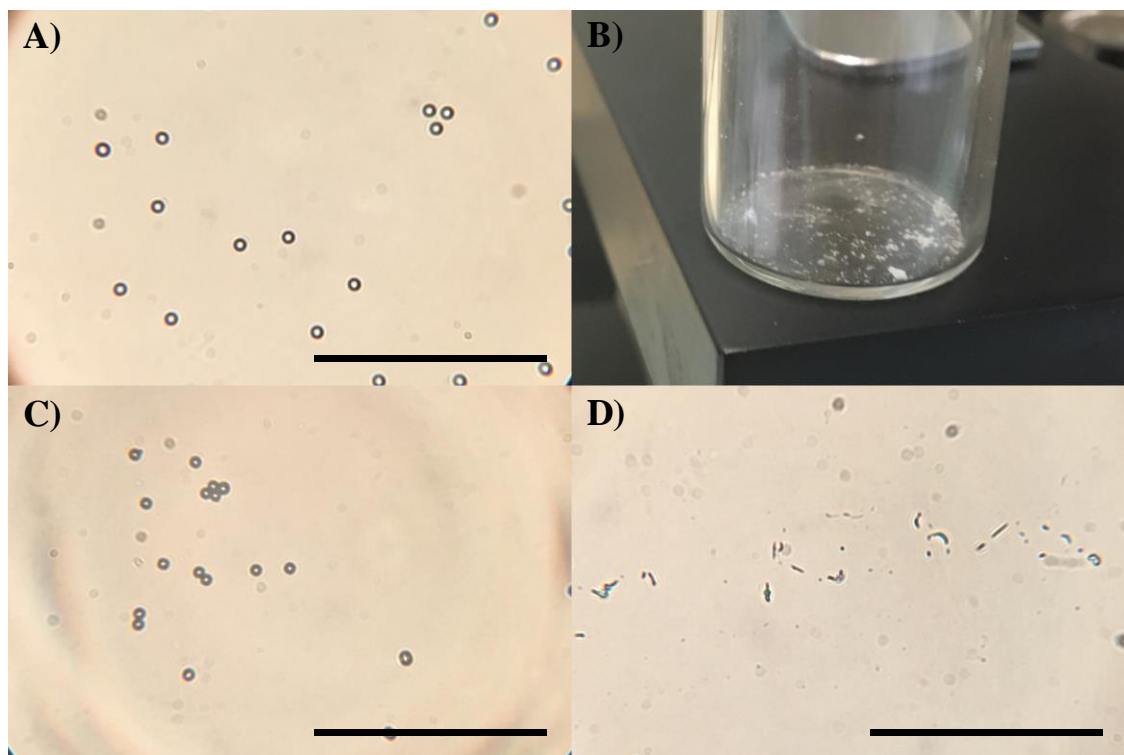


Fig. S1. Effect of different solvents on 4.5 µm MP integrity. A) Original MP stock in water, B) MPs after freeze-drying, C) MPs after 1 h in methanol, D) MPs after 1 h in dichloromethane. Scale bars: 100 µm.

Gas chromatography-mass spectrometry instrumentation, quality assurance and quality control. A GC/MS system (Agilent 7890A/ Agilent MSD-5795C, Agilent Technologies, California, USA) operated with an energy of ionization of 70 eV in ionisation mode par electronic impact equipped with an HP5MS-UI column (5% phenyl methylpolysiloxane; 30 m x 0,25 mm i.d.; 0,25 µm sorbent, Agilent Technologies) was used to analyse the selected PAHs. Injection in the GC/MS system was made with the inlet temperature at 280 °C in the pulsed splitless mode: a pulse pressure of 25 psi was maintained for 1.5 min, the purge flow the pulse vent was 60 mL/min after 1.5 min. The injection volume was 1 µL with a helium (purity 6.0) constant flow rate of 1.3 mL/min. The column temperature was initially held at 50 °C for 2 min, and was then increased to 250 °C at 10 °C/min for 1 min, to 280 °C for 2 min and to 310 at 10 °C/min, where it was held for 3 min. The compound determination was operated in the selected ion monitoring (SIM). The selected 18 PAHs were determined by isotope dilution (naphthalene d₈, acenaphthylene d₁₀, acenaphthene d₁₀, fluorene d₁₀, anthracene d₁₀, phenanthrene d₁₀, fluoranthene d₁₀, pyrene d₁₀, benzo(a)anthracene d₁₂, chrysene d₁₂, benzo(e)pyrene d₁₂, perylene d₁₂, benzo(b)fluoranthene d₁₂,

Results and discussion

benzo(k)fluoranthene d_{12} , indeno(1,2,3-cd)pyrene d_{12} , benzo(ghi)perylene d_{12} and dibenz(a,h)anthracene d_{14} .

All the precautions were taken to prevent contamination from laboratory operators, reagents and materials. Blanks were run in parallel for each batch of experiments in order to monitor the background contamination (microwave extraction blank, SPME blank and injection blank). For SPME, blanks were obtained by the desorption of the fibre without immersion (empty vial) and for injection blank with immersion in a sample with water medium. Recovery from MPs (freeze dried) precontaminated in water media spiked with a known B(a)P concentration (100 $\mu\text{g/L}$) was analysed after sequential microwave extraction with 10 mL of methanol in triplicate (**Fig. S2**) in order to validate the extraction method. Recovery was $95.1 \pm 1.6\%$ after two sequential extractions, which indicated a good extraction efficiency. Previously, an experiment with spiked sand was performed in order to establish a methodology that did not result into PAH loss during extraction. For that, sand was spiked with PAHs and precontaminated as described for MPs; after 24 h the sand with sorbed PAH was extracted by microwave with 10 mL of methanol spiked with the internal standard (B(a)P d_{12}). Previous to the injection a solution called syringe with a PAH deuterated (benzo(b)fluoranthene d_{12}) was added to calculate raw recovery for surrogate internal standards. The recovery of B(a)P d_{12} related to benzo(b)fluoranthene d_{12} was $99.44 \pm 12.54\%$, ($n=6$).

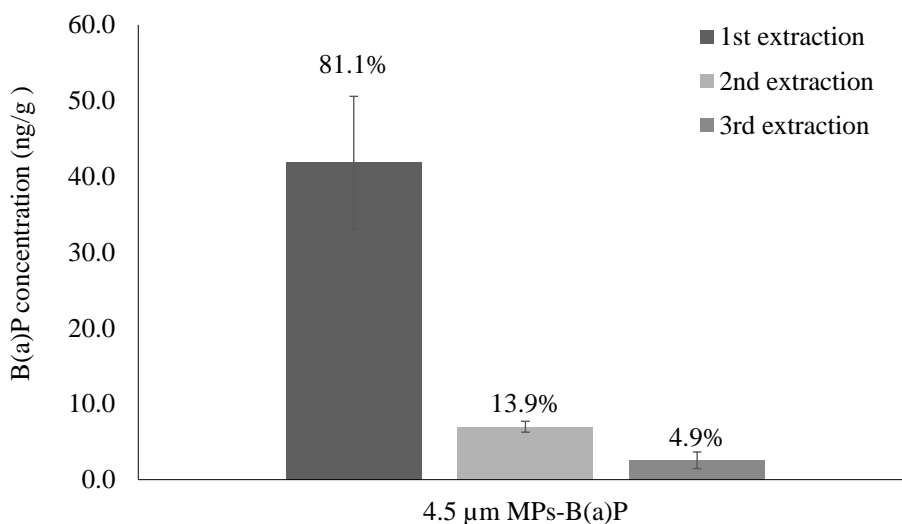


Fig S2. Concentration of B(a)P measured after sequential microwave assisted extraction steps with methanol with the representative recovery percentage from the total.

Accuracy of the method was determined by extracting water samples spiked at 10 ng/L. Method limit of quantification (MLOQ) was determined by extracting spiked water samples. Signal to noise ratio (S/N) was determined by peak to peak method and MLOQ were calculated for $S/N=9$.

Performances for B(a)P and for the PAHs in the WAF mixture are given in **Table S1**. Method performances were good for B(a)P with a recovery comprised between 94.1% and 107.5% (median recovery = 100.8%) (**Table S2**). Method performances were good for the 16 PAHs with a recovery ranging from 78% to 108% (median recovery = 103.5%). The 16 PAHs showed a MLOQ in MilliQ water similar than in conditioned water with a MLOQ up to 37.3 ng/L (median MLOQ = 14.2±7.7 ng/L) (**Table S3**).

Table S1. Limits of quantification determined for SPME (ng/L) and LIQ injection (ng/g) sample analysis. Data are expressed as mean ± S.D.

	naphthalene	fluorene	phenanthrene	benzo(a)pyrene
SPME (standard concentration B(a)P: 10 ng/L)	9.2±5.1 (N=3)	6.7±2.1 (N=3)	7.9±5.3 (N=3)	4.7±1.4 (N=4)
LIQ injection	8.0 (N=1)	0.7 (N=1)	5.0 (N=1)	1.7 (N=1)

LIQ: liquid

Table S2. Control chart with response factor and % of efficiency for SPME and LIQ sample analysis. Data are expressed as mean ± S.D.

naphthalene/ naphthalene d ₈		fluorene/ fluorene d ₁₀		phenanthrene/ phenanthrene d ₁₀		benzo(a)pyrene/ benzo(a)pyrene d ₁₂		
SPME								
K _i /K _e	%	K _i /K _e	%	K _i /K _e	%	K _i /K _e	%	
N=4	0.7±0.4	92.5±7.8	0.6±0.1	94.1±1.2	0.6±0.1	96.2±4.0	0.9±0.1	100.8±6.7
LIQ								
K _i /K _e	%	K _i /K _e	%	K _i /K _e	%	K _i /K _e	%	
N=4	0.7	100.7	0.5	100.0	0.7	101.3	0.7±0.2	103.2±11.5

SPME: solid phase micro extraction; LIQ: liquid; K_i/K_e: response factor.

Results and discussion

Table S3. Control chart with response factor and % of efficiency for SPME of WAF sample analysis in different aqueous media: MilliQ (MQ) and conditioned water (CW).

		Naphthalene	Acenaphthylene	Acenaphthene	Fluorene	Anthracene	Phenanthrene	Fluoranthene	Pyrene	Benz(a)anthracene
MQ	K _i /K _e	0.6	0.8	0.9	0.6	0.7	0.6	0.7	0.7	0.5
	%	83.9	109.7	121.2	93.3	108.0	85.2	104.2	103.7	100.2
CW	K _i /K _e	0.5	0.7	0.7	0.5	0.7	0.6	0.7	0.61	0.6
	%	78.8	88.9	100.7	101.4	95.1	97.7	96.0	94.0	95.1
		Chrysene	Benzo(e)pyrene	Benzo(a)pyrene	Perylene	Benzo(b)fluoranthene	Benzo(k)fluoranthene	Indeno(1,2,3-cd)pyrene	Benzo(ghi)perylene	Dibenz(a,h)anthracene
MQ	K _i /K _e	0.7	0.6	0.5	0.4	0.6	0.7	0.6	0.6	0.8
	%	113.0	102.0	113.3	104.4	104.4	97.5	126.2	96.3	97.2
CW	K _i /K _e	0.7	0.6	0.5	0.4	0.6	0.7	0.4	0.6	0.7
	%	96.8	93.7	92.5	100.1	95.1	94.4	89.8	95.3	101.4

K_i/K_e: response factor.

Characteristics of the crude oil used for WAF preparation. The oil was a very light naphthenic crude oil, with density of 0.84 g/cc at 15 °C and pour point at -15 °C, rich in branched and cyclic saturated hydrocarbons, little wax content, poor thermal and oxidative stability and high octane content (1).

Table S4. Concentration of PAHs ($\mu\text{g/L}$) measured in the WAF of a naphthenic North Sea crude oil used for sorption experiments. Values are means of 3 replicates.

Compound	Molecular weight (g/mol)	WAF dilution						L.Q.
		25%		50%		100%		
		Average	SD	Average	SD	Average	SD	
Naphthalene	128	53.9	1.4	115.7	3.176	292.6	30.8	$1.5 \cdot 10^{-2}$
Acenaphthylene	152	n.d.		n.d.		n.d.		$1.9 \cdot 10^{-2}$
Acenaphthene	154	0.3	0.02	0.6	0.04	0.6	0.05	$7.1 \cdot 10^{-3}$
Fluorene	166	1.0	0.04	2.0	0.1	4.4	0.2	$8.3 \cdot 10^{-3}$
Anthracene	178	<L.Q.		<L.Q.		0.07	0.03	$2.5 \cdot 10^{-2}$
Phenanthrene	178	0.71	0.01	1.39	0.03	3.1	0.2	$1.4 \cdot 10^{-2}$
Fluoranthene	202	<L.Q.		<L.Q.		0.03	0.001	$9.3 \cdot 10^{-3}$
Pyrene	202	<L.Q.		<L.Q.		0.03	0.001	$7.5 \cdot 10^{-3}$
Benz(a)anthracene	228	n.d.		n.d.		<L.Q.	<L.Q.	$1.5 \cdot 10^{-2}$
Chrysene	228	n.d.		n.d.		0.015	0.001	$1.5 \cdot 10^{-2}$
Benzo(e)pyrene	252	n.d.		n.d.		n.d.		$1.4 \cdot 10^{-2}$
Benzo(a)pyrene	252	n.d.		n.d.		n.d.		$6.0 \cdot 10^{-3}$
Perylene	252	n.d.		n.d.		n.d.		$1.4 \cdot 10^{-2}$
Benzo(b)fluoranthene	252	n.d.		n.d.		n.d.		$7.9 \cdot 10^{-3}$
Benzo(k)fluoranthene	252	n.d.		n.d.		n.d.		$7.9 \cdot 10^{-3}$
Indeno(1,2,3-cd)pyrene	276	n.d.		n.d.		n.d.		$3.7 \cdot 10^{-2}$
Benzo(ghi)perylene	276	n.d.		n.d.		n.d.		$1.7 \cdot 10^{-2}$
Dibenz(a,h)anthracene	278	n.d.		n.d.		n.d.		$1.9 \cdot 10^{-2}$
Total PAHs (Σ PAHs)		55.9		119.7		300.9		

n.d.: not detected; L.Q.: limit of quantification;

- Statoil. 2011. Crude summary report. Available at: <https://www.statoil.com/content/dam/statoil/documents/crude-oil-assays/Statoil-TROLL-BLEND-2011-01.xls> (Accessed Nov 2018)

Results and discussion

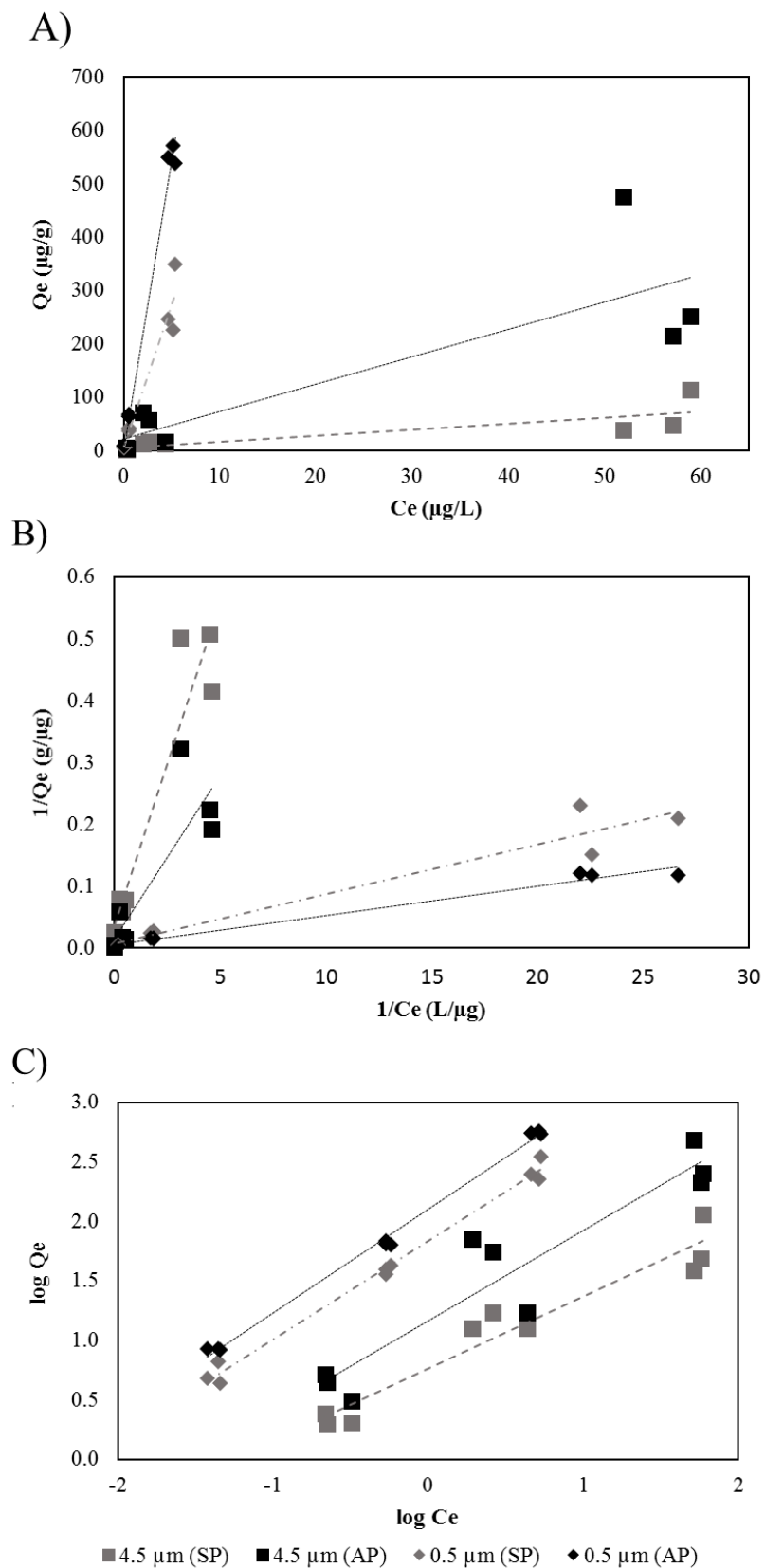


Fig. S3. Models for the sorption of B(a)P to MPs of different sizes depending on the analysed fraction (AP, SP). A) Linear model, B) Langmuir model and C) Freundlich model.

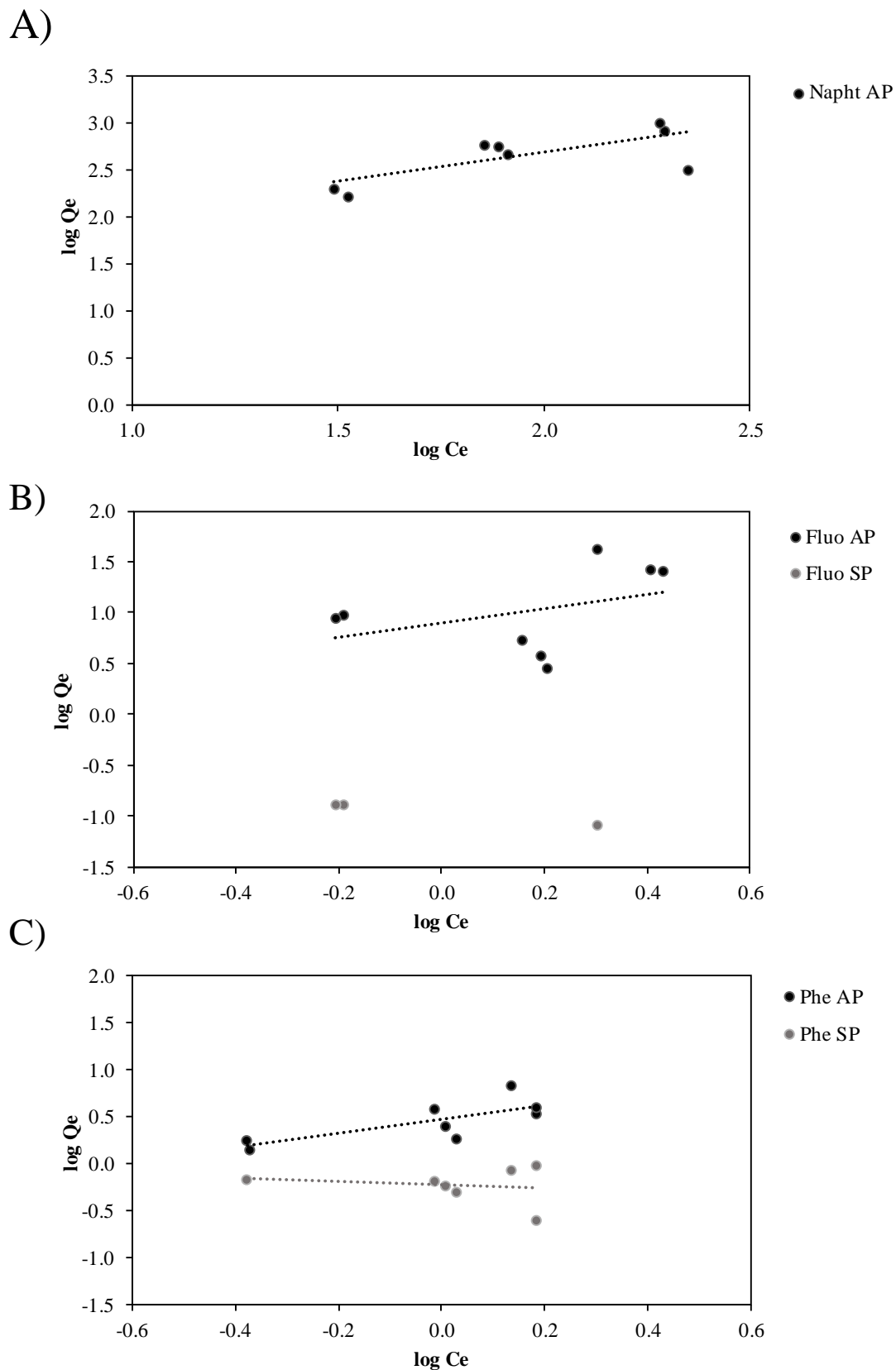
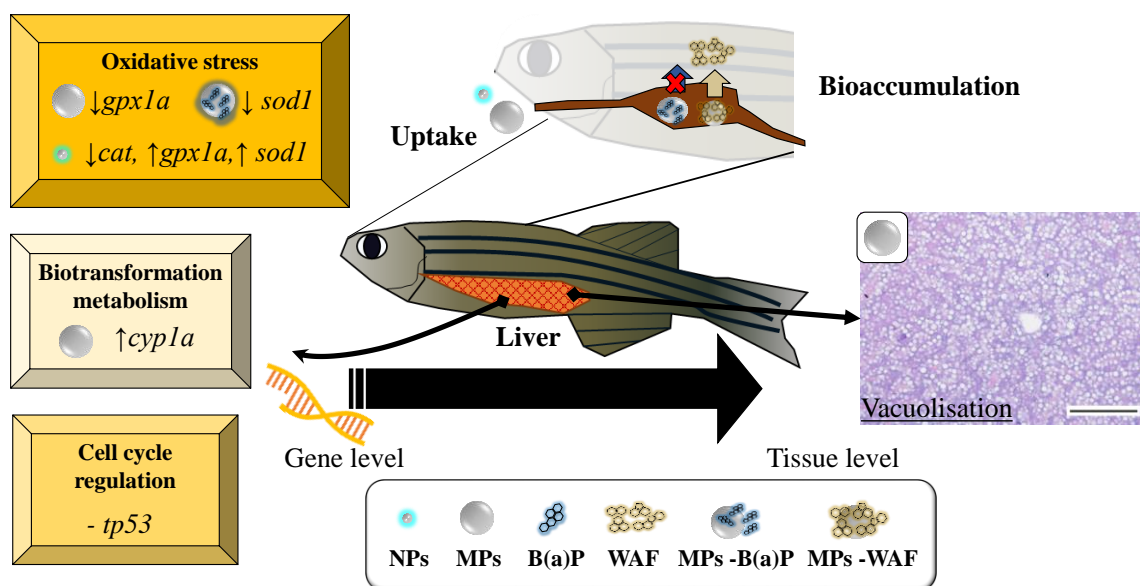


Fig. S4. Freundlich model for the sorption of different PAHs present in the WAF to 4.5 μm MPs depending on the analysed fraction (AP, SP). A) Naphthalene, B) fluorene and C) phenanthrene.

CHAPTER 3. Effects of polystyrene nano- and microplastics and of microplastics with sorbed polycyclic aromatic hydrocarbons in adult zebrafish



ABBREVIATIONS

B(a)P, Benzo(a)pyrene

CAT, Catalase

DMSO, Dimethylsulfoxide

EC₅₀, Effective concentration 50

EE2, 17 α -ethynylestradiol

EROD, 7-ethoxyresorufin O-deethylase activity

GC/MS, Gas chromatography and mass spectrometry

GPx, Glutathione peroxidase

GSH, Glutathione

GST, Glutathione S-transferase

LC₅₀, Lethal concentration 50

L.Q., Limit of quantification

MPs, Microplastics

n.d., Not detected

NNS, Naphthenic North Sea

NPs, Nanoplastics

PAHs, Polycyclic aromatic hydrocarbons

PE, Polyethylene

PP, Polypropylene

PS, Polystyrene

PVC, Polyvinyl chloride

ROS, Reactive oxygen species

SOD, Superoxide dismutase

SPME, Solid phase microextraction

TEM, Transmission electron microscopy

WAF, Water accommodated fraction

WWTPs, Wastewater treatment plants

ABSTRACT

The increasing presence of nanoplastics (<100 nm, NPs) and microplastics (<5 mm, MPs) in the aquatic environment is being recognised as a global-scale problem. NPs and MPs are susceptible of being ingested by organisms and, depending on the particle size, could be internalised into the tissues, entering into the food web. Moreover, due to their hydrophobic nature and large specific surface, NPs and MPs can adsorb other contaminants, especially hydrophobic organic pollutants, such as polycyclic aromatic hydrocarbons (PAHs), already present in the environment, and can modulate their bioavailability and hazard. This study aimed at (1) assessing the effects of polystyrene NPs (50 nm) and MPs (4.5 µm) in zebrafish and (2) studying the potential role of MPs as carriers of PAHs. For that, different groups of adult zebrafish were exposed for 3 and 21 days to 0.07 mg/L (10^{12} particles/L) of NPs to 0.05 mg/L (10^6 particles/L) of MPs, to MPs with sorbed PAHs present in the water accommodated fraction (WAF) of a naphthenic crude oil (MPs-WAF) and to MPs with sorbed B(a)P (MPs-B(a)P). In addition, two groups of zebrafish were exposed to 5% WAF or to 21 µg/L B(a)P. An unexposed control group was run in parallel. Some electron-dense particles resembling NPs were seen in the intestine lumen close to microvilli. MPs were abundantly found in the lumen of the intestine, but without signs of internalisation into the tissues. According to chemical analysis in fish tissues, at the contaminant level used, MPs did not act as vehicles of PAHs to zebrafish tissue. Transcription levels of liver *cyp1a* were significantly upregulated in fish exposed to MPs for 21 days and higher mean levels than in control fish were measured in fish exposed to MPs-WAF, WAF and MPs-B(a)P. A similar pattern was observed for *gstp1*. 21 days of exposure to NPs, but not to MPs, caused a significant downregulation of *cat*, and upregulation of *gpx1a* and *sod1* compared to control fish. Liver vacuolisation was the histopathological condition most frequently found, being its prevalence significantly increased in fish exposed to MPs for 21 days. Histopathological alterations were not observed in gills for any treatment. Thus, the presence of NPs or MPs in the environment could change the bioavailability of PAHs, mostly decreasing the PAHs toxicity and reducing their effect in antioxidant and biotransformation systems of zebrafish.

Key words: Nanoplastics, microplastics, polycyclic aromatic hydrocarbons, zebrafish

INTRODUCTION

Plastic debris have been identified as a source of contamination of high concern in aquatic ecosystems (Villarubia-Gómez et al., 2018). The main focus of the investigation, in terms of debris density, is been put in the marine ecosystems (Pham et al., 2014; Werner et al., 2016), outshining freshwater ecosystems which have been mainly considered only as pathways to the marine ecosystems (Schmidt et al., 2017) and not as a plastic debris storage compartment. As seen by Driedger et al. (2015), some locations of the Laurentian Great Lakes presented debris density in surface water (0.0425 items/m^2) at the same level as reported in marine ecosystems (0.0269 items/m^2). Within debris, a large amount in terms of items are microplastics (MPs, $<5 \text{ mm}$) (Barnes et al., 2009; Lechner et al., 2014; Sadri and Thompson, 2014), while the smallest particles, NPs ($<100 \text{ nm}$), are unquantified due to the lack of quantification techniques. Nevertheless, NPs are expected to appear in similar amount as MPs (Gigault et al., 2016). Due to the manufacture of NPs and MPs (primary plastics) for many industrial, biomedical and domestic applications, such as personal care products, and breaking down of larger plastic to NPs and MPs (secondary plastics), the amount of NPs and MPs present in aquatic ecosystems will continue increasing in the next years (Besseling et al., 2019). High concentrations of MPs have been already reported in fresh waters (lakes and rivers) all over the world (Xu et al., 2020). In the case of Austrian Danube River, $0.0551 \pm 0.0754 \text{ MP items /m}^3$ were found (Lechner et al., 2014), and much higher concentrations, up to 288 items/m^3 , were recorded in a tropical Indian river which debouches into the Arabian Sea (Amrutha and Warriar, 2020).

Due to the abundant presence of MPs in aquatic ecosystems, it becomes necessary to analyse their possible impacts on aquatic organisms. Due to their feeding habit, fish are target species for MP ingestion because of the similar size of plastic particles and their preys, such as planktonic species. Moreover, plankton can also accumulate MPs, increasing the risk for fish to ingest and accumulate MPs through a biomagnification process (Saley et al., 2019; Elizalde-Velazquez et al., 2020). Ingestion of noticeable amounts of MPs (1-20 items/individual) have been reported in freshwater fish inhabiting areas with high population pressure (Sanchez et al., 2014; Jabeen et al., 2017; Wang et al., 2020), being polyethylene (PE), polypropylene (PP) and polystyrene (PS) the three polymer types most abundantly found in freshwater fish (Bordós et al., 2019; Egessa et al., 2020). Among them, PS shows an intermediate density ($0.96\text{-}1.05 \text{ g/cm}^3$), similar to that of water, which allows this polymer to be distributed on surface waters or to sink to bottom waters and sediments, being a polymer with higher contribution in freshwater than in ocean compartments and that could be ingested by numerous freshwater organisms with different feeding habits (Schwarz et al., 2019).

Results and discussion

The ingestion of PS plastic particles has been reported for many aquatic organisms, such as algae, crustacean and fish embryos (Chae et al., 2018). A recent work that summarised the ecotoxicological effects of MPs using the biomarker approach showed that MPs can alter normal metabolism, induce oxidative stress and produce neurotoxic, genotoxic and inflammatory effects on aquatic organisms (Prokić et al., 2019). Zebrafish is a common experimental freshwater species used in toxicology to assess the impact of NPs and MPs (Chen et al., 2017a; Jin et al., 2018; Lei et al., 2018; Lu et al., 2018). MPs of different size (0.1-90 µm), composition (PS, PP, PE, polyvinyl-chloride (PVC)) and concentrations (1-10000 µg/L) were evaluated in zebrafish and results showed gut inflammation and changes in genes related with the immune system of zebrafish gills driven by concentration and MP size but not by polymer type (Jin et al., 2018; Lei et al., 2018; Lu et al., 2018). Oxidative stress in zebrafish was also observed after exposure to 70 nm PS NPs. Increased ROS level in zebrafish muscle along with a neurotoxic effect in brain (decreased acetylcholinesterase activity) was reported in zebrafish exposed for 7 days to 1.5 mg/L of NPs (Sarasamma et al., 2020). In addition to size, other characteristic of the MPs, such as shape and additives, can affect to aquatic organisms (Teuten et al., 2009; Ašmonaitė et al., 2018).

One of the most concerning characteristic of NPs and MPs is their capability to sorb organic pollutants due to their porosity and large surface area to volume ratio (Wang et al., 2019b; Wirnkor et al., 2019; **Chapter 2**). MPs arrive to sites with high contamination pressure, such as wastewater treatment plants (WWTPs; Xu et al., 2019) where plastic could act as a sponge for contaminants and return back to aquatic ecosystems through WWTP effluents, and to other contaminated places, such as harbours, where crude oil pollution is common. Polycyclic aromatic hydrocarbons (PAHs) are dominant compounds in this type of contamination and, due to their high hydrophobicity, can be sorbed to MPs (Rochman et al., 2013; Bouhroum et al., 2019; **Chapter 2**). PAHs sorbed to MPs could produce toxicological effects on aquatic organisms after ingestion, as sorbed pollutants could be released within of the organism causing the so called “Trojan horse effect”. Some studies have already addressed the transfer of PAHs from contaminated MPs to adult fish (Batel et al., 2016; Karami et al., 2016; Ašmonaitė et al., 2018; Batel et al., 2018; Bussolaro et al., 2019). In rainbow trout, co-exposure to 200 nm PS MPs and benzo(a)pyrene (B(a)P) or 3-nitrobenzanthrone altered PAH genotoxicity, causing increased DNA damage in gill and gut cells (Bussolaro et al., 2019). Genotoxicity analysis were also performed by Karami et al. (2016) to assess the potential transfer of phenanthrene (10 and 100 µg/L) from low-density PE MPs (50 and 500 µg/L) to African catfish. Gills and brain of African catfish were analysed after 96 h of exposure and results showed that MPs were able to reduce the toxicity of phenanthrene inhibiting the induction of specific biomarkers caused by phenanthrene exposure alone, such as change in glycogen stores and cholesterol production with further liver pathologies. 100-140 µm contaminated plastic pellets by in situ exposure in a sewage effluent and

in a harbour were used by Ašmonaitė et al. (2018) for toxicity evaluation and quality for consumption of rainbow trout (*Oncorhynchus mykiss*). Results showed that compounds (PAHs, surfactants and plasticizers) that were sorbed to the MPs (5 pellets/fish/day) produced hepatic stress through induction of the transcription of genes and the activity of enzymes related to biotransformation metabolism, but without loss of fillet quality after 28 days of exposure. Exposure of adult zebrafish to PE MPs (10^6 particles) of two size ranges (1-5 μm and 10-20 μm) with sorbed B(a)P (incubated in 252 $\mu\text{g/L}$) led to transport of B(a)P to the organism via the resolution into the exposure media or via direct contact, specifically with gills (Batel et al., 2018). As previously mentioned, MPs could act as a potential source of toxicity for aquatic life, but some work has to be still done to elucidate whether MPs with sorbed compounds could be a source of other contaminants and modulate their availability to aquatic organisms.

The aim of the present study was to test the toxicity of polystyrene NPs and MPs alone and of MPs with sorbed PAHs to assess the potential Trojan horse effect in zebrafish. Therefore, the specific objectives were: (1) to assess the sublethal toxicity of 50 nm PS NPs and 4.5 μm PS MPs alone and with sorbed B(a)P, as a model pyrolytic PAH, or with sorbed petrogenic PAHs from an environmentally relevant mixture, such as the water accommodated fraction (WAF) of a naphthenic North Sea crude oil; (2) to assess the potential transfer and bioaccumulation of PAHs from 4.5 μm PS MPs to adult zebrafish.

MATERIALS AND METHODS

Plastic particles and chemicals. 50 nm fluorescent Fluoresbrite® carboxylate polystyrene NPs (excitation/emission wavelength of 360/407 nm) and 4.5 μm polystyrene MPs in aqueous suspensions were purchased from Polysciences, Inc. (Warrington, PA, USA). Benzo(a)pyrene (B(a)P, $\text{C}_{20}\text{H}_{12}$, purity $\geq 96\%$) and dimethyl sulfoxide (DMSO, purity $\geq 96\%$) were purchased from Sigma-Aldrich. The naphthenic North Sea (NNS) crude oil was provided by Driftslaboratoriet Mongstad, Equinor (former Statoil). The oil was a very light naphthenic crude oil, with density of 0.845 g/cc at 15 °C and pour point at -15 °C, rich in branched and cyclic saturated hydrocarbons, little wax content, poor thermal and oxidative stability and high octane content (Statoil, 2011). Deuterated PAHs (naphthalene d_8 , acenaphthylene d_{10} , acenaphthene d_{10} , fluorene d_{10} , anthracene d_{10} , phenanthrene d_{10} , fluoranthene d_{10} , pyrene d_{10} , benzo(a)anthracene d_{12} , chrysene d_{12} , benzo(e)pyrene d_{12} , benzo(a)pyrene d_{12} , perylene d_{12} , benzo(b)fluoranthene d_{12} , benzo(k)fluoranthene d_{12} , indeno(1,2,3-cd)pyrene d_{12} , benzo(ghi)perylene d_{12} and dibenz(a,h)anthracene d_{14}) used for chemical analyses were also purchased from Sigma-Aldrich.

Results and discussion

Preparation of PAH solutions and MPs with sorbed PAHs. B(a)P was firstly dissolved in 100% DMSO at a concentration of 10 g/L. This solution was diluted in pure DMSO to obtain a B(a)P stock of 1 g/L. Then, a 1:10000 dilution was made in MilliQ water to obtain a B(a)P solution of 100 µg/L (0.01% DMSO (v/v)) used to contaminate MPs. The WAF was prepared based on Singer et al. (2000). A 5 L glass bottle was filled with 4 L of conditioned water (600 µS/cm, 7-7.5 pH) and 20 g of NNS oil. The bottle was wrapped with aluminium foil and placed in a magnetic stirrer (IKA®-Werke GmbH & Co. KG, Staufen, Germany) at 800 rpm and 21 °C. After 40 h, the aqueous phase was collected in a glass bottle avoiding taking oil droplets. MPs with sorbed PAHs were prepared as described in **Chapter 1**. Briefly, 1.75 mg of 4.5 µm MPs were incubated in a glass bottle containing 35 mL of 100 µg/L B(a)P (0.01% DMSO) prepared in MilliQ water or 35 mL of 100% WAF in order to maintain the plastic mass to incubation volume ratio used in **Chapter 2**. MP suspensions were wrapped with aluminium foil and shaken at 300 rpm for 24 h at 20 °C. Then, samples were filtered through a polyethersulfone filter (0.45 µm filter pore, Sarstedt AG & Co., Nümbrecht, Germany) and washed two times with 10 mL of MilliQ water. MPs were recovered from the filter using 10 mL of conditioned water. These MPs-B(a)P and MPs-WAF suspensions were added to the exposure water tanks (35 L) to reach the desired MP concentration (0.05 mg/L). This process was repeated every three days to prepare freshly contaminated MPs for each redosing.

Water borne exposure of adult zebrafish. The wild type zebrafish stock was maintained in a temperature-controlled room at 28 °C with a 14 hour light/10 hour dark cycle in 100 L tanks provided with mechanic and biological filters following standard protocols for zebrafish culture. Conditioned water (600 µS/cm and 7-7.5 pH) was prepared from deionised water and commercial salt (SERA, Heinsberg, Germany). Fish were fed with Vipagran baby (Sera) and brine shrimp larvae (Artemia Koral GmbH, Nürnberg, Germany) twice per day. The experimental procedure described herein was approved by the Ethics Committee in Animal Experimentation of the UPV/EHU (M20/2017/152) according to the current regulations. Adult fish of >7 months old were placed in 35 L aquaria with conditioned water. Fish were exposed to NPs, MPs, MPs-WAF, WAF, MPs-B(a)P and B(a)P for 21 days. In the case of 50 nm NPs, fish were exposed to ~0.07 mg/L equivalent to 10^{12} particles/L. In the treatments containing 4.5 µm MPs (MPs, MPs-B(a)P and MPs-WAF), fish were exposed to ~0.05 mg/L equivalent to 10^6 particles/L. A group of fish was exposed to the B(a)P alone (21 µg/L), which was equivalent to the B(a)P sorbed to MPs and another group of fish was exposed to 5% WAF, a WAF dilution containing an equivalent PAH amount to that sorbed to MPs. Those concentration of B(a)P and PAH mixture alone were calculated from chemical analyses performed in **Chapter 2** and based on Chen et al. (2017b). Briefly, the percentage of the sorbed fraction that was calculated by chemical analyses (21 % for B(a)P from an initial concentration of 100 µg/L) and the WAF dilution containing an equivalent

PAH amount (21 µg/L of total PAHs is the fraction corresponding to 5% WAF) were used as representative part of the sorbed compounds to 4.5 µm MPs. Finally, an unexposed control group was run in parallel in identical experimental conditions. Every 3 days, 2/3 of the water volume of each tank were renewed. This allowed maintaining water parameters without the need of biological filters and contaminant concentrations along the whole experiment. Over the first three days of the experiment, fish were distributed in two aquariums per experimental group in order to maintain a fish density of 1-2 fish/L. During the experimental period, fish were feed with live brine shrimp larvae twice per day. Fish samples were collected after 3 and 21 days of exposure after euthanasia by overdose of anaesthetic (200 mg/L benzocaine).

Measurement of PAH concentration in water and fish tissue. In the treatments containing PAHs (MPs-WAF, WAF, MPs-B(a)P and B(a)P) and in the control group, water samples were taken in triplicate in glass vials at day 0, 9 and 18 (1st, 4th and 7th dose) 30 min after dosing and at day 3, 12 and 21 just before water renewal. PAH quantification in water was performed by gas chromatography and mass spectrometry (GC/MS) after solid phase micro extraction (SPME). SPME consisted in a heating process at 40 °C with 35 min stirring period at 250 rpm of the polydimethylsiloxane (100 µm PDMS) fibre (Supelco, Sigma-Aldrich, South Africa). After extraction, the fibre was thermally desorbed into the GC/MS system (Agilent GC 7890A/Agilent MSD 5975C, Agilent Technology, California) for 10 min at 280 °C.

At 3 and 21 days of exposure, 20 fish per experimental groups (control, MPs-WAF, WAF, MPs-B(a)P and B(a)P) were collected and grouped in 4 pools of 5 fish of similar weight (≈1 g wet weight). Samples were immediately frozen in liquid nitrogen and stored at -80 °C until analysis. Samples were freeze dried (Power Dry LL3000, ThermoFisher Scientific, Vantaa, Finland) before being grinded in a IKA tube mill (ThermoFisher Scientific). PAHs were extracted from 0.2 g of dry weight samples by microwave-assisted extraction (Start E, Milestone, Italy) with dichloromethane (5 min at 900W, 2nd 5 min at 500W 70 °C). After extraction, dichloromethane was reconcentrated to 500 µL using a Vacuum Evaporation System (Rapidvap Labconco, Kansas city, USA). The organic extracts followed a purification step through alumina and silica micro-columns in order to remove macromolecules and polar molecules to avoid interference with PAH quantification. First, the extracts were passed through alumina column by dichloromethane elution. Extract was reconcentrated with gas nitrogen and then samples were passed through a silica column. The aliphatic fraction was eluted with pentane and discarded, followed by PAH fraction elution with a first elution using a mix of pentane/dichloromethane (65/35, v/v) and second elution using dichloromethane. The final extracts were reconcentrated again with gas nitrogen in 150 µL isoctane and analysed by GC-MS.

Results and discussion

Analysis of gene transcription levels. The liver of 15 male zebrafish per experimental group were dissected, placed in cryovials, frozen in liquid nitrogen and stored at -80 °C. Analysis of the transcription levels of target genes was done in pools of three livers resulting in five biological replicates per experimental group and exposure time. The analysed genes were: cytochrome P450 1A1 (*cyp1a*, ID: Dr03112441_m1) and glutathione S-transferase pi 1 (*gstp1*, ID: Dr03118992_g1) as genes related with biotransformation metabolism of organic compounds; catalase (*cat*, ID: Dr03099094_m1), superoxide dismutase 1 (*sod1*, ID: Dr03074068_g1) and glutathione peroxidase 1a (*gpx1a*, ID: Dr03071768_m1) as genes related with oxidative stress; and tumour protein 53 (*tp53*, ID: Dr03112086_m1) as gene related with cell cycle regulation. Ribosomal protein S18 (*rps18*, ID: Dr03144509_m1) was used as housekeeping gene. Taqman® probes were purchased from ThermoFisher Scientific. RNA extraction was carried out by homogenisation of the sample in cold TRIzol® using an electric disperser. RNA was measured for integrity and purity before cDNA synthesis. 3 µg of total RNA were retrotranscribed using the Affinity Script Multiple Temperature cDNA synthesis Kit (Agilent Technologies) following manufacturer's instructions in a 2720 Thermal Cycler (ThermoFisher Scientific). qPCRs were run in 7300 Applied Biosystems thermocycler (ThermoFisher Scientific). A dilution 1:5 of cDNA was done for each target gene. A final volume of 2.5 µL cDNA sample and 22.5 µL mix TaqMan® reaction (12.5 µl master mix + 1.25 µl primer probe + 8.75 µl water RNase free) was used. Relative transcription levels were calculated based on the $2^{-\Delta\Delta CT}$ method (Livak and Schmittgen, 2001) using the mean value of the control group at each corresponding exposure time as calibrator and *rps18* transcription levels as reference gene. *rps18* transcription levels presented a coefficient of variation of 3.46% among all the samples. Results of transcription levels are represented as $RQ = \log_2(2^{-\Delta\Delta CT})$.

Histopathology. Visceral mass and gills were dissected from 10 female fish per experimental group after 3 and 21 days of exposure. Samples were processed for histological analysis using N-butyl alcohol (Stiles, 1934) instead other organic solvents in order to prevent the degradation of the PS MPs during standard histology tissue processing. Tissues were placed in histological cassettes and immersed in neutral buffered formalin (4% formaldehyde) overnight at 4 °C. Then, samples were dehydrated in ascending ethanol/N-butyl solutions and embedded in paraffin wax. 5 µm sections were cut in a RM2125RT microtome (Leica Microsystems, Wetzlar, Germany). Afterwards, sections were dewaxed utilising n-butyl alcohol and stained with haematoxylin/eosin (H/E) in an Auto Stainer XL (Leica Microsystems) and manually mounted in glycerol (Sigma-Aldrich). After staining and mounting, samples were examined and photographed under a BX51 light microscope (Olympus, Tokyo, Japan). For MP quantification in the lumen of zebrafish, four sections per individual were used and the quantity of particles found in the three sections of each individual were summed.

Subcellular localisation of NPs: transmission electron microscopy (TEM) analysis. Gills, liver and intestine from control fish and fish exposed to NPs for 21 days were dissected and fixed for 1 h at 4 °C in sodium cacodylate (sigma-Aldrich buffer 0.1 M, pH 7.2, containing 2.5% glutaraldehyde (Panreac, Barcelona, Spain). Zebrafish tissue samples were treated and processed as described in Lacave et al. (2018). Ultrathin sections of 50 nm in thickness were cut using a Reichert Ultracut S ultramicrotome (Leica Microsystems, Wetzlar, Germany). Sections were picked up in 150 mesh copper grids, contrasted with 1% uranyl acetate (Fluka, Steinheim, Germany) for 3 min and with 0.3% lead citrate (Fluka) for 4 min and, finally, examined and photographed using a Hitachi HT7700 transmission electron microscope (Tokyo, Japan) at 60 kV. Additionally, the NP stock suspension was also observed at TEM. For that, one drop of the suspension (3.64×10^{14} particles/mL or 25 g/L) was placed over a 150 mesh copper grid previously covered with Formvar® (Sigma Aldrich) and dried at 35 °C.

Data analysis and statistics. Data were tested for normality (Kolmogorov-Smirnov test) and homogeneity of variance (Bartlett test) using the GraphPad Prism version 5.00 for Windows (GraphPad Software, La Jolla, California, USA). Data following a normal distribution were analysed by one-way ANOVA followed by the Tukey post-hoc test. For non-parametric data, Kruskal-Wallis test was applied followed by the Dunn's post hoc test. For number of particles per fish, Mann-Whitney U was applied. For prevalence of histopathological alterations, Fisher's exact test was applied. In all cases, significance level was established at $p < 0.05$.

RESULTS

Localisation of plastic particles. 50 nm NPs particles were visualised at the TEM as small electron-dense structures (**Fig. 1A**). Presence of small electron-dense structures resembling NPs according to the appearance shown in **Fig. 1A** were localised among microvilli located in the apical zone of the intestine cells (**Fig. 1B**). Inside cells, vesicles that could contain NPs internalised by endocytic processes were not observed and free particles in the cytosol could not be distinguished from other cell structures. In the secondary lamella of the gills and in liver of fish exposed to NPs presence of round structures with similar size to the commercial NPs were observed inside the tissues but could not be distinguished from other cell structures.

Results and discussion

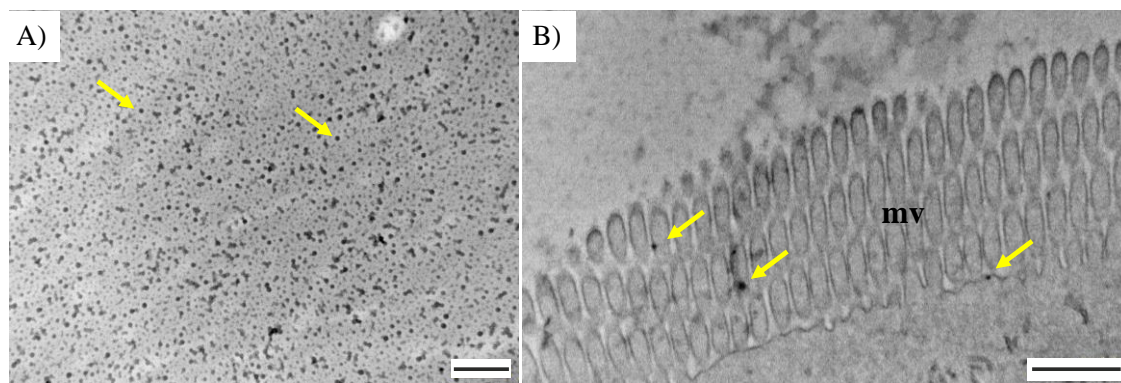


Fig. 1- TEM micrographs showing A) 50 nm NPs; B) apical zone of the enterocytes of adult zebrafish after 21 days of exposure to 0.07 mg/L of NPs. The presence of electron-dense structures resembling NPs (yellow arrows) was detected close to the microvilli (mv). Scale bars: 500 nm.

Fluorescent NPs of 50 nm could not be localised in paraffin tissues due to high autofluorescence of the sample. Ingestion of 4.5 μm MPs was observed in all groups exposed to MPs (MPs, MPs-WAF, MPs-B(a)P) as can be seen in **Fig. 2**. Abundant presence of MPs was detected in the lumen of the intestine of the zebrafish at the two exposure times. Unexposed fish did not show presence of MPs. At light microscopy level, MPs were not seen inside the cells of the tissues of the different organs examined (intestine, liver and gills). The quantification of number of MPs was done in the intestine lumen for fish exposed to MPs alone or in combination with PAHs (**Fig. 3**). The amount of MPs found in the intestine lumen was less at 3 days than at 21 days. After 3 days, fish exposed to MPs-B(a)P presented 30.5 ± 37.37 particles/fish, followed by fish exposed to pristine MPs with 6.4 ± 16.574 particles/fish and finally by fish exposed to MPs-WAF with a presence of 0.44 ± 1.33 particles/fish. After 21 days, fish exposed to MPs-WAF showed the highest presence of particles with a value of 112.78 ± 222.32 particles/fish, being significantly higher than those scored in the same exposure group at 3 days. Similar values were obtained in fish exposed to pristine MPs and to MPs-B(a)P with values of 45.5 ± 63.92 and 38.3 ± 60.89 particles/fish, respectively. The amount of particles scored in fish exposed to pristine MPs for 21 days was also significantly higher than after 3 days of exposure.

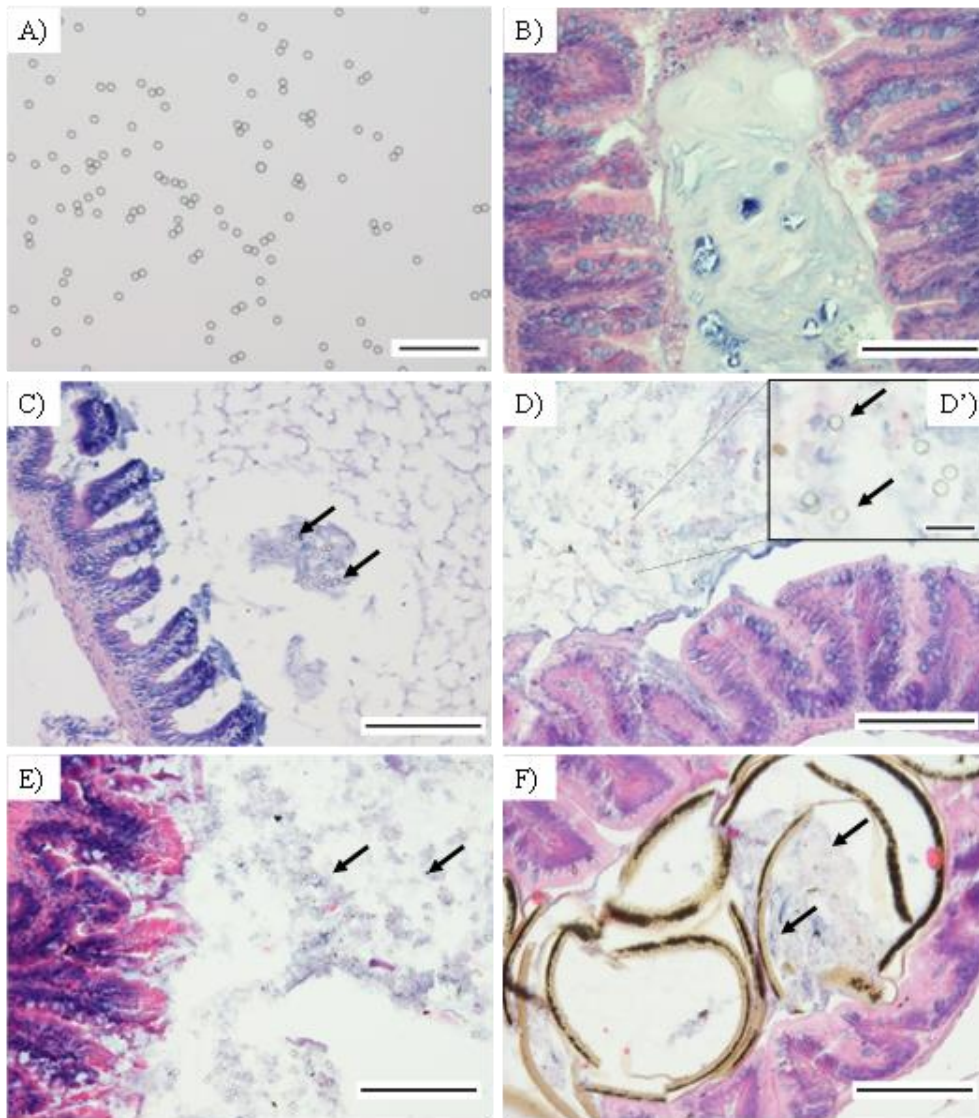


Fig. 2- Micrographs of 4.5 μm MPs and of histological sections of zebrafish intestine. A) 4.5 μm MPs; B) control zebrafish at 3 days; C) zebrafish exposed to 4.5 μm pristine MPs for 3 days showing accumulation of MPs in the intestine lumen (black arrows); D) zebrafish exposed to 4.5 μm pristine MPs for 21 days; D') MPs (black arrows) in the intestinal lumen observed at higher magnification; E) zebrafish exposed to MPs-WAF for 21 days, also showing abundant MPs (black arrows) in the lumen; F) zebrafish exposed to MPs-B(a)P for 21 days, MPs (black arrows) appear together with empty *Artemia* cysts in the lumen of the intestine. Scale bars: 50 μm (A), 100 μm (B-F) and 15 μm (D').

Results and discussion

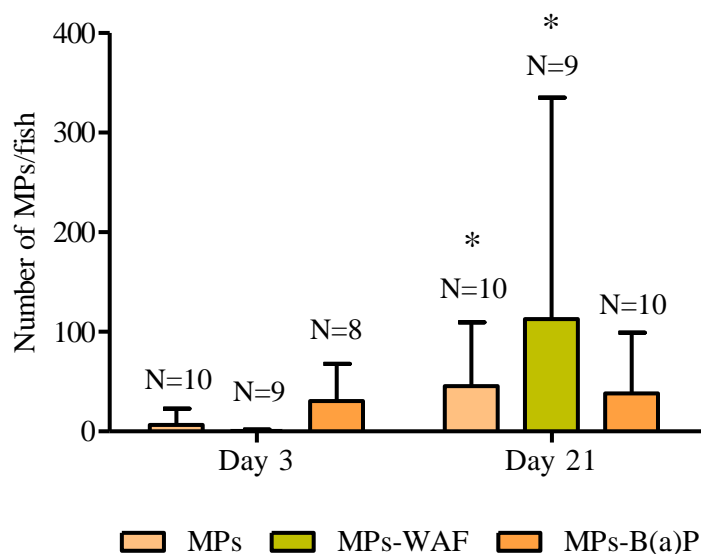


Fig. 3- MPs found in the lumen of the intestine. Data are shown as means \pm SD. Asterisks indicate statistically significant differences ($p < 0.05$) for the same treatment between exposure days according to Mann Whitney U test. N = individuals per experimental group. In some cases $N < 10$ because the intestine tissue was not always present in the histological sections used for the analysis.

PAH concentration in water and fish tissues. Results of the chemical analysis of PAH concentration in the WAF stock solution are shown in **Table 1** and PAH concentrations measured in exposure tanks are given in **Table 2**. Control tanks did not show detectable levels of PAHs, except for naphthalene that appeared at low concentrations only in one water sample out of three collected 30 min after dosing ($0.0326 \mu\text{g/L}$) and after 3 days ($0.0172 \mu\text{g/L}$) of the first dose. In the tank dosed with 5% WAF, measured PAH concentration was lower than the concentration expected based on the measures done in the WAF stock solution (**Table 1**). For example, naphthalene concentration in water samples from the 5% WAF tank was $6.556 \pm 0.963 \mu\text{g/L}$, 43 times lower than in the 100% WAF stock ($286.768 \pm 37.490 \mu\text{g/L}$). Similar concentration ratio was measured for fluorene and phenanthrene, with a concentration in the 5% WAF tank 30 min after dosing of $0.123 \pm 0.013 \mu\text{g/L}$ and $0.094 \pm 0.016 \mu\text{g/L}$, respectively, when the concentration in the 100% stock was $4.658 \pm 0.995 \mu\text{g/L}$ and $3.333 \pm 1.483 \mu\text{g/L}$. Three days after redosing, almost all the PAHs disappeared from the 5% WAF exposure tank or were lower than the limits of quantification, except for naphthalene ($0.327 \pm 0.410 \mu\text{g/L}$), fluorene ($0.01 \mu\text{g/L}$) and phenanthrene ($0.02 \mu\text{g/L}$).

In MPs-WAF the experimental group, only naphthalene was detected at a concentration of $0.063 \pm 0.042 \mu\text{g/L}$ 30 min after dosing and $0.037 \pm 0.03 \mu\text{g/L}$ after 3 days. Regarding the B(a)P alone exposure group, the measured concentration in the tank was $4.923 \pm 3.161 \mu\text{g/L}$ after 30 min when the nominal exposure concentration was $21 \mu\text{g/L}$. After 3 days, B(a)P concentration was

reduced to 0.160 ± 0.117 $\mu\text{g/L}$. Finally, water samples from MPs-B(a)P exposure group did not presented detectable values of B(a)P.

Table 1- Concentration of PAHs ($\mu\text{g/L}$) in 100% WAF of the naphthenic North Sea crude oil. Values are expressed as mean \pm S.D.

Compound	MW	Concentration	L.Q.
Naphthalene	128	286.768 ± 37.490	0.005
Acenaphthylene	152	n.d.	0.004
Acenaphthene	154	1.643 ± 0.820	0.004
Fluorene	166	4.658 ± 0.995	0.004
Anthracene	178	0.119 ± 0.026	0.003
Phenanthrene	178	3.333 ± 1.483	0.003
Fluoranthene	202	0.041 ± 0.024	0.005
Pyrene	202	0.042 ± 0.023	0.005
Benz(a)anthracene	228	<L.Q.	0.012
Chrysene	228	<L.Q.	0.006
Benzo(e)pyrene	252	<L.Q.	0.014
Benzo(a)pyrene	252	<L.Q.	0.006
Perylene	252	<L.Q.	0.014
Benzo(b)fluoranthene	252	<L.Q.	0.008
Benzo(k)fluoranthene	252	<L.Q.	0.008
Indeno(1,2,3-cd)pyrene	276	<L.Q.	0.037
Benzo(ghi)perylene	276	<L.Q.	0.017
Dibenz(a,h)anthracene	278	<L.Q.	0.019
Total PAHs (Σ PAHs)		296.603	

MW: molecular weight (g/mol); L.Q.: limit of quantification; n.d.: not detected.

PAH accumulation after 3 and 21 days of exposure was analysed in all groups of fish exposed to PAHs alone or sorbed to MPs and in control fish (**Table 3**). Unexposed fish showed a total PAH concentration of 68.65 ± 8.19 ng/g at 3 days and 64.01 ± 17.49 ng/g at 21 days. Similar concentrations were quantified in fish exposed to MPs-WAF, 78.67 ± 22.05 ng/g and 77.98 ± 25.65 ng/g at 3 and 21 days, respectively, showing no increased accumulation along exposure time. The most accumulated PAHs were fluorene with values of about 25 ng/g at 3 and 21 days, and phenanthrene with values of 38.98 ± 3.04 ng/g at 3 days and 35.21 ± 4.40 ng/g at 21 days. Fish exposed to WAF accumulated a higher amount of PAHs with values of total PAHs of 910.03 ± 203.69 ng/g and 736.53 ± 108.83 ng/g at 3 and 21 days, respectively. Naphthalene was the most concentrated compound at 3 days, but concentration dropped from 502.88 ± 94.10 ng/g to 109.16 ± 41.84 ng/g at 21 days. On the contrary, concentration of other PAHs in whole fish tissues, such as acenaphthene, fluorene, phenanthrene and anthracene, increased with exposure time (**Table 3**). In fish exposed to MPs-B(a)P, B(a)P was quantifiable only in one replicate at 21 days of exposure, with a value of 3 ng/g. For fish exposed to B(a)P alone, B(a)P concentration did not

Results and discussion

increased along exposure time with values of $40.25 \pm 4.09 \mu\text{g/L}$ at 3 days of exposure and of $33.00 \pm 3.5 \mu\text{g/L}$ at 21 days.

Table 2- Mean (\pm S.D.) of PAH concentration ($\mu\text{g/L}$) in exposure media at 30 minutes and 3 days after dosing in three medium renewal cycles. Acenaphthylene, anthracene, fluoranthene, pyrene, benzo(a)anthracene, chrysene, benzo(e)pyrene, perylene, benzo(b)fluoranthene, benzo(k)fluoranthene, indeno(1,2,3-cd)pyrene, benzo(ghi)perylene and dibenz(a,h)anthracene were not detected in any water samples.

	Control		MPs-WAF		WAF		MPs-B(a)P		B(a)P	
	30'	3 d	30'	3 d	30'	3 d	30'	3 d	30'	3 d
Naphthalene	0.03*	0.02*	0.06 \pm 0.04	0.04 \pm 0.03	6.57 \pm 0.96	0.33 \pm 0.41	-	-	-	-
Acenaphthene	n.d.	n.d.	n.d.	n.d.	0.038 \pm 0.004	n.d.	-	-	-	-
Fluorene	n.d.	n.d.	n.d.	n.d.	0.12 \pm 0.01	0.01*	-	-	-	-
Phenanthrene	n.d.	n.d.	n.d.	n.d.	0.09 \pm 0.02	0.02*	-	-	-	-
Benzo(a)pyrene	n.d.	n.d.	n.d.	n.d.	n.d.	n.d.	n.d.		4.92 \pm 3.16	0.16 \pm 0.12
Σ PAHs	0.03	0.02	0.06	0.04	6.80	0.36	-	-	-	-

n.d.: not detected; *: values corresponding to a single replicate in where PAHs were detected; - : not measured.

Transcription levels of target genes. The gene transcription levels in the liver of fish exposed to NPs and pristine MPs are shown in **Fig. 4**. Exposure to NPs for 3 or 21 days did not significantly alter the transcription level of genes related to biotransformation metabolism (*cyp1a* and *gstp1*) and cell cycle regulation (*tp53*). Exposure to MPs for 21 days resulted in a significant up-regulation of *cyp1a* and *gstp1* compared to control fish and to fish exposed to NPs, respectively. Regarding the genes coding for the antioxidant enzymes, exposure to NPs for 3 days did not provoke any effect, but at 21 days significant alteration of the transcription levels of the three genes investigated was observed. Whereas *cat* resulted downregulated compared to control fish and fish exposed to MPs, transcription levels of *gpx1a* and *sod1* were upregulated. Exposure to MPs alone only provoked downregulation of *gpx1a*, compared to the control group and to fish exposed to NPs, after 3 days of exposure. The transcription levels of *cyp1a*, *gstp1* and *tp53* in the liver of fish exposed to MPs alone or with sorbed PAHs and to PAHs alone are shown in **Fig. 5**. *Cyp1a* only showed a significant up-regulation in fish exposed to MPs-WAF for 3 days compared to fish exposed to MPs, MPs-B(a)P and B(a)P. Exposure for 21 days to MPs with sorbed PAHs or to WAF alone provoked elevated levels of *cyp1a*, but these changes were not statistically significant respect to control fish. However, *cyp1a* transcription levels in fish exposed to WAF were significantly higher than in individuals exposed to B(a)P.

Table 3- Concentration of PAHs (ng/g dry weight) in adult zebrafish at 3 and 21 days of exposure. Values are expressed as mean±S.D. of fourth replicates for 3 days and sixth replicates for 21 days. Concentration of benzo(a)anthracene, perylene, benzo(b)fluoranthene, benzo(k)fluoranthene, indeno(1,2,3-cd)pyrene, benzo(ghi)perylene and dibenz(a,h)anthracene in all the quantified samples were not detected or under limit of quantification.

	Control		MPs-WAF		WAF		MPs-B(a)P		B(a)P		L.Q.
	3 d	21 d	3 d	21 d	3 d	21 d	3 d	21 d	3 d	21 d	
Naphthalene	7.49±1.64	6.89±1.98	9.33±0.12	8.90±0.78	502.88±94.10	109.16±41.84	-	-	-	-	9.50
Acenaphthylene	2.23±0.26	<L.Q.	1.87±0.84	1.92±0.41	2.52±0.67	1.92±0.51	-	-	-	-	0.60
Acenaphthene	9.55±1.20	11.14±5.23	8.55±4.74	11.19±1.80	46.2±16.73	52.80±6.94	-	-	-	-	0.88
Fluorene	19.77±2.77	21.51±7.83	25.43±4.67	25.06±5.56	138.03±103.47	260.61±22.81	-	-	-	-	0.80
Phenanthrene	23.85±6.02	21.55±3.57	38.98±3.04	35.21±4.40	163.52±42.98	293.63±45.79	-	-	-	-	5.50
Anthracene	1.46±0.75	0.89±0.38	2.61±0.33	1.57±0.45	4.81±3.25	16.29±7.44	-	-	-	-	0.58
Fluoranthene	3.55±3.55	1.61±0.00	2.56±0.28	2.1±0.27	2.96±0.75	2.47±0.26	-	-	-	-	1.60
Pyrene	2.60±1.47	2.11±0.39	2.26±0.50	2.33±0.22	2.4±0.11	2.82±0.00	-	-	-	-	1.88
Chrysene ⁺ triphenylene	<L.Q.	<L.Q.	<L.Q.	<L.Q.	1.12*	<L.Q.	-	-	-	-	0.50
Benzo(e)pyrene	<L.Q.	<L.Q.	<L.Q.	<L.Q.	1.04*	<L.Q.	-	-	-	-	1.00
Benzo(a)pyrene	<L.Q.	<L.Q.	<L.Q.	<L.Q.	<L.Q.	<L.Q.	<L.Q.	3*	40.25±4.09	33.00±3.5	1.00
ΣPAHs	68.65±8.19	64.01±17.49	78.67±22.05	77.98±25.65	910.03±203.69	736.53±108.83	-	-	-	-	

L.Q.: limit of quantification; *: value corresponding to a single replicate where PAHs were detected; -: not measured.

Results and discussion

Regarding *gstp1*, significant differences were observed only at 21 days (**Fig. 5**). Fish exposed to MPs-WAF and WAF presented significantly higher transcription levels than fish exposed to B(a)P, whereas no differences were found among fish treated with MPs alone or with sorbed PAHs. Significant differences were not observed for *tp53* transcription levels at any exposure time in any treatment.

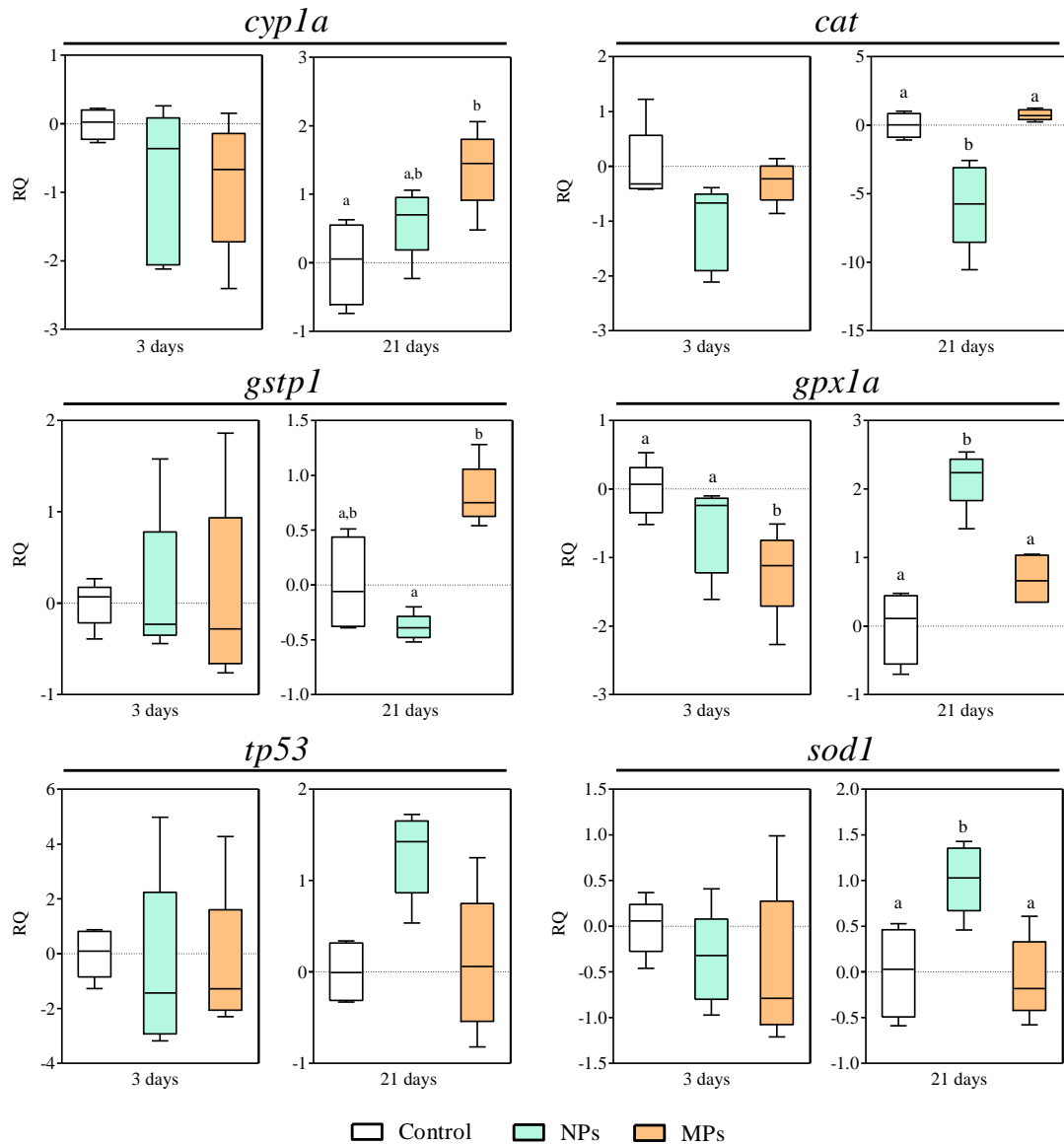


Fig. 4- Relative quantification (RQ) of transcription levels of the biotransformation metabolism related genes A) *cypla* and B) *gstp1*, cell cycle related gene C) *tp53* and oxidative stress related genes D) *cat*, E) *gpx1a* and F) *sod1* in adult zebrafish liver after 3 and 21 days of exposure. Box-plots represent the percentage data value in between the 25th and the 75th percentile, median indicated by a line in the middle of the box. Whiskers are the data values in up to the 5th percentile and 95th percentile. Different letters indicate statistically significant differences (p<0.05) within each exposure time according to the Kruskal-Wallis test followed by the post hoc Dunn's test for the non-parametric data sets (B, C, D, E) and one-way ANOVA followed by the post hoc Tukey test for the parametric data sets (A, F).

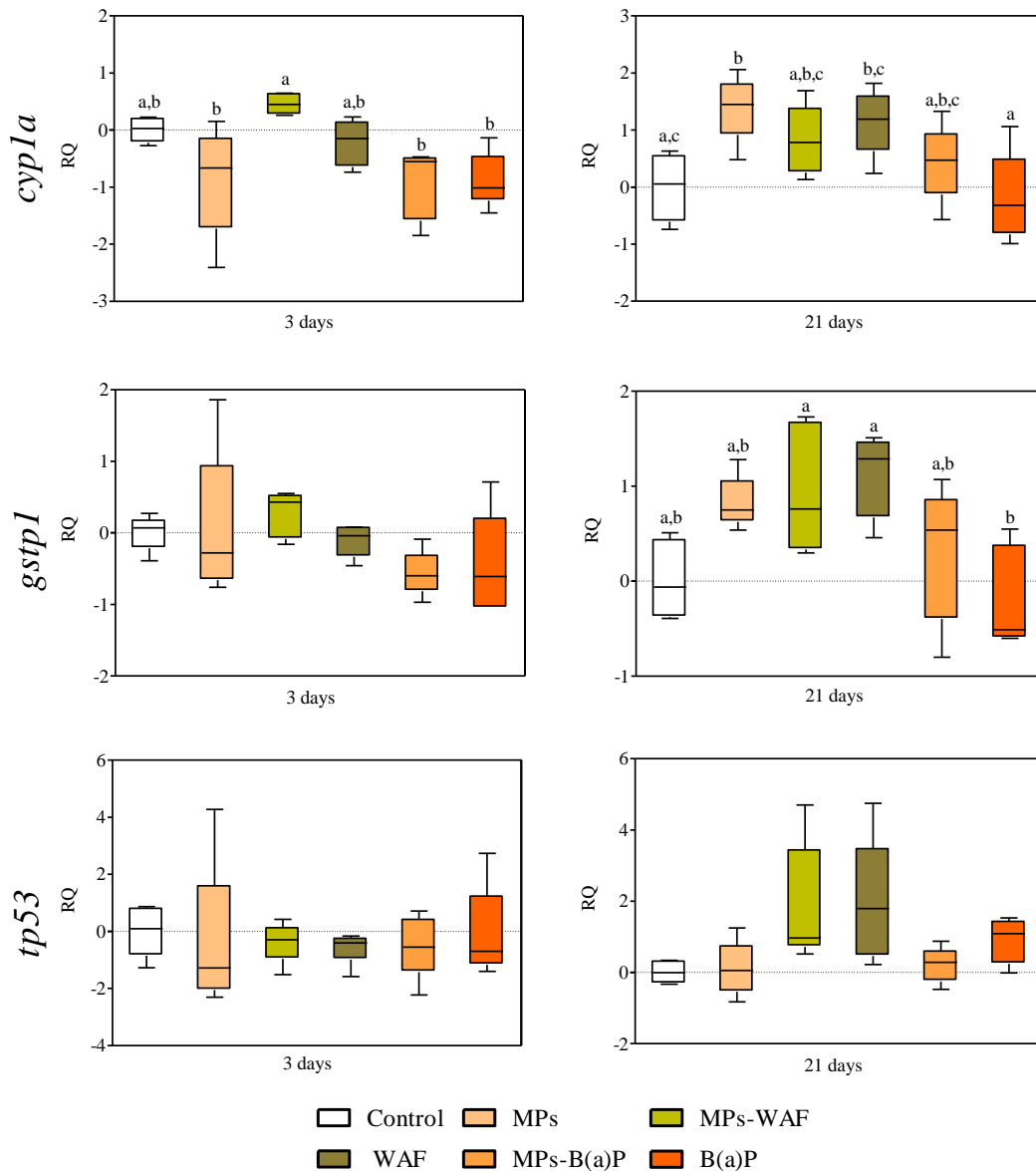


Fig. 5-Relative quantification (RQ) of transcription levels of the biotransformation metabolism related genes A) *cyp1a* and B) *gstp1* and cell cycle related gene C) *tp53* in adult zebrafish liver after 3 and 21 days of exposure. Data representation as in Fig. 4. Different letters indicate statistically significant differences ($p < 0.05$) within each exposure time according to the Kruskal-Wallis test followed by the post hoc Dunn's test (C) and one-way ANOVA followed by the post hoc Tukey test (A, B).

Results of the transcription levels of genes coding for the antioxidant enzymes in liver of fish exposed to MPs alone or in combination with PAHs are shown in **Fig. 6**. In the case of fish exposed to MPs contaminated with WAF, to WAF alone and to B(a)P alone, only effects compared to control fish were recorded at 3 days in fish exposed to MPs-B(a)P for the *sod1* gene. Nevertheless, fish exposed to MPs-WAF for 3 days showed significantly higher transcription levels of *gpx1a* than fish exposed to MPs alone. Compared to fish exposed to MPs-WAF, fish

Results and discussion

exposed to MPs-B(a)P for 3 days displayed significantly lower transcription levels for the three genes and, although not significantly, also lower levels than fish exposed to B(a)P alone.

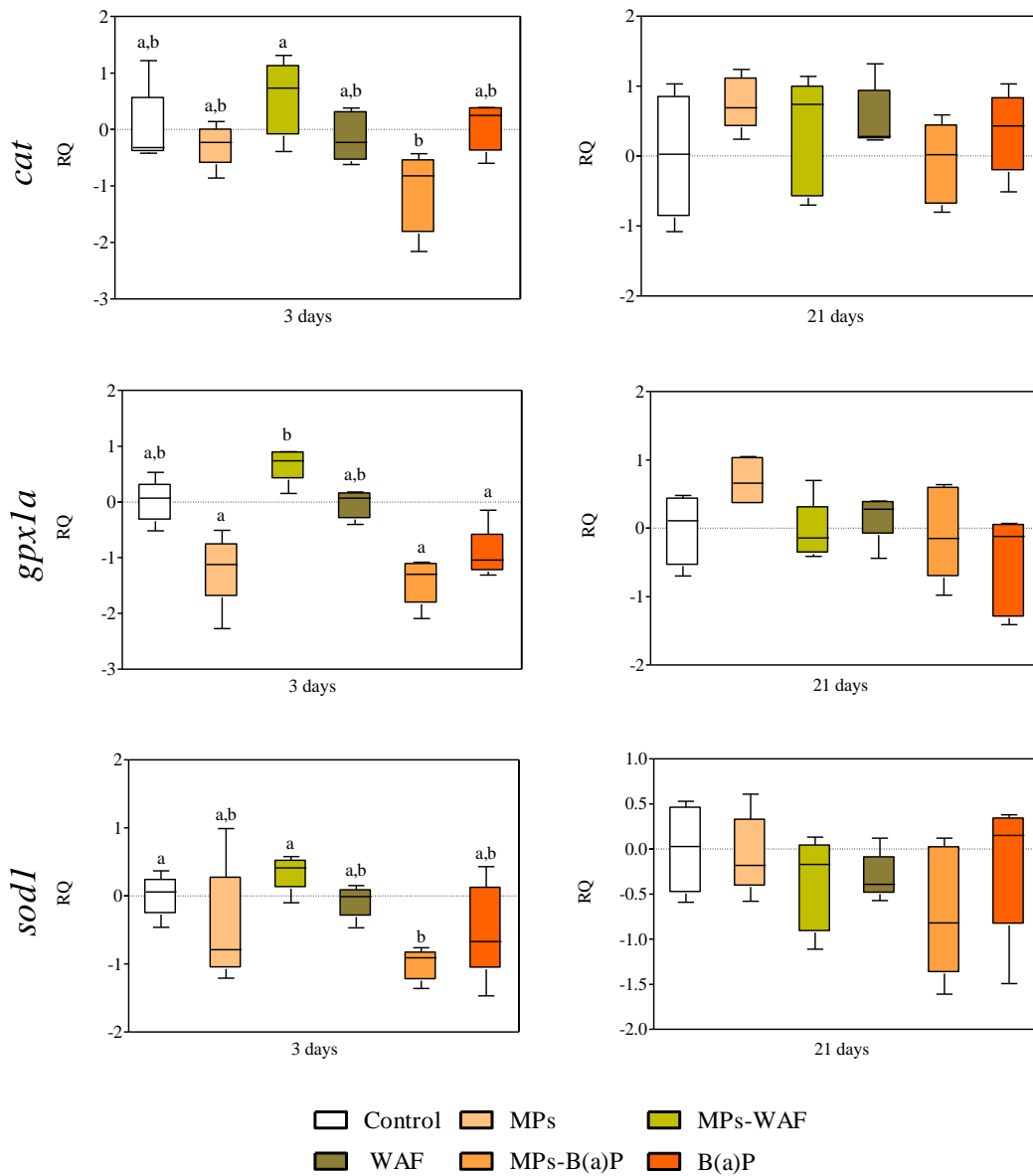


Fig. 6- Relative quantification (RQ) of transcription levels of the oxidative stress related genes A) *cat*, B) *gpx1a* and C) *sod1* in adult zebrafish liver after 3 and 21 days of exposure. Data representation as in Fig. 4. Different letters indicate statistically significant differences ($p < 0.05$) within each exposure time according to the Kruskal-Wallis test followed by the post hoc Dunn's test (A, B) and one-way ANOVA followed by the post hoc Tukey test (C).

Histopathological alterations. In liver, different pathological conditions, such as vacuolisation, presence of megalocytosis, necrotic focus and eosinophilic focus were observed in exposed fish. Prevalence of the histopathological alterations found in zebrafish liver is shown in **Table 4**. Control fish showed normal architecture of the liver (**Fig. 7A**), although two individuals at each

sampling time showed vacuolisation. Treated fish presented, in general, higher prevalence of vacuolisation (**Fig. 7B**), being this increase (up to 80%) statistically significant in the liver of fish exposed to MPs for 21 days (**Fig. 7C**) and noticeable (70%) in the case of fish exposed to WAF for 3 days. At 21 days, vacuolisation prevalence was reduced to 44.4% in fish exposed to WAF (**Fig. 7E**). Other histopathological conditions, such as megalocytosis and necrotic focus (**Fig. 7D and 7F**) appeared at low prevalence in fish exposed to NPs, MPs-WAF and WAF.

Table 4- Prevalence (%) of histopathological alterations in the liver of zebrafish. Asterisks indicate statistically significant differences ($p < 0.05$) according to the Fisher's exact test compared to the control group at the same exposure day.

		n	Vacuolisation	Megalocytosis	Necrotic focus	Total
Control	3 d	10	20	n.o.	n.o.	20
	21 d	10	20	n.o.	n.o.	20
NPs	3 d	10	30	10	n.o.	30
	21 d	10	40	n.o.	10	50
MPs	3 d	10	40	n.o.	n.o.	40
	21 d	10	80*	n.o.	n.o.	80*
MPs-WAF	3 d	9	33.33	11.11	n.o.	44.44
	21 d	9	11.11	11.11	n.o.	22.22
WAF	3 d	10	70	n.o.	20	80*
	21 d	9	44.4	11.11	n.o.	55.55
MPs-B(a)P	3 d	10	20	n.o.	n.o.	20
	21 d	10	50	n.o.	n.o.	50
B(a)P	3 d	9	55.56	n.o.	n.o.	55.56
	21 d	10	30	n.o.	n.o.	30

n: number of individuals per experimental group (in some cases $n < 10$ because the liver tissue was not always present in the histological sections used for the histological analysis); n.o.: not observed.

Overall, prevalence of histopathological alterations gills was low. Control fish showed normal architecture of the gills (**Fig. 8A**). Besides one individual showing inflammation (**Fig. 8B**), fish exposed to NPs also presented normal gill histology. Inflammation was also seen in few individuals exposed to MPs (**Fig. 8C**), but not in the other treatment groups. Aneurisms were found on one individual exposed to MPs for 21 days (**Fig. 8D**) and in one individual (out of four) exposed to B(a)P for 3 days. Finally, one individual exposed to MPs for 3 days presented hyperplasia.

Results and discussion

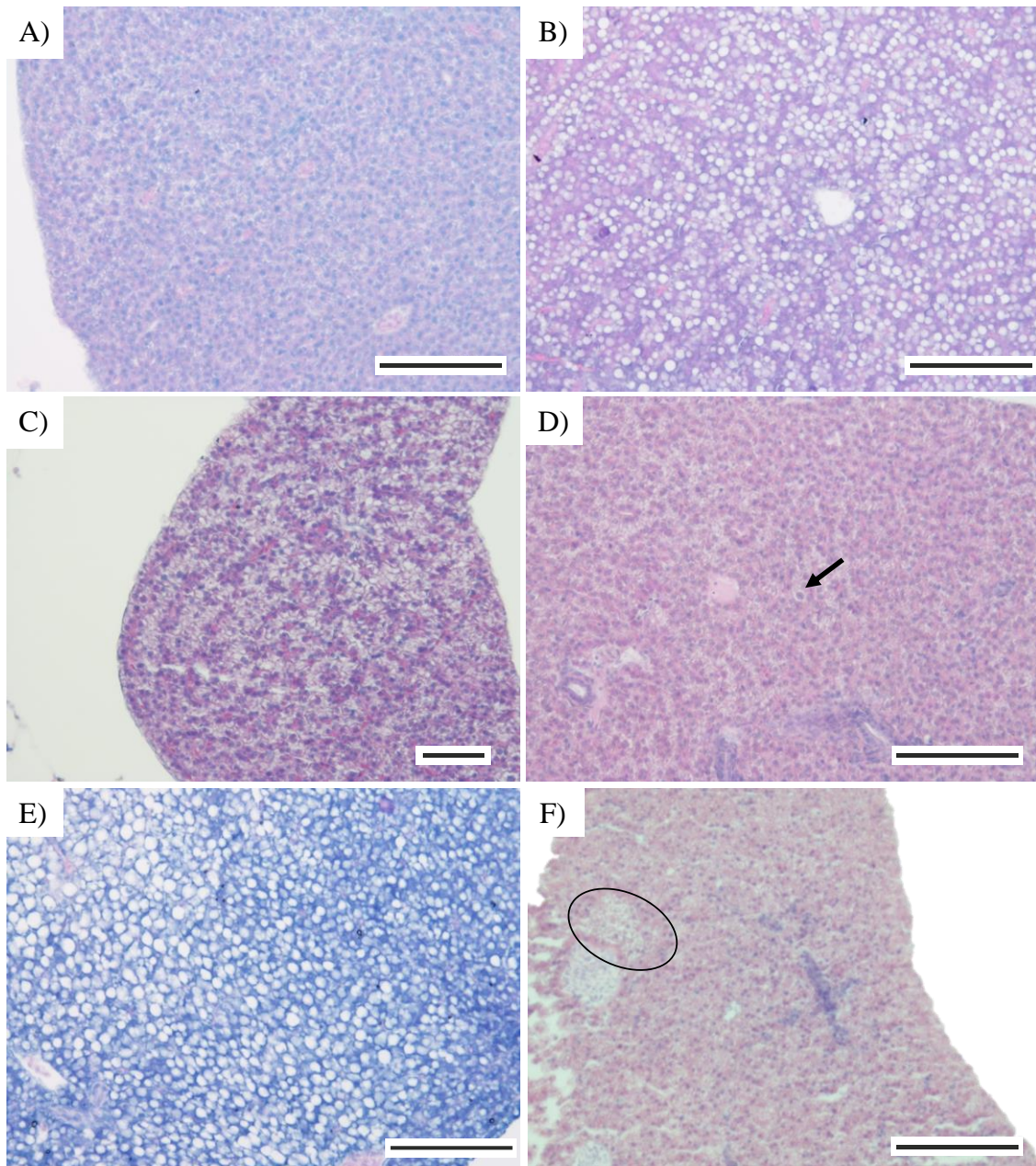


Fig. 7- Micrographs of histological sections of zebrafish liver. A) Liver of unexposed adult zebrafish at 21 days showing normal morphology; B) Liver of a zebrafish exposed to NPs for 21 days showing vacuolisation; C) Liver of a zebrafish exposed to MPs for 21 days showing vacuolisation; D) Liver of a zebrafish exposed to MPs-WAF for 21 days showing megalocytosis (black arrow); E) Liver of a zebrafish exposed to WAF for 21 days showing liver vacuolisation; F) Liver of a zebrafish exposed to WAF for 3 days showing a necrotic focus (black circle). Scale bars: 100 μm .

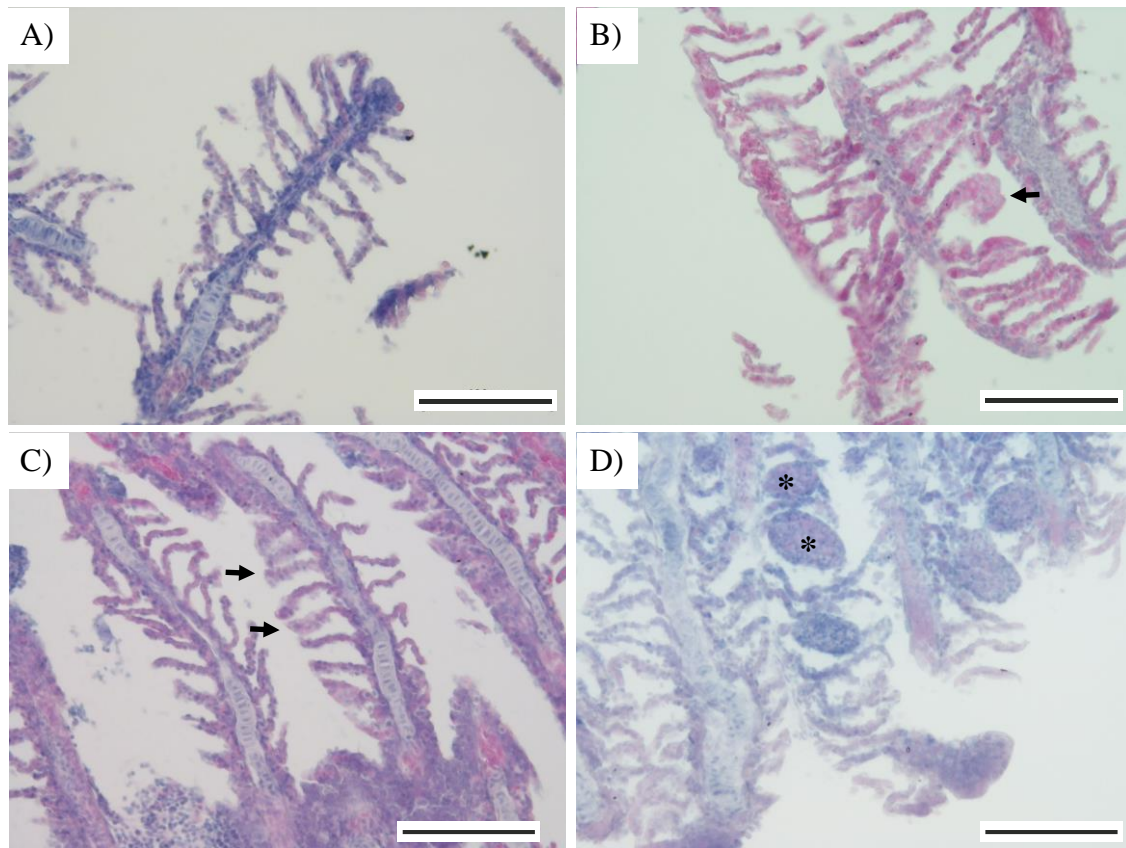


Fig. 8- Micrographs of histological section of zebrafish gills. A) Gills of unexposed zebrafish at 21 days showing normal morphology; B) Gills of zebrafish exposed to NPs for 3 days, showing inflammation (arrow); C) Gills of a zebrafish exposed to MPs for 3 days, showing inflammation (arrows); D) Gills of a zebrafish exposed to MPs for 21 days showing aneurism (asterisks). Scale bars: 100 μ m.

DISCUSSION

In the present study, the potential harmful effects produced by polystyrene NPs (50 nm) and MPs (4.5 µm) were studied in adult zebrafish. Ingestion and internalisation of fluorescent NPs could not be demonstrated in histological sections of intestine and gills due to the high autofluorescence of the samples. At TEM, NPs could be seen as a well dispersed suspension of round particles, although some aggregates could be observed. Round electron dense particles resembling NPs were found in intestine lumen close to microvilli. Inside cells, NPs could not be clearly identified; vesicles containing particles as those seen in the suspension were not found. In previous studies, NP ingestion has been observed in zebrafish embryos (**Chapter 1**; Pitt et al., 2018b) and in adult zebrafish (Skjolding et al., 2017). Fluorescent NPs have been identified by light sheet microscopy in intestine, gills and head of zebrafish but no evidence of translocation to inner tissues was observed (Skjolding et al., 2017). NPs can also be transferred from adults to embryos (F1) as reported by Pitt et al. (2018b). *In vitro* studies with rainbow trout intestinal cells have also demonstrated accumulation of fluorescent PS NPs (73 ± 18 nm) and their ability to prevent the translocation of PS-NPs to the basolateral compartment (Geppert et al., 2016), but further *in vivo* studies are required to study the potential translocation (internalisation) to the tissues.

MPs were observed in the intestinal lumen of zebrafish exposed to all treatments containing MPs, but not inside cells or tissues. Several studies have reported the ingestion of MPs of different size by zebrafish (Karami et al., 2017; Lei et al., 2018; Qiao et al., 2019; Batel et al., 2020). MPs (5 µm) were numerously localised in the gut duct of zebrafish exposed for 21 days to 50 and 500 µg/L of PS (Qiao et al., 2019). Similar results were obtained by Karami et al. (2016), who detected an abundant presence of low-density PE fragments (<18 µm) in the intestinal lumen of adult zebrafish after 10 days of exposure (50 and 500 µg/L). As observed in the present study, MPs are commonly found in the intestinal lumen of fish, but their ability to internalise into fish tissues is still being questioned (Batel et al., 2020).

The discussion on whether MPs act as vectors for adsorbed hazardous chemicals is also open (Batel et al., 2020). Thus, to address this issue zebrafish were also exposed to MPs contaminated with PAHs and to the corresponding dissolved fraction of the sorbed PAHs. The actual PAH concentration was measured along exposure time in tanks. In the WAF tank, PAH concentration in water was lower than the corresponding dilution (nominal 5%, measured 2.3%) according to concentration measured in the 100% WAF stock. WAF used in the study is mainly composed by low weight polycyclic aromatic hydrocarbons and represented by naphthalene as expected for a low energy WAF of a NNS crude oil (Perrichon et al., 2016; **Chapter 2**). In addition, the WAF stock used to contaminate the aquaria was prepared in advance to be also used to contaminate MPs for 24 h before dosage. The WAF stock was stored in the fridge overnight, which could also

lead to some PAH loss. Lower concentration than the nominal concentration was also measured in the B(a)P exposure tank. This has also been reported in previous exposure experiments with freshwater fish (Zhao et al., 2013) and in sorption experiments of PAHs to MPs (**Chapter 2**) and could be due to the low solubility of B(a)P in water (1.64 µg/L; May et al., 1983).

PAH concentration in exposure tanks was notably reduced after 3 days of dosing, which could be due to PAH uptake by zebrafish and to other processes like PAH adsorption to the tank walls, degradation and volatilisation, the latter especially in the case of the low molecular weight PAHs present in the WAF. In the case of B(a)P alone, 97% of the B(a)P was lost after 3 days. Similar results were obtained by Costa et al. (2011), who reported a 96.97% of B(a)P loss after 24 h of exposure of Nile tilapia. In the exposure tanks containing MPs with sorbed PAHs (MPs-B(a)P and MPs-WAF), PAH concentration in water were below the limit of quantification showing that probably MPs with sorbed PAHs did not released these compounds to the water. After incubation in the PAH solution and filtering, MPs were rinsed with clean water to remove the dissolved PAH fraction not sorbed to MPs. As observed by Zuo et al. (2019), 250 µm PS MPs showed less desorption of phenanthrene than other polymers, like PE or PVC, indicating that the interaction of this PAH and PS was stronger than in the other cases.

Fish accumulated higher concentration of PAHs after exposure to dissolved PAHs than after exposure to MPs with sorbed PAHs. With the exception of phenanthrene and fluorene, fish exposed to MPs with sorbed PAHs showed similar PAH concentration to control fish. Only in fish exposed to WAF, an exposure time dependent increase in the concentration of four PAHs (acenaphthene, fluorene, phenanthrene and anthracene) was observed. It is well known that PAHs are accumulated, but also easily metabolised by fish (Livingstone, 1998), being the metabolism of low molecular weight PAHs ($\log K_{ow} < 5$) slower than the metabolism of high molecular weight PAHs ($\log K_{ow} > 5$) (Budzinski et al., 2004) due to their higher ability to induce the aryl hydrocarbon receptor (AHR). In addition, the higher solubility of low molecular weight PAHs in water make them available through the gills-water barrier, while high molecular weight PAHs are more prone to be assimilated by digestive system (Jafarabadi et al., 2019). This would also explain the lower B(a)P accumulation compared to PAHs from WAF, even when the measured concentration of B(a)P during exposure was higher than for individual PAHs from WAF.

To assess the effects of exposure to NPs and MPs alone and in combination with PAHs, a set of well established biomarkers of biotransformation metabolism, cell cycle regulation and oxidative stress were selected. Cytochrome P450 1A (*cyp1a*) and glutathione S-transferase pi (*gstp1*) play an important role in metabolic activation and detoxification of PAHs in fish liver. Compared to control fish, only fish exposed to MPs for 21 days showed a significant upregulation of *cyp1a* transcription levels, along with an increase of *gstp1* transcription levels. Our results are

Results and discussion

comparable to those reported in red tilapia by Ding et al. (2018), who observed that short-term exposure of 1, 3 or 6 days to 10 and 100 µg/L of PS MPs (100 nm) resulted in inhibition of liver 7-ethoxyresorufin O-deethylase (EROD) activity, enzyme coded by *cyp1a*, but at longer term (14 days) induction of EROD was observed. On the contrary, in adult marine medaka, 60 days of exposure to 10 µm PS MPs caused inhibition of hepatic GST enzyme activity at all tested concentrations (2, 20 and 200 µg/L) (Wang et al., 2019a). In the present study *cyp1a* and *gstp1* were not affected by NPs exposure, suggesting that size of plastic could influence the pathways in which the organism are affected. The potential causes of CYP P450 increased activity as result of MPs exposure in fish are unknown.

No significant alteration of *cyp1a* and *gstp1* transcription levels was seen in zebrafish liver exposed to PAHs or PAH-contaminated MPs, although at 21 days higher mean values were measured in fish exposed to PAH-contaminated MPs and to WAF than in control fish and fish exposed to B(a)P. Rainbow trout exposed to 100-400 µm PS MPs (5 pellets/fish/day) contaminated with sewage or harbour waters did neither show significant differences in mRNA levels of *cyp1a*, *gstp1* or *cat*, compared to fish exposed to pristine PS MPs (Ašmonaitė et al., 2018). The two fractions obtained after filtration of a solution containing 200-250 µm PVC MPs (500 mg/L) and phenanthrene (0.5 mg/L) were used to assess the capacity of MPs to act as vectors of PAHs in zebrafish larvae. *Cyp1a* as a marker of PAH exposure showed that larvae exposed to the filtered fraction (PAHs alone) presented a significant up-regulation of transcription levels compared to larvae exposed to MPs with sorbed phenanthrene due to a reduction of the phenanthrene bioavailability when sorbed to the MPs (Sleight et al., 2016). On the contrary, zebrafish exposed to 0.5 µM (126 µg/L) B(a)P presented lower liver EROD activity than fish exposed to 1-5 µm MPs and 10-20 µm MPs spiked with B(a)P. Only exposure to 1 µM (252 µg/L) B(a)P induced EROD activity significantly (Batel et al., 2016). In our study, the measured concentration of B(a)P (4.923±3.161 µg/L) was lower than concentrations found in the literature able to induce *cyp1a* on zebrafish liver. On the other hand, the lack of response to MPs with sorbed PAHs could be explained by the limited bioavailability of the compounds (especially in MPs-B(a)P as reflected by PAH bioaccumulation analyses) or by the fact that the PAH concentrations were not enough to trigger responses in the selected biotransformation markers. Given the low weight PAH composition of the WAF from the NNS crude oil, strong induction of liver transcription levels of *cyp1a* was not expected. According to the results obtained in zebrafish embryos by Perrichon et al. (2016), significant upregulation of *cyp1a* was only measured at concentrations higher than 10% WAF of different types of crude oil (brut Arabian Light and Erika heavy fuel oil). Wang et al. (2018) obtained similar results, where significant upregulation of *cyp1a* in 15 days post fertilisation (dpf) and 30 dpf juvenile zebrafish exposed to PAHs from a

crude oil (5 and 50 µg/L total PAHs) compared to control was observed along with a down-regulation of *gstp1* on 15 dpf juvenile zebrafish exposed to 5 and 50 µg/L total PAHs.

The tumour suppressor gene *tp53* has been often used in fish toxicology as a biomarker for genotoxicity (Bhaskaran et al., 1999; Ruiz et al., 2012). In this study, significant differences in its transcription levels were not observed in any treatment, although higher mean values were measured in all fish groups exposed to PAHs for 21 days than in control fish or fish exposed to pristine MPs. To the best of our knowledge, there are not previous data on the effects of NP exposure on fish *tp53* transcription levels. Only some studies have been carried out on zebrafish exposed to MPs and PAHs (Zaho et al., 2013; Karami et al., 2017; Martins et al., 2018; Perrichon et al., 2018). Karami et al. (2007) did neither see differences in zebrafish embryos exposed to <18 µm low-density PE (5-500 µg/L) fragments for 10 and 20 days compared to control embryos. In zebrafish embryos exposed to the WAF of a light crude oil, significant upregulation of *p53* transcription levels only occurred at 100% WAF (Perrichon et al., 2016). For individual PAHs, exposure of zebrafish or medaka to 0.5 or 1.21 µg/L of B(a)P, respectively, did not cause effects on *tp53* transcription levels (Zaho et al., 2013; Martins et al., 2018). The WAF and B(a)P concentrations used in the present study were again maybe too low to produce significant changes of *tp53* transcription levels.

Metabolism of organic pollutants can enhance the production of reactive oxygen species (ROS) that leads to oxidative stress, which has also been addressed regarding potential MP and NP toxicity (Karami et al., 2017; Chen et al., 2017a; Espinosa et al., 2019; Ding et al., 2018). The antioxidant enzymes CAT and GPx are in charge of cell protection against peroxidation by decomposing reactive species and SOD is in charge of the control of superoxide transformation to hydrogen peroxide (Di Giulio et al., 1989). In this work, statistically significant downregulation of liver *cat* and upregulation of *gpx1a* and *sod1* was observed in zebrafish exposed to NPs for 21 days. Chen et al. (2017a) reported reduced levels of glutathione in zebrafish embryos exposed to 1 mg/L of PS NPs (50 nm) for 5 days whilst no significant changes were recorded in CAT and GPx activities. Exposure to 100 nm PS MPs produced an induction of SOD liver activity on red tilapia at 1, 6, 10 and 14 days when fishes were exposed to 1-100 µg/L of PS MPs (Ding et al., 2018). For larger plastic particles, downregulation of *cat* was reported in zebrafish larvae (5 hours post fertilisation) exposed to 5, 50 and 500 µg/L of low-density PE fragments (<18 µm) for 20 days (Karami et al., 2017). Dietary exposure to PE, but not to PVC, MPs of 40-150 µm (500 mg MPs/Kg diet) inhibited liver SOD and CAT enzyme activities, as well as *sod1* transcription levels, in European sea bass (Espinosa et al., 2019). In our study, exposure to pristine PS MPs did not significantly altered transcription levels of genes coding for the antioxidant enzymes, suggesting that polymer type and particle size can modulate the response of the fish antioxidant system. Plastic size, in particular, seems to be an important characteristic driving oxidative stress in

Results and discussion

aquatic organisms, being the particle size decrease a potential factor of increased oxidative stress in zebrafish. A size dependent toxicity of PS MPs was observed in adult zebrafish exposed for 21 days to 100 nm, 5 µm and 200 µm PS MPs. Decreasing size altered the expression of genes related to phagocyte-produced reactive oxygen species (ROS) generation in zebrafish intestine (Gu et al., 2020). Smaller size can confer NPs more ability to cross the physical defence of fish formed by intestine and gill epithelia (Pitt et al., 2018a).

Cat transcription levels were significantly reduced in fish exposed for 3 days to MPs-B(a)P compared to fish exposed to MPs-WAF. In addition, downregulation of *sod1* was observed in fish exposed to MPs-B(a)P compared to control fish. Absence of oxidative stress in zebrafish embryos co-exposed to MPs/NPs and POPs was reported in the literature, assuming that MPs/NPs alleviated the reported oxidative stress in embryos exposed to POPs alone (Chen et al., 2017a). Oxidative stress is an effect commonly reported in organism exposed to xenobiotics, including PAHs (Vieira et al., 2008; Salazar-Coria et al., 2019). Exposure to WAF of Maya crude oil prepared in a proportion of 100 g/L for 24 h and then diluted at 10, 100 and 1000 mg/L caused significant inhibition of SOD activity in Nile tilapia liver only at the highest concentration while no effect was reported for CAT or GPx in zebrafish liver (Salazar-Coria et al., 2019). Exposure of common goby for 96 h to B(a)P (1-16 µg/L) and to anthracene (0.25-4 µg/L) caused a significant induction of CAT; SOD, GPX and GR activities in liver, while a mixture of PAHs from the WAF of fuel-oil #4 (7.5-30% of 100 g fuel-oil/L) only provoked significant induction of CAT activity (Vieira et al., 2008). In the present study, exposure to MPs alone or to PAHs alone did not alter the transcription levels of the genes coding for the main antioxidant enzymes but, interestingly, exposure to MPs with sorbed B(a)P provoked downregulation of *sod1* suggesting a differential effect of the combined exposure.

Liver is the main organ for metabolic activation and detoxification of PAHs and fish liver histopathology has been studied after exposure to pollutants, showing multiple alterations and being liver vacuolisation one of the most frequently reported (Chae et al., 2018; Chen et al., 2018; Hook et al., 2018; Espinosa et al., 2019; Mai et al., 2019; De Sales-Ribeiro et al., 2020). In the present study, liver vacuolisation was the unique pathological condition showing statistically higher prevalence in fish exposed to MPs for 21 days compared to control fish. Similar significant increase in the prevalence of liver vacuolisation in fish exposed to WAF was observed at short term (3 days). High concentration of PS NPs (5 mg/L) was also found to alter liver histology in the freshwater fish *Zacco temminckii*, causing liver vacuolisation and cell destruction after 7 days of exposure (Chae et al., 2018). Liver vacuolisation was also observed in liver of European sea bass exposed to 40-150 µm PE and PVC MPs (100 and 500 mg/Kg) for 21 days (Espinosa et al., 2019). Similar pathology was observed in liver of zebrafish exposed for longer periods (30 and 45 days) to 1-5 µm PE fragments and fibres (2.1 10⁻² g/cm³, 2% of the total food delivered) but

this time without significant differences among treatments (De Sales-Riberio et al., 2020). When adult zebrafish were exposed for 3 weeks to a combination of 125-250 μm PE MPs (4 mg/g food) with persistent organic pollutants (PCBs, PBDEs, PFCs and methylmercury, 77.9 ng/g food), a greater liver vacuolisation was provoked than when fish were exposed to MPs or POPs alone (Rainieri et al., 2018).

In gills, significant increase in the prevalence of pathological lesions was not recorded after 3 nor 21 days of exposure, but some pathologies were observed, such as inflammation, that is known as a mechanism of defence in fish exposed to MPs and B(a)P (Martins et al., 2018; Limonta et al., 2019). Accordingly, Martins et al. (2018) reported that zebrafish exposure to 0.5 $\mu\text{g/L}$ of B(a)P for 14 days also provoked gill inflammation. A mix of PS and high-density PE MPs at environmentally relevant concentrations (100 and 1000 $\mu\text{g/L}$) caused damage on zebrafish gills integrity (adhesion and partial fusion of secondary lamellae and mucous hypersecretion) after 21 days of exposure (Limonta et al., 2019). Gills are the first barrier to be impacted on fish because of their direct contact with pollutants present on water. However, relevant effects were not observed on this study suggesting again that the pollutant concentrations used were not enough toxic to impair gill structure.

The results of the present work show the different effects caused on zebrafish depending on the size of PS plastics. 4.5 μm PS MPs induced biotransformation metabolism in liver, showing further liver injury characterised by tissue vacuolisation, whereas 50 nm NPs mainly affected the antioxidant system. The ability of 4.5 μm PS MPs to act as vector of PAHs was not observed. Only a slight higher bioaccumulation of PAHs in fish exposed to MPs-WAF than in those exposed to MPs-B(a)P was observed without an increased accumulation of PAHs over time in both groups. Analysis of the gene transcription levels showed an upregulation of biotransformation metabolism and oxidative stress in fish exposed to MPs-WAF compared to those exposed to MPs-B(a)P. Nevertheless, significant differences were not observed compared to controls or fish exposed to PAHs alone showing that the PAH concentration values used were not enough to induce these parameters. Looking at tissue level, only MPs or PAHs from WAF alone caused injury on fish liver (vacuolisation). The results highlighted the importance to assess the potential risk of MPs and NPs to aquatic biota.

REFERENCES

1. Amrutha, K., Warriar, A.K., 2020. The first report on the source-to-sink characterization of microplastic pollution from a riverine environment in tropical India. *Sci. Total Environ.* 739, 140377.
2. Ašmonaitė, G., Larsson, K., Undeland, I., Sturve, J., Carney Almroth, B., 2018. Size matters: ingestion of relatively large microplastics contaminated with environmental pollutants posed little risk for fish health and fillet quality. *Environ. Sci. Technol.* 52, 14381-14391.

Results and discussion

3. Barnes, D.K.A., Galgani, F., Thompson, R.C., Barlaz, M., 2009. Accumulation and fragmentation of plastic debris in global environments. *Phil. Trans. Royal Soc. B Biol. Sci.* 364, 1985-1998.
4. Batel, A., Borchert, F., Reinwald, H., Erdinger, L., Braunbeck, T., 2018. Microplastic accumulation patterns and transfer of benzo[a]pyrene to adult zebrafish (*Danio rerio*) gills and zebrafish embryos. *Environ. Pollut.* 235, 918-930.
5. Batel, A., Linti, F., Scherer, M., Erdinger, L., Braunbeck, T., 2016. Transfer of benzo[a]pyrene from microplastics to *Artemia* nauplii and further to zebrafish via a trophic food web experiment: *CYP1A* induction and visual tracking of persistent organic pollutants: Trophic transfer of microplastics and associated POPs. *Environ. Toxicol. Chem.* 35, 1656-1666.
6. Batel, A., Baumann, L., Carteny, C.C., Cormier, B., Keiter, S.H., Braunbeck, T. 2020. Histological, enzymatic and chemical analyses of the potential effects of differently sized microplastic particles upon long-term ingestion in zebrafish (*Danio rerio*). *Mar. Pollut. Bull.* 153, 111022.
7. Besseling, E., Redondo-Hasselerharm, P., Foekema, E.M., Koelmans, A.A., 2019. Quantifying ecological risks of aquatic micro- and nanoplastics. *Crit. Rev. Environ. Sci. Technol.* 49, 32-80.
8. Bhaskaran, A., May, D., Rand-Weber, M., Tyler, C.R., 1999. Fish *p53* as a possible biomarker for genotoxins in the aquatic environment. *Environ. Mol. Mutagen.* 33, 177-184.
9. Bordós, G., Urbányi, B., Micsinai, A., Kristz, B., Palotai, Z., Szabó, I., Hantosi, Z., Szoboszlai, S., 2019. Identification of microplastics in fish ponds and natural freshwater environments of the Carpathian basin, Europe. *Chemosphere* 216, 110-116.
10. Bouhroum, R., Boulkamh, A., Asia, L., Lebarillier, S., Halle, A.T., Syakti, A.D., Doumenq, P., Malleret, L., Wong-Wah-Chung, P., 2019. Concentrations and fingerprints of PAHs and PCBs adsorbed onto marine plastic debris from the Indonesian Cilacap coast and the North Atlantic gyre. *Reg. Stud. Mar. Sci.* 29, 100611.
11. Budzinski, H., Mazéas, O., Tronczynski, J., Désaunay, Y., Bocquené, G., Claireaux, G., 2004. Link between exposure of fish (*Solea solea*) to PAHs and metabolites: Application to the "Erika" oil spill. *Aquat. Living Resour.* 17, 329-334.
12. Bugiak, B., Weber, L.P., 2009. Hepatic and vascular mRNA expression in adult zebrafish (*Danio rerio*) following exposure to benzo-a-pyrene and 2,3,7,8-tetrachlorodibenzo-p-dioxin. *Aquat. Toxicol.* 95, 299-306.
13. Bussolaro, D., Wright, S.L., Schnell, S., Schirmer, K., Bury, N.R., Arlt, V.M., 2019. Co-exposure to polystyrene plastic beads and polycyclic aromatic hydrocarbon contaminants in fish gill (RTgill-W1) and intestinal (RTgutGC) epithelial cells derived from rainbow trout (*Oncorhynchus mykiss*). *Environ. Pollut.* 248, 706-714.
14. Chae, Y., Kim, D., Kim, S.W., An, Y-J., 2018. Trophic transfer and individual impact of nano-sized polystyrene in a four-species freshwater food chain. *Sci. Rep.* 8, 284.
15. Chen, H., Sheng, L., Gong, Z., Ru, S., Bian, H., 2018. Investigation of the molecular mechanisms of hepatic injury upon naphthalene exposure in zebrafish (*Danio rerio*). *Ecotoxicol.* 27, 650-660.
16. Chen, Q., Gundlach, M., Yang, S., Jiang, J., Velki, M., Yin, D., Hollert, H. 2017a. Quantitative investigation of the mechanisms of microplastics and nanoplastics toward zebrafish larvae locomotor activity. *Sci. Total Environ.* 584-585, 1022-1031.
17. Chen, Q., Yin, D., Jia, Y., Schiwy, S., Legradi, J., Yang, S., Hollert, H. 2017b. Enhanced uptake of BPA in the presence of nanoplastics can lead to neurotoxic effects in adult zebrafish. *Sci. Total Environ.* 609, 1312-1321.

18. Compa, M., March, D., Deudero, S., 2019. Spatio-temporal monitoring of coastal floating marine debris in the Balearic Islands from sea-cleaning boats. *Mar. Pollut. Bull.* 141, 205-214.
19. Corrales, J., Fang, X., Thornton, C., Mei, W., Barbazuk, W.B., Duke, M., Scheffler, B.E., Willett, K.L., 2014. Effects on specific promoter DNA methylation in zebrafish embryos and larvae following benzo[a]pyrene exposure. *Comp. Biochem. Physiol. Part C: Toxicol. Pharmacol.* 163, 37-46.
20. Costa, J., Ferreira, M., Rey-Salgueiro, L., Reis-Henriques, M.A., 2011. Comparison of the waterborne and dietary routes of exposure on the effects of Benzo(a)pyrene on biotransformation pathways in Nile tilapia (*Oreochromis niloticus*). *Chemosphere* 84, 1452-1460.
21. De Sales-Ribeiro, C., Brito-Casillas, Y., Fernández, A., Caballero, M.J., 2020. An end to the controversy over the microscopic detection and effects of pristine microplastics in fish organs. *Sci. Rep.* 10, 12434.
22. Di Giulio, R.T., Washburn, P.C., Wenning, R.J., Winston, G.W., Jewell, C.S., 1989. Biochemical responses in aquatic animals: a review of determinants of oxidative stress. *Environ. Toxicol. Chem.* 8, 1103-1123.
23. Ding, J., Zhang, S., Razanajatovo, R.M., Zou, H., Zhu, W., 2018. Accumulation, tissue distribution, and biochemical effects of polystyrene microplastics in the freshwater fish red tilapia (*Oreochromis niloticus*). *Environ. Pollut.* 238, 1-9.
24. Driedger, A.G.J., Dürr, H.H., Mitchell, K., Van Cappellen, P., 2015. Plastic debris in the Laurentian Great Lakes: A review. *J. Great Lake Res.* 41, 9-19.
25. Egezza, R., Nankabirwa, A., Ocaya, H., Pabire, W.G., 2020. Microplastic pollution in surface water of Lake Victoria. *Sci. Total Environ.* 741, 140201.
26. Elizalde-Velázquez, A., Carcano, A.M., Crago, J., Green, M.J., Shah, S.A., Cañas-Carell, J.E., 2020. Translocation, trophic transfer, accumulation and depuration of polystyrene microplastics in *Daphnia magna* and *Pimephales promelas*. *Environ. Pollut.* 259, 113937.
27. Espinosa, C., Esteban, M.A., Cuesta, A., 2019. Dietary administration of PVC and PE microplastics produces histological damage, oxidative stress and immunoregulation in European sea bass (*Dicentrarchus labrax* L.). *Fish Shellfish Immunol.* 95, 574-583.
28. Geppert, M., Sigg, L., Schirmer, K., 2016. A novel two-compartment barrier model for investigating nanoparticle transport in fish intestinal epithelial cells. *Environ. Sci. Nano* 3, 388-395.
29. Gigault, J., Pedrono, B., Maxit, B., Ter Halle, A., 2016. Marine plastic litter: the unanalysed nano-fraction. *Environ. Sci. Nano* 3, 346.
30. Gregory, M.R., 2009. Environmental implications of plastic debris in marine settings entanglement, ingestion, smothering, hangers-on, hitchhiking and alien invasions. *Philos. Trans. R. Soc. B: Biol. Sci.* 364, 2013-2025.
31. Gu, W., Liu, S., Chen, L., Liu, Y., Gu, C., Ren, H., Wu, B., 2020. Single-cell RNA sequencing reveals size-dependent effects of polystyrene microplastics on immune and secretory cell populations from zebrafish intestines. *Environ. Sci. Technol.* 54, 3417-3427.
32. Hook, S.E., Mondon, J., Revill, A.T., Greenfield, P.A., Stephenson, S.A., Strzelecki, J., Corbett, P., Armstrong, E., Song, J., Doan, H., Barrett, S., 2018. Monitoring sublethal changes in fish physiology following exposure to a light, unweathered crude oil. *Aquat. Toxicol.* 204, 27-45.
33. Jabeen, K., Su, L., Li, J., Yang, D., Tong, C., Mu, J., Shi, H., 2017. Microplastics and mesoplastics in fish from coastal and fresh waters of China. *Environ. Pollut.* 221, 141-149.

Results and discussion

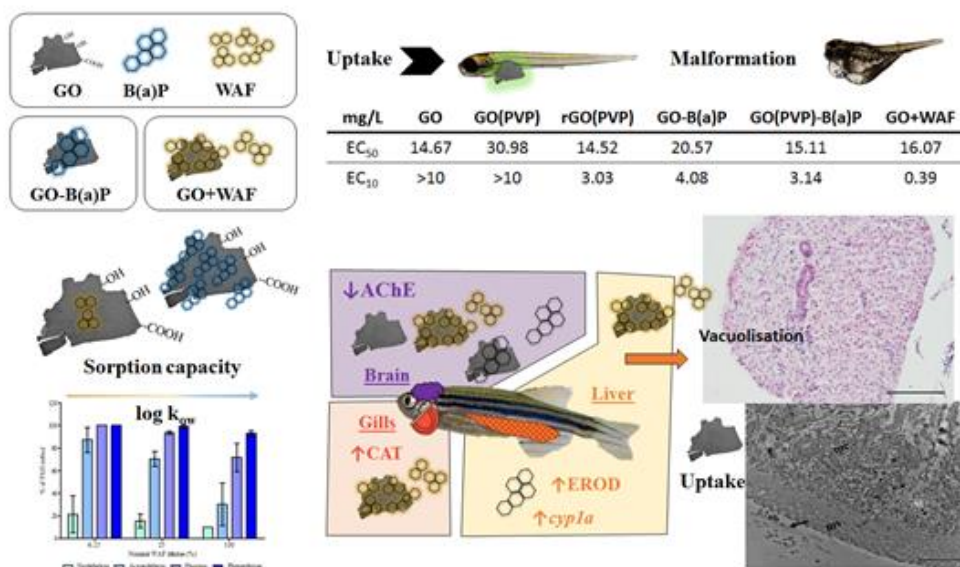
34. Jafarabadi, A.R., Bakhtiari, A.R., Yaghoobi, Z., Yap, C.K., Maisano, M., Cappello, T. 2019. Distributions and compositional patterns of polycyclic aromatic hydrocarbons (PAHs) and their derivatives in three edible fishes from Kharg coral Island, Persian Gulf, Iran. *Chemosphere* 215, 835-845.
35. Jin, Y., Xia, J., Pan, Z., Yang, J., Wang, W., Fu, Z., 2018. Polystyrene microplastics induce microbiota dysbiosis and inflammation in the gut of adult zebrafish. *Environ. Pollut.* 235, 322-329.
36. Karami, A., Romano, N., Galloway, T., Hamzah, H., 2016. Virgin microplastics cause toxicity and modulate the impacts of phenanthrene on biomarker responses in African catfish (*Clarias gariepinus*). *Environ. Res.* 151, 58-70.
37. Lacave, J.M., Vicario-Parés, U., Bilbao, E., Gilliland, D., Mura, F., Dini, L., Cajaraville, M.P., Orbea, A., 2018. Waterborne exposure of adult zebrafish to silver nanoparticles and to ionic silver results in differential silver accumulation and effects at cellular and molecular levels. *Sci. Total Environ.* 642, 1209-1220.
38. Lechner, A., Keckeis, H., Lumesberger-Loisl, F., Zens, B., Krusch, R., Tritthart, M., Glas, M., Schludermann, E., 2014. The Danube so colourful: A potpourri of plastic litter outnumbers fish larvae in Europe's second largest river. *Environ. Pollut.* 188, 177-181.
39. Lei, L., Wu, S., Lu, S., Liu, M., Song, Y., Fu, Z., Shi, H., Raley-Susman, K.M., He, D., 2018. Microplastic particles cause intestinal damage and other adverse effects in zebrafish *Danio rerio* and nematode *Caenorhabditis elegans*. *Sci. Total Environ.* 619-620, 1-8.
40. Limonta, G., Mancina, A., Benkhalqui, A., Bertolucci, C., Abelli, L., Fossi, M.C., Panti, C., 2019. Microplastics induce transcriptional changes, immune response and behavioural alterations in adult zebrafish. *Sci. Rep.* 9, 15775.
41. Liu, X., Xu, J., Zhao, Y., Shi, H., Huang, C. 2019. Hydrophobic sorption behaviours of 17 β -Estradiol on environmental microplastics. *Chemosphere* 226, 726-735.
42. Livak, K.J., Schmittgen, T.D., 2001. Analysis of Relative Gene Expression Data Using Real-Time Quantitative PCR and the 2 $^{-\Delta\Delta CT}$ Method. *Methods* 25, 402-408.
43. Livingstone, D.R., 1998. The fate of organic xenobiotics in aquatic ecosystems: quantitative and qualitative differences in biotransformation by invertebrates and fish. *Comp. Biochem. Physiol. Part A* 120, 43-49.
44. Lu, C., Kania, P.W., Buchmann, K., 2018. Particle effects on fish gills: An immunogenetic approach for rainbow trout and zebrafish. *Aquaculture* 484, 98-104.
45. Mai, Y., Peng, S., Li, H., Lai, Z., 2019. Histological, biochemical and transcriptomic analyses reveal liver damage in zebrafish (*Danio rerio*) exposed to phenanthrene. *Comp. Biochem. Physiol. Part C: Toxicol. Pharmacol.* 225,
46. Martins, M., Silva, A., Costa, M.H., Miguel, C., Costa, P.M., 2018. Co-exposure to environmental carcinogens in vivo induces neoplasia-related hallmarks in low-genotoxicity events, even after removal of insult. *Sci. Rep.* 8, 3649.
47. May, W.E., Wasik, S.P., Miller, M.M., Tewari, Y.B., Brown-Thomas, J.M., Goldberg, R.N., 1983. Solution thermodynamics of some slightly soluble hydrocarbons in water. *J. Chem. Eng. Data* 28, 197-200.
48. Perrichon, P., Le Menach, K., Akcha, F., Cachot, J., Budzinski, H., Bustamante, P., 2016. Toxicity assessment of water-accommodated fractions from two different oils using a zebrafish (*Danio rerio*) embryo-larval bioassay with a multilevel approach. *Sci. Total Environ.* 568, 952-966.
49. Pham, C. K., Ramirez-Llodra, E., Alt, C. H. S., Amaro, T., Bergmann, M., Canals, M., Company, J.B., Davies, J., Duineveld, G., Galgani, F., Howell, K.L., Huvenne, A.J., Isidro,

- E., Jones, D.O.B., Lastras, G., et al., 2014. Marine litter distribution and density in European Seas, from the shelves to deep basins. *PLoS ONE* 9, e95839.
50. Pitt, J.A., Kozal, J.S., Jayasundara, N., Massarsky, A., Trevisan, R., Geitner, N., Wiesner, M., Levin, E.D., Di Giulio, R.T. 2018a. Uptake, tissue distribution, and toxicity of polystyrene nanoparticles in developing zebrafish (*Danio rerio*). *Aquat. Toxicol.* 194, 185-194.
 51. Pitt, J.A., Trevisan, R., Massarsky, A., Kozal, J.S., Levin, E.D., Di Giulio, R.T., 2018b. Maternal transfer of nanoplastics to offspring in zebrafish (*Danio rerio*): A case study with nanopolystyrene. *Sci. Total Environ.* 643, 324-334.
 52. Prokić, M.D., Radovanović, T.B., Gavrić, J.P., Faggio, C., 2019. Ecotoxicological effects of microplastics: Examination of biomarkers, current state and future perspectives. *Trends Anal. Chem.* 111, 37-46.
 53. Qiao, R., Sheng, C., Lu, Y., Zhang, Y., Ren, H., Lemos, B., 2019. Microplastics induce intestinal inflammation, oxidative stress, and disorders of metabolome and microbiome in zebrafish. *Sci. Total Environ.* 662, 246-253.
 54. Rainieri, S., Conlledo, N., Larse, B.K., Granby, K., Barranco, A., 2018. Combined effects of microplastics and chemical contaminants on the organ toxicity of zebrafish (*Danio rerio*). *Environ. Res.* 162, 135-143.
 55. Rochman, C.M., Hoh, E., Kurobe, T., Teh, S.J., 2013. Ingested plastic transfers hazardous chemicals to fish and induces hepatic stress. *Sci. Rep.* 3, 3263.
 56. Ruiz, P., Orbea, A., Rotchell, J.M., Cajaraville, M.P., 2012. Transcriptional responses of cancer-related genes in turbot *Scophthalmus maximus* and mussels *Mytilus edulis* exposed to heavy fuel oil no. 6 and styrene. *Ecotoxicol.* 21, 820-831.
 57. Sadri, S.S., Thompson, R.C., 2014. On the quantity and composition of floating plastic debris entering and leaving the Tamar Estuary, Southwest England. *Mar. Pollut. Bull.* 81, 55-60.
 58. Saley, A.M., Smart, A.C., Bezerra, M.F., Brunham, T.L.U., Capece, L.R., Lima, L.F.O., Carsh, A.C., Williams, S.L., Morgan, S.G., 2019. Microplastic accumulation and biomagnification in a coastal marine reserve studied in a sparsely populated area. *Mar. Pollut. Bull.* 146, 54-59.
 59. Salazar-Coria, L., Rocha-Gómez, M.A., Matadamas-Martínez, F., Yépez-Mula, L., Vega-López, A., 2019. Proteomic analysis of oxidized proteins in the brain and liver of the Nile tilapia (*Oreochromis niloticus*) exposed to a water-accommodated fraction of Maya crude oil. *Ecotoxicol. Environ. Saf.* 171, 609-620.
 60. Sanchez, W., Bender, C., Porcher, J.M., 2014. Wild gudgeons (*Gobio gobio*) from French rivers are contaminated by microplastics: Preliminary study and first evidence. *Environ. Res.* 128, 98-100.
 61. Schmidt, C., Krauth, T., Wagner, S. 2017. Export of plastic debris by rivers into the sea. *Environ. Sci. Technol.* 51, 12246-12253.
 62. Schwarz, A.E., Lighthart, T.N., Boukris, E., van Harmelen, T., 2019. Sources, transport, and accumulation of different types of plastic litter in aquatic environments: A review study. *Mar. Pollut. Bull.* 143, 92-100.
 63. Singer, M.M., Aurand, D., Bragins, G.E., Clark, J.R., Coelho, G.M., Sowby, M.L., Tjeerdema, R.S., 2000. Standardization of the preparation and quantitation of water-accommodated fractions of petroleum for toxicity testing. *Mar. Pollut. Bull.* 40, 1007-1016.
 64. Skjolding, L.M., Ašmonaitė, G., Jølcck, R.I., Andresen, T.L., Selck, H., Baun, A., Sturve, J., 2017. An assessment of the importance of exposure routes to the uptake and internal localisation of fluorescent nanoparticles in zebrafish (*Danio rerio*), using light sheet microscopy. *Nanotoxicology* 11, 351-359.

Results and discussion

65. Sleight, V.A., Bakir, A., Thompson, R.C., Henry, T.B., 2017. Assessment of microplastic-sorbed contaminant bioavailability through analysis of biomarker gene expression in larval zebrafish. *Mar. Pollut. Bull.* 116, 291-297.
66. Statoil, 2011. Crude summary report. Available at: <https://www.statoil.com/content/dam/statoil/documents/crude-oil-assays/Statoil-TROLL-BLEND-2011-01.xls> (Accessed Nov 2018).
67. Teuten, E.L., Rowland, S.J., Galloway, T.S., Thompson, R.C., 2007. Potential for plastics to transport hydrophobic contaminants. *Environ. Sci. Technol.* 41, 7759-7764.
68. Vieira, L.R., Sousa, A., Frasco, M.F., Lima, L., Morgado, F., Guilhermino, L., 2008. Acute effects of benzo(a)pyrene, anthracene and a fuel oil on biomarkers of the common goby *Pomatoschistus microps* (Teleostei, Gobiidae). *Sci. Total Environ.* 395, 87-100.
69. Villarubia-Gómez, P., Cornell, S.E., Fabres, J. 2018. Marine plastic pollution as a planetary boundary threat – The drifting piece in the sustainability puzzle. *Mar. Policy* 96, 213-220.
70. Wang, J., Li, Y., Lu, L., Zheng, M., Zhang, X., Tian, H., Wang, W., Ru, S., 2019a. Polystyrene microplastics cause tissue damages, sex-specific reproductive disruption and transgenerational effects in marine medaka (*Oryzias melastigma*). *Environ. Pollut.* 254, 113024.
71. Wang, J., Liu, X., Liu, G., Zhang, Z., Wu, H., Cui, B., Bai, J., Zhang, W., 2019b. Size effect of polystyrene microplastics on sorption of phenanthrene and nitrobenzene. *Ecotoxicol. Environ. Saf.* 173, 331-338.
72. Wang, Y., Shen, C., Wang, C., Zhou, Y., Gao, D., Zuo, Z., 2018. Maternal and embryonic exposure to the water soluble fraction of crude oil or lead induces behavioural abnormalities in zebrafish (*Danio rerio*), and the mechanisms involved. *Chemosphere* 191, 7-16.
73. Werner, S., Budziak, A., van Franeker, J., Galgani, F., Hanke, G., Maes, T., Matiddi, M., Nilsson, P., Oosterbaan, L., Priestland, E., Thompson, R., Veiga, J. and Vlachogianni, T.; 2016; Harm caused by Marine Litter. MSFD GES TG Marine Litter - Thematic Report; JRC Technical report; EUR 28317 EN.
74. Wirnkör, V.A., Eberé, E.C., Ngozi, V.E., Oharley, N.K., 2019. Microplastic-toxic chemical interaction: a review study on quantified levels, mechanism and implication. *SN Appl. Sci.* 1, 1400.
75. Xu, S., Ma, J., Ji, R., Pan, K., Miao, A.J., 2020. Microplastics in aquatic environments: Occurrence, accumulation, and biological effects. *Sci. Total Environ.* 703, 134699.
76. Xu, X., Jian, Y., Xue, Y., Hou, Q., Wang, L., 2019. Microplastics in the wastewater treatment plants (WWTPs): Occurrence and removal. *Chemosphere* 235, 1089-1096.
77. Zhang, W., Ma, X., Zhang, Z., Wang, Y., Wang, J., Wang, J., Ma, D., 2015. Persistent organic pollutants carried on plastic resin pellets from two beaches in China. *Mar. Pollut. Bull.* 99, 28-34.
78. Zhao, Y., Luo, K., Fan, Z., Huang, C., Hu, J., 2013. Modulation of benzo[a]pyrene-induced toxic effects in japanese medaka (*Oryzias latipes*) by 2,2',4,4'-tetrabromodiphenyl ether. *Environ. Sci. Technol.* 47, 13068-13076.
79. Zuo, L.Z., Li, H.X., Lin, L., Sun, Y.X., Diao, Z.H., Liu, S., Zhang, Z.Y., Xu, X.R., 2019. Sorption and desorption of phenanthrene on biodegradable poly(butylene adipate co-terephthalate) microplastics. *Chemosphere* 215, 25-32.

CHAPTER 4. Uptake and effects of graphene oxide nanomaterials alone and in combination with polycyclic aromatic hydrocarbons in zebrafish



ABBREVIATIONS

AChE, Acetylcholinesterase

AFM, Atomic force microscopy

B(a)P, Benzo(a)pyrene

CAT, Catalase

DMSO, Dimethyl sulfoxide

EC₁₀, Effective concentration to 10% of the population

EC₅₀, Effective concentration to 50% of the population

EROD, 7-ethoxyresorufin O-deethylase

Fl-rGO, Fluorescent reduced graphene oxide

GC/MS, Gas chromatography/mass spectrometry

GO, Graphene oxide

GST, Glutathione-s-transferase

NMs, Nanomaterials

NNS, Naphthenic North Sea crude oil

PAHs, Polycyclic aromatic hydrocarbons

PVP, Poly N-vinyl-2-pyrrolidone

rGO(PVP), Reduced graphene oxide coated with poly N-vinyl-2-pyrrolidone

SOD, Superoxide dismutase

SPME, Solid phase micro extraction

TEM, Transmission electron microscopy

WAF, Water accommodated fraction

ABSTRACT

Graphene is a carbon nanomaterial (NM) being increasingly implemented in multiple applications. Because of its surface characteristics, once in the aquatic environment, graphene could act as a carrier of pollutants, such as polycyclic aromatic hydrocarbons (PAHs), to aquatic organisms. In this study we aimed to (1) assess the capacity of graphene oxide (GO) to sorb PAHs and (2) to evaluate the toxicity of GO alone and in combination with PAHs on zebrafish embryos and adults. GO showed a high sorption capacity for benzo(a)pyrene (B(a)P) (98% of B(a)P sorbed from a nominal concentration of 100 µg/L) and for other PAHs of the water accommodated fraction (WAF) of a naphthenic North Sea crude oil, depending on their log K_{ow} (95.7% of phenanthrene, 84.4% of fluorene and 51.5% of acenaphthene). In embryos exposed to different GO nanomaterials alone and with PAHs, no significant mortality was recorded for any treatment. Nevertheless, malformation rate increased significantly in embryos exposed to the highest concentrations (5 or 10 mg/L) of GO and reduced GO (rGO) alone and with sorbed B(a)P (GO-B(a)P). On the other hand, adults were exposed for 21 days to 2 mg/L of GO, GO-B(a)P and GO co-exposed with WAF (GO+WAF) and to 100 µg/L B(a)P. Fish exposed to GO presented GO in the intestine lumen and liver vacuolisation. Transcription level of genes related to cell cycle regulation and oxidative stress was not altered, but the slight up-regulation of *cyp1a* measured in fish exposed to B(a)P for 3 days resulted in a significantly increased EROD activity. Fish exposed to GO-B(a)P and to B(a)P for 3 days and to GO+WAF for 21 days showed significantly higher catalase activity in the gills than control fish. Significantly lower acetylcholinesterase activity, indicating neurotoxic effects, was also observed in all fish treated for 21 days. Results demonstrated the capacity of GO to carry PAHs and to exert sublethal effects in zebrafish.

Key words: Carbon based nanomaterials, organic pollutants, adsorption, aquatic nanotoxicity.

INTRODUCTION

Graphene is a two-dimensional carbon nanomaterial (NM) formed by a single layer of carbon atoms densely packed into a benzene-ring structure (Chen et al., 2012). Large specific surface area, mechanical strength, and remarkable electric and thermal properties make graphene suitable for many new applications (Ghosal and Sarkar, 2018; Kinloch et al., 2018). The two dimensional single layer of carbon can be chemically functionalised to produce derivatives, such as graphene oxide (GO) and reduced graphene oxide (rGO). Functionalisation of graphene NMs confers them different characteristics, like higher dispersability and adaptability, and consequently allows additional applications (Wang et al., 2011). Due to the recent discovery of their potential applications, the scarce implementation in the market (Kong et al., 2019) and the analytical limitations, graphene NM concentrations in ecosystems are not reported yet. Nevertheless, predicted concentrations in aquatic ecosystems range from 0.001 to 1000 µg/L, which are similar to those reported for carbon nanotubes (De Marchi et al., 2018). Further the production of graphene NMs is expected to increase in the following years (Ciriminna et al., 2015).

The potential risk of graphene NMs for aquatic organisms is currently being investigated (De Marchi et al., 2018). The driving characteristics of their potential toxicity are surface properties (radicals and functional groups) that can change due to chemical reactions that occur in ecosystems, which could, in turn, alter the bioavailability of graphene NMs for organisms. Effects of graphene NMs are poorly understood, but evidence shows that graphene is able to go through cell membranes in invertebrates and fish (Lammel et al., 2014; Lammel and Navas, 2014; Katsumiti et al., 2017). In zebrafish, which has been reported as a suitable model organism for the assessment of graphene NMs toxicity (Dasmahapatra et al., 2019), GO has been shown to translocate from the water to the brains of parental and offspring fish, leading to remarkable neurotoxicity in the offspring (Hu et al., 2017). Several studies indicate that zebrafish larval stages are sensitive to graphene NMs toxicity (Liu et al., 2014; Chen et al., 2016a; Ren et al., 2016; d'Amora et al., 2017; Soares et al., 2017; Zhang et al., 2017b; Pecoraro et al., 2018). Acute effects have not been reported under exposure to high GO concentrations (1-100 mg/L), but several sublethal effects including development delay, hatching rate alterations, neurotoxic effects, oxidative stress, cardiac alterations and locomotor alterations have been observed (Chen et al., 2016a; d'Amora et al., 2017; Soares et al., 2017). In embryos exposed to environmental concentrations of GO (0.01-100 µg/L) sublethal effects, such as oxidative stress, skeletal developmental delay and alterations in the nervous system have been reported even at the lowest exposure concentration (0.01 µg/L) (Ren et al., 2016; Zhang et al., 2017b). Toxicity of graphene NMs has also been tested in adult zebrafish (Chen et al., 2016b; Souza et al., 2017). Exposure to 1-50 mg/L GO for 14 days provoked oxidative stress at short term (4 days) and induction of tissue

Results and discussion

damage, such as increase of liver vacuolisation, at all the exposure concentrations tested (Chen et al., 2016b). Zebrafish exposed to GO (2-20 mg/L) showed similar effects with alterations in the liver (vacuolisation and pycnotic nuclei) and in the gills, such as lamellar fusion and clubbed tips (Souza et al., 2017).

One characteristic of graphene NMs that could modulate the previously described effects on aquatic organisms is their ability to sorb organic compounds, especially polycyclic aromatic hydrocarbons (PAHs). Due to the surface hydrophobicity, surface area and micropore volume, graphene NMs display a high PAH sorption capacity (Apul et al., 2013; Ji et al., 2013; Pei et al., 2013; Wang et al., 2014; Zhao et al., 2014) based on hydrophobic interactions (π - π interactions). In addition, graphene NMs can sorb pollutants by other interaction types, such as ion exchange or hydrogen bonding thanks to the presence of different functional groups (epoxy groups, C-O-C; hydroxyl groups, C=O; carboxylic groups, C-OOH) (Wang et al., 2015; Smith and Rodrigues 2015; Yan et al., 2015). Based on this characteristic, carbon NMs are being investigated as remediation materials for water treatment (Tabish et al., 2018; Baig et al., 2019). One example of this application is the use of 3D materials containing NMs such as graphene for remediation of oil spill scenarios (mainly PAHs) (Niu et al., 2014). These uses could represent an additional source of graphene into aquatic ecosystems that could modulate the availability of PAHs for aquatic organisms (Naasz et al., 2018). To the best of our knowledge, only two studies have addressed the potential “Trojan horse effect” of graphene NMs contaminated with persistent organic pollutants to zebrafish (Yang et al., 2019a; Liu et al., 2020). Mortality increase and hatching delay were reported in zebrafish embryos exposed to irradiated graphene aerogel combined with naphthalene (Liu et al., 2020). In contrast, GO reduced the bioavailability of the endocrine disruptor bisphenol A to early stages of zebrafish embryos (Yang et al., 2019a). Other carbon NMs were previously studied for potential transfer of PAHs to zebrafish (Falconer et al., 2015; Della Torre et al., 2017). Carbon nanopowder promoted the bioaccumulation of benzo(a)pyrene (B(a)P), enhanced the cytotoxicity, and the number of necrotic cells in zebrafish embryos (Della Torre et al., 2017). On the contrary, carbon nanotubes (CNTs) in combination with phenanthrene increased the survival rate of zebrafish embryos compared to phenanthrene alone, showing the capacity of some carbon NMs to reduce the availability of PAHs to zebrafish (Falconer et al., 2015). Although some studies have already addressed this issue, work is still to be done to elucidate the role of graphene NMs to affect and modulate PAH availability and effects to aquatic organisms. The aims of the present work were: (1) to assess the sorption capacity of GO NMs for a model pyrolytic PAH such as B(a)P and for an environmentally relevant mixture of petrogenic PAHs from the water accommodated fraction (WAF) of a crude oil; (2) to assess the uptake and potential acute toxicity of GO NMs alone or in combination with PAHs to

zebrafish embryos; (3) to evaluate the sublethal toxicity of GO alone and in combination with PAHs to adult zebrafish.

MATERIALS AND METHODS

Nanomaterials and chemicals. GO was originally purchased from Graphenea (San Sebastian, Spain) in form of a stable suspension. According to manufacturer's information, nanoplatelets showed lateral dimensions ranging from 500 nm to few microns and thickness < 2 nm. Oxygen content was about 40% wt. Part of the GO suspension was stabilised with 2% of poly N-vinyl-2-pyrrolidone (PVP, Sigma-Aldrich, St. Louis, MO, USA) to produce GO(PVP). After stabilisation GO(PVP) samples were dialysed (12–14,000 Da spectral/Por® membranes, Spectrumlabs (Piraeus, Greece)), in order to remove the excess of PVP, until samples reached a neutral pH. To obtain reduced rGO, GO was chemically reduced by hydrazine monohydrate (5:1) at 60 °C for 2 h in the presence of PVP as stabilising agent. Afterwards, rGO samples were also dialysed (12–14,000 Da spectral/Por® membranes, Spectrumlabs (Piraeus, Greece)), in order to remove secondary products of the reduction of GO and excess of PVP. Final rGO suspensions contained 2% PVP (rGO(PVP)). Fluorescent rGO (Fl-rGO) was produced from GO originally purchased to Graphene Supermarket (Graphene Laboratories Inc., Ronkonkoma, NY, USA). Fluorescent GO was reduced in the same way as GO. After reduction and fluorescent labelling with fluorescein, the Fl-rGO was dialysed as previously explained and was stabilised with 2% of PVP.

Benzo(a)pyrene (B(a)P, C₂₀H₁₂, purity ≥ 96%), its internal standard (B(a)P d₁₂), other deuterated PAHs (naphthalene d₈, acenaphthylene d₁₀, acenaphthene d₁₀, fluorene d₁₀, anthracene d₁₀, phenanthrene d₁₀, fluoranthene d₁₀, pyrene d₁₀, benzo(a)anthracene d₁₂, chrysene d₁₂, benzo(e)pyrene d₁₂, perylene d₁₂, benzo(b)fluoranthene d₁₂, benzo(k)fluoranthene d₁₂, indeno(1,2,3-cd)pyrene d₁₂, benzo(ghi)perylene d₁₂ and dibenz(a,h)anthracene d₁₄) and dimethyl sulfoxide (DMSO, purity ≥ 96%) were purchased from Sigma-Aldrich. The naphthenic North Sea (NNS) crude oil was provided by Driftslaboratoriet Mongstad, Equinor (former Statoil; Statoil, 2011). The oil was a very light naphthenic crude oil, with a density of 0.845 g/cc at 15 °C and pour point at -15 °C, rich in branched and cyclic saturated hydrocarbons, little wax content, poor thermal and oxidative stability and high octane content (Statoil, 2011).

PAH sorption to GO NMs. B(a)P was firstly dissolved in 100% DMSO at a concentration of 10 g/L. Successive dilutions were made in pure DMSO to obtain B(a)P stocks of 1, 0.1 and 0.01 g/L. From each of them, a 1:10000 dilution in conditioned water (600 µS/cm, 7-7.5 pH) was prepared to obtain the nominal B(a)P concentrations that were used in the sorption experiments: 1, 10 and 100 µg/L (0.01% DMSO (v/v)). WAF was prepared, based on Singer et al. (2000), in a glass bottle of 150 mL filled with conditioned water and NNS oil (1/50, NNS to conditioned water). The bottle was wrapped with aluminium foil and placed in a magnetic stirrer (IKA®-Werke GmbH

Results and discussion

& Co. KG, Staufen, Germany) at 800 rpm without vortexing and 21 °C. After 40 h, the aqueous phase was collected in a clean glass bottle avoiding taking oil droplets. 100% WAF samples were stored at -20 °C until chemical analysis.

For sorption experiments, 50 mg/L GO, GO(PVP) or rGO(PVP) were incubated in triplicate for 24 h in capped aluminium-wrapped glass vials containing 10 mL of 1, 10 and 100 µg/L of B(a)P or of 6.25, 25 and 100% WAF (v/v). Vials containing the corresponding PAH solutions without graphene were processed in parallel to monitor potential PAH loss due to degradation, sorption onto the vial walls or other factors during the experimental procedure. Vials were kept in an orbital shaker (M1000 VWR, Thorofare, USA) at 300 rpm in darkness in a temperature-controlled room (21±1 °C). After incubation, samples were centrifuged (Hettich Universal 32R centrifuge, Tuttlingen, Germany) at 9509 g for 30 min. Recovery of GO NMs after centrifugation was assessed by spectrophotometry at 230 nm (**Fig. S1**). Then, supernatants were diluted up to 1 µg/L according to nominal PAH concentration with deionised water in 10 mL glass solid phase micro extraction (SPME) vials. The 18 PAHs (16 priority PAHs selected by the US EPA (Environmental Protection Agency) and 2 additional parent PAHs (benzo(e)pyrene and perylene)) were quantified by isotopic dilution using deuterated standards added prior the extraction to calculate raw recoveries for surrogate internal standards. B(a)P d₁₂ and the 18 deuterated PAHs were dissolved separately in ethanol at a concentration of 20 ng/g for SPME extraction. A blank analysis was carried out to ensure the absence of contamination prior and during analysis. SPME consisted in a heating process at 40 °C with 35 min stirring period at 250 rpm of the polydimethylsiloxane fibre (100 µm PDMS, Supelco, Sigma-Aldrich, Johannesburg, South Africa). After extraction, the fibre was thermally desorbed into the gas chromatography/mass spectrometry (GC/MS) system (Agilent GC 7890A/Agilent MSD 5975C, Agilent Technology, California) for 10 min at 280 °C. Limits of detection and quantification (L.Q.) were defined at which the signal to noise ratio was >3 and 10, respectively, in spiked water samples. The GC/MS instrumentation, quality assurance and controls (L.Q., control charts and percentage of PAH recovery in control samples) that were carried out are reported on the Supporting Information (**Tables S1 and S2**).

Based on the PAH concentration measured in the aqueous phase, sorption of PAHs to GO was indirectly calculated. Values of sorption were expressed as Q_e (µg/g), which is the sorption concentration of PAH to GO at equilibrium and it was calculated as follows (equation 1):

$$Q_e = \frac{(C_0 - C_e)V}{M} \quad (1)$$

where C_e (µg/L) is the equilibrium concentration in the aqueous phase, C₀ (µg/L) is the average PAH concentration of the control sample after centrifugation, V (L) is the medium volume and M (g) is the GO mass. When the 100% of a given PAH was sorbed to GO, L.Q. value of that PAH was used as C_e. In order to evaluate PAH sorption to GO, the linear and Freundlich sorption

isotherm models were applied. Linear model (equation 2) was applied from Q_e and C_e values obtained for the sorption capacity of GO for PAHs:

$$Q_e = k_d C_e \quad (2)$$

where K_d (L/g) is the partition coefficient of the PAH between GO and the aqueous phase.

Freundlich model (equation 3) was used for parameter acquisition:

$$Q_f = k_f C_e^N \quad (3)$$

where K_f [($\mu\text{g/g}$)/($\mu\text{g/L}$)^N] is the Freundlich affinity coefficient, and N is the exponential coefficient.

Characterisation of the GO NMs. GO-B(a)P and GO(PVP)-B(a)P were prepared as described above by incubating GO and GO(PVP) for 24 h in 100 $\mu\text{g/L}$ B(a)P (0.01% DMSO). GO, GO(PVP), rGO(PVP) and GO-B(a)P and GO(PVP)-B(a)P were diluted in conditioned water at a concentration of 100 mg/L for transmission electron microscopy (TEM) and at 10 mg/L for atomic force microscopy (AFM). For TEM, one drop of each NM dispersion was placed over a 150 mesh copper grid previously covered with Formvar® (Sigma Aldrich) and dried at 35 °C. Micrographs were taken using a high resolution JEOL 2000 microscope (JEOL Co., Tokyo, Japan) operated at 80 kV. For atomic force microscopy (AFM) each NM dispersion was placed in grade V mica disks and deposited by spin coating. AFM measurements were performed using Dimension ICON AFM (Bruker Corporation, Massachusetts, USA) and micrographs were obtained in the intermittent-contact (tapping) mode (320 KHz) with a TESP-V2 cantilever with a spring constant of 40 N/m. Three representative platelets were taken from each sample to measure their length and thickness using the NanoScope Analysis 1.9 software (Bruker Corporation, Santa Barbara, USA).

Zebrafish maintenance and egg production. The zebrafish (wild type AB Tübingen) stock was maintained in a temperature-controlled room at 28 °C with a 14-hour light/10-hour dark cycle in 100 L tanks provided with mechanic and biological filters following standard protocols for zebrafish culture. Conditioned water was prepared from deionised water and commercial salt (SERA, Heinsberg, Germany). Fish were fed with Vipagran baby (Sera) and brine shrimp larvae (Artemia Koral GmbH, Nürnberg, Germany) twice per day.

Breeding female fish were selected and maintained separately in fish breeding nets inside the same tanks in order to avoid continuous spawning. The day before the assay, one female and two male zebrafish were placed separately in the same breeding tramp, which had previously been located in a 2 L tank containing conditioned water. Fish were left overnight and, just before the light switched on, the separation barrier was removed. The fertilised eggs were collected in a Petri

Results and discussion

dish with the help of a Pasteur pipette. The eggs selected as viable under a stereoscopic microscope (Nikon smz800, Kanagawa, Japan) were transferred to the exposure microplates.

Embryo toxicity test. For the embryo toxicity tests, GO NMs alone, GO NMs with sorbed PAHs and B(a)P solutions were diluted in embryo water (600-800 μ S/cm, 6.5-6.8 pH, Brand et al., 2002) at the desired nominal concentrations: 0.1, 0.5, 1, 5 and 10 mg/L GO or B(a)P. GO NMs with sorbed B(a)P were prepared as described above by incubating GO and GO(PVP) in 100 μ g/L B(a)P (0.01% DMSO) for 24 h followed by centrifugation to separate GO from the incubation medium. In the case of GO with sorbed PAHs from WAF, GO was incubated in 100% WAF for 24 h and, then, diluted at the above mentioned concentrations. Thus, in the case of GO+WAF, co-exposure to adsorbed and soluble PAHs took place. The toxicity tests were carried out in covered 24-well polystyrene microplates placing one embryo per well in 2 mL of test solution based on the OECD guideline TG236 (2013). In each microplate, two different concentrations were tested (10 embryos per concentration). In the remaining wells, four control embryos were placed in embryo water. For each compound three replicates were prepared, resulting in 30 embryos exposed to each concentration and 36 control embryos. Embryos were exposed up to 120 hours post fertilisation (hpf). The test was considered as valid only when the survival of the control group of each replicate was $\geq 90\%$. Daily and up to the end of the test, embryos were examined to determine survival rate (as the percentage of alive embryos at 120 hpf), hatching time (as the time that embryos needed to hatch) and malformation prevalence (as the percentage of malformed embryos over surviving embryos at 120 h). Normal embryo morphology and malformation identification were based on Fako and Furgeson (2009). Developmental abnormalities scored as malformations were spinal cord flexure, caudal fin alteration, tail malformation, pericardial edema, yolk sac edema, eye abnormality and stunted body. Malformations were recorded and photographed under a stereoscopic microscope (Nikon AZ100, Kanagawa, Japan).

Groups of 10 embryos were exposed in Petri dishes for 120 h to fluorescent rGO (1 and 10 mg/L) in order to analyse the uptake and distribution in the embryo body. At 120 h of exposure the individuals were observed under a fluorescence stereoscopic microscope (Nikon AZ100). For the micrographs, the organisms were anaesthetised with benzocaine (200 mg/L).

Waterborne exposure of adult zebrafish. The experimental procedure described herein was approved by the Ethics Committee in Animal Experimentation of the UPV/EHU (NoRefCEID: M20/2018/232) according to the current regulations. Adult fish more than 7 months old were placed in 35 L aquaria with conditioned water. Fish were exposed to 2 mg/L of GO alone, 2 mg/L of GO with sorbed B(a)P, 2 mg/L of GO+WAF and to 100 μ g/L B(a)P alone for 21 days. Water and pollutants were renewed every 3 days by changing 5/7 of the tank volume (25 L from a total of 35 L). This allowed maintaining water quality parameters along the whole experiment without

the need of biological filters that could interfere with the exposure. An unexposed control group was run in parallel in identical experimental conditions. Fish were feed with live brine shrimp larvae twice per day. Samples were taken after 3 and 21 days of exposure after euthanasia by overdose of anaesthetic (200 mg/L benzocaine).

For the preparation of the exposure media containing GO with sorbed PAHs, the GO mass/PAH mass ratio used in the sorption experiments was maintained. For the initial dose, 70 mg GO were incubated for 24 h in 100 mL of 1400 µg/L of B(a)P prepared in MilliQ water. For the following doses, 50 mg GO were incubated in 71 mL of 1400 µg/L of B(a)P. After centrifugation, the pellet was resuspended with conditioned water and added to the 35 L exposure tanks, resulting in a nominal exposure concentration of 2 mg/L GO-B(a)P. The concentration used in the group exposed to B(a)P alone was based on the results of the sorption experiments. In the case of GO incubated in 100 µg/L B(a)P, 96.7% B(a)P was lost from the aqueous phase. Thus, considering that almost all B(a)P was sorbed onto GO nanoplatelets, this B(a)P incubation concentration was used for adult zebrafish exposure.

Due to the low PAH concentration of the produced WAF, in the case of GO+WAF, a co-exposure scenario was established. For this, for the initial dose, 70 mg GO were incubated in 1.4 L of 100% WAF, prepared as described before, for 24 h. As this WAF volume was too high for further centrifugation, this mixture was added to the exposure tanks to achieve a nominal concentration of 2 mg/L GO and 4% WAF (co-exposure), considering that the most hydrophobic PAHs from WAF are highly sorbed by GO while less hydrophobic PAHs are more volatile. For the following doses, 50 mg of GO were incubated for 24 h in 1 L of 100% WAF.

Monitoring of GO and PAH concentrations in water and PAH bioaccumulation in adult zebrafish. In order to monitor the GO concentration in exposure tanks, water samples were taken in triplicate in glass vials from tanks containing GO (GO, GO+WAF and GO-B(a)P) after 5 min, 4 h, 24 h, 48 h and 72 h of the 3rd and 7th doses. GO was quantified by UV/Vis spectrophotometry at 230 nm using a microplate reader (Multiskan Spectrum, Thermo Fisher Scientific Oy, Vantaa, Finland). Absorbance values of each sample were converted into GO concentrations using a GO calibration curve (0.5-10 mg/L) prepared in conditioned water. For PAH quantification in the exposure media, water samples were taken in triplicate in glass vials from the same experimental groups (GO, GO+WAF, GO-B(a)P and B(a)P) after 5 min, 4 h, 8 h, 24 h, 48 h and 72 h of the initial dose. PAH quantification was performed as described above for the sorption experiments.

After 21 days of exposure, 20 fish per experimental group (control, GO+WAF, GO-B(a)P and B(a)P) were collected and grouped in 4 pools of 5 fish of similar weight (≈1 g wet weight). Samples were immediately frozen in liquid nitrogen and stored at -80 °C until analysis. Concentrations of PAHs in fish tissues were analysed using established analytical methods

Results and discussion

(Baumard et al., 1997) as described in detail in Turja et al. (2013; 2014). Samples were freeze dried (Power Dry LL3000, ThermoFisher Scientific) before being grinded in IKA tube mill (ThermoFisher Scientific). PAHs were extracted from 0.2 g of dry weight samples by microwave-assisted extraction (Start E, Milestone, Leutkirch, Germany) using dichloromethane (5 min at 900 W and 5 min at 500 W 70 °C). PAHs were quantified by isotopic dilution using deuterated internal standards added prior the extraction according to a protocol adapted from Baumard et al. (1997; 1999). After extraction, dichloromethane was concentrated to 500 µL using a Vacuum Evaporation System (Rapidvap Labconco, Kansas city, USA). The organic extracts followed a purification step through alumina and silica micro-columns in order to remove macromolecules and polar molecules to avoid interference on PAH quantification. First, the extracts were passed through an alumina column by dichloromethane elution. Extracts were reconcentrated with gas nitrogen and, then, passed through a silica column. The aliphatic fraction was eluted with pentane and discarded, followed by PAH fraction elution with a first elution using a mix of pentane/dichloromethane (65/35, v/v) and second elution using dichloromethane. The final extracts were reconcentrated again with gas nitrogen in 150 µL isooctane and analysed by GC-MS. Syringe deuterated PAHs (pyrene d_{10} and benzo(b)fluoranthene d_{12}) were added prior the injection to calculate raw recoveries for surrogate internal standards (**Table S3**). All steps of the analytical protocol were validated in terms of reproducibility and accuracy; procedural blanks were systematically checked and certified reference mussel tissues (2974a NIST for PAHs,) were analysed together with the actual samples. The obtained recoveries ranged between 70-120% with coefficient of variation < 20%. The detection limits of individual compounds in mussel tissues were in the range 0.1-1 ng/g dry weight for all PAHs.

Subcellular localisation of GO: transmission electron microscopy (TEM) analysis. Gills, liver and intestine from control fish and fish exposed to GO for 21 days were dissected and fixed for 1 h at 4 °C in sodium cacodylate (Sigma-Aldrich) buffer 0.1 M, pH 7.2 containing 2.5% glutaraldehyde (Panreac, Barcelona, Spain). Zebrafish tissue samples were treated and processed as described in Lacave et al. (2018). Ultrathin sections of 50 nm in thickness were cut using a Reichert Ultracut S ultramicrotome (Leica Microsystems, Wetzlar, Germany). Sections were picked up in 150 mesh copper grids, contrasted with 1% uranyl acetate (Fluka, Steinheim, Germany) for 3 min and with 0.3% lead citrate (Fluka) for 4 min and, finally, examined and photographed using a Hitachi HT7700 transmission electron microscope (Tokyo, Japan) at 60 kV.

Analysis of gene transcription levels. The liver of 15 male zebrafish per experimental group after 3 and 21 days of exposure were dissected, placed in cryovials with RNA later® (Sigma-Aldrich), frozen in liquid nitrogen and stored at -80 °C. Analysis of the transcription levels of target genes was done in pools of three livers resulting in five biological replicates per

experimental group and exposure time. The analysed genes were: cytochrome P450 1A1 (*cyp1a*, ID: Dr03112441_m1) and glutathione S-transferase pi 1 (*gstp1*, ID: Dr03118992_g1) as genes related with biotransformation of organic compounds; catalase (*cat*, ID: Dr03099094_m1), superoxide dismutase 1 (*sod1*, ID: Dr03074068_g1) and glutathione peroxidase 1a (*gpx1a*, ID: Dr03071768_m1) as genes related with oxidative stress; and tumour suppressor protein 53 (*tp53*, ID: Dr03112086_m1) as gene related with cell cycle regulation. Ribosomal protein S18 (*rps18*, ID: Dr03144509_m1) was used as housekeeping gene. Taqman® probes were purchased from ThermoFisher Scientific. RNA extraction was carried out by homogenisation of the tissues in cold TRIzol® using an electric disperser (PELLET PESTLE- Cordless Motor, Kimble Kontes, U.S.A). RNA was measured for integrity and purity before cDNA synthesis. 3 µg of total RNA were retrotranscribed using the Affinity Script Multiple Temperature cDNA synthesis Kit (Agilent Technologies) following manufacturer's conditions in a 2720 Thermal Cycler (ThermoFisher Scientific). qPCRs were run in a 7300 Applied Biosystems thermocycler (ThermoFisher Scientific). A dilution 1:5 of cDNA was done for each target gene. A final volume of 2.5 µL cDNA sample and 22.5 µL mix TaqMan® reaction (12.5 µL master mix + 1.25 µL primer probe + 8.75 µL RNase free water) was used. Relative transcription levels were calculated based on the $2^{-\Delta\Delta ct}$ method (Livak and Schmittgen, 2001) using the mean value of the corresponding control group at each exposure time as calibrator and *rps18* transcription levels as reference gene. *rps18* transcription levels presented a coefficient of variation of 2.34% among all the samples. Results of transcription levels are represented as $RQ = \log_2(2^{-\Delta\Delta CT})$.

Analysis of biochemical biomarkers. Liver, gills and brains collected from 15 female fish per experimental group after 3 and 21 days of exposure were dissected, immediately frozen in liquid nitrogen and kept into cryovials at -80 °C until analysis. Pools of three livers, gills or brains were homogenised in 300 µL cold homogenisation buffer (50 mM potassium phosphate buffer containing 1 mM ethylenediaminetetraacetic acid, 0.5 mM dithiothreitol and 0.4 mM phenylmethylsulfonyl fluoride, pH 7.5) for 15 s on ice using an electric disperser resulting in 5 samples per treatment. The homogenates were centrifuged at 10000 g and 4 °C for 15 min (Eppendorf 5415R refrigerated centrifuge, Eppendorf AG, Hamburg, Germany). Supernatants were carefully transferred to new micro test tubes, aliquoted on ice for different enzymatic and protein measurements and stored at -80 °C until further use. Four biochemical biomarkers were analysed: 7-ethoxyresorufin O-deethylase (EROD) activity, glutathione-S-transferase (GST) activity and catalase (CAT) activity in gills and liver and acetylcholinesterase (AChE) activity in brains.

EROD activity in liver and gill tissues was measured according to Kennedy and Jones (1994). Briefly, 20 µL of samples (in triplicate) and of resorufin standards were preincubated in 200 µL of 7-ethoxyresorufin (0.5 µM) for 10 min at room temperature. 20 µL NADPH (1 mM) were

Results and discussion

added to each well to activate the deethylation of 7-ethoxyresorufin to fluorescent resorufin. Resorufin was measured at 540/590 nm excitation/emission wavelengths for 25 min in 30 s intervals in a microplate reader (FLx800, Bio-Tek Instruments, INC, Winooski, U.S.A). The standard curve was prepared using a resorufin concentration range from 0.004 to 1 μ M on Tris-KCl buffer (pH 7.4). EROD activity was expressed as nmol of resorufin produced per min and mg protein.

GST activity in liver and gill tissues was measured according to Habig and Jakoby (1981) with the modifications done by Velki et al. (2017) for 96-well microplates. The conjugation of glutathione (GSH) was assessed by adding 12 μ L of sample, in quadruplicate, to 180 μ L of 1 mM 1-chloro-2,4-dinitrobenzene and 50 μ L of reduced GSH (25 mM). Activity was assessed through the increase of absorbance due to the conjugation of GSH at 340 nm for 15 min in 10 s intervals in a microplate reader (Multiskan Spectrum). Values of sample activity were validated when they fulfilled two criteria: a linear increase of absorbance ($R^2 \geq 0.98$) and a minimum increase of absorbance over time ($\Delta t_{3\text{min}} \geq 0.1$). GST activity was expressed as nmol of conjugated GSH per min and mg protein.

CAT activity in liver and gill tissues was assayed according to Aebi (1984) adapted to UV 96-well microplates (Thermo Fisher Scientific). 5 μ L of each sample, in quadruplicate, were added to 295 μ L of 20.28 mM H_2O_2 in potassium phosphate buffer (0.5 mM, pH 7). Consumption of H_2O_2 by catalase was monitored at 240 nm for 5 min in 5 s intervals in the same microplate reader. The standard curve of H_2O_2 was prepared at a concentration range from 0.4 to 20.28 mM. CAT activity was expressed as μ mol H_2O_2 consumption per min and mg protein.

AChE activity in brain tissues was measured according to the initial protocol established by Ellman et al. (1961) with modifications according to Velki et al. (2017) for 96-well microplates. The hydrolysis of acetylthiocholine (7.52 mM) was evaluated in a final volume of 207.5 μ L of 86.7 mM of potassium phosphate buffer (pH 7.2) and 7.52 mM of 5,5'-dithiobis-(2-nitrobenzoic acid). 7.5 μ L of sample were used in triplicate. Activity was measured by the increase of absorbance at 412 nm for 25 min in 10 s intervals using the same microplate reader. Values of sample activity were validated when they fulfilled the criteria used for GST. AChE was expressed as nmol of acetylcholine hydrolysed per min and mg of protein. Protein concentration was measured using the Bio-Rad DC protein assay (Bio-Rad Laboratories Inc., Hercules, California, USA) based on Lowry's method following instructions of the manufacturer.

Histopathology. Visceral mass and gills were dissected from 10 zebrafish per experimental group after 3 and 21 days of exposure. The collected tissues were placed in histological cassettes and immersed in neutral buffered formalin (4% formaldehyde) for 13 h at 4 $^\circ\text{C}$. Then, samples were dehydrated in a graded ethanol series (70%, 96% and 100% ethanol) and immersed in xylene at

room temperature by an Automatic Tissue Processor MTP (SLEE medical GmbH, Mainz, Germany) for a total of 11 h before embedding in paraffin at 60 °C. Paraffin blocks were done using plastic moulds. 5 µm sections were cut in a RM2125RT microtome (Leica Microsystems). Afterwards, sections were stained with haematoxylin/eosin in an Auto Stainer XL (Leica Microsystems) and mounted in DPX (Sigma-Aldrich) by means of a CV5030 Robotic Coverslipper (Leica Microsystems). After staining and mounting, samples were examined and photographed using a BX51 light microscope (Olympus, Tokyo, Japan).

Data analysis and statistics. Data on survival and malformations for zebrafish embryos were analysed by binomial logistic regression (Lacave et al., 2017; Orbea et al., 2017). Odd ratios were calculated in order to estimate and to compare the risk associated with the exposure to the GO NMs alone and in combination with PAHs. EC₅₀ and EC₁₀ values were calculated using a Probit model. For binomial logistic regression and Probit model, R package (R Foundation for Statistical Computing, Vienna, Austria) was used. Data on hatching time of zebrafish embryos followed a Normal distribution, therefore data were analysed by one-way ANOVA followed by the Tukey's post-hoc test. Data obtained from adult zebrafish were tested for normality (Kolmogorov-Smirnov test) and homogeneity of variances (Bartlett test) using the GraphPad Prism version 5.00 for Windows (GraphPad Software, La Jolla, California, USA). Data following a normal distribution were analysed by one-way ANOVA followed by the Tukey's post-hoc test, otherwise the non-parametric Kruskal-Wallis test was applied followed by the Dunn's post hoc test. Prevalence of histopathological alterations in gill and liver tissues was analysed by Fisher's exact test. In all cases, statistical significance was established at $p < 0.05$.

RESULTS

PAH sorption to GO NMs. B(a)P recovery after centrifugation of the control samples of GO experiments was 45.26% of the 0.69 ± 0.12 µg/L of B(a)P measured in the samples prepared at a nominal concentration of 1 µg/L (**Table S2**). As shown in **Fig. 1A**, at this incubation concentration, 100% of the B(a)P was sorbed to GO. In the nominal B(a)P incubation concentrations of 10 and 100 µg/L, measured B(a)P concentrations were 6.23 ± 0.23 µg/L and 118.5 ± 4.78 µg/L and recovery values were 69.79 and 76.91%, respectively. At these concentrations, B(a)P sorption percentages were $87.2 \pm 2.1\%$ and $96.68 \pm 0.5\%$, respectively. In the case of GO(PVP), $96.96 \pm 5.26\%$ of B(a)P was sorbed from a measured concentration of 0.81 ± 0.08 µg/L (nominal concentration 1 µg/L). At nominal B(a)P concentrations of 10 and 100 µg/L, measured B(a)P concentration values were 7.11 ± 0.28 µg/L and 149.8 ± 1.65 µg/L and the sorption percentages $90.44 \pm 2.3\%$ and $96.44 \pm 0.3\%$, respectively. Results could not be obtained for rGO(PVP) due to the remaining rGO(PVP) platelets in the supernatant after centrifugation, which interfered with the SPME/GC/MS analysis resulting in no signal for PAHs or deuterated PAHs.

Results and discussion

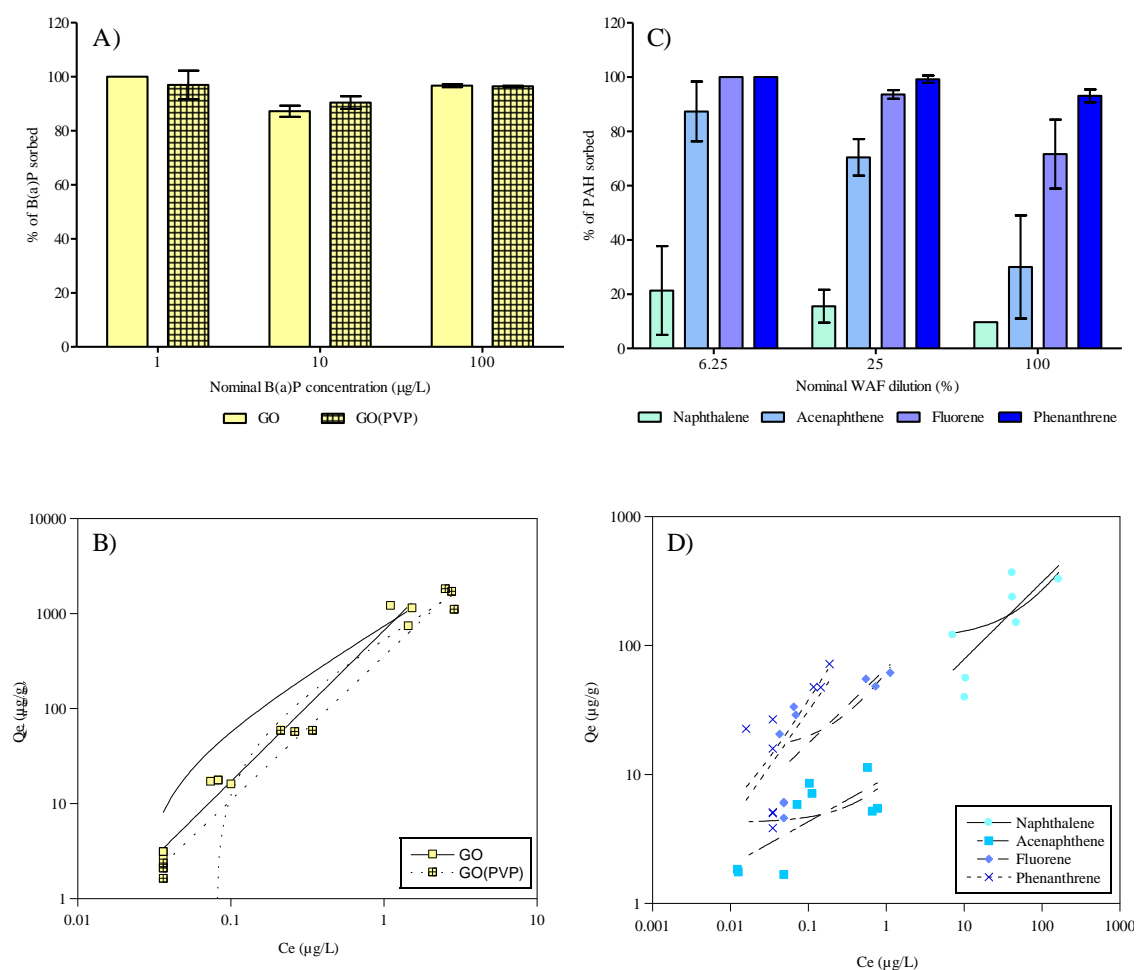


Fig. 1- Percentage of A) B(a)P sorbed to GO and to GO(PVP), and B) of PAHs from WAF sorbed to GO for the three nominal incubation concentrations and WAF dilutions tested. Sorption isotherms of C) B(a)P to GO and to GO(PVP) and D) of the four WAF PAHs studied to GO. Lines represent isotherms fitted by the Linear (curved line) and Freundlich model (straight line).

The sorption isotherms of B(a)P to GO and GO(PVP) are represented in **Fig. 1B**. The corresponding constants and parameters obtained from Linear and Freundlich models for GO and GO(PVP) are shown in **Table 1**. Regarding the Linear model, values of the distribution coefficient (K_d) for B(a)P sorption to GO and to GO(PVP) were 756.58 L/g and 575.05 L/g, respectively. Values of correlation coefficient (R^2) for the Linear model (0.88 and 0.91, respectively) were similar to those obtained for the Freundlich model (0.83 for GO and 0.89 for GO(PVP)). The Freundlich affinity coefficient (K_f) was higher for B(a)P sorption to GO ($665.47 (\mu\text{g/g})/(\text{L}/\mu\text{g})^N$) than to GO(PVP) ($357.78 (\mu\text{g/g})/(\text{L}/\mu\text{g})^N$). In addition, the Freundlich “N” cooperation factor was similar for B(a)P sorption to GO or GO(PVP), 1.59 and 1.52, respectively.

The PAH concentration of the three WAF dilutions (6.25, 25 and 100%) of the NNS crude oil is shown in **Table S4**. The WAF produced from NNS oil presented low concentrations of the 18 PAHs analysed (Σ PAHs = 171.06 $\mu\text{g/L}$ for 100% WAF).

Table 1- Estimated parameters for the Linear and the Freundlich models explaining the sorption of B(a)P to GO and to GO(PVP), and the sorption of PAHs from a naphthenic North Sea oil WAF to GO.

		Linear model		Freundlich model			
		K_d	R^2	K_f	N	R^2	n
GO	Benzo(a)pyrene	756.58	0.88	665.47	1.59	0.83	9
GO(PVP)	Benzo(a)pyrene	575.05	0.91	357.78	1.52	0.89	9
	Naphthalene	1.55	0.44	19.71	0.60	0.53	7
	Acenaphthene	4.56	0.18	9.40	0.34	0.34	9
GO	Fluorene	46.92	0.85	73.85	0.49	0.89	9
	Phenanthrene	307.27	0.92	188.87	0.65	0.87	9

K_d = partition coefficient of B(a)P between GO and the aqueous phase at equilibrium (L/g); K_f = Freundlich affinity coefficient [$(\mu\text{g/g})/(\text{L}/\mu\text{g})^N$]; N= site energy heterogeneity factor; n= number of samples.

The compounds that could be measured in the three WAF dilutions were naphthalene, acenaphthene, fluorene and phenanthrene, with concentrations in the 100% sample of 163.245 $\mu\text{g/L}$, 0.951 $\mu\text{g/L}$, 3.779 $\mu\text{g/L}$ and 2.874 $\mu\text{g/L}$, respectively. Thus, analyses of the sorption to GO were done for these four PAHs (**Fig. 1C**) that showed good recovery values (88.76-150.55%) after centrifugation of the control samples (**Table S2**). Phenanthrene was the PAH showing the highest sorption to GO with a 95.7% of sorption for 100% WAF, 99.2% for 25% WAF and 100% for 6.25% WAF. This was followed by fluorene with sorption values between 84.4 and 100%, while acenaphthene and naphthalene presented values of sorption to GO that ranged from 51.5 to 87.3% and from 9.7 to 21.3%, respectively. These results clearly indicated that the ability of PAHs to sorb to GO was dependent on their hydrophobicity.

Constants and parameters for WAF PAH sorption isotherm models are given in **Table 1**. Sorption isotherm models (**Fig. 1D**) were applied only for those PAHs detected in control samples ($C_e > L.Q.$) of the three WAF dilutions. According to the Linear sorption model, naphthalene and acenaphthene showed a nonlinear trend with a R^2 coefficient of 0.44 and 0.18, respectively. For the more hydrophobic PAHs, fluorene and phenanthrene, a linear trend was observed (R^2 of 0.85 and 0.92, respectively). K_d values were closely related to PAH hydrophobicity showing the following trend: phenanthrene > fluorene > acenaphthene > naphthalene. According to the Freundlich model, phenanthrene ($R^2 = 0.87$) and fluorene ($R^2 = 0.89$) fitted better than

Results and discussion

acenaphthene ($R^2 = 0.34$) and naphthalene ($R^2 = 0.53$), as also seen in the Linear model. In addition, values of sorption capacity (K_f) agreed with K_d values, with the exception of naphthalene and acenaphthene. Naphthalene showed higher K_f value than acenaphthene (19.71 versus 9.40 $(\mu\text{g/g})/(\text{L}/\mu\text{g})^N$, but lower K_d value (1.55 versus 4.56 L/g). Cooperation between the PAHs and GO (N) was higher for naphthalene (N = 0.60) and phenanthrene (N = 0.65) than for fluorene (N = 0.49) or acenaphthene (N = 0.34).

Characterisation of GO NMs. Micrographs of the three GO NMs obtained by TEM and AFM are shown in **Fig. S2**. At TEM, platelets with different sizes and shapes were observed, being the maximum length of the platelets always below 13 μm . According to AFM analysis, thickness of GO platelets was 0.612 ± 0.176 nm (n = 3), in agreement with the information provided by the provider. An increase of thickness was observed for GO(PVP) platelets with a value of 1.994 ± 0.319 nm (n = 3). rGO(PVP) platelets appeared thicker than GO and GO(PVP) platelets, with a value of 4.174 ± 0.179 nm. Platelets of GO-B(a)P and GO(PVP)-B(a)P showed similar length to GO or GO(PVP) alone (**Fig. S3**). GO-B(a)P presented a thickness of 0.796 ± 0.177 nm (n = 3) and GO(PVP)-B(a)P presented a thickness of 3.995 ± 0.221 nm (n = 3). No relevant aggregation of GO platelets was observed with or without B(a)P, but an increase of thickness was observed in GO(PVP)-B(a)P platelets compared to GO(PVP) alone.

Embryo toxicities tests. The results of the developmental parameters of zebrafish embryos exposed to GO NMs alone or in combination with PAHs are shown in **Table 2** and the odd ratio values for each treatment showing statistically significant differences and their corresponding confidence intervals are shown in **Table S5**. Survival at 120 hpf and hatching time did not show statistically significant differences between treated and control embryos, neither for GO alone nor in combination with PAHs. Regarding malformation prevalence at 120 hpf, unexposed control embryos showed values ranging from 0 to 11.4%. Exposure to 5 and 10 mg/L of GO caused a significant increase in total malformation prevalence, reaching to 33.3% and 23.3%, respectively. Exposure to 10 mg/L of rGO(PVP) also caused significantly higher malformation prevalence (26.7%) than in control embryos. Embryos exposed to GO(PVP) did not show any significant difference on malformation prevalence for the exposure concentrations used. Looking at malformation prevalences produced by the GO NMs in combination with PAHs, GO(PVP)-B(a)P was the most toxic combination to zebrafish embryos. Embryos exposed to 0.5, 5 and 10 mg/L of GO(PVP)-B(a)P presented a significant increase (20%, 13.8% and 26.7%, respectively) compared to unexposed embryos. In the case of GO-B(a)P, only embryos exposed to 5 mg/L showed a malformation prevalence (28.6%) higher than controls. None of the GO+WAF concentrations used caused significant toxicity to embryos in terms of increased malformation prevalence.

Table 2- Results of the developmental parameters (% of surviving embryos at 120 h, hatching time and % of malformed embryos at 120 h) of zebrafish embryo exposed to graphene NMs alone and in combination with PAHs. Asterisks indicate statistically significant differences ($p < 0.05$) compared to the control group according to the binomial logistic regression. The values of the corresponding odd ratios are given in **Table S4**. Values for hatching time are given as means \pm S.D.

	Conc. (mg/L)	Surv. (%)	Hatching time (h)	Malform. (%)	Type of malform. (%)			
					SC	PE	YE	EA
GO	0	100	72	8.3	8.3	8.3	0	0
	0.1	100	72	20	20	20	0	0
	0.5	90	70.4 \pm 6.41	13.8	13.8	3.5	3.5	3.5
	1	100	72	3.3	3.3	0	0	0
	5	96.7	71.2 \pm 4.46	33.3*	25.9	7.4	7.4	7.4
	10	100	72.0	23.3*	23.3	0	0	0
GO(PVP)	0	97.2	66.91 \pm 9.74	11.4	11.4	0	0	0
	0.1	96.7	70.22 \pm 8.42	16.7	16.7	0	0	0
	0.5	100	68 \pm 10.32	24.1	13.8	10.3	6.9	6.9
	1	100	67.2 \pm 9.76	20	16.7	3.3	0	0
	5	96.7	66.4 \pm 9.23	30	26.7	3.3	0	0
	10	100	68.8 \pm 6.09	20.7	13.8	6.9	0	0
rGO(PVP)	0	100	68.67 \pm 8.42	5.6	2.8	2.8	0	0
	0.1	100	68 \pm 4.38	3.3	3.3	0	0	0
	0.5	100	66.4 \pm 4.38	6.7	0	6.7	0	0
	1	100	66.4 \pm 10.32	6.7	6.7	0	0	0
	5	100	71.2 \pm 10.32	20	16.7	3.3	0	0
	10	100	71.2 \pm 9.10	26.7*	10	20	0	0
GO+WAF	0	94.4	70.55 \pm 5.73	2.9	2.9	0	0	0
	0.1	96.7	69.42 \pm 7.82	3.8	3.8	0	0	0
	0.5	86.7	70 \pm 4.71	19.2	15.4	3.8	0	0
	1	93.3	70.31 \pm 6.29	10.7	7.1	3.6	0	0
	5	86.7	71.2 \pm 6.52	23.1	23.1	0	0	0
	10	86.7	69.33 \pm 7.4	25.1	25.1	3.4	3.4	3.4
GO-B(a)P	0	97.2	72	5.7	5.7	0	0	0
	0.1	100	71.2 \pm 4.38	3.7	0	3.7	0	0
	0.5	93.3	71.2 \pm 4.54	0	0	0	0	0
	1	93.3	72	3.6	3.6	0	0	0
	5	90	70.86 \pm 4.62	28.6*	10.7	17.9	0	0
	10	90	71 \pm 4.62	10	3.3	6.7	0	0
GO(PVP)-B(a)P	0	100	72	0	0	0	0	0
	0.1	100	72	0	0	0	0	0
	0.5	96.7	72	20*	20	0	0	0
	1	96.7	72	6.9	3.4	3.4	0	0
	5	100	72	13.8*	10.3	6.9	0	0
	10	96.7	72	26.7*	13.4	16.7	0	0

Conc. = concentration; Surv. = survival; Malform. = malformation; SC= spinal cord flexure; PE= pericardial edema; YE= yolk sac edema; EA: eye abnormality.

Results and discussion

At the same exposure concentration, no significant differences were found between embryos exposed to GO NMs alone or with sorbed PAHs.

The most prevalent malformation among exposed embryos was spinal cord flexure (**Fig. S4B**). This malformation was mostly observed in embryos exposed to 5 mg/L of GO and GO(PVP) with a malformation prevalence of 25.9% and 26.7%, respectively. The highest prevalence of pericardial edema was observed in embryos exposed to 10 mg/L of rGO(PVP) (**Fig. S4C**) with a 20% of prevalence and in embryos exposed to 5 mg/L of GO-B(a)P with a prevalence of 17.9% (**Fig. S4D**). Embryos exposed to 10 mg/L of GO(PVP)-B(a)P also showed a high prevalence of pericardial edema (16.7%). Embryos showing yolk sac edema and eye abnormality were found among those exposed to GO (**Fig. S4E**), GO(PVP) (**Fig. S4F**) and GO+WAF (**Table 2**).

Values of EC_{50} and EC_{10} for malformation occurrence calculated for all the treatments are shown in **Table S6**. GO+WAF was the most toxic treatment for embryos according to the EC_{10} value (0.39 ± 2.11 mg/L). EC_{10} values were similar for embryos exposed to rGO(PVP), GO(PVP)-B(a)P and GO-B(a)P (3.03 ± 1.37 mg/L, 3.14 ± 1.43 mg/L and 4.08 ± 1.99 mg/L, respectively). These values could not be calculated for GO and GO(PVP). EC_{50} values for all the treatments were higher than the highest exposure concentration (10 mg/L). The lowest EC_{50} values corresponded to GO (14.67 ± 4.03 mg/L) and to rGO(PVP) (14.52 ± 3.12 mg/L). Similar values were estimated for zebrafish embryos exposed to GO+WAF (16.07 ± 4.98 mg/L) and GO(PVP)-B(a)P (15.11 ± 3.51 mg/L). The highest EC_{50} values among treatments for zebrafish embryos were recorded for GO-B(a)P (20.57 ± 8.03 mg/L) and GO(PVP) (30.98 ± 26.7 mg/L).

Localisation of fluorescent rGO in zebrafish embryos. Zebrafish embryos were exposed for 120 h to FI-rGO in order to track rGO fate in the embryos. At 120 hpf, unexposed embryos did not show fluorescence (**Fig. S5A-B**) whereas fluorescence was observed in the yolk sac and digestive tract of zebrafish embryos exposed to 1 (**Fig. S5C-D**) and 10 mg/L (**Fig. S5E-F**) of FI-rGO.

GO and PAH concentrations in water and PAH bioaccumulation in adult fish. Up to 24 h after dosing, measured GO concentrations in exposure tanks containing GO (GO, GO+WAF and GO-B(a)P) were close to the nominal GO concentration (2 mg/L) in the two assessed cycles (3rd and 7th, **Fig. S6**). Then, GO concentration decreased close to the limit of detection (0.5 mg/L) at 72 h, except in the case of GO-B(a)P and GO+WAF tanks during the third dose, where an unexpected GO concentration increase was measured.

Summarised results of PAH concentrations over time for each tank during the first three days of exposure of adult zebrafish are shown in **Table S7**. Control tank presented low concentrations of the analysed PAHs, below or near the limit of quantification, and with similar values along time.

Total PAH concentration in GO+WAF tank decreased 130 times from 5 min (8044.1 ng/L) to 72 h after adding the contaminants (61.1 ng/L). Naphthalene was the most abundant PAH in the water samples with a decrease of concentration from 7,788.9±491.9 ng/L at 5 min to 4,730.9±122.1 ng/L at 8 h after dosing. Naphthalene concentration reached 34.9±3.4 ng/L after 72 h. The concentration of the other measured PAHs, acenaphthene, fluorene, phenanthrene and anthracene also decreased progressively along time almost reaching limits of quantification after 72 h of dosing. B(a)P was not detected in this treatment. B(a)P concentration in the GO-B(a)P exposure tank was more stable than in the previous case with an initial concentration of 1,743.2±117.3 ng/L and a concentration at 72 h of 1,293.2±309.2 ng/L. In the case of exposure to B(a)P alone, measured concentration at 5 min was 29,440.3±4582.1 ng/L, remained stable up to 8 h (34,682.5±4147 ng/L) and decreased progressively up to 7,956.7±1,723.1 ng/L at 72 h.

PAH accumulation in whole zebrafish after 21 days of exposure is shown in **Table 3**. While control fish presented a total PAH value of 44.82±10.20 ng/g, fish exposed to GO+WAF presented a total PAH concentration of 139.16±24.79 ng/g, being fluorene and phenanthrene the most accumulated compounds. B(a)P was not detected in these treatments. Fish exposed to GO-B(a)P accumulated B(a)P up to a concentration of 37.49±11.28 ng/g, while B(a)P concentration in fish exposed only to B(a)P reached 10,065.38±1,444.03 ng/g.

Table 3- Concentration of PAHs (ng/g) in adult zebrafish at 21 days of exposure. Values are represented as mean±S.D.

	Control	GO+WAF	GO-B(a)P	B(a)P	L.Q.
Naphthalene	<L.Q.	<L.Q.	-	-	9.0
Acenaphthylene	1.07±0.12	2.60±0.63	-	-	0.6
Acenaphthene	4.69±0.42	18.21±3.68	-	-	2.0
Fluorene	9.48±0.62	56.57±9.91	-	-	1.0
Phenanthrene	18.30±5.84	44.84±6.92	-	-	10.0
Anthracene	0.94±0.83	4.72±0.70	-	-	0.5
Fluoranthene	4.61±1.53	4.13±1.01	-	-	3.0
Pyrene	5.74±0.84	8.08±1.95	-	-	4.0
Benzo(a)pyrene	<L.Q.	<L.Q.	37.49±11.28	10,065.38±1,444.03	1.0
ΣPAHs	44.82±10.20	139.16±24.79			

L.Q.: limit of quantification; -: not measured.

Localisation of GO in adult zebrafish. Rod-like structures resembling longitudinal sections of GO platelets were detected at histological level in the lumen of the intestine of the zebrafish exposed to all treatments that contained GO (GO, GO+WAF, GO-B(a)P) at the two exposure times (**Fig. 2**). Unexposed embryos did not show the presence of these putative GO platelets.

Results and discussion

TEM analysis also showed the presence of GO platelets in the lumen of the intestine of zebrafish (**Fig. 2**). The length of the GO platelets found in the intestine ranged from 0.9 to 2.7 μm which agreed well with the data of isolated GO platelets analysed by AFM and TEM ($<10 \mu\text{m}$). GO was not seen inside the cells, neither at light microscopy nor at TEM level.

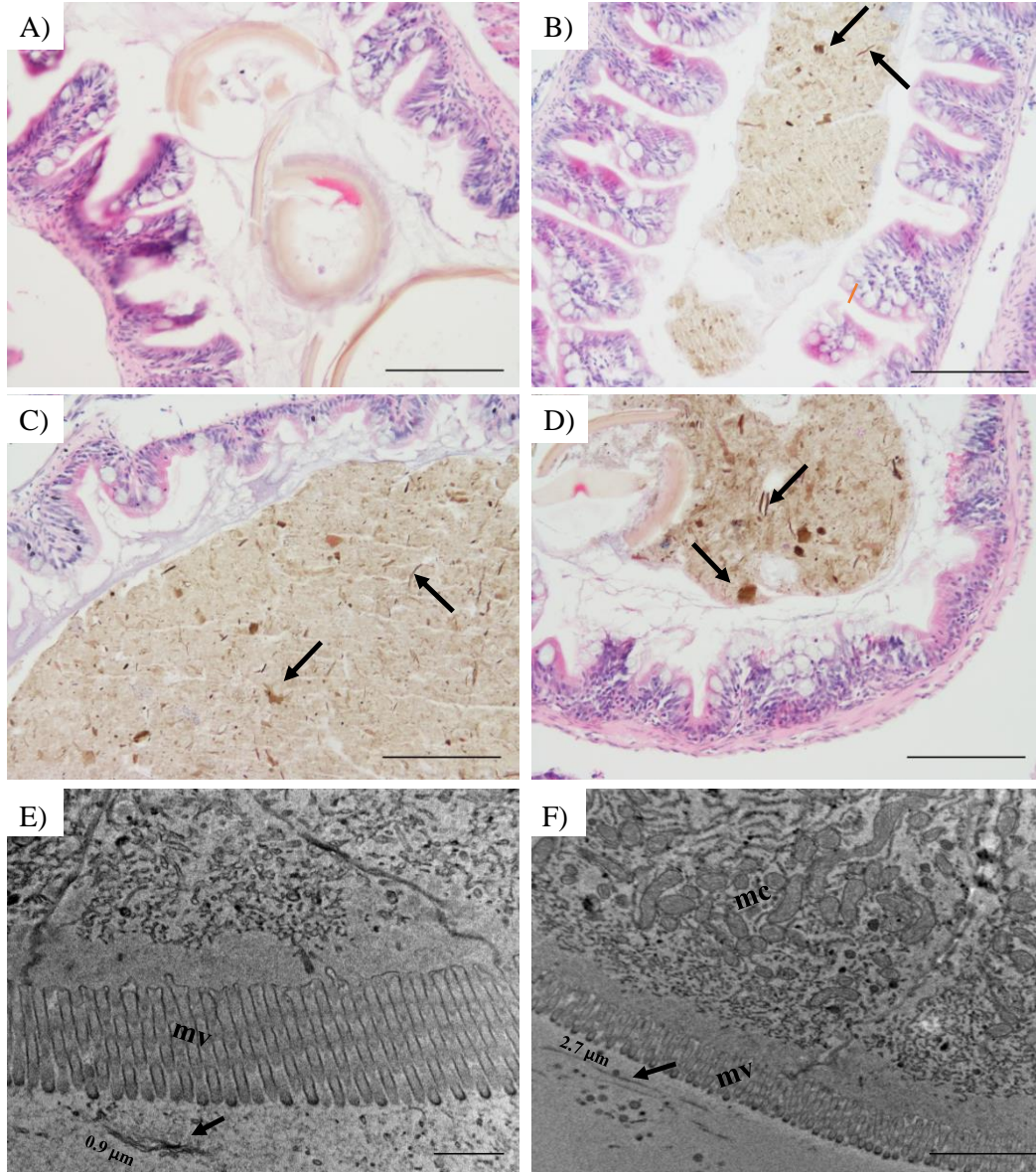


Fig. 2- Localisation of GO in adult zebrafish intestine. Micrographs of histological sections of A) unexposed adult zebrafish at 21 days showing normal intestine histology and remnants of brine shrimp capsules in the lumen; B) adult zebrafish exposed to 2 mg/L of GO for 21 days; C) adult zebrafish exposed to 2 mg/L of GO+WAF for 21 days; D) adult zebrafish exposed to 2 mg/L of GO-B(a)P for 21 days. Fish exposed to treatments containing GO showed abundant putative GO platelets in the lumen of the intestine (arrows). E-F) TEM micrographs showing the apical zone of the enterocytes of adult zebrafish after 21 days of exposure to 2 mg/L GO. The presence of GO platelets (arrows) was detected in the digestive lumen, but not inside enterocytes. Microvilli (mv), mitochondria (mc). Scale bars: A-D) 100 μm , E) 0.5 μm and F) 2 μm .

Transcription levels of target genes. The transcription levels of selected genes are represented in **Fig. 3**. For genes related with biotransformation metabolism, only *cyp1a* transcription levels showed significant differences between fish exposed to GO and those exposed to B(a)P at 3 days. In the case of transcription levels of *tp53*, only fish exposed to GO-B(a)P showed a significantly higher transcription level than fish exposed to GO+WAF at 3 days. Regarding the transcription level of genes related with oxidative stress, no significant differences were found among groups at 3 or 21 days of exposure (**Fig. 3**).

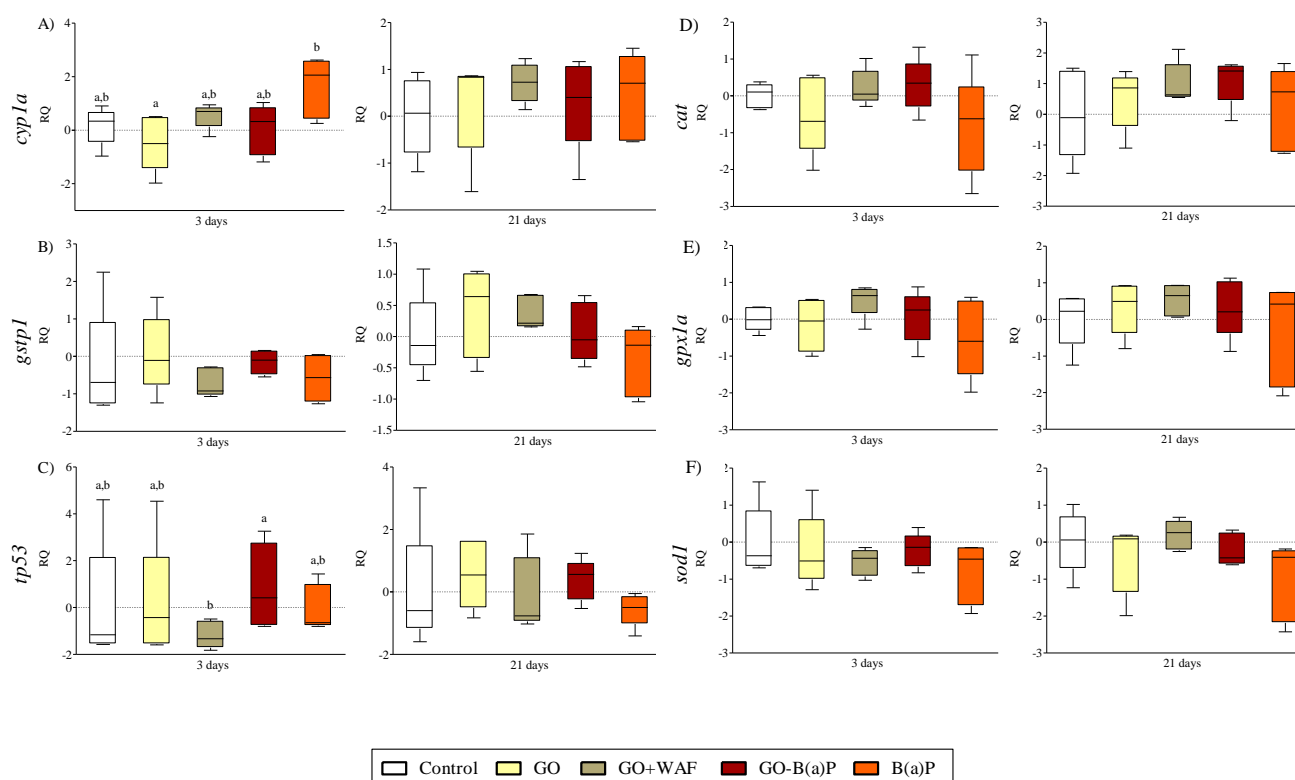


Fig. 3- Relative quantification (RQ) of transcription levels of the biotransformation metabolism related genes A) *cyp1a* and B) *gstp1*, C) tumour suppressor gene *tp53* and oxidative stress related genes D) *cat*, E) *gpx1a* and F) *sod1* in adult zebrafish liver after 3 and 21 days of exposure to GO, GO+WAF, GO-B(a)P and B(a)P. Box-plot boxes represent the percentage data values in between the 25th and the 75th percentile, median indicated by a line in the middle of the box. Whiskers are the data values in up to the 5th percentile and 95th percentile. Different letters indicate statistically significant differences ($p < 0.05$) within each sampling time according to the Kruskal-Wallis test followed by C, E) the post hoc Dunn's test for non-parametric data and to A, B, D, F) one-way ANOVA followed by the post hoc Tukey's test.

Biochemical biomarkers. Results of the biotransformation metabolism and oxidative stress biochemical biomarkers in liver and gills of adult zebrafish are shown in **Fig. 4**. All treated groups showed higher EROD activity in liver than controls fish at 3 days, being significantly higher in B(a)P-exposed fish. After 21 days of exposure, significant differences among groups were not observed, although fish exposed to B(a)P maintained the highest EROD activity (**Fig. 4A**). EROD

Results and discussion

activity in gills did not show any significant differences, neither among experimental groups nor between exposure times (**Fig. 4B**).

After 3 days of exposure, GST activity in liver did not show any significant differences compared to control fish. After 21 days, fish exposed to B(a)P alone showed significantly higher activity than fish exposed to GO-B(a)P, but no differences were detected respect to control fish. A significant increase of activity at 21 days compared to 3 days was recorded for control fish, and in fish exposed to GO+WAF and to B(a)P (**Fig. 4C**). In gills, GST activity was significantly higher in fish exposed to GO+WAF than in fish exposed GO for 3 days (**Fig. 4D**). After 21 days, GST activity in gills of fish exposed to GO+WAF decreased compared to fish sampled after 3 days of exposure. Also at 21 days, fish exposed to GO-B(a)P presented significantly higher activity than fish exposed to GO. Catalase activity did not change significantly in zebrafish liver among exposure groups or between exposure times (**Fig. 4E**). In gills, at 3 days, catalase activity was higher in all exposed groups than in control fish, being significantly higher for fish exposed to GO-B(a)P and B(a)P (**Fig. 4F**). After 21 days, CAT activity remained higher in treated fish than in control fish, but only in fish exposed to GO-WAF it was significantly higher than in control fish.

Regarding AChE activity in brain, no significant differences were detected at 3 days of exposure (**Fig. 4G**). At 21 days, AChE was significantly lower in the brain of all exposed fish than in the brain of control fish, suggesting signs of neurotoxicity. A significant increase of activity was recorded in control fish at 21 days compared to 3 days while a significant decrease was measured in GO+WAF exposed fishes.

Histopathological alterations. Results of the histopathological evaluation of liver tissue is shown in **Table S8**. Control fish showed, in general, normal architecture of the liver (**Fig. 5A**). An overall increase in the prevalence of liver vacuolisation was recorded in all treated groups, being significant compared to the control group in fish exposed to GO+WAF for 3 days (60%) and 21 days (50%) (**Table S8**). Megalocytosis was found in two individuals, one exposed to GO+WAF and another treated with B(a)P (**Fig. 5C**). Other histopathological alterations that are commonly found in liver, such as necrotic foci or eosinophilic foci were not observed in the liver of any treated or control individual. In gill tissues, not significant differences in the prevalences of histopathological conditions were observed, as shown in **Table S9**. Control fish showed in general normal architecture of the gills (**Fig. 5E**). Some of the histopathological lesions found in gills were inflammation and aneurism of the secondary lamella, being the highest prevalence of

aneurism observed in fish exposed to B(a)P (33.3%) and to GO-B(a)P (20%) for 21 days (**Fig. 5H**). Only one individual presented hyperplasia of the primary lamellae.

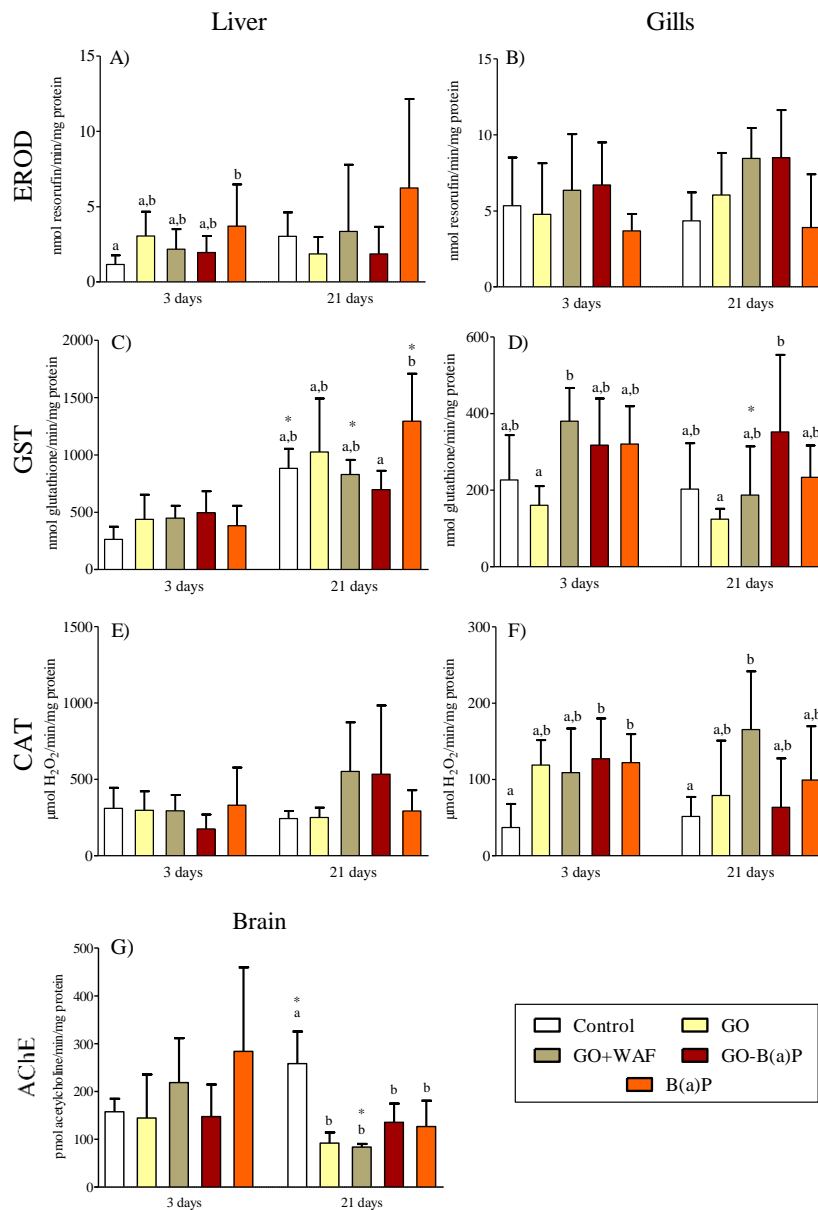


Fig. 4- Results of the biochemical biomarkers measured in adult zebrafish after 3 and 21 days of exposure to GO, GO+WAF, GO-B(a)P and B(a)P. A) EROD activity in liver and B) gills, C) GST activity in liver and D) gills, E) CAT activity in liver and F) gills and G) AChE activity in brain. Different letters indicate statistically significant differences ($p < 0.05$) within each sampling time according to A, B, C, E, G) the Kruskal-Wallis test followed by the post hoc Dunn's test for non-parametric data and D, F) one-way ANOVA followed by the post hoc Tukey's test for parametric data. Asterisks indicate statistically significant differences ($p < 0.05$) for the same treatment between exposure days according to the Mann-Whitney's U test for non-parametric data and Student's t test for parametric data

Results and discussion

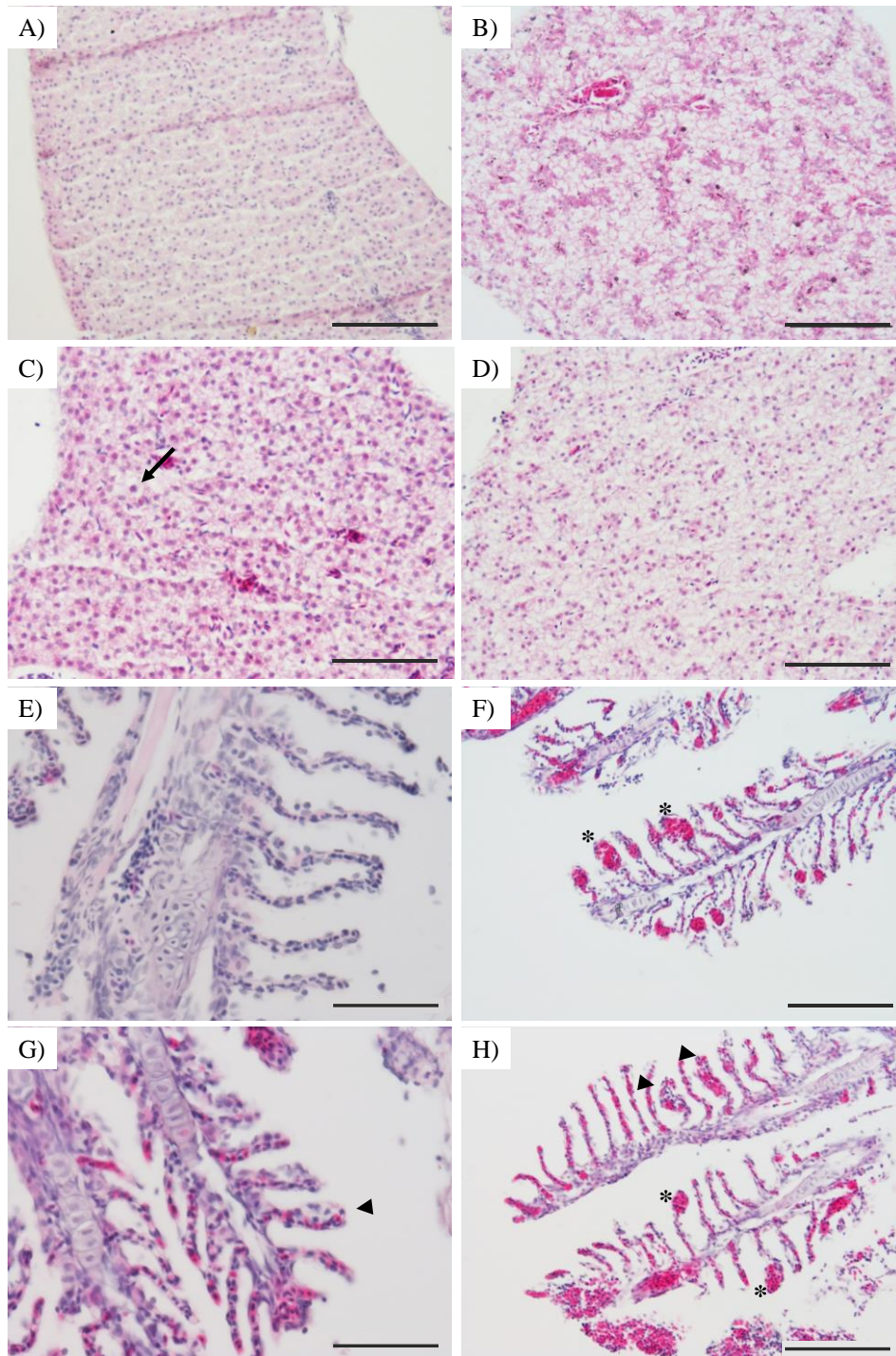


Fig. 5- Micrographs of histological sections of zebrafish liver and gills. A) Liver of unexposed adult zebrafish at 21 days showing normal morphology; B) Liver of zebrafish exposed to GO for 3 days showing liver vacuolisation; C) Liver of a zebrafish exposed to GO+WAF for 21 days showing megalocytosis (black arrow); D) Liver of a zebrafish exposed to GO-B(a)P for 21 days showing liver vacuolisation; E) Gills of unexposed adult zebrafish at 3 days showing normal morphology; F) Gills of zebrafish exposed to GO for 3 days, showing aneurisms (asterisks) of the secondary lamellae; G) Gills of a zebrafish exposed to GO+WAF for 3 days, showing inflammation (arrow head); H) Gills of a zebrafish exposed to GO-B(a)P for 3 days, showing inflammation (arrow head) and aneurisms (asterisks) of the secondary lamellae. Scale bars: A-D) 100 μm , G) 50 μm and E, F, H) 25 μm .

DISCUSSION

To assess the potential risk of graphene NMs as vectors of PAHs, the capacity of the NMs to sorb these organic compounds needs to be analysed. In the present work, we selected for this analysis B(a)P, as a model pyrolytic PAH, and the WAF of a crude oil, as an environmentally relevant mixture of petrogenic PAHs. B(a)P recovery in the control samples after centrifugation needed to separate GO platelets from the liquid phase was lower than expected, due to its high hydrophobicity. In addition, measured B(a)P concentration in water differed from the nominal concentration (sorption experiments, adult exposure group). B(a)P use above saturation point (B(a)P water solubility, 1.62 µg/L; ChemIDplus 2020) usually leads to lower concentration in water than expected (Zhao et al., 2013). Working with over saturated B(a)P concentration was needed to achieve high levels of PAH sorption to GO that could further produce toxic effects in aquatic organisms. According to the results, GO showed a great ability to sorb B(a)P; between 87.2% and 100% of the total B(a)P in the incubation media was sorbed to GO. B(a)P also showed the highest K_f value ($665.47 (\mu\text{g/g})/(\mu\text{g/L})^N$) and a Freundlich N factor of 1.59. In the case of the complex mixture formed in the WAF of the NNS crude oil, the sorption of PAHs to GO was mainly explained by their hydrophobicity. According to the K_f values of the Freundlich isotherm model, sorption of PAHs to GO was as follows: acenaphthene < naphthalene < fluorene < phenanthrene. The highest K_f value was obtained for phenanthrene ($188.87 (\mu\text{g/g})/(\mu\text{g/L})^N$) with a Freundlich N factor of 0.65. Those values were lower than those obtained for B(a)P, as expected based on their lower hydrophobicity and number of aromatic rings. To the best of our knowledge, no previous works have experimentally studied the sorption of B(a)P to GO, but Li et al. (2018) published some predictive simulations that agree with our results. Regarding other PAHs, Wang et al. (2014) evaluated the sorption capacity of naphthalene, phenanthrene and pyrene to graphene and to GO. Values of K_f for GO increased with the increase in the number of aromatic rings and hydrophobicity of each PAH, with values of $0.776\pm 0.0328 (\text{mg/g})/(\text{L/mg})^N$, $8.12\pm 0.257 (\text{mg/g})/(\text{L/mg})^N$ and $42.3\pm 5.39 (\text{mg/g})/(\text{L/mg})^N$, respectively. This tendency was also observed in the present study, with the exception of the higher K_f value ($19.71 (\mu\text{g/g})/(\text{L}/\mu\text{g})^N$) and N factor (0.60) obtained for the sorption of naphthalene to GO compared to those reported in the literature (Pei et al., 2013; Wang and Chen, 2015) and even higher than the values obtained for acenaphthene (a PAH heavier than naphthalene) in the present study. The WAF produced from NNS oil presented low concentrations of the 18 PAHs analysed ($\Sigma\text{PAHs} = 171,059.5 \text{ ng/L}$ for 100% WAF), partially due to the low energy (no vortex) used for its production, as it has been reported for other crude oils. In the case of the Deepwater Horizon oil, PAH concentration increased from 4-196 µg/L in WAFs produced at low energy to 263-6006 µg/L in WAFs produced at higher energy (Forth et al. 2017). In the present study, naphthalene was the most abundant PAH in the WAF ($163,244.5\pm 1,961.3 \text{ ng/L}$), representing 95% of the total PAH concentration.

Results and discussion

Competition among PAHs for sorption onto GO surface could explain the K_f and N factor values estimated. Low values of the Freundlich fitted “ N ” factor indicate an inhomogeneous distribution of PAHs onto GO surface with a wide adsorption site distribution of the PAHs (Carter et al., 1995). The competition between PAHs on GO platelets was higher for phenanthrene and naphthalene being distributed more homogeneously and less widely than the other PAHs. In accordance, a higher K_f coefficient was obtained for naphthalene than for acenaphthene, but values for phenanthrene and fluorene were still higher than for naphthalene. Only one work that studied the potential sorption of a complex PAH mixture to rGO was found in the literature (Sun et al., 2013). In this case, sorption of the PAHs to rGO was mainly driven by the initial concentration and not by the PAH characteristics (Sun et al., 2013). Naphthalene, as the most concentrated PAH in the WAF, was expected to cover the surface of GO at a higher extent than the other PAHs. Nevertheless, initial concentration is not the only parameter regulating the sorption process to GO; the main parameter, as previously mentioned, was hydrophobicity.

GO showed a high capacity to sorb B(a)P, without major differences in the presence of PVP. Nevertheless, when applying isotherm sorption models, values of K_d and K_f were higher for GO (756.58 L/g and 665.45 ($\mu\text{g/g}/(\text{L}/\text{mg})^N$) than for GO(PVP) (575.05 L/g and 357.55 ($\mu\text{g/g}/(\text{L}/\mu\text{g})^N$). The use of PVP (polymer-surfactant) that interacts with GO through hydrogen bonds, allows to disperse GO in the suspension by changing its surface characteristics and making GO platelets completely compatible with water (Zhang et al., 2016). The lower hydrophobicity of the GO(PVP) platelets due to the presence of the surfactant makes GO less likely for hydrophobic compounds sorption than GO alone.

Addition of PVP and reduction of GO resulted into thicker GO(PVP) and rGO(PVP) platelets than GO platelets, as previously reported in the literature (Luque-Alled et al., 2020; Zhang et al., 2010); this increase is suggested to be caused by PVP nanospheres that make the platelets thicker. The GO centrifugation process after contamination with B(a)P did not alter the lateral dimensions or the thickness of the platelets and no evidence of stacking was observed. In the case of GO(PVP) platelets, an increase of thickness was observed after contamination with B(a)P, which suggested that the proven sorption of B(a)P to GO(PVP) and the previously reported PVP effect on thickness could change the surface charge producing the stacking and aggregation of the platelets.

Given the capacity of GO to sorb PAHs, GO contaminated with B(a)P and with PAHs from WAF was assessed for potential toxicity on zebrafish development. Survival and hatching time of zebrafish embryos were not significantly altered by any treatment or concentration used. A significant increase of malformation prevalence was observed only for the highest concentrations assayed and for 0.5 mg/L of GO(PVP)-B(a)P, although all EC_{50} values were higher than the highest concentration tested (10 mg/L). Based on calculated EC_{50} values for malformation

occurrence, the following toxicity ranking was observed: rGO(PVP) > GO > GO(PVP)-B(a)P > GO+WAF > GO-B(a)P > GO(PVP). As reported in the literature, zebrafish embryos exposed to GO (0.01-100 mg/L) presented malformations, such as yolk sac edema and spinal cord flexure, for GO concentrations ranging from 1-5 to 100 mg/L (Chen et al., 2015; D'amora et al., 2017). In addition, changes in hatching rate of zebrafish embryos exposed from 50 to 100 mg/L of GO have been reported (D'amora et al., 2017). Yang et al. (2019b) observed similar malformations in embryos exposed to 1 and 10 mg/L of GO, which showed upregulation of immune response related genes and signs of oxidative stress (increased superoxide dismutase and catalase activities and glutathione concentration) compared to control embryos for the highest GO concentration. Regarding different types of GO NMs, exposure of 5 and 50 mg/L of rGO, but not of GO, provoked changes in hatching rate and body length of zebrafish embryos, although no significant effects on zebrafish malformation and mortality were observed at the tested concentrations (Liu et al., 2014). Thus, evidences point that rGO is more toxic than GO as observed in our results in zebrafish embryos and in the literature, mainly due to the higher bioavailability of rGO (Katsumiti et al., 2017; Yan et al., 2017).

As to the best of our knowledge, modulation of PAH toxicity to zebrafish embryos in presence of GO has not been reported in the literature yet. Nevertheless, toxicity of another persistent pollutant, such as bisphenol A, in combination with GO was assessed by Yang et al. (2019a). The availability of bisphenol A to zebrafish embryos was reduced in the presence of GO and adverse effects caused by bisphenol A on zebrafish embryos (larvae malformation and hatching delay) were alleviated. Similar findings have been published for other non-planar carbon NMs, such as fullerenes (C₆₀) and carbon nanotubes, in combination with PAHs (Della Torre et al., 2019; Falconer et al. 2015). The accumulation of B(a)P (1 mg/L) was reduced in presence of C₆₀ (20 mg/L), but similar toxicity was observed for C₆₀ alone or in combination with B(a)P (Della Torre et al., 2019). Phenanthrene (10 mg/L) was also less available to zebrafish embryos in presence of multiwalled carbon nanotubes (50-200 mg/L MWCNTs) (Falconer et al., 2015). An increase of MWCNTs concentration to 200 mg/L, with the same phenanthrene concentration, increased the survival rate of zebrafish embryos compared to embryos exposed to phenanthrene alone. Presence of GO might reduce the availability of PAHs decreasing their toxicity at the tested concentrations, and it can be suggested that the toxicity observed on zebrafish embryo development was mainly due to the GO characteristics rather than to PAH toxicity.

The effects produced by GO on zebrafish embryos could be due to the ingestion-internalisation of GO (Chen et al., 2015; Zhang et al., 2017a). Thus, GO labelled with fluorescein was observed inside zebrafish embryos at early development (24 hpf), indicating the ability of GO to cross the chorion barrier. Fluorescence produced by GO was more intense in the chest than in the head or in the tail. A similar accumulation pattern was observed for fluorescent rGO on zebrafish embryos

Results and discussion

(Chen et al., 2015). rGO internalisation was already observed at 12 hpf in exposed embryos, while GO was first internalised in zebrafish embryos at 24 hpf (Zhang et al., 2017a).

To further understand the effects of GO alone or in combination with PAHs, an experiment with adult zebrafish was carried out. The selected GO concentration (2 mg/L) has been used in previous studies (Souza et al., 2017) and showed effects in adult zebrafish, while being a relatively low concentration. GO is stable at long term in freshwater (Chowdhury et al., 2013), but the presence of fish and, consequently, of organic matter due to fish feeding could produce GO aggregation in the exposure tanks (Souza et al., 2017; Castro et al., 2018), which could lead to an heterogeneous dispersion of GO in the tanks and could explain the variability in GO concentrations measured in water, especially during the first three days of the experiment. Nevertheless, the system appeared to stabilise and in the last three days of exposure, the concentration of GO in the three GO-containing tanks behaved similarly. Changes in GO concentration in water could also be due to the ingestion of GO by zebrafish as proved in the present study. The ingestion of GO by aquatic organisms has been shown by TEM analysis (Hu et al., 2017). GO translocation from water to adult zebrafish brain was reported by Hu et al. (2017). Also, GO was found in the diencephalon of the offspring of the adult zebrafish exposed to 1 µg/L of GO, demonstrating that GO can be transferred from the adult to the offspring through gametes. In our study GO was identified in the lumen of the intestine of adult zebrafish but evidences of GO translocation to the tissues were not found.

Along with the quantification of the GO concentration in the exposure tanks, PAH levels were also measured. PAH concentration in the control tank was close to the limit of quantification. In the co-exposure GO+WAF tank, total PAH concentration was progressively reduced along the 72 h of the dosing cycle, mainly due to the reduction in naphthalene concentration. As previously discussed, naphthalene was only partially sorbed to GO. Thus, the loss of naphthalene concentration could be expected due to its low hydrophobicity and high volatility (Salazar-Coria et al., 2019). A similar decrease of PAH concentration over time was measured in the B(a)P alone exposure tank, where B(a)P concentration was reduced from 29,440.3±4,582.1 ng/L to 7,956.7±1,723.1 ng/L over 72 h, a reduction that could be partially explained by the high capacity of fish to uptake and metabolise PAHs (Livingstone, 1998). Overall, PAH exposure levels were not constant over time, except in the case of GO-B(a)P exposure group, where B(a)P concentration remained almost stable for 72 h (1,743.2 ng/L to 1,293.2 ng/L), possibly as a consequence of adsorption of B(a)P to GO.

PAH bioaccumulation was also analysed in zebrafish in order to confirm fish exposure. Except for naphthalene, PAH accumulation in zebrafish exposed to GO+WAF reflected the PAH concentration in exposure media. Despite of the high concentration of naphthalene in the

GO+WAF exposure tank, accumulation of this compound in zebrafish was not detected in this study. The bioavailability of PAHs sorbed to carbon NMs was studied by Linard et al. (2017) who concluded that bioavailability to freshwater fish of PAHs associated with graphene was higher for the most hydrophobic PAH phenanthrene (90% of adsorbed phenanthrene was bioavailable), than for anthracene, fluorene or naphthalene (35%, 40% and 20%, respectively). A lower PAH bioaccumulation was measured in fish exposed to GO-B(a)P than in those co-exposed to GO+WAF in agreement with PAH concentration in exposure media. Another factor to be considered regarding PAH bioaccumulation is the capacity of the fish to metabolise those compounds, being more hydrophobic PAHs more easily metabolised and excreted than lower weight PAHs being, in turn, less accumulated in fish (Livingstone, 1998). In addition, a noticeable accumulation of B(a)P in the whole body of fish exposed for 21 days to B(a)P alone was recorded, while fish exposed to GO-B(a)P showed much lower levels of B(a)P in their tissues as could be expected based on B(a)P levels measured in water. These results indicated that B(a)P sorbed to GO was less bioavailable than dissolved B(a)P, as previously discussed.

Analyses of the biological responses in adult zebrafish showed that fish exposed to B(a)P alone for 3 days presented the highest transcription levels of hepatic *cyp1a*. This up-regulation of *cyp1a* could have been translated into a significant induction of EROD activity in the liver of fish exposed to B(a)P for 3 days, that remained the highest among treatments after 21 days of exposure. This response is linked to the previously mentioned bioaccumulation of B(a)P in fish tissue at 21 days of exposure, although elimination (biotransformation metabolism) of B(a)P seemed to be slower than uptake, resulting in a net B(a)P bioaccumulation. For the same nominal B(a)P concentration used in the present study (100 µg/L), previous studies have also reported an up-regulation of *cyp1a* and induction of EROD activity in the liver of zebrafish exposed for 7 days (Thompson et al., 2010). This response was not observed in the gills. On the other hand, exposure to GO alone did not alter liver biotransformation metabolism (*cyp1a* or EROD) at any exposure time. Other works, however, have reported that a high concentration of rGO quantum dots (100 mg/L) significantly up-regulated *cyp1a*, through interaction with the AhR pathway in zebrafish embryos (Zhang et al., 2017a). Apart from differences in exposure concentrations, effects produced by different graphene derivatives can differ completely depending on the surface characteristics of each NM (Guo and Mei, 2014; Jia et al., 2019), being the oxygen content on the surface one of the potential driving factors. When carbon NMs were combined with PAHs in the present study, the observed ability of B(a)P alone exposure to induce *cyp1a* and EROD in fish liver was not observed in fish exposed to GO with sorbed B(a)P. The lack of response of PAH exposure biomarkers in fish exposed to GO-B(a)P could be due to the lower level of exposure to B(a)P when sorbed to GO, as was reported for other carbon NMs in combination with PAHs (Della Torre et al., 2017) as well as consequent lower bioavailability and bioaccumulation.

Results and discussion

Similarly, the level of PAH exposure achieved in the GO+WAF treatment did not result enough to regulate the *cyp1a* transcription levels in zebrafish liver. According to Salaberria et al. (2010), a 50% WAF (1:40 North Sea crude oil/water), with a PAH content similar to that of the WAF used herein, was needed to cause *cyp1a* up-regulation in zebrafish liver after 24 and 72 h of exposure.

The transcription levels of liver *gstp1*, analysed as a key gene of phase II biotransformation metabolism, did not show significant changes in any treated group. Nevertheless, liver GST activity in fish exposed to B(a)P for 21 days presented a significant induction compared to GO-B(a)P exposed fishes. Whereas, Thompson et al. (2010) did not report induction of GST liver activity in zebrafish exposed to B(a)P for 7 days, exposure of red tilapia to 300 µg/L B(a)P for 10 days resulted in liver GST induction (Rodrigues et al., 2015). The presence of GO could inhibit the effect on liver GST activity induced by B(a)P exposure. Exposure to GO (1, 5 and 10 mg/L) has been reported to reduce the levels of glutathione (GSH), the co-factor of GST closely related with its activity (Chen et al., 2016), which could lead to the inhibition of GST activity (Glisic et al., 2015). On the contrary, GST activity was significantly induced in gills of fishes exposed for 3 days to GO+WAF and for 21 days to GO-B(a)P compared to fish exposed to GO, which showed the lowest gill GST activity among all treated fish. An inhibition of GST activity in gills was also observed in zebrafish after 48 h of injection of 50 mg/L of graphene (Fernandes et al., 2018). The fact that GST activity was induced significantly in gills of fish exposed to GO combined with PAHs (GO-B(a)P and GO+WAF), while the same response was not observed in the liver, suggests that the principal uptake route for these PAHs associated to GO could be through the gills. The contaminated GO (particulate) can directly impact on gills that are directly exposed to the water column and accumulate released PAHs as it has been demonstrated for other PAHs adsorbed on suspended particles (Zhai et al., 2020).

Analysis of *tp53* transcription levels in liver was carried out because of the involvement of this gene in cell cycle regulation. Its overexpression is considered a sign of protection against DNA damage that can trigger apoptosis or hepatocarcinogenesis in zebrafish (Lu et al., 2013). Metabolism of PAHs can lead to the formation of DNA damaging reactive intermediates (Storer and Zon, 2010). GO has been reported as an inducer of *tp53* in zebrafish embryos exposed to 50 mg/L of GO for 72 hpf (Jia et al., 2019). Regarding PAHs, no changes in the transcription levels of *tp53* were detected 14 days after injection of rainbow trout with 100 mg/Kg of B(a)P (Phalen et al., 2017). In the present study, the *tp53* transcription levels were only significantly higher in fish exposed to GO-B(a)P compared to fish exposed to GO+WAF for 3 days, which presented the lowest values, and no significant differences were found compared to control fish, suggesting that the exposure concentrations were not high enough to induce DNA damage and to activate cell cycle regulation pathways.

Similarly, *cat*, *gpx1a* or *sod1* did not show any significant change among treatments, even though GO is known to affect antioxidant enzymes in zebrafish embryos as consequence of ROS generation (Zhang et al., 2017b; Zou et al., 2018; Souza et al., 2019). Zou et al. (2018) reported an up-regulation of *gpx4b*, *sod2*, and *prdx1* in embryos exposed to 100 µg/L of GO. Zhang et al. (2017b) also observed generation of ROS by 1-100 µg/L of GO with a consequent oxidative stress reflected by the significant increase of malondialdehyde content in GO exposed zebrafish. To the best of our knowledge, no previous works have reported effects in the transcription levels of oxidative stress-related genes caused by GO in adult zebrafish liver, but zebrafish embryos are expected to be more sensitive to GO compared with adult individuals. Accordingly, no significant effects were observed in liver CAT activity, which showed only significant differences in gills. All exposed fish presented higher CAT activity than controls, being significant in fish exposed to GO-B(a)P and B(a)P for 3 days and to GO+WAF for 21 days. Souza et al. (2019) reported induction of CAT activity in zebrafish gills exposed to 2, 10 and 20 mg/L of GO for 48 h. This early response of the antioxidant system of zebrafish was reduced after 168 h of recovery in clean water. Other carbon NMs, such as C₆₀ (20 mg/L), combined with B(a)P (8 µg/L), or B(a)P alone (8 µg/L) provoked a reduction of CAT activity in zebrafish embryos, while C₆₀ alone produced induction of CAT (Della Torre et al., 2018).

AChE, that regulates the activity of acetylcholine, an important neurotransmitter involved in synaptic transmission of nerve impulses, was inhibited in all fish exposed for 21 days compared to control fish, but not in fish exposed for three days except in the case of the GO+WAF group. Hu et al. (2017) demonstrated that for a range of GO concentrations (0.01-1 µg/L), GO translocated to the brain of adult zebrafish and of their offspring with a subsequent inhibition of AChE activity in the offspring of exposed adults. AChE has also been typically reported to be altered in fish by xenobiotics, such as pesticides and PAHs (Holth and Tollefsen, 2012; Vieira et al., 2008; Kim et al., 2018). Phenanthrene, a common PAH present in most WAFs of crude oil, inhibited AChE activity in the head of adult zebrafish after 96 h of exposure to 750 µg/L (Kim et al., 2018). Another freshwater fish, *Electrophorus electricus*, showed inhibition of AChE after exposure to the produced water effluents from oil production platforms in the North Sea, being the aromatic PAHs, and not the polar and aliphatic fractions responsible of AChE inhibition (Holth and Tollefsen, 2012). In the common goby, exposure to 2 to 16 µg/L of B(a)P for 96 h also caused inhibition of AChE (Vieira et al., 2008).

Regarding histopathological alterations, a significant increase in the prevalence of liver vacuolisation was observed in fish exposed to GO+WAF for 3 and 21 days. Previous works observed 71.4% and 80% liver vacuolisation in zebrafish exposed to 2 mg/L and 20 mg/L of GO, respectively, for 14 days (Chen et al., 2016; Souza et al., 2017), but this was not observed in the present work. WAF from naphthenic crude oils have also been reported as disruptors of hepatic

Results and discussion

tissue. Agamy (2012) found the presence of lipid droplets in the liver of juvenile rabbit fish (*Siganus canaliculatus*) after 15 days and less frequently after 21 days of exposure to WAF. Co-exposure to GO+WAF PAHs, as in the present study, might increase the prevalence of hepatic pathologies compared to the effect of each treatment alone. Regarding gill tissues, none of the treatments of our study produced any significant histopathological alteration. Other studies did neither report remarkable effects on zebrafish gill tissue after exposure to GO at the same concentration used herein (Chen et al., 2016; Souza et al., 2017). Only at exposures from 10 to 20 mg/L of GO, gills of zebrafish presented some pathologies, such as lamellar fusion, clubbed tips, swollen mucocytes, epithelial lifting, aneurysms, and necrosis and these effects were closely related to ROS production due to GO exposure (Souza et al., 2017).

In summary, GO presented a high sorption capacity for PAHs that was driven mainly by the hydrophobicity of each PAH. Thus, GO in the environment could play a potential role as carrier of organic pollutants to aquatic organisms. Environmentally relevant concentrations of GO and rGO(PVP) did not cause significant effects on zebrafish embryo development ($EC_{50} > 10$ mg/L), even when they were combined with PAHs. Regarding sublethal effects in adult zebrafish, some evidences of toxicity were observed according to the results of catalase activity in zebrafish gills, but without further appearance of histopathological alterations in the gill tissue. The inhibition of AChE activity in all fish treated for 21 days indicated a potential neurotoxic effect. Only dissolved B(a)P provoked changes in liver biotransformation biomarkers, even at gene level, and these effects were reduced when zebrafish were exposed to GO combined with PAHs. At tissue level, hepatic vacuolisation was observed in fish co-exposed to GO+WAF, which is possibly linked to the bioavailability of the PAHs from WAF when they are associated with GO. Taken together, the results suggested that graphene oxide NMs, alone and in combination with PAHs, are a potential source of toxicity to fish, but at concentrations that are currently above the expected environmental levels.

REFERENCES

1. Aebi H., 1984. Catalase in vitro. *Meth. Enzymol.* 105, 121-126.
2. Agamy, E., 2012. Histopathological liver alterations in juvenile rabbit fish (*Siganus canaliculatus*) exposed to light Arabian crude oil, dispersed oil and dispersant. *Ecotoxicol. Environ. Saf.* 75, 171-179.
3. Apul, O.G., Wang, Q., Zhou, Y., Karanfil, T., 2013. Adsorption of aromatic organic contaminants by graphene nanosheets: Comparison with carbon nanotubes and activated carbon. *Water Res.* 47, 1648-1654.
4. Baig, N., Ihsanullah, Sajid, M., Saleh, T.A., 2019. Graphene-based adsorbents for the removal of toxic organic pollutants: A review. *J. Environ. Manage.* 244, 370-382.
5. Baumard, P., Budzinski, H., Garrigues, P., 1997. Analytical procedure for the analysis of PAHs in biological tissues by gas chromatography coupled to mass spectrometry: application to mussels. *Fresenius J. Anal. Chem.* 359, 502-509.

6. Baumard P., Budzinski H., Garrigues P., Dizer H., Hansen P.D., 1999. Polycyclic aromatic hydrocarbons in recent sediments and mussels (*Mytilus edulis*) from the Western Baltic Sea: occurrence, bioavailability and seasonal variations. *Mar. Environ. Res.* 47, 17-47.
7. Butala, H., Metzger, C., Rimoldi, J., Willett, K.L., 2004. Microsomal estrogen metabolism in channel catfish. *Mar. Environ. Res.* 58, 489-494.
8. Brand, M., Granato, M., Nüsslein-Volhard, C., 2002. Chapter 1: Keeping and raising zebrafish. In: *Zebrafish: A practical approach*; Nusslein-Volhard C., Eds.; Dahm, R., Oxford University Press, New York, pp. 7-37.
9. Carter, M.C., Kilduff, J.E., Weber Jr., W.J., 1995. Site energy distribution analysis of preloaded adsorbents. *Environ. Sci. Technol.* 29, 1773-1780.
10. Castro, V.L., Clemente, Z., Jonsson, C., Silva, M., Vallim, J.H., de Medeiros, A.M.Z., Martinez, D.S.T., 2018. Nanoecotoxicity assessment of graphene oxide and its relationship with humic acid: Nanoecotoxicity of graphene oxide and humic acid. *Environ. Toxicol. Chem.* 37, 1998-2012.
11. ChemIDplus by SRC, Inc. [http://chem.sis.nlm.nih.gov/chemidplus/name/benzo\(a\)pyrene](http://chem.sis.nlm.nih.gov/chemidplus/name/benzo(a)pyrene) (accessed Jan 20, 2020).
12. Chen, L., Hernandez, Y., Feng, X., Müllen, K., 2012. From nanographene and graphene nanoribbons to graphene sheets: chemical synthesis. *Angew. Chem. Int. Ed.* 51, 764-7654.
13. Chen, M., Yin, J., Liang, Y., Yuan, S., Wang, F., Song, M., Wang, H., 2016a. Oxidative stress and immunotoxicity induced by graphene oxide in zebrafish. *Aquat. Toxicol.* 174, 54-60.
14. Chen, Y., Hu, X., Sun, J., Zhou, Q., 2016b. Specific nanotoxicity of graphene oxide during zebrafish embryogenesis. *Nanotoxicology* 1-11.
15. Cheng, X., Kan, A.T., Tomson, M.B., 2004. Naphthalene adsorption and desorption from aqueous C60 fullerene. *J. Chem. Eng. Data* 49, 675-683.
16. Chowdhury, I., Duch, M.C., Mansukhani, N.D., Hersam, M.C., Bouchard, D., 2013. Colloidal properties and stability of graphene oxide nanomaterials in the aquatic environment. *Environ. Sci. Technol.* 47, 6288-6296.
17. Cimbalk, G.V., Ramsdorf, W.A., Perussolo, M.C., Santos, H.K.F., Da Silva De Assis, H.C., Schnitzler, M.C., Schnitzler, D.C., Carneiro, P.G., Cestari, M.M., 2018. Evaluation of multiwalled carbon nanotubes toxicity in two fish species. *Ecotoxicol. Environ. Saf.* 150, 215-223.
18. Ciriminna, R., Zhang, N., Yang, M., Meneguzzo, F., Xu, Y., Pagliaro, M., 2016. Commercialization of graphene-based technologies: a critical insight. *Chem. Comm.* 51, 7090-7095.
19. D' Amora, M., Camisasca, A., Lettieri, S., Giordani, S., 2017. Toxicity assessment of carbon nanomaterials in zebrafish during development. *Nanomaterials* 7, 414.
20. Dasmahapatra, A.K., Dasari, T.P.S., Tchounwou, P.B., 2018. Graphene-Based Nanomaterials Toxicity in Fish, in: de Voogt, P. (Ed.), *Reviews of Environmental Contamination and Toxicology Volume 247*. Springer International Publishing, Cham, pp. 1-58.
21. Della Torre, C., Maggioni, D., Ghilardi, A., Parolini, M., Santo, N., Landi, C., Madaschi, L., Magni, S., Tasselli, S., Ascagni, M., Bini, L., La Porta, C., Del Giacco, L., Binelli, A., 2018. The interactions of fullerene C60 and Benzo(α)pyrene influence their bioavailability and toxicity to zebrafish embryos. *Environ. Pollut.* 241, 999-1008.
22. Della Torre, C., Parolini, M., Del Giacco, L., Ghilardi, A., Ascagni, M., Santo, N., Maggioni, D., Magni, S., Madaschi, L., Prosperi, L., La Porta, C., Binelli, A., 2017. Adsorption of B(α)P on carbon nanopowder affects accumulation and toxicity in zebrafish (*Danio rerio*) embryos. *Environ. Sci. Nano* 4, 1132-1146.

Results and discussion

23. De Marchi, L., Pretti, C., Gabriel, B., Marques, P.A.A.P., Freitas, R., Neto, V., 2018. An overview of graphene materials: Properties, applications and toxicity on aquatic environments. *Sci. Total Environ.* 631-632, 1440-1456.
24. Ellman, G.L., Courtney, K.D., Andres, V., Featherstone, R.M., 1961. A new and rapid colorimetric determination of acetylcholinesterase activity. *Biochem. Pharmacol.* 7, 88-90.
25. Fako, V.E., Furgeson, D.Y., 2009. Zebrafish as a correlative and predictive model for assessing biomaterial nanotoxicity. *Adv. Drug Deliv. Rev.* 61, 478-486.
26. Falconer, J.L., Jones, C.F., Lu, S., Grainger, D.W., 2015. Carbon nanomaterials rescue phenanthrene toxicity in zebrafish embryo cultures. *Environ. Sci. Nano* 2, 645-652.
27. Fernandes, A.L., Nascimento, J.P., Santos, A.P., Furtado, C.A., Romano, L.A., Eduardo da Rosa, C., Monserrat, J.M., Ventura-Lima, J., 2018. Assessment of the effects of graphene exposure in *Danio rerio*: A molecular, biochemical and histological approach to investigating mechanisms of toxicity. *Chemosphere* 210, 458-466.
28. Forth, H.P.; Mitchelmore, C.L.; Morris, J.M.; Lipton, J., 2017. Characterization of oil and water accommodated fractions used to conduct aquatic toxicity testing in support of the Deepwater Horizon oil spill natural resource damage assessment. *Environ. Toxicol. Chem* 36, 1450-1459.
29. Ghosal, K., Sarkar, K., 2018. Biomedical applications of graphene nanomaterials and beyond. *ACS Biomater. Sci. Eng.* 4, 2653-2703.
30. Glisic, B., Mihaljevic, I., Popovic, M., Zaja, R., Loncar, J., Fent, K., Kovacevic, R., Smital, T., 2015. Characterization of glutathione-S-transferases in zebrafish (*Danio rerio*). *Aquat. Toxicol.* 158, 50-62.
31. Guo, X., Mei, N., 2014. Assessment of the toxic potential of graphene family nanomaterials. *J. Food Drug Anal.* 22, 105-115.
32. Habig, W.H., Jakoby W.B., 1981. Assays for differentiation of glutathione S-transferases. *Methods Enzymol.* 77, 398-405.
33. Holth, T.F, Tollefsen, K.E., 2012. Acetylcholine esterase inhibitors in effluents from oil production platforms in the North Sea. *Aquat. Toxicol.* 112-113, 92-98.
34. Hu, X., Wei, Z., Mu, L., 2017. Graphene oxide nanosheets at trace concentrations elicit neurotoxicity in the offspring of zebrafish. *Carbon* 117, 182-191.
35. Ji, L., Chen, W., Xu, Z., Zheng, S., Zhu, D., 2013. Graphene nanosheets and graphite oxide as promising adsorbents for removal of organic contaminants from aqueous solution. *J. Environ. Qual.* 42, 191-198.
36. Jia, P.-P., Sun, T., Junaid, M., Yang, L., Ma, Y.-B., Cui, Z.-S., Wei, D.-P., Shi, H.-F., Pei, D.-S., 2019. Nanotoxicity of different sizes of graphene (G) and graphene oxide (GO) *in vitro* and *in vivo*. *Environ. Pollut.* 247, 595-606.
37. Katsumiti, A., Tomovska, R., Cajaraville, M.P., 2017. Intracellular localization and toxicity of graphene oxide and reduced graphene oxide nanoplatelets to mussel hemocytes *in vitro*. *Aquat. Toxicol.* 188, 138-147.
38. Kennedy S.W., Jones S.P., 1994. Simultaneous measurement of cytochrome P4501A catalytic activity and total protein concentration with a fluorescence plate reader. *Anal. Biochem.* 222(1), 217-223.
39. Kim, K., Jeon, H., Choi, S., Tsang, D.C.W., Oleszczuk, P., Ok, Y.S, Lee, H., Lee, S., 2018. Combined toxicity of endosulfan and phenanthrene mixtures and induced molecular changes in adult zebrafish (*Danio rerio*). *Chemosphere* 194, 30-41.
40. Kinloch, I.A, Suhr, J., Lou, J., Young, R.J., Ajayan, P.M., 2018. Composites with carbon nanotubes and graphene: An outlook. *Science* 362, 547-553

41. Kong, W., Kum, H., Bae, S., Shim, J., Kim, H., Kong, L., Meng, Y., Wang, K., Kim, C., Kim, J., 2019. Path towards graphene commercialization from lab to market. *Nat. Nanotechnol.* 14, 927-938.
42. Lacave J.M., Fanjul, A., Bilbao, E., Gutierrez, N., Barrio, I., Arostegui, I., Cajaraville, M.P., Orbea, A., 2017. Acute toxicity, bioaccumulation and effects of dietary transfer of silver from brine shrimp exposed to PVP/PEI-coated silver nanoparticles to zebrafish. *Comp. Biochem Physiol. Part C* 199, 69-80.
43. Lacave, J.M., Vicario-Parés, U., Bilbao, E., Gilliland, D., Mura, F., Dini, L., Cajaraville, M.P., Orbea, A., 2018. Waterborne exposure of adult zebrafish to silver nanoparticles and to ionic silver results in differential silver accumulation and effects at cellular and molecular levels. *Sci. Total Environ.* 642, 1209-1220.
44. Lammel, T., Navas, J.M., 2014. Graphene nanoplatelets spontaneously translocate into the cytosol and physically interact with cellular organelles in the fish cell line PLHC-1. *Aquat. Toxicol.* 150, 55-65.
45. Lammel, T., Boisseaux, P., Navas, J.M., 2014. Potentiating effect of graphene nanomaterials on aromatic environmental pollutant-induced cytochrome P450 1A expression in the topminnow fish hepatoma cell line PLHC-1. *Environ. Toxicol.* 30, 1192-1204.
46. Li, B., Ou, P., Wei, Y., Zhang, X., Song, J., 2018. Polycyclic aromatic hydrocarbons adsorption onto graphene: a DFT and AIMD study. *Materials* 11, 726.
47. Linard, E.N., Apul, O.G., Karanfil, T., van den Hurk, P., Klaine, S.J., 2017. Bioavailability carbon nanomaterial-adsorbed polycyclic aromatic hydrocarbons to *Pimephales promelas*: influence of adsorbate molecular size and configuration. *Environ. Sci. Technol.* 51, 9288-9296.
48. Liu, X.T., Mu, X.Y., Wu, X.L., Meng, L.X., Guan, W.B., Ma, Y.Q., Sun, H., Wang, C.J., Li, X.F., 2014. Toxicity of multi-walled carbon nanotubes, graphene oxide, and reduced graphene oxide to zebrafish embryos. *Biomed. Environ. Sci.* 27(9), 676-683.
49. Liu, Y., Bai, J., Yao, H., Li, G., Zhang, T., Li, S., Zhang, L., Si, J., Zhou, R., Zhang, H., 2020. Embryotoxicity assessment and efficient removal of naphthalene from water by irradiated graphene aerogels. *Ecotoxicol. Environ. Saf.* 189, 110051.
50. Livak, K.J., Schmittgen, T.D., 2001. Analysis of relative gene expression data using real-time quantitative PCR and the 2- $\Delta\Delta$ CT method. *Methods* 25, 402-408.
51. Livingstone, D.R., 1998. The fate of organic xenobiotics in aquatic ecosystems: quantitative and qualitative differences in biotransformation by invertebrates and fish. *Comp. Biochem Physiol. Part A* 120, 43-49.
52. Lu, J., Yang, W., Tsai, S., Lin, Y., Chang, P., Chen, J., Wang, H., Wu, J., Jin, S.C., Yuh, C., 2013. Liver-specific expressions of *HBx* and *src* in the *p53* mutant trigger hepatocarcinogenesis in zebrafish. *PLOS One* 8, e76951.
53. Luque-Alled, J.M., Abdel-Karim, A., Alberto, M., Leaper, S., Perez-Page, M., Huang, K., Vijayaraghavan, A., El-Kalliny, A.S., Holmes, S.M., Gorgojo, P., 2020. Polyethersulfone membranes: From ultrafiltration to nanofiltration via the incorporation of APTS functionalized-graphene oxide. *Sep. Purif. Technol.* 230, 115836.
54. Montagner, A., Bosi, S., Tenori, E., Bidussi, M., Alshatwi, A.A., Tretiach, M., Prato, M., Syrgiannis, Z., 2017. Ecotoxicological effects of graphene-based materials. *2D Materials* 4(1), 1-9.
55. Naasz, S., Altenburger, R., Kühnel, D., 2018. Environmental mixtures of nanomaterials and chemicals: The Trojan-horse phenomenon and its relevance for ecotoxicity. *Sci. Total Environ.* 635, 1170-1181.

Results and discussion

56. Niu, Z., Liu, L., Zhang, L., Chen, X., 2014. Porous graphene materials for water remediation. *Small* 10, 3434-3441.
57. OECD TG236. 2013. OECD guidelines for the testing of chemicals. Section 2: Effects on biotic systems Test No. 236: Fish embryo acute toxicity (FET) test. Organization for Economic Cooperation and Development, Paris, France, 22 pp.
58. Orbea, A., González-Soto, N., Lacave, J.M., Barrio, I., Cajaraville, M.P., 2017. Developmental and reproductive toxicity of PVP/PEI-coated silver nanoparticles to zebrafish. *Comp. Biochem. Physiol. Part C: Toxicol. Pharmacol.* 199, 59–68.
59. Pecoraro, R., D'Angelo, D., Filice, S., Scalese, S., Capparucci, F., Marino, F., Iaria, C., Guerriero, G., Tibullo, D., Scalisi, E.M., Salvaggio, A., Nicotera, I., Brundo, M.V., 2018. Toxicity evaluation of graphene oxide and titania loaded nafion membranes in zebrafish. *Front. Physiol.* 8, 1039.
60. Pei, Z., Li, L., Sun, L., Zhang, S., Shan, X., Yang, S., Wen, B., 2013. Adsorption characteristics of 1,2,4-trichlorobenzene, 2,4,6-trichlorophenol, 2-naphthol and naphthalene on graphene and graphene oxide. *Carbon* 51, 156-163.
61. Phalen, L.J., Köllner, B., Hogan, N.S., van den Heuvel, M.R., 2017. Transcriptional response in rainbow trout (*Oncorhynchus mykiss*) B cells and thrombocytes following *in vivo* exposure to benzo[a]pyrene. *Environ. Toxicol. Pharmacol.* 53, 212-218.
62. Ren, C., Hu, X., Li, X., Zhou, Q., 2016. Ultra-trace graphene oxide in a water environment triggers Parkinson's disease-like symptoms and metabolic disturbance in zebrafish larvae. *Biomaterials* 93, 83-94.
63. Rodrigues, A.F.C., Moneró, T.O., Frighetto, R.T.S., de Almeida, E.A., 2015 E2 potentializes benzo(a)pyrene-induced hepatic cytochrome P450 enzyme activities in Nile tilapia at high concentrations. *Environ. Sci. Pollut. Res.* 22, 17367-17374.
64. Salaberria, I., Brakstad, O.G., Olsen, A.J., Nordtug, T., Hansen, B.H., 2014. Endocrine and AhR-CYP1A pathway responses to the water-soluble fraction of oil in zebrafish (*Danio rerio* Hamilton). *J. Toxicol. Environ. Health, Part A* 77, 506-515.
65. Salazar-Coria, L., Rocha-Gómez, M.A., Matadamas-Martínez, F., Yépez-Mulia, L., Vega-López, A., 2019. Proteomic analysis of oxidized proteins in the brain and liver of the Nile tilapia (*Oreochromis niloticus*) exposed to a water-accommodated fraction of Maya crude oil. *Ecotoxicol. Environ. Saf.* 17, 609-620.
66. Singer, M.M., Aurand, D., Bragins, G.E., Clark, J.R., Coelho, G.M., Sowby, M.L., Tjeerdema, R.S., 2000. Standardization of the Preparation and Quantitation of Water-accommodated Fractions of Petroleum for Toxicity Testing. *Mar. Pollut. Bull.* 40, 1007-1016.
67. Smith, S.C., Rodrigues, D.F., 2015. Carbon-based nanomaterials for removal of chemical and biological contaminants from water: A review of mechanisms and applications. *Carbon* 91, 122-143.
68. Soares, J., Pereira, T., Costa, K., Maraschin, T., Basso, N., Bogo, M., 2017. Developmental neurotoxic effects of graphene oxide exposure in zebrafish larvae (*Danio rerio*). *Colloids Surf. B: Biointerfaces* 157, 335-346.
69. Souza, J.P., Baretta, J.F., Santos, F., Paino, I.M.M., Zucolotto, V., 2017. Toxicological effects of graphene oxide on adult zebrafish (*Danio rerio*). *Aquat. Toxicol.* 186, 11-18.
70. Statoil. 2011. Crude summary report. Available at: <https://www.statoil.com/content/dam/statoil/documents/crude-oil-assays/Statoil-TROLL-BLEND-2011-01.xls> (Accessed Nov 2018).
71. Storer, N.Y., Zon, L.I., 2010. Zebrafish models of p53 functions. *Cold Spring Harb. Perspect. Med.* 2, a001123.

72. Sun, Y., Yang, S., Zhao, G., Wang, Q., Wang, X., 2013. Adsorption of polycyclic aromatic hydrocarbons on graphene oxides and reduced graphene oxides. *Chem. Asian J.* 8, 2755-2761.
73. Tabish, T.A., Memon, F.A., Gomez, D.E., Horsell, D.W., Zhang, S., 2018. A facile synthesis of porous graphene for efficient water and wastewater treatment. *Sci. Rep.* 8, 1817-1831.
74. Thompson, E.D., Burwinkel, K.E., Chava, A.K., Notch, E.G., Mayer, G.D., 2010. Activity of Phase I and Phase II enzymes of the benzo[a]pyrene transformation pathway in zebrafish (*Danio rerio*) following waterborne exposure to arsenite. *Comp. Biochem. Physiol. Part C: Toxicol. Pharmacol.* 152, 371-378.
75. Turja, R., Höher, N., Snoejis, P., Baršienė, J., Butrimavičienė, L., Kuznetsova, T., Kholodkevich, S.V., Devier, M.H., Budzinski, H., Lehtonen, K.K., 2014. A multibiomarker approach to the assessment of pollution impacts in two Baltic Sea coastal areas in Sweden using caged mussels (*Mytilus trossulus*). *Sci. Total Environ.* 473, 398-409.
76. Turja, R., Soirinsuo, A., Budzinski, H., Devier, M.H., Lehtonen, K.K., 2013. Biomarker responses and accumulation of hazardous substances in mussels (*Mytilus trossulus*) transplanted along a pollution gradient close to an oil terminal in the Gulf of Finland (Baltic Sea). *Comp. Biochem. Physiol. Part C: Toxicol. Pharmacol.* 157, 80-92.
77. Vance, M.E., Kuiken, T., Vejerano, E.P., McGinnis, S.P., Hochella, M.F., Rejeski, D., Hull, M.S., 2015. Nanotechnology in the real world: Redeveloping the nanomaterial consumer products inventory. *Beilstein J. Nanotechnol.* 6, 1769-1780.
78. Velki, M., Meyer-Alert, H., Seiler, T.-B., Hollert, H., 2017. Enzymatic activity and gene expression changes in zebrafish embryos and larvae exposed to pesticides diazinon and diuron. *Aquat. Toxicol.* 193, 187-200.
79. Vieira, L.R., Sousa, A., Frasco, M.F., Lima, I., Morgado, F., Guilhermino, L., 2008. Acute effects of Benzo[a]pyrene, anthracene and a fuel oil on biomarkers of the common goby *Pomatoschistus microps* (Teleostei, Gobiidae). *Sci. Total Environ.* 395, 87-100.
80. Wang, F., Haftka, J.J.-H., Sinnige, T.L., Hermens, J.L.M., Chen, W., 2014. Adsorption of polar, nonpolar, and substituted aromatics to colloidal graphene oxide nanoparticles. *Environ. Pollut.* 186, 226-233.
81. Wang, F., Jia, Z., Su, W., Shang, Y., Wang, Z.-L., 2019. Adsorption of phenanthrene and 1-naphthol to graphene oxide and L-ascorbic-acid-reduced graphene oxide: effects of pH and surfactants. *Environ. Sci. Pollut. Res.* 26, 11062-11073.
82. Wang, H., Xia, X., Liu, R., Wang, Z., Lin, X., Muir, D.C.G., Wang, W., 2020. Multicompartmental toxicokinetic modeling of discrete dietary and continuous waterborne uptake of two polycyclic aromatic hydrocarbons by zebrafish *Danio rerio*. *Environ. Sci. Technol.* 54, 1054-1065.
83. Wang, J., Chen, B., 2015. Adsorption and coadsorption of organic pollutants and a heavy metal by graphene oxide and reduced graphene materials. *Chem. Eng. J.* 281, 379-388.
84. Wang, J., Chen, Z., Chen, B., 2014. Adsorption of polycyclic aromatic hydrocarbons by graphene and graphene oxide nanosheets. *Environ. Sci. Technol.* 48, 4817-4825.
85. Wang, Y., Li, Z., Wang, J., Li, J., Lin, Y., 2011. Graphene and graphene oxide: biofunctionalization and applications in biotechnology. *Trends Biotechnol.* 29, 205-212.
86. Wu, W., Jiang, W., Zhang, W., Lin, D., Yang, K., 2013. Influence of functional groups on desorption of organic compounds from carbon nanotubes into water: insight into desorption hysteresis. *Environ. Sci. Technol.* 47, 8373-8382.
87. Yan, H., Wu, H., Li, K., Wang, Y., Tao, X., Yang, H., Li, A., Cheng, R., 2015 Influence of the surface structure of graphene oxide on the adsorption of aromatic organic compounds from water. *Appl. Mater. Interfaces* 7, 6690-6697.

Results and discussion

88. Yan, J., Chen, L., Huang, C., Lung, S.C., Yang, L., Wang, W., Lin, P., Suo, G., Lin, C., 2017. Consecutive evaluation of graphene oxide and reduced graphene oxide nanoplatelets immunotoxicity on monocytes. *Colloids Surf. B: Biointerfaces* 153, 300-309.
89. Yang, J., Zhong, W., Chen, P., Zhang, Y., Sun, B., Liu, M., Zhu, Y., Zhu, L., 2019a. Graphene oxide mitigates endocrine disruption effects of bisphenol A on zebrafish at an early development stage. *Sci. Total Environ.* 697, 134158.
90. Yang, Z., Yang, Q., Zheng, G., Han, S., Zhao, F., Hu, Q., Fu, Z., 2019b. Developmental neurotoxicity and immunotoxicity induced by graphene oxide in zebrafish embryos. *Environ. Toxicol.* 34, 415-423.
91. Yang, K., Wang, X., Zhu, L., Xing, B., 2006. Competitive sorption of pyrene, phenanthrene, and naphthalene on multiwalled carbon nanotubes. *Environ. Sci. Technol.* 40, 5804–5810.
92. Yang, K., Xing, B., 2007. Desorption of polycyclic aromatic hydrocarbons from carbon nanomaterials in water. *Environ. Pollut.* 145, 529-537.
93. Zhai, Y., Xia, X., Wang, H., Lin, H., 2020. Effect of suspended particles with different grain sizes on the bioaccumulation of PAHs by zebrafish (*Danio rerio*). *Chemosphere* 242, 125299.
94. Zhang, J.-H., Sun, T., Niu, A., Tang, Y.-M., Deng, S., Luo, W., Xu, Q., Wei, D., Pei, D.-S., 2017a. Perturbation effect of reduced graphene oxide quantum dots (rGOQDs) on aryl hydrocarbon receptor (AhR) pathway in zebrafish. *Biomaterials* 133, 49-59.
95. Zhang, J., Shen, G., Wang, W., Zhou, X., Guo, S., 2010. Individual nanocomposite sheets of chemically reduced graphene oxide and poly(N-vinyl pyrrolidone): preparation and humidity sensing characteristics. *J. Mater. Chem.* 20, 10824.
96. Zhang, X., Zhou, Q., Zou, W., Hu, X., 2017b. Molecular mechanisms of developmental toxicity induced by graphene oxide at predicted environmental concentrations. *Environ. Sci. Technol.* 51, 7861-7871.
97. Zhang, Y., Chi, H., Zhang, W., Sun, Y., Liang, Q., Gu, Y., Jing, R., 2014. Highly efficient adsorption of copper ions by a PVP-reduced graphene oxide based on a new adsorptions mechanism. *Nano-Micro Let.* 6.
98. Zhao, Y., Luo, K., Fan, Z., Huang, C., Hu, J., 2013. Modulation of benzo[a]pyrene-induced toxic effects in japanese medaka (*Oryzias latipes*) by 2,2',4,4'-tetrabromodiphenyl ether. *Environ. Sci. Technol.* 47, 13068–13076.
99. Zhao, J., Wang, Z., Zhao, Q., Xing, B., 2014. Adsorption of phenanthrene on multilayer graphene as affected by surfactant and exfoliation. *Environ. Sci. Technol.* 48, 331-339.
100. Zhu, S., Luo, F., Chen, W., Zhu, B., Wang, G., 2017. Toxicity evaluation of graphene oxide on cysts and three larval stages of *Artemia salina*. *Sci. Total Environ.* 595, 101-109.
101. Zou, W., Zhou, Q., Zhang, X., Mu, L., Hu, X., 2018. Characterization of the effects of trace concentrations of graphene oxide on zebrafish larvae through proteomic and standard methods. *Ecotoxicol. Environ. Saf.* 159, 221-231.

SUPPORTING INFORMATION

Spectrophotometrical measurement of graphene oxide (GO) concentration. GO concentration was spectrophotometrically estimated based on an absorption peak at 230 nm. This wavelength is assigned to the representative $\pi-\pi^*$ transitions of the aromatic C=C bonds.

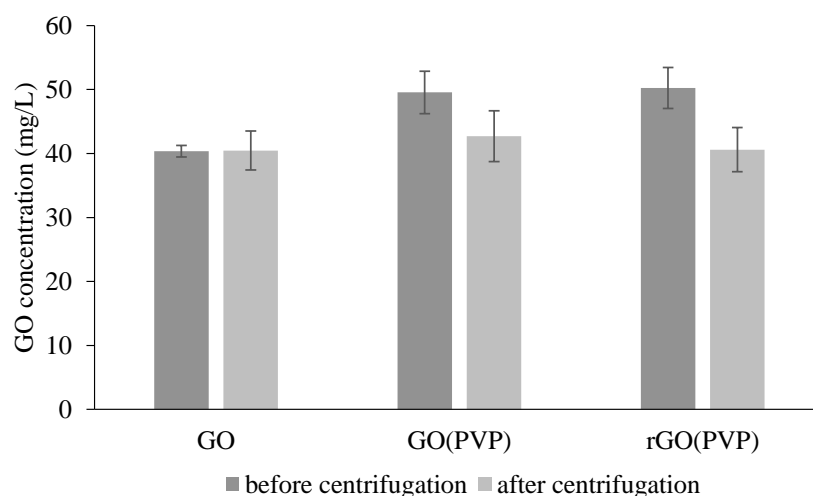


Fig. S1- GO measured by UV/vis spectrophotometry before and after centrifugation using a microplate reader (Thermo Scientific Multiskan Spectrum, Thermo Fisher Scientific Oy, Vantaa, Finland) at 230 nm. A concentration of 50 mg/L in 10 mL MilliQ water was prepared for the three different graphene NMs and, then, centrifuged at 9509 g for 30 min. The supernatant was removed and the pellet was resuspended in the same volume.

Gas chromatography/mass spectrometry (GC/MS) instrumentation, quality assurance and quality control. A GC/MS system (Agilent 7890A/ Agilent MSD-5795C, Agilent Technologies, California, USA) operated with an energy of ionization of 70 eV in ionisation mode par electronic impact equipped with an HP5MS-UI column (5% phenyl methylpolysiloxane; 30 m x 0.25 mm i.d.; 0.25 μ m sorbent, Agilent Technologies) was used to analyse the selected PAHs. Injection in GC/MS system was made with the inlet temperature at 280 °C in the pulsed splitless mode: a pulse pressure of 25 psi was maintained for 1.5 min, the purge flow to split vent was 60 mL/min after 1.5 min. The injection volume was 1 μ L with a helium (purity 6.0) constant flow rate of 1.3 mL/min. The column temperature was initially held at 50 °C for 2 min, and was then increased to 250 °C at 10 °C/min for 1 min, to 280 °C for 2 min and to 310 °C at 10 °C/min, where it was held for 3 min. Compound determination was operated in the selected ion monitoring (SIM). The selected 18 PAHs were determined by isotope dilution (naphthalene d_8 , acenaphthylene d_{10} , acenaphthene d_{10} , fluorene d_{10} , anthracene d_{10} , phenanthrene d_{10} , fluoranthene d_{10} , pyrene d_{10} , benzo(a)anthracene d_{12} , chrysene d_{12} , benzo(e)pyrene d_{12} , perylene d_{12} , benzo(b)fluoranthene d_{12} , benzo(k)fluoranthene d_{12} , indeno(1,2,3-cd)pyrene d_{12} , benzo(ghi)perylene d_{12} and dibenz(a,h)anthracene d_{14}). All the precautions were taken to prevent contamination from personnel, reagents and materials. Blanks were run in parallel for each batch of experiments in order to monitor the background contamination. Recovery values of deuterated standards were

Results and discussion

good for the 18 PAHs with values ranging from 84.68% to 108.84% (mean recovery = 95.76%) (**Table S1**). Accuracy of the method was determined by extracting water samples spiked with 10 ng/L of each deuterated PAH. Method limit of quantification (MLOQ) was determined by extracting spiked water samples. Signal to noise ratio (S/N) was determined by peak to peak method and MLOQ were calculated for S/N=9. The 18 PAHs showed a MLOQ in MilliQ water similar than in conditioned water with a MLOQ up to 9.04 ng/L (mean MLOQ = 5.41 ± 2.16 ng/L). Percentage of PAH recovery in control samples after the procedure employed to sorb PAHs to graphene NMs is detailed in **Table S2**. Resulting values were used as initial concentration for the sorption models. Similar precautions and controls were run for the PAH bioaccumulation analysis. Recovery values of deuterated standards were good for the 18 PAHs with values ranging from 59% to 98% (mean recovery = 85%) (**Table S3**). Accuracy of the method was determined by extracting mussel tissue spiked with each deuterated PAH. Method limit of quantification (MLOQ) was determined by extracting spiked mussel tissue. Signal to noise ratio (S/N) was determined by peak to peak method and MLOQ were calculated for S/N=9. The 18 PAHs showed a MLOQ up to 10 ng/L in mussel tissue (mean MLOQ = 2.3 ± 2.9 ng/L).

Table S1- Control chart with response factor and % of efficiency for SPME analysis. Values are represented as means \pm S.D. of three replicates.

Compound	K_i/K_e	%
Naphthalene/naphthalene d ₈	0.67 \pm 0.02	100.57 \pm 27.60
Acenaphthylene/acenaphthylene d ₈	0.82 \pm 0.15	108.84 \pm 20.65
Acenaphthene/acenaphthene d ₁₀	0.85 \pm 0.13	101.53 \pm 15.90
Fluorene/fluorene d ₁₀	0.69 \pm 0.12	101.95 \pm 8.91
Anthracene/anthracene d ₁₀	0.86 \pm 0.12	84.68 \pm 13.08
Phenanthrene/phenanthrene d ₁₀	0.87 \pm 0.17	103.05 \pm 876
Fluoranthene/fluoranthene d ₁₀	0.89 \pm 0.16	97.3 \pm 1.3
Pyrene/pyrene d ₁₀	0.80 \pm 0.13	96.68 \pm 0.85
Benz(a)anthracene/benz(a)anthracene d ₁₂	0.82 \pm 0.12	86.68 \pm 15.00
Chrysene/chrysene d ₁₂	0.85 \pm 0.13	87.09 \pm 11.94
Benzo(e)pyrene/benzo(e)pyrene d ₁₂	0.81 \pm 0.04	93.29 \pm 0.73
Benzo(a)pyrene/benzo(a)pyrene d ₁₂	0.75 \pm 0.09	106.05 \pm 14.15
Perylene/perylene d ₁₂	0.81 \pm 0.04	93.05 \pm 1.21
Benzo(b)fluoranthene/benzo(b)fluoranthene d ₁₂	0.76 \pm 0.06	91.82 \pm 2.52
Benzo(k)fluoranthene/benzo(k)fluoranthene d ₁₂	0.86 \pm 0.07	89.58 \pm 0.2
Indeno(1,2,3-cd)pyrene/indeno(1,2,3-cd)pyrene d ₁₂	0.77 \pm 0.01	92.01 \pm 12.8
Benzo(ghi)perylene/benzo(ghi)perylene d ₁₂	0.79 \pm 0.03	91.18 \pm 5.88
Dibenz(a,h)anthracene/dibenz(a,h)anthracene d ₁₄	0.79 \pm 0.03	91.96 \pm 3.7

SPME: solid phase micro extraction; K_i/K_e : response factor.

Results and discussion

Table S2- Percentage of PAH recovery in control samples after centrifugation to separate GO NMs from the aqueous phase during sorption experiments. In the case of the WAF PAHs, recovery values in the control samples were calculated in relation to PAH concentrations measured in the WAF samples shown in Table S3.

Nominal B(a)P concentration (µg/L)	1	10	100
Measured initial B(a)P concentration in GO experiment (µg/L)	0.69	6.21	118.5
B(a)P recovery (%) from initial concentration in GO experiment	45.26	69.79	76.91
Measured initial B(a)P concentration in GO(PVP) experiment (µg/L)	0.81	7.11	149.8
B(a)P recovery (%) from initial concentration in GO(PVP) experiment	55.77	69.85	77.48
WAF (%)	6.5	25	100
Naphthalene	95.43	104.74	108.74
Acenaphthylene	n.d.	n.d.	n.d.
Acenaphthene	119.73	150.55	126.34
Fluorene	96.50	101.13	94.82
Anthracene	<L.Q.	54.25	120.77
Phenanthrene	88.76	95.35	90.16
Fluoranthene	<L.Q.	<L.Q.	67.72
Pyrene	<L.Q.	<L.Q.	67.28
Benz(a)anthracene	n.d.	n.d.	n.d.
Chrysene	n.d.	n.d.	n.d.
Benzo(e)pyrene	n.d.	n.d.	n.d.
B(a)P	n.d.	n.d.	n.d.
Perylene	n.d.	n.d.	n.d.
Benzo(b)fluoranthene	n.d.	n.d.	n.d.
Benzo(k)fluoranthene	n.d.	n.d.	n.d.
Indeno(1,2,3-cd)pyrene	n.d.	n.d.	n.d.
Benzo(ghi)perylene	n.d.	n.d.	n.d.
Dibenz(a,h)anthracene	n.d.	n.d.	n.d.

L.Q.: limit of quantification; n.d.: not detected.

Table S3- Recovery (%) of surrogate internal standards obtained for the PAH bioaccumulation analysis in adult zebrafish.

Internal standard	Syringe perdeuterated	Mean (%)	S.D. (%)
Naphthalene d ₈	Pyrene d ₁₀	59	8
Acenaphthylene d ₈	Pyrene d ₁₀	91	5
Acenaphthene d ₁₀	Pyrene d ₁₀	94	6
Fluorene d ₁₀	Pyrene d ₁₀	94	4
Phenanthrene d ₁₀	Pyrene d ₁₀	96	4
Anthracene d ₁₀	Pyrene d ₁₀	97	4
Fluoranthene d ₁₀	Pyrene d ₁₀	98	5
Benzo(a)anthracene d ₁₂	Benzo(b)fluoranthene d ₁₂	89	11
Chrysene d ₁₂	Benzo(b)fluoranthene d ₁₂	70	5
Benzo(k)fluoranthene d ₁₂	Benzo(b)fluoranthene d ₁₂	76	6
Benzo(e)pyrene d ₁₂	Benzo(b)fluoranthene d ₁₂	92	6
Benzo(a)pyrene d ₁₂	Benzo(b)fluoranthene d ₁₂	87	7
Indeno(1,2,3 -c,d)pyrene d ₁₂	Benzo(b)fluoranthene d ₁₂	80	5
Dibenzo(a,h)anthracene d ₁₄	Benzo(b)fluoranthene d ₁₂	81	6
Benzo(g,h,i)perylene d ₁₂	Benzo(b)fluoranthene d ₁₂	74	6

Results and discussion

Table S4- Concentration of PAHs (ng/L) measured in the three dilutions of the WAF of the naphthenic North Sea crude oil used for sorption experiments. Values are represented as means \pm S.D of three replicates. Concentration of acenaphthylene, benzo(e)pyrene, benzo(a)pyrene, perylene, benzo(b)fluoranthene, benzo(k)fluoranthene, indeno(1,2,3-cd)pyrene, benzo(ghi)perylene and dibenz(a,h)anthracene in the three dilutions were not detected.

	MW	WAF dilution			L.Q.
		6.25%	25%	100%	
Naphthalene	128	12,965.2 \pm 1,228.8	29,953.9 \pm 367.7	163,244.5 \pm 1,961.3	7.5
Acenaphthene	154	57.6 \pm 0.1	196.9 \pm 5.3	951.2 \pm 13.6	5.3
Fluorene	166	194.7 \pm 6.5	840.2 \pm 25.7	3,779.4 \pm 67.6	7.5
Anthracene	178	n.d.	28.8 \pm 0.5	119.1 \pm 2.12	7
Phenanthrene	178	177.1 \pm 3.1	658.2 \pm 9.8	2,874.3 \pm 27.3	4.3
Fluoranthene	202	<L.Q.	9.4 \pm 5.3	42.7 \pm 1.5	4.8
Pyrene	202	<L.Q.	7 \pm 0.2	33 \pm 1.2	5
Benz(a)anthracene	228	<L.Q.	<L.Q.	<L.Q.	6
Chrysene	228	<L.Q.	<L.Q.	15.1 \pm 0.4	6
Total PAHs (Σ PAHs)		13,394.5	31,694.6	171,059.5	

MW: molecular weight (g/mol); L.Q.: limit of quantification; n.d.: not detected.

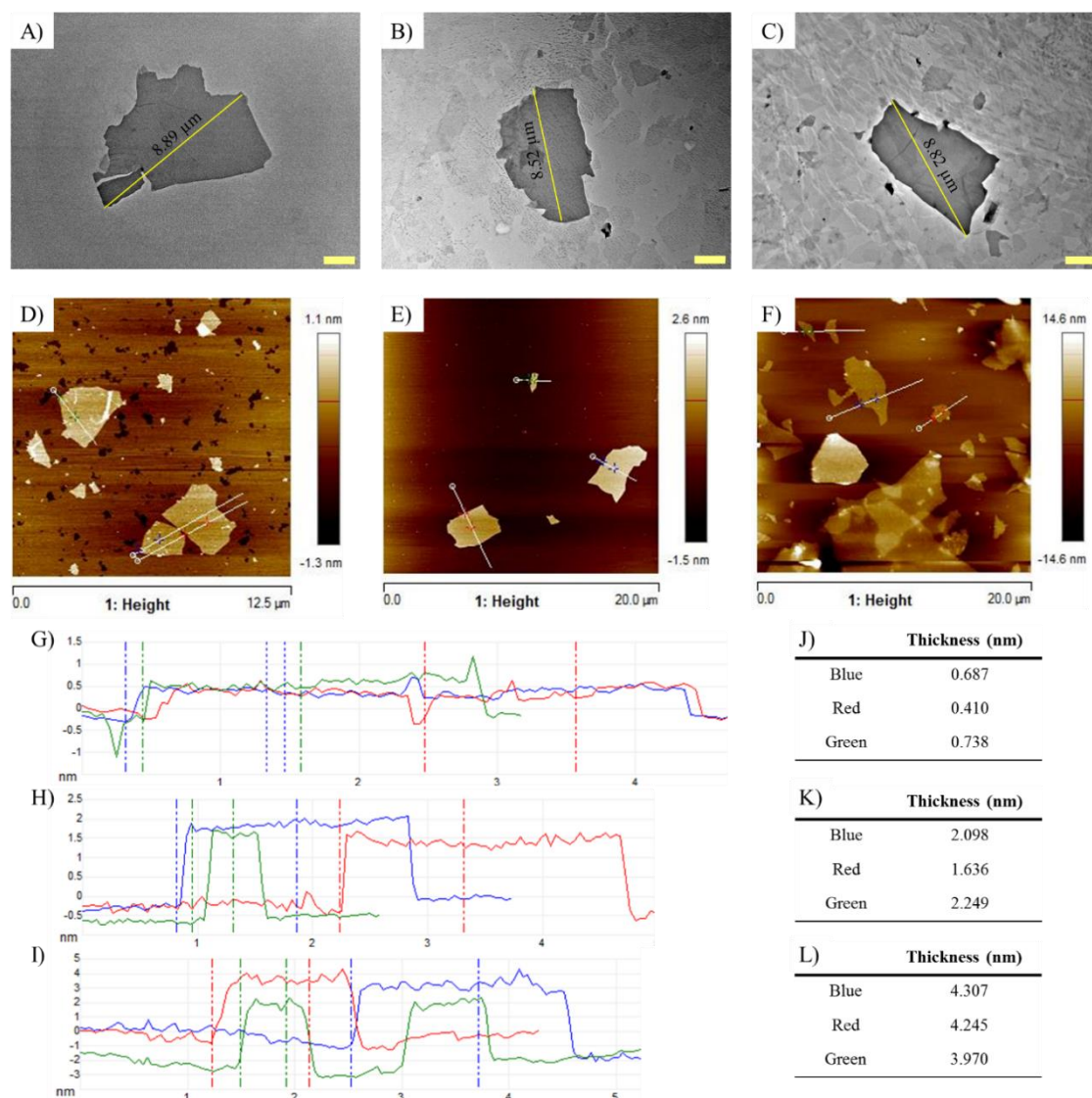


Fig. S2- TEM micrographs of individual platelets of A) GO, B) GO(PVP) and C) rGO(PVP). Yellow line: maximum length of each platelet. AFM micrographs of D) GO, E) GO(PVP) and F) rGO(PVP). Height profile of G) GO, H) GO(PVP) and I) rGO(PVP) obtained from AFM micrographs. Maximum thickness of the platelets of J) GO, K) GO(PVP) and L) rGO(PVP). Scale bars for TEM micrographs: 2 μm .

Results and discussion

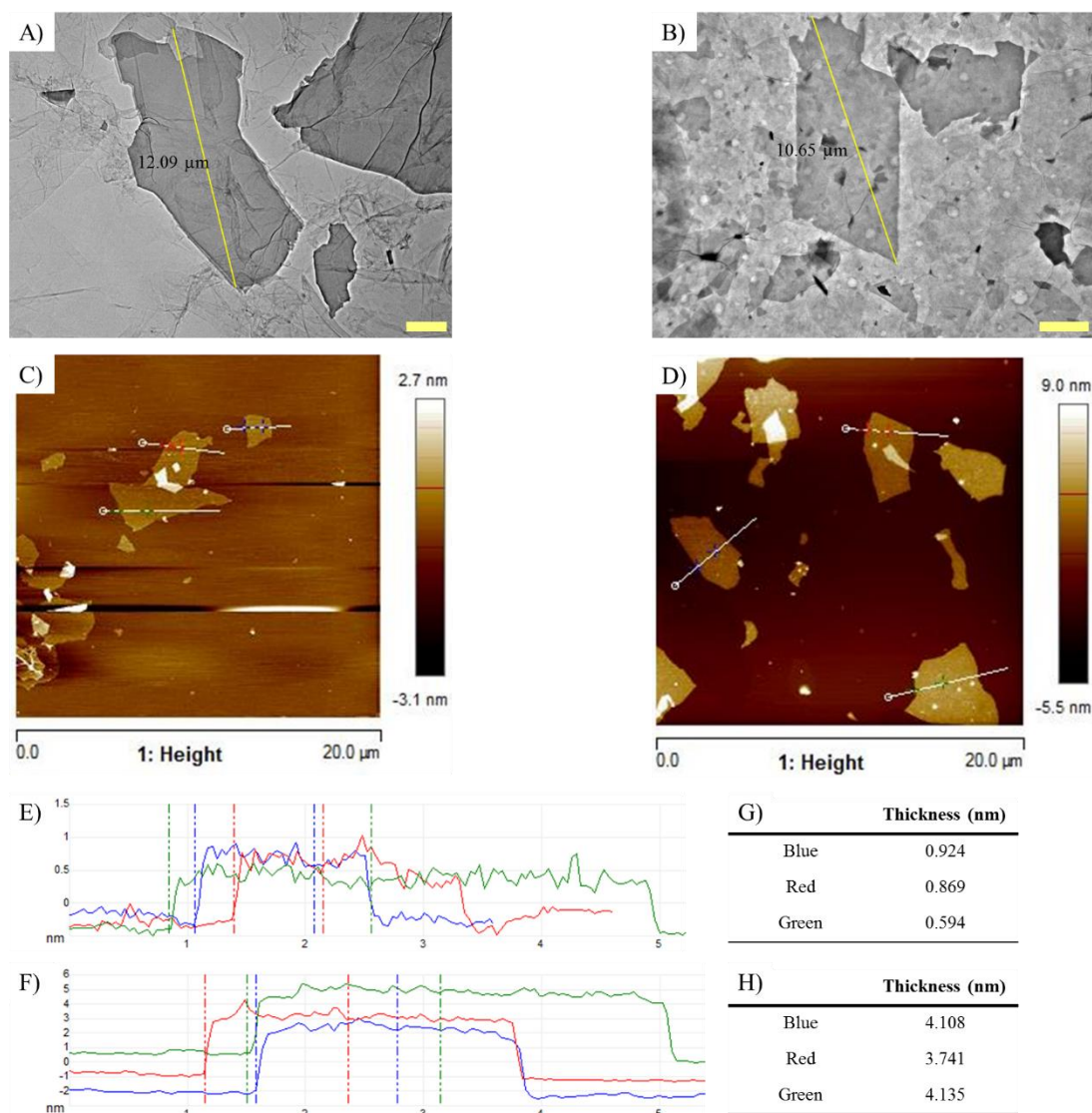


Fig. S3- TEM micrographs of individual platelets of A) GO-B(a)P and B) GO(PVP)-B(a)P. Yellow line: maximum length of each platelet. AFM micrographs of C) GO-B(a)P and D) GO(PVP)-B(a)P. Height profile of E) GO-B(a)P and F) GO(PVP)-B(a)P obtained from AFM micrographs. Maximum thickness of the platelets of G) GO-B(a)P and H) GO(PVP)-B(a)P. Scale bars for TEM micrographs: 2 μm .

Table S5. Odd ratio values indicating the risk of malformation in 120 hpf zebrafish embryos depending on the exposure treatment. Data are shown only for the cases indicated as significant in **Table 2**.

Treatment test	Treatment for comparison	Concentration (mg/L)	Odd ratio	Confidence interval (5%, 95%)		P value
GO	Control	5	1.38*	1.037	1.829	0.018
		10	1.168*	1.013	1.345	0.022
rGO(PVP)	Control	10	1.199*	1.018	1.414	0.015
GO-B(a)P	Control	5	1.350*	1.012	1.802	0.031
		0.5	407.69*	4.89	7.17 10 ⁶	0.004
GO(PVP)-B(a)P	Control	5	1.654*	1.044	4.411	0.029
		10	1.400*	1.127	2.280	0.000

Results and discussion

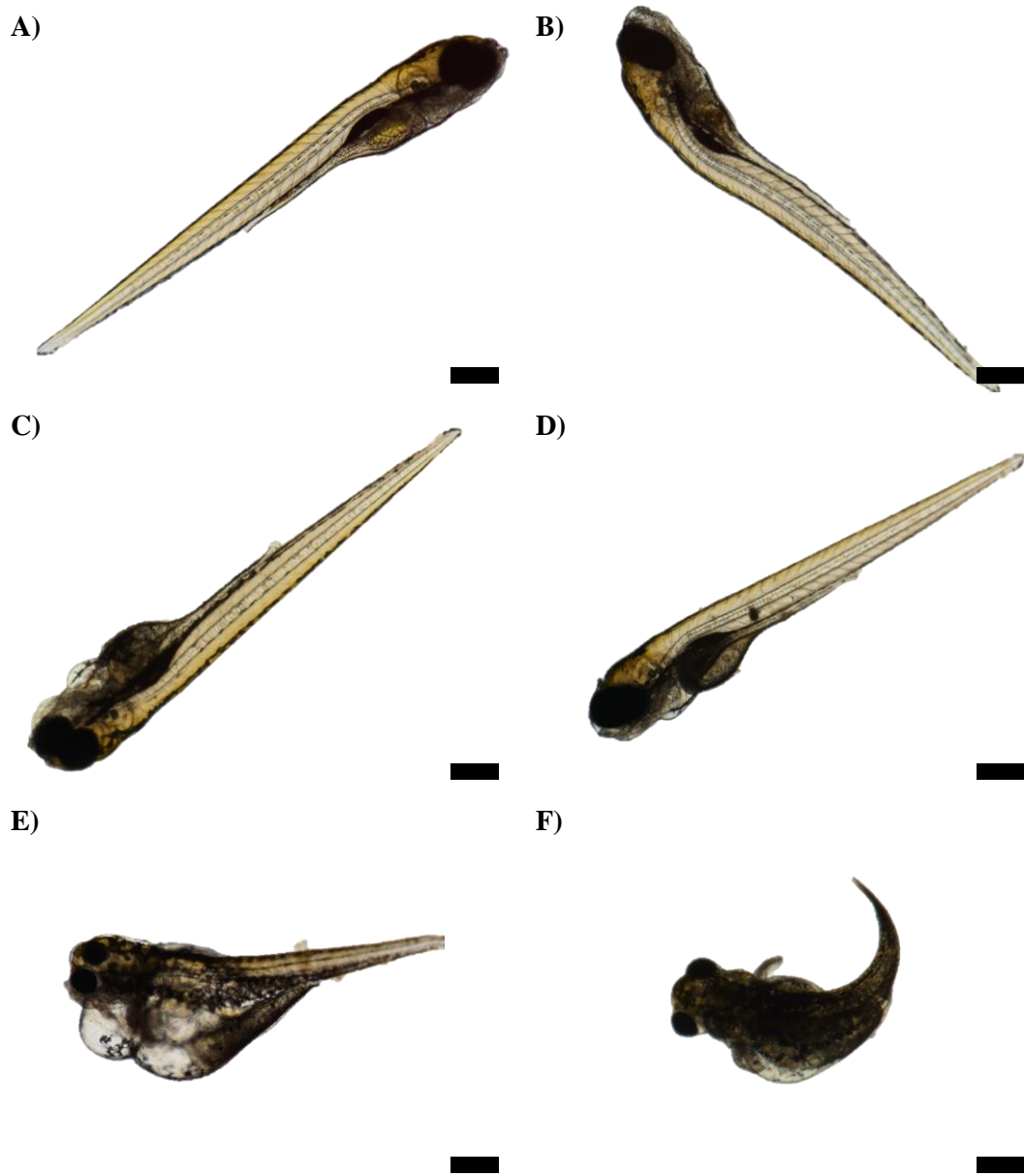


Fig. S4- Micrographs of zebrafish embryos at 120 hpf. A) Unexposed control embryo showing normal morphology; B) embryo exposed to 0.5 mg/L of GO(PVP)-B(a)P showing spinal cord flexure; C) embryo exposed to 5 mg/L of rGO(PVP) showing pericardial edema; D) embryo exposed to 10 mg/L of GO-B(a)P showing pericardial edema; E) embryo exposed to 5 mg/L of GO showing multiple malformations, such as pericardial edema, yolk sac edema and eye abnormality; F) embryo exposed to 0.5 mg/L of GO(PVP) showing spinal cord flexure, pericardial edema and yolk sac edema. Scale bars: 100 μ m.

Table S6- EC₁₀ and EC₅₀ values of malformation occurrence obtained for the different exposure treatments. Values are represented by mean ± S.E.

	EC ₁₀ (mg/L)	EC ₅₀ (mg/L)
GO	-	14.67±4.03 (6.61 – 22.73)
GO(PVP)	-	30.98±26.7 (-22.47 – 84.44)
rGO(PVP)	3.03±1.37 (0.29 – 5.76)	14.52±3.12 (8.27 – 20.76)
GO+WAF	0.39±2.11 (-3.82 – 4.62)	16.07±4.98 (6.12 – 26.04)
GO-B(a)P	4.08±1.99 (0.09 – 8.08)	20.57±8.03 (4.51 – 36.62)
GO(PVP)-B(a)P	3.14±1.43 (0.29 – 5.99)	15.11±3.51 (8.07 – 22.13)

-: values could not be calculated by the Probit model.

Results and discussion

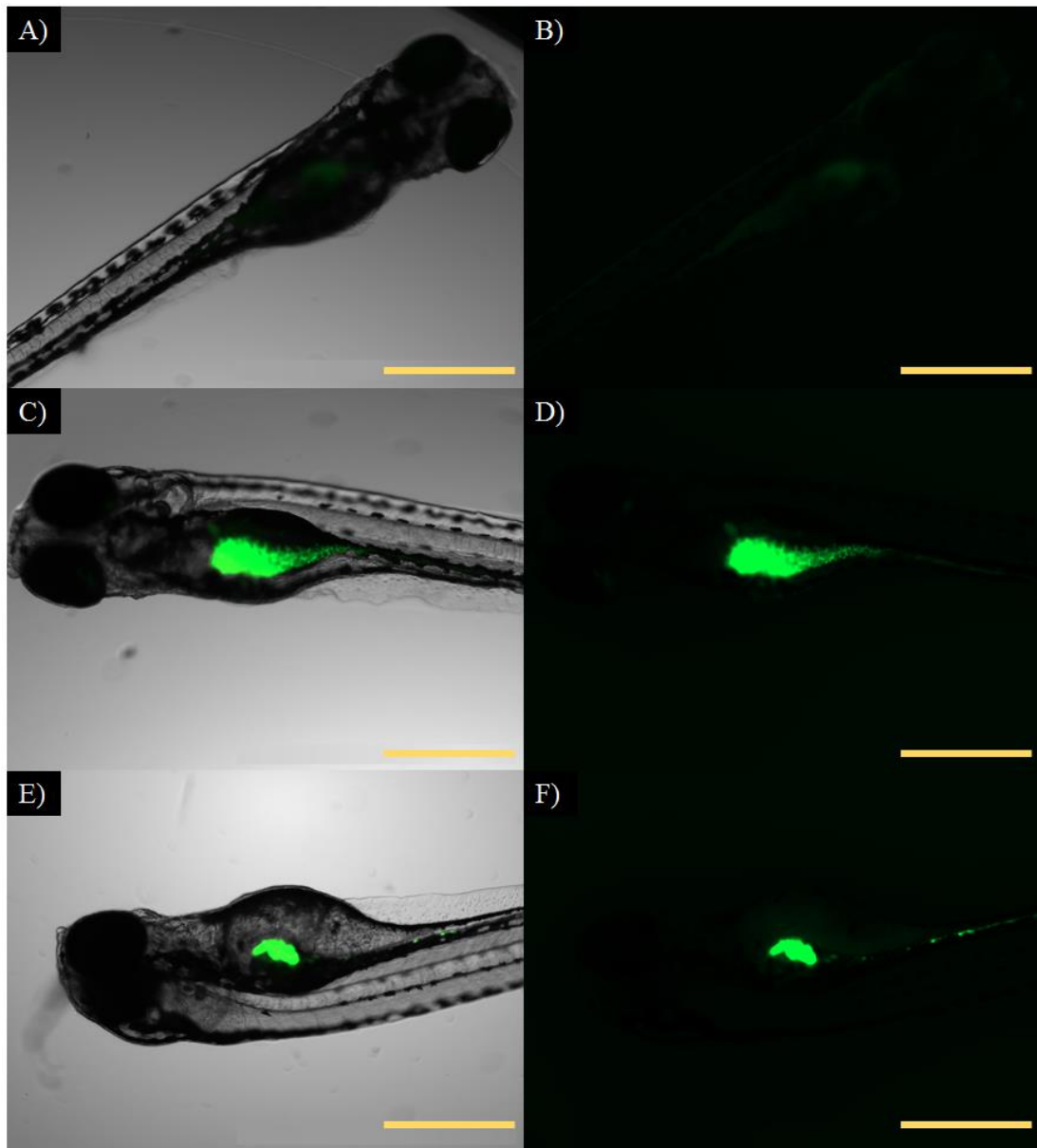


Fig. S5- Micrographs of 120 hpf zebrafish embryos. A-B) unexposed control embryo; C-D) embryo exposed to 1 mg/L of FI-rGO; E-F) embryo exposed to 10 mg/L of FI-rGO. Scale bars: 500 μm .

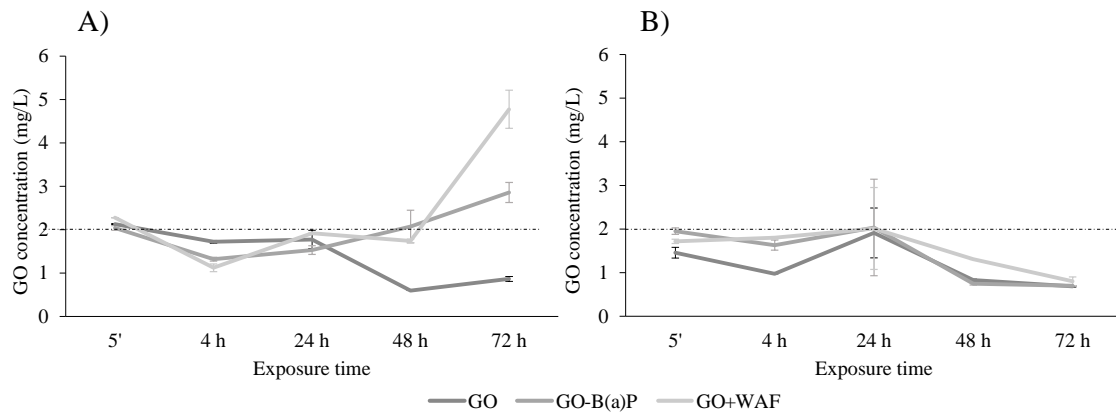


Fig. S6- Measured GO concentration in exposure tanks along the 3 days cycle for the A) 3rd dose and B) 7th dose. Straight lines show the nominal GO concentration added to the exposure tanks.

Results and discussion

Table S7- PAH concentration (ng/L) in water samples along the three first days of exposure. Values are shown as mean±S.D.

PAH	Control					
	5'	4 h	8 h	24 h	48 h	72 h
Naphthalene	5.2±0.9	7.7±1.1	8.5±0.5	5.4±0.2	<L.Q.	<L.Q.
Acenaphthene	<L.Q.	<L.Q.	<L.Q.	<L.Q.	<L.Q.	<L.Q.
Fluorene	0.8± 0.2	0.8± 0.04	0.6± 0.05	0.6± 0.04	0.7± 0.05	0.6± 0.04
Phenanthrene	2.0± 0.4	2.0± 0.1	1.8± 0.05	1.7± 0.1	1.6± 0.06	1.7± 0.14
Anthracene	<L.Q.	<L.Q.	<L.Q.	<L.Q.	<L.Q.	<L.Q.
Benzo(a)pyrene	<L.Q.	<L.Q.	<L.Q.	<L.Q.	<L.Q.	<L.Q.
ΣPAHs	8.0	10.5	10.9	7.7	2.3	2.3

	GO+WAF					
	5'	4 h	8 h	24 h	48 h	72 h
Naphthalene	7,788.9 ± 491.9	5,558.6± 505.1	4,730.9± 122.1	1,742.9± 103.8	246.0± 5.8	34.9± 3.4
Acenaphthene	44.2 ± 1.1	33.3± 1.4	31.7± 3.8	18.0± 6.2	12.2± 0.9	10.6± 3.2
Fluorene	127.3 ± 7.3	97.7± 6.9	80.17± 3.8	32.6± 0.6	12.6± 0.9	5.5± 0.7
Phenanthrene	69.3 ± 6.50	64.7± 6.4	54.5± 3.3	24.7± 0.4	13.5± 2.1	8.2± 2.7
Anthracene	14.4 ± 1.5	13.5± 2.5	10.8± 0.97	4.7± 0.3	2.8± 0.7	1.9± 0.9
Benzo(a)pyrene	<L.Q.	<L.Q.	<L.Q.	<L.Q.	<L.Q.	<L.Q.
ΣPAHs	8,044.1	5,767.8	4,907.9	1,822.9	287.1	61.1

	GO-B(a)P					
	5'	4 h	8 h	24 h	48 h	72 h
Benzo(a)pyrene	1,743.2± 117.3	2,054.3± 213.6	1,548.8± 255.9	1,388.6± 186.5	964.9± 98.7	1,293.2± 309.2

	B(a)P					
	5'	4 h	8 h	24 h	48 h	72 h
Benzo(a)pyrene	29,440.3± 4,582.1	32,980.5± 10,154.4	34,682.5± 4,147	24,414.7± 5,015.8	16,138.3± 2,882.2	7,956.7± 1,723.1

L.Q.: limit of quantification.

Table S8. Prevalence (%) of histopathological alterations in liver of zebrafish. Asterisks indicate statistically significant differences ($p < 0.05$) according to the Fisher's exact test compared to the control group at the same sampling time.

		n	Vacuolisation	Megalocytosis	Total
Control	3 d	9	11.1	n.o.	11.1
	21 d	10	n.o.	n.o.	0
GO	3 d	10	40	n.o.	40
	21 d	9	22.2	n.o.	22.2
GO+WAF	3 d	10	60*	n.o.	60*
	21 d	10	50*	10	50*
GO-B(a)P	3 d	10	50	n.o.	50
	21 d	10	30	n.o.	30
B(a)P	3 d	10	20	n.o.	20
	21 d	10	30	10	40

n: number of individuals per experimental group (in some cases $n < 10$ because the tissue was not always present in the histological sections used for the histological analysis); n.o.: not observed

Table S9- Prevalence (%) of histopathological alterations in gills of zebrafish.

		n	Secondary lamellae		Primary lamellae	Total
			Inflammation	Aneurism	Hyperplasia	
Control	3 d	8	12.5	12.5	n.o.	25
	21 d	10	n.o.	10	n.o.	10
GO	3 d	10	10	n.o.	n.o.	10
	21 d	10	n.o.	20	n.o.	20
GO+WAF	3 d	9	11.1	n.o.	n.o.	11.1
	21 d	9	n.o.	n.o.	11.1	11.1
GO-B(a)P	3 d	9	11.1	11.1	n.o.	22.2
	21 d	10	n.o.	20	n.o.	20
B(a)P	3 d	9	n.o.	11.1	n.o.	11.1
	21 d	9	n.o.	33.3	n.o.	33.3

n: number of individuals per experimental group (in some cases $n < 10$ because the gill tissue was not always present in the histological sections used for the histological analysis); n.o.: not observed.

GENERAL DISCUSSION

ABBREVIATIONS

B(a)P, Benzo(a)pyrene

EC₅₀, Effective concentration 50

GNMs, Graphene family nanomaterials

GO, Graphene oxide

LC₅₀, Lethal concentration 50

MPs, Microplastics

NMs, Nanomaterials

NPs, Nanoplastics

PAHs, Polycyclic aromatic hydrocarbons

POPs, Persistent organic pollutants

PVP, Poly N-vinyl-2-pyrrolidone

rGO, Reduced graphene oxide

WAF, Water accommodated fraction

Engineered materials in micro and nano scale have been incorporated into a wide range of products (personal and health care, electronics, packaging...) (Bandala and Berli, 2019). Among these materials, those made of carbon displayed several new characteristics that allowed new applications due to the carbon properties (resistant, easily to handle and versatile). The most used in the industry worldwide is plastic, which is a main concern in aquatic pollution due to its occurrence in the ecosystems. Plastic in micro (microplastics, MPs, $5 < \mu\text{m}$) and nano (nanoplastics, NPs, 100 nm) size is being manufactured and incorporated into consumer products (microbeads from personal care products) but they are also produced accidentally by the use or degradation of larger plastics upon arrival to the ecosystems (Picó and Barceló, 2019). One of the outstanding carbon-based nanomaterial is graphene which, due to its unusual properties, is being incorporated in many new applications (electronics, desalination, remediation of water pollution, cancer treatments). Graphene is the base of other graphene based NMs (GNMs), such as graphene oxide (GO) and reduced graphene oxide (rGO), and consists of a single layer of carbon atoms arranged in a two-dimensional honeycomb lattice (Chen et al., 2012).

MPs are materials already present in the environment with alarming concentrations in aquatic ecosystems (Li et al., 2018). The entrance of NPs (Koelmans et al., 2015) and GNMs is not yet quantified, but they are expected to reach the aquatic ecosystems due to their current applications and predicted increase in their corresponding market and future uses (Kong et al., 2019). In the aquatic ecosystems, MPs/NPs and GNMs undergo different process that change their fate (**Fig. 1**). Their availability for a wide range of organisms and capacity to cross biological barriers due to their small size are the main characteristics ruling their potential toxicity (Vijver et al., 2018; Ribeiro et al., 2019). Moreover, once MPs/NPs and GNMs arrive to the aquatic ecosystems they could act as vectors of hydrophobic organic pollutants (specially polycyclic aromatic hydrocarbons, PAHs) due to their surface characteristics (Koelmans et al., 2016; Liu et al., 2018; Shen et al., 2019). MPs/NPs and GNMs can alter the bioavailability of hydrophobic organic pollutants and modulate their toxicity for aquatic organisms (Ziccardi et al., 2016).

In the present PhD thesis two organisms were used, a small invertebrate (brine shrimp, *Artemia salina*) and a vertebrate model (zebrafish, *Danio rerio*), in order to assess the potential effects of the exposure to polystyrene (PS) NPs, and to MPs and GNMs alone and in combination with PAHs. In addition, the sorption capacity of these materials for an individual pyrogenic PAH, benzo(a)pyrene (B(a)P), and for a complex mixture of PAHs from the water accommodated fraction (WAF) of a naphthenic North Sea crude oil was investigated.

General discussion

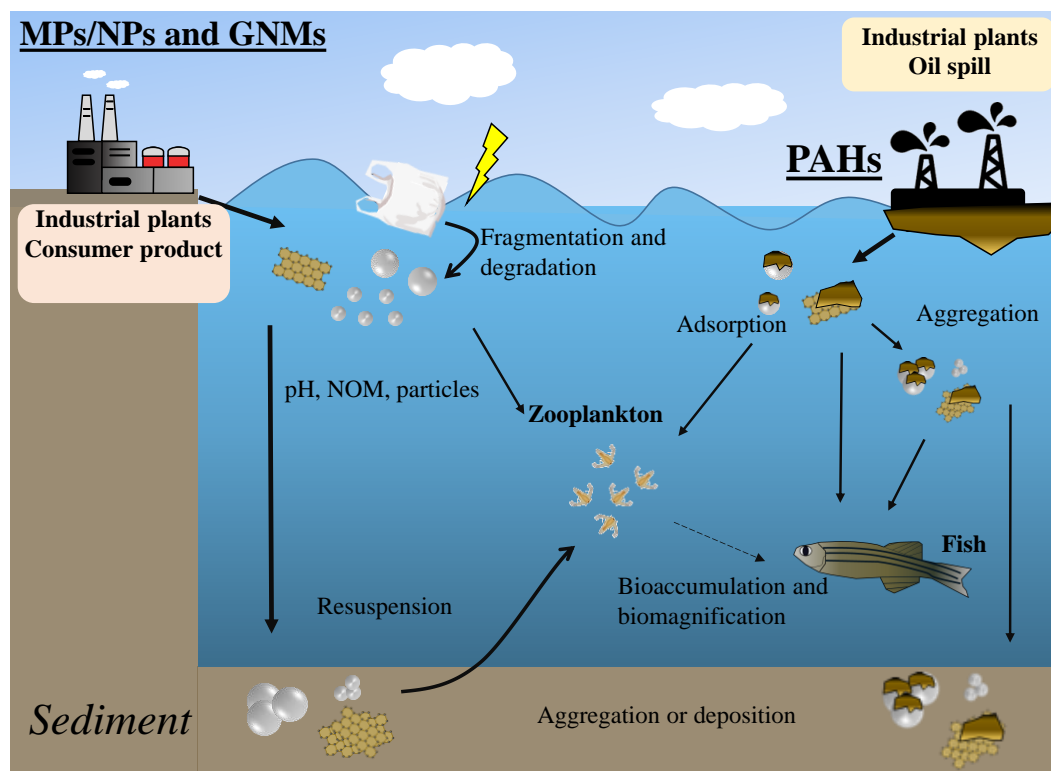


Fig. 1- Fate of MPs/NPs and GNMs alone or with PAHs in the aquatic environment (based on Yu et al. (2019) and He et al. (2017)).

MPs/NPs are reported as non-acutely toxic materials, but they exert some sublethal effects in aquatic organisms, such as oxidative stress, neurotoxicity, inflammation, feeding and growth reduction (Franzellitti et al., 2019; Shen et al., 2019; Bhagat et al., 2020). According to the results obtained in **Chapter 1**, the two PS MP sizes tested (4.5 and 0.5 μm) and the NPs (50 nm) in a wide range of concentrations (0.000069 to 50.1 mg/L) did not cause acute toxic effects in brine shrimp larvae and zebrafish embryos. Given the size of both MPs and NPs, ingestion of 4.5 μm MPs and 50 nm fluorescent NPs was observed by brine shrimps, and ingestion of fluorescent NPs was observed in zebrafish embryos along with an accumulation in specific organs (eye, yolk sac and tail). Even with the demonstrated capacity of the tested organism to ingest MP and accumulate NPs (van Pomeroy et al., 2017; Pitt et al., 2018; Duan et al., 2020) alterations in the organisms (immobilisation, mortality or malformation) were not reported. To assess the potential capacity of MPs to act as vectors of PAHs, zebrafish embryos and brine shrimp larvae were exposed to MPs of both sizes with sorbed B(a)P and to B(a)P alone. Exposure of brine shrimps to 0.5 μm MPs with sorbed B(a)P caused mortality at a concentrations of 6.87 mg/L (LC_{50} value of 4.75 mg/L). Only the exposure of zebrafish embryos to the highest concentration (50.1 mg/L) of 4.5 μm MPs with sorbed B(a)P (EC_{50} value of 45.57 ± 9.12 mg/L) provoked a significant increase in malformation prevalence. The exposure to PS MPs associated with persistent organic pollutants

(POPs) in early developmental stages of brine shrimps and *Daphnia magna* (Horton et al., 2018; Lin et al., 2019) and zebrafish (Ma et al., 2016; Chen et al., 2017a; Sleight et al., 2017; Cormier et al., 2019) did not provoke increased effects than those caused by POPs alone. Sometimes the effects produced by the pollutant alone were alleviated in presence of MPs. In the present study, malformations observed in 120 hours post fertilisation (hpf) embryos exposed to 4.5 µm MPs-B(a)P were similar to those provoked by exposure to B(a)P. 30% of the embryos exposed to 52.5 mg/L of 4.5 µm MPs-B(a)P presented pericardial edema. PAHs are known to cause cardiotoxicity (Incardona et al., 2013). In our case, acute tests reflected that the B(a)P associated with MPs was the cause of the observed toxicity, suggesting that MPs acted as vectors of B(a)P maintaining, its toxicity, which was supported by the successful transfer of B(a)P by MP as observed by confocal microscopy.

In **Chapter 2**, PAH sorption analyses were carried out with both MP sizes (4.5 and 0.5 µm) based on the analysis of aqueous (water medium) and solid phases (particles) to obtain information that could help to understand the potential capacity of plastics to transport PAHs. This information would further support the design of experiments to study the potential toxicity of MPs with sorbed PAHs in adult zebrafish (**Chapter 3**) and would help to understand the results obtained in developing organisms (brine shrimp larvae and zebrafish embryos) (**Chapter 1**). Results showed that 0.5 µm MPs sorbed higher amounts of B(a)P than 4.5 µm MPs, indicating that size is a key parameter influencing the role of MPs as carriers of organic pollutants. Previous studies have demonstrated the capacity of MPs to sorb PAHs, being the smallest MPs those with a higher sorption capacity of PAHs due to their higher surface to volume ratio (Ma et al., 2016; Wirnkör et al., 2019; Wang et al., 2019a). In the case of 4.5 µm MPs incubated in an environmentally relevant mixture of PAHs, as that formed in the WAF of a naphthenic North Sea crude oil, sorption was mainly driven by PAH hydrophobicity and initial PAH concentration in the mixture. Moreover, competition among PAHs for binding sites of MPs resulted into complex interactions between PAHs and MPs. Competition among PAHs for sorption to MPs is expected to occur in the environment, as was described for marine ecosystems where competition was promoted for those PAHs more hydrophobic and present at higher concentration (Bakir et al., 2012).

In **Chapter 3**, sublethal effects of the exposure to 4.5 µm MPs (0.05 mg/L) and 50 nm NPs (0.07 mg/L) were assessed in the liver of adult zebrafish at molecular level (biotransformation metabolism, cell cycle regulation and oxidative stress related genes) and tissue level (histopathological alterations). Results indicated that 4.5 µm MPs induced biotransformation metabolism in liver and produced liver injury characterised by tissue vacuolisation. Liver is known to be the principal organ for detoxification and vacuolisation is one of the main histopathological alteration found in fish exposed to organic xenobiotic (Wolf and Wheeler, 2018). 50 nm NPs did mainly affected the antioxidant system of adult zebrafish, which could be

General discussion

explained by the higher availability of these particles and their higher capacity to cross biological barriers compared with MPs (Pitt et al., 2018a). Several studies reported this size dependent oxidative stress in embryos and in the intestine of adult zebrafish (Chen et al., 2017; Gu et al., 2020). Again, ingestion was demonstrated for 4.5 µm MPs and suspected to be occurred for 50 nm NPs as electron-dense particles resembling NPs were found in intestine lumen. Nevertheless, internalisation and accumulation of MPs and NPs was not demonstrated in tissues (intestine, liver and gills) of adult fish. Previous studies reported ingestion of MPs and NPs by adult zebrafish (Skjolding et al., 2017; Karami et al., 2017; Pitt et al., 2018b; Lei et al., 2018; Qiao et al., 2019; Batel et al., 2020) and MP/NP internalisation in the intestinal wall, liver and brain of zebrafish was reported for particle sizes below 5 µm (van Pomeran et al., 2017; Pitt et al., 2018a; De Sales-Ribeiro et al., 2020). Small plastic particles seem to be able to cross biological barriers, mainly those of the digestive system and spread via the blood vessels of the fish to the other organs (De Sales-Ribeiro et al., 2020).

In **Chapter 3**, adult zebrafish were also exposed to MPs with sorbed PAHs and to PAHs alone to assess sublethal effects in liver and bioavailability of PAHs. In addition, gills were analysed for histopathological alterations as the primary organ in contact with the water column. The selected biomarkers of the biotransformation metabolism to detect PAH exposure associated with MPs did not respond to any treatment, even for PAHs alone (21 µg/L of B(a)P and 5% WAF), suggesting that the selected concentrations were not enough to induce this pathway. In the literature, only concentrations above 252 µg/L of PAHs alone or co-exposed with MPs are reported to produce induction of this pathway in fish (Batel et al., 2016; Sleight et al., 2016). Alteration of cell cycle regulation was neither observed, indicating that higher level of toxicity was not induced. Looking at tissue level, only PAHs from WAF caused damage to fish liver at early exposure time, probably connected to the PAH bioaccumulation found in those fish. The efficient system of fish to metabolise and excrete PAHs (Honda and Suzuki, 2020) and the non reported bioavailability of PAHs associated with MPs (Sleight et al., 2017) could explain the lack of bioaccumulation and effects in biotransformation metabolism routes of PAHs associated with MPs. Oxidative stress was the only significant response found in the liver of zebrafish exposed to MPs-B(a)P. On the contrary, according to the literature zebrafish embryos co-exposed to MPs and POPs showed a reduction of the oxidative stress produced by the POPs alone when MPs were present in the exposure (Chen et al., 2017). PAHs from WAF and B(a)P are been reported as oxidative stress inducers in the liver of exposed fish (Vieira et al., 2008; Salazar-Coria et al., 2019).

The GNMs are known to be toxic materials at elevated concentrations (< 10 mg/L) due to their reactive surface area (highly hydrophobic) and small size (crossing biological barriers) potentially causing oxidative stress and DNA damage in fish (**Fig. 2**; Sanchez et al., 2012; Guo and Mei, 2014; De Marchi et al., 2018). In **Chapter 4**, GO and rGO(PVP) (0.1-1 mg/L) did not cause

significant effects on zebrafish embryo development ($EC_{50} > 10$ mg/L). Only the highest concentrations (5 and 10 mg/L) of GO and rGO(PVP) tested in zebrafish embryos provoked a significant increase in the prevalence of malformed embryos. Sublethal effects at molecular, biochemical or tissue level in adult zebrafish exposed to GO (2 mg/L) for 3 and 21 days were neither detected. In addition, uptake of rGO(PVP) in zebrafish embryos and ingestion of GO by adults was demonstrated without evidence of internalisation into the inner tissues. Nevertheless, some studies have reported ingestion and internalisation of GO in adult zebrafish due to their sharp edges of the GO platelets (Chen et al., 2015; Zhang et al., 2017a).

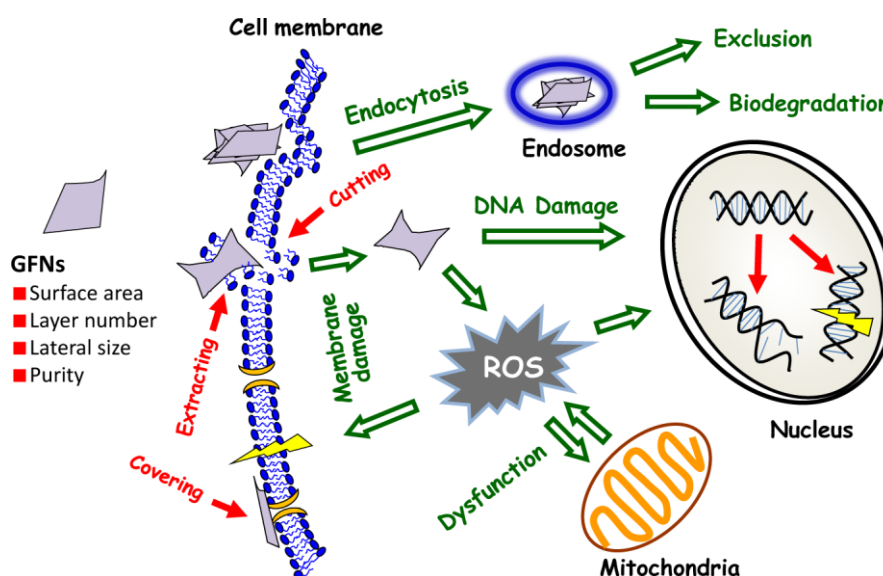


Fig. 2- The different potential interactions of GNMs with aquatic organisms at cellular level (from Zhao et al., 2014a).

GNMs have been reported as great sorbents for PAHs (Apul et al., 2013; Ji et al., 2013; Pei et al., 2013; Wang et al., 2014; Zhao et al., 2014), allowing their use for remediation of water pollution (Niu et al., 2014; Tabish et al., 2018; Baig et al., 2019). In the present work, B(a)P sorption to three GNMs (GO, GO with poly N-vinyl-2-pyrrolidone (GO(PVP)) and reduced graphene oxide with poly N-vinyl-2-pyrrolidone (rGO(PVP))) was analysed. GO showed higher capacity to sorb B(a)P than GO(PVP). In the case of rGO(PVP), the methodology was not appropriate for the analysis (velocity and time of centrifugation required for a completely precipitation of rGO(PVP) platelets was not satisfactorily achieved). For some B(a)P concentrations (1 and 10 $\mu\text{g/L}$), GO and GO(PVP) were able to sorb practically the total of the B(a)P present in the aqueous phase. The characteristics of their reactive surface (hydrophobicity, area and micropore volume) make them a recognised sorbent for PAHs, showing their capacity to be potential vectors of these pollutants for aquatic organism. GO was selected as the material with the highest capacity to sorb the B(a)P and, therefore, it was selected to analyse the sorption capacity for PAHs from the WAF of a naphthenic North Sea crude oil. Results showed a close relation of PAH sorption with their

General discussion

hydrophobicity. The naphthalene as the most abundant PAH and the less hydrophobic in the WAF was the less sorbed in terms of percentage, while phenanthrene presented a higher sorption to MPs. The complexity of the phenomenon in terms of competition is been described in the literature, highlighting the importance of PAH molecular size and hydrophobicity as parameters ruling the sorption competition among PAHs (Sun et al., 2013).

After demonstrating the capacity of GO to sorb PAHs, acute and sublethal effects were investigated in zebrafish embryos and adults, respectively. GNMs combined with B(a)P did not cause significant mortality on zebrafish embryo development, but some malformations were reported ($EC_{50} > 10$ mg/L). Significant differences between exposure to GO alone or to GO with sorbed PAHs were neither found. Other carbon NMs have shown the capacity to increase or inhibit the effects of POPs combined with carbon NMs in zebrafish embryos (Falconer et al., 2015; Della Torre et al., 2019; Yang et al., 2019).

Endpoints at molecular and biochemical level in the liver (biotransformation metabolism) showed that only fish exposed to B(a)P alone for 3 days presented an increase in biotransformation metabolism. These results suggested that PAHs associated with GO (co-exposure with WAF and sorbed with B(a)P) were not bioavailable enough to induce the biotransformation metabolism in the liver of adult zebrafish. Indeed, fish exposed to B(a)P for 21 days presented also an increase of glutathione S-transferase activity compared to GO-B(a)P exposed fish. This indicated lower bioavailability of PAHs when they are associated with GO, as reported by Linard et al. (2017). For this reason PAH bioaccumulation analysis indicated a noticeable accumulation of B(a)P in the whole body of fish exposed for 21 days to B(a)P alone, while fish exposed to GO-B(a)P showed much lower concentration of B(a)P. The less hydrophobic PAHs from WAF were less bioavailable for fish co-exposed to GO+WAF. Linard et al. (2017) also demonstrated that the less hydrophobic PAHs are less bioavailable for fish when they are sorbed to GO.

The activity of glutathione S-transferase was significantly induced in gills of fish exposed to GO combined with PAHs (GO-B(a)P and GO+WAF), while the same response was not observed in the liver. This suggested that the principal uptake route for these PAHs associated to GO could be through the gills (Zhai et al., 2020). The B(a)P concentration used in the present study (100 μ g/L) has been previously reported as a concentration able to induce biotransformation metabolism in the liver of zebrafish (Thompson et al., 2010). This indicated that GO has probably sequestered PAHs making them less bioavailable for adult zebrafish.

Cell cycle regulation did not show significant alterations on the liver of fish exposed to any treatment compared to control fish. As previously mentioned, fish exposed to PAHs alone, to GO alone or in combination with PAHs, could be able to impact this cell process (**Fig. 1**; Perrichon et al., 2016; Jia et al., 2019). Regarding histopathological alterations in liver, a significant increase

in the prevalence of vacuolisation was observed in fish exposed to GO+WAF for 3 and 21 days which can be probably linked to the reported bioavailability of the PAHs from WAF when they co-exposed with GO. Liver vacuolisation has been reported in fish exposed to GO (Chen et al., 2016; Souza et al., 2017) and also in fish exposed to PAHs from WAF (Agamy, 2012).

The other common response of zebrafish exposure to GNMs is oxidative stress (**Fig. 1**; Zhang et al., 2017b; Zou et al., 2018; Souza et al., 2019). In **Chapter 4**, biomarkers of oxidative stress did not show any significant change in the liver of fish exposed to any treatments. Only significant differences in gills were reported. All exposed fish presented higher catalase (CAT) activity than controls, being this increase significant in fish exposed to GO-B(a)P and B(a)P for 3 days and to GO+WAF for 21 days. Gills did not show oxidative stress after exposure to GO in the present study. In contrast, oxidative stress is often reported in the literature for GO exposed fish (Souza et al., 2019). No data have been found in the literature regarding the impact of GNMs or any CNMs combined with PAHs on gills antioxidant systems of fish. Appearance of histopathological alterations in the gill tissue was not reported in the present study. Other studies did neither report remarkable effects of GO exposure on zebrafish gill tissue (Chen et al., 2016; Souza et al., 2017).

Finally, a remarkable neurotoxic effect was provoked in all fish exposed for 21 days compared to control fish. As previously mentioned, translocation of graphene to the brain of adult zebrafish was previously reported in the literature (Hu et al., 2017). Even if not previous data was found on the neurotoxic effect produced by exposure to GNMs in fish, this effect could be expected due to the capacity of NMs to cross biological barriers up to the brain of fish. In addition, PAHs are reported as neurotoxic compounds in fish (Vieira et al., 2008; Holth and Tollefsen, 2012; Kim et al., 2018). Thus, the combination of GO and PAHs is a potential source of neurotoxicity to aquatic organisms.

LC₅₀ and EC₅₀ values are useful tools for environmental risk assessment of environmental pollutants (Vestel et al., 2016). According to results obtained in **Chapter 1** and **Chapter 4** for brine shrimp larvae and zebrafish embryos, exposure to B(a)P alone resulted the most toxic treatment for both developing organisms, as shown by the estimated LC₅₀ and EC₅₀ values (**Table 1**). At certain developmental stage B(a)P posed a higher risk for brine shrimp larvae than for zebrafish embryos. In the case of brine shrimps, EC₅₀ value was close to B(a)P solubility point in water (1.64 µg/L; May et al., 1983) and to environmentally relevant concentrations for this compound. This increased sensitivity could be related with the moulting event during early development, the brine shrimp older than 48 h has been demonstrated as the most sensitive larval stages (Barahona and Sánchez-Fortún, 1996). The second most toxic treatment was 0.5 µm MPs-B(a)P, but only for brine shrimps (24 hph) exposed for 48 h. In this case, a potential risk of MPs as vector of PAHs to brine shrimp is evidenced, being size of MPs the main explaining factor for

General discussion

concentrations higher than those that could be expected in the aquatic ecosystems. 4.5 µm MPs-B(a)P showed low potential risk for zebrafish (EC₅₀ of 45.57 mg/L), as these concentrations would be hardly present in the aquatic ecosystems. Regarding zebrafish embryos exposure to graphene family NMs alone and in combination with PAHs, some potential risk would be only forecast for concentrations above 10 mg/L and with a sorbed PAH amount unlike to be reported in the aquatic ecosystems.

Table 1- LC₅₀ values (mg/L) for brine shrimp based on the immobilisation and EC₅₀ values (mg/L) for zebrafish embryo based on malformation prevalence.

		4.5 µm MPs	0.5 µm MPs	50 nm NPs	4.5 µm- B(a)P	0.5 µm- B(a)P	B(a)P
BS	24 hph 24 h	>50.1	>6.9	>6.9	>50.1	>6.9	>10
	24 hph 48 h	>50.1	>6.9	>6.9	>50.1	4.75± 1.03	>10
	48 hph 24 h	>50.1	>6.9	>6.9	>50.1	>6.9	0.004± 0.197
	48 hph 48 h	>50.1	>6.9	>6.9	>50.1	>6.9	0.002± 0.119
ZF	120 hpf	>50.1	>6.9	>6.9	45.57± 9.12	>6.9	3.55± 0.68
		GO	GO(PVP)	rGO(PVP)	GO+WAF	GO-B(a)P	GO(PVP)- B(a)P
ZF	120 hpf	14.67± 4.03	30.98± 26.7	14.52± 3.12	16.07± 4.98	20.57± 8.03	15.11± 3.51

BS: brine shrimp; hpf: hours post fertilisation; hph: hours post hatch; ZF: zebrafish.

A summary of all the results is shown in **Table 2** and **Table 3**. Each endpoint was classified into three categories: red colour represents significant difference (except for uptake and chemical analyses) between the treated organisms and the control group, yellow colour represents a difference, although not significant, compared to control group and green colour represents endpoints showing no difference between treatments. This classification helped to visualise the treatments that produced a higher impact in each organism. According to the summary of endpoints for brine shrimp larvae and zebrafish (embryos and adults) exposed to NPs, MPs alone and in combination with PAHs (**Table 2**), B(a)P was the treatment that showed the greatest impact, followed by 0.5 µm MPs-B(a)P, 4.5 µm MPs-B(a)P and 50 nm NPs. The 0.5 µm MPs-B(a)P treatment impacted principally on brine shrimp, while zebrafish embryos presented a lower impact.

In the case of zebrafish, when results obtained in adults and embryos are compared, exposure to 4.5 μm MPs seemed to have greater impact on adults according to established classification, even when adult organisms were exposed to a lower concentration, but for longer time. Nevertheless, the relevance of assessed endpoints in each developmental stage needs to be considered. The other treatments showed similar record of endpoints between embryos and adults.

For zebrafish exposed to GNMs alone and with sorbed PAHs (**Table 3**), the treatments that caused the highest impact were B(a)P, GO-B(a)P and GO+WAF. GO contaminated with PAHs presented a higher impact on zebrafish in comparison with GO alone according to the established classification. rGO(PVP) that was only studied in zebrafish embryos provoked an important impact being an interesting NM to be further studied in combination with PAHs. Differences between the different developmental stages of zebrafish (embryos versus adults) were not observed, being both successful models for the study of the potential toxicity produced by micro and NMs as carriers of pollutants.

Table 2-Summary of all the endpoints studied in the test organisms exposed to NPs and MPs, PAHs alone and to MPs with sorbed PAHs.

		4.5 μm	0.5 μm	50 nm	4.5 μm -WAF	WAF	4.5 μm - B(a)P	0.5 μm - B(a)P	B(a)P
Brine shrimp larvae	Uptake	Red		Red			Red	Red	Red
	Internalisation/transfer	Green		Yellow			Red	Red	Red
	Immobilisation	Green	Green	Green			Green	Red	Red
Embryo	Uptake	Yellow	Yellow	Red			Yellow	Yellow	Yellow
	Internalisation/transfer	Green	Yellow	Red			Red	Red	Red
	Malformation	Green	Green	Green			Red	Yellow	Red
	→ Cardiotoxicity	Green	Green	Green			Yellow	Yellow	Red
Zebrafish	Adult	Uptake	Red		Red	Red	Red		Yellow
		Internalisation	Green		Yellow	Green		Green	Yellow
	PAH bioaccumulation				Yellow	Yellow			Yellow
	Oxidative stress (liver)	Yellow		Red	Yellow	Green	Red		Green
	Biotransformation (liver)	Red		Green	Yellow	Yellow	Green		Green
	Cell cycle (liver)	Green			Yellow	Yellow			Green
	Liver tissue alteration	Red		Green	Green	Red	Green		Green
	Gill tissue alteration	Green		Green	Green	Green	Green		Green

Table 3- Summary of all the endpoints studied in the test organisms exposed to GNMs, PAH alone and GNMs contaminated with PAHs.

		GO	GO(PVP)	rGO(PVP)	GO+WAF	GO-B(a)P	GO(PVP)-B(a)P	B(a)P
Embryo	Uptake			Red				Red
	Internalisation/transfer			Yellow				Red
	Malformation	Red	Yellow	Red	Yellow	Red	Red	Red
	→ Cardiotoxicity	Green	Green	Red	Green	Red	Red	Red
Zebrafish	Uptake	Red			Red	Red		
	Internalisation	Yellow			Yellow	Yellow		
	PAH Bioaccumulation				Yellow	Yellow		Yellow
	Oxidative stress (liver)	Green			Green	Green		Green
	Biotransformation metabolism (liver)	Green			Green	Green		Red
	Adult				Yellow	Green		Green
	Cell cycle regulation (liver)	Green			Yellow	Green		Green
	Oxidative stress (gills)	Green			Red	Red		Red
	Biotransformation metabolism (gills)	Green			Yellow	Yellow		Green
	Neurotoxicity	Red			Red	Red		Red
	Liver tissue alterations	Green			Red	Yellow		Green
	Gills tissue alterations	Green			Green	Green		Green

Red colour represents significant difference (except for uptake and chemical analyses) between the treated organisms and the control group, yellow colour represents a difference, although not significant, compared to control group and green colour represents endpoints showing no difference between treatments.

REFERENCES

- Agamy, E., 2012. Histopathological liver alterations in juvenile rabbit fish (*Siganus canaliculatus*) exposed to light Arabian crude oil, dispersed oil and dispersant. *Ecotoxicol. Environ. Saf.* 75, 171-179.
- Apul, O.G., Wang, Q., Zhou, Y., Karanfil, T., 2013. Adsorption of aromatic organic contaminants by graphene nanosheets: Comparison with carbon nanotubes and activated carbon. *Water Res.* 47, 1648-1654.
- Baig, N., Ihsanullah, Sajid, M., Saleh, T.A., 2019. Graphene-based adsorbents for the removal of toxic organic pollutants: A review. *J. Environ. Manage.* 244, 370-382.
- Bakir, A., Rowland, S.J., Thompson, R.C., 2012. Competitive sorption of persistent organic pollutants onto microplastics in the marine environment. *Mar. Pollut. Bull.* 64, 2782-2789.
- Bandala, E.R., Berli, M., 2019. Engineered nanomaterials (ENMs) and their role at the nexus of food, energy, and water. *Mater. Sci. Energ. Technol.* 2, 29-40.
- Barahona, M.V., Sánchez-Fortún, S., 1996. Comparative sensitivity of three age classes of *Artemia salina* larvae to several phenolic compounds. *Bull. Environ. Contam. Toxicol.* 56, 271-278.
- Batel, A., Baumann, L., Carteny, C.C., Cormier, B., Keiter, S.H., Braunbeck, T. 2020. Histological, enzymatic and chemical analyses of the potential effects of differently sized microplastic particles upon long-term ingestion in zebrafish (*Danio rerio*). *Mar. Pollut. Bull.* 153, 111022.
- Batel, A., Linti, F., Scherer, M., Erdinger, L., Braunbeck, T., 2016. Transfer of benzo[a]pyrene from microplastics to artemia nauplii and further to zebrafish via a trophic food web experiment: *cyp1a* induction and visual tracking of persistent organic pollutants. *Environ. Toxicol. Chem.* 35, 1656-1666.
- Bhagat, J., Zang, L., Nishimura, N., Shimada, Y., 2020. Zebrafish: An emerging model to study microplastic and nanoplastics toxicity. *Sci. Total Environ.* 728, 138707.
- Chen, L., Hernandez, Y., Feng, X., Müllen, K., 2012. From nanographene and graphene nanoribbons to graphene sheets: chemical synthesis. *Angew. Chem. Int. Ed.* 51, 7640-7654.
- Chen, Q.Q., Gundlach, M., Yang, S.Y., Jiang, J., Velki, M., Yin, D.Q., Hollert, H., 2017. Quantitative investigation of the mechanisms of microplastics and nanoplastics toward zebrafish larvae locomotor activity. *Sci. Total Environ.* 584, 1022-1031.
- Chen, Y., Ren, C., Ouyang, S., Hu, X., Zhou, Q., 2015. Mitigation in multiple effects of graphene oxide toxicity in zebrafish embryogenesis driven by humic acid. *Environ. Sci. Technol.* 49, 10147-10154.
- Chen, M., Yin, J., Liang, Y., Yuan, S., Wang, F., Song, M., Wang, H., 2016a. Oxidative stress and immunotoxicity induced by graphene oxide in zebrafish. *Aquat. Toxicol.* 174, 54-60.
- Cormier, B., Batel, A., Cachot, J., Bégout, M.-L., Braunbeck, T., Cousin, X., Keiter, S.H., 2019. Multi-laboratory hazard assessment of contaminated microplastic particles by means of enhanced fish embryo test with the zebrafish (*Danio rerio*). *Front. Environ. Sci.* 7, 135.

General discussion

- Della Torre, C., Parolini, M., Del Giacco, L., Ghilardi, A., Ascagni, M., Santo, N., Maggioni, D., Magni, S., Madaschi, L., Prosperi, L., La Porta, C., Binelli, A., 2017. Adsorption of B(α)P on carbon nanopowder affects accumulation and toxicity in zebrafish (*Danio rerio*) embryos. *Environ. Sci. Nano*. 4, 1132-1146.
- De Marchi, L., Pretti, C., Gabriel, B., Marques, P.A.A.P., Freitas, R., Neto, V., 2018. An overview of graphene materials: Properties, applications and toxicity on aquatic environments. *Sci. Total Environ*. 631-632, 1440-1456.
- De Sales-Ribeiro, C., Brito-Casillas, Y., Fernández, A., Caballero, M.J., 2020. An end to the controversy over the microscopic detection and effects of pristine microplastics in fish organs. *Sci. Rep.* 10, 12434.
- Falconer, J.L., Jones, C.F., Lu, S., Grainger, D.W., 2015. Carbon nanomaterials rescue phenanthrene toxicity in zebrafish embryo cultures. *Environ. Sci. Nano* 2, 645-652.
- Franzellitti, S., Canesi, L., Auguste, M., Wathsala, R.H.G.R., Fabbri, E., 2019. Microplastic exposure and effects in aquatic organisms: A physiological perspective. *Environ. Toxicol. Pharmacol.* 68, 37-51.
- Gu, W., Liu, S., Chen, L., Liu, Y., Gu, C., Ren, H.Q., Wu, B., 2020. Single-cell RNA sequencing reveals size-dependent effects of polystyrene microplastics on immune and secretory cell populations from zebrafish intestines. *Environ. Sci. Technol.* 54, 3417-3427.
- Guo, X., Mei, N., 2014. Assessment of the toxic potential of graphene family nanomaterials. *J. Food Drug Anal.* 22, 105-115.
- He, K., Chen, G., Zeng, G., Peng, M., Huang, Z., Shi, J., Huang, T., 2017. Stability, transport and ecosystem effects of graphene in water and soil environments. *Nanoscale* 9, 5370-5388.
- Holth, T.F., Tollefsen, K.E., 2012. Acetylcholine esterase inhibitors in effluents from oil production platforms in the North Sea. *Aquat. Toxicol.* 112-113, 92-98.
- Honda, M., Suzuki, N., 2020. Toxicity of polycyclic aromatic hydrocarbons for aquatic animals. *Environ. Res. Public Health* 17, 1363.
- Horton, A.A., Walton, A., Spurgeon, D.J., Lahive, E., Svendsen, C., 2017. Microplastics in freshwater and terrestrial environments: Evaluating the current understanding to identify the knowledge gaps and future research priorities. *Sci. Total Environ.* 586, 127-141.
- Hu, X., Wei, Z., Mu, L., 2017. Graphene oxide nanosheets at trace concentrations elicit neurotoxicity in the offspring of zebrafish. *Carbon* 117, 182-191.
- Ji, L., Chen, W., Xu, Z., Zheng, S., Zhu, D., 2013. Graphene nanosheets and graphite oxide as promising adsorbents for removal of organic contaminants from aqueous solution. *J. Environ. Qual.* 42, 191-198.
- Jia, P.-P., Sun, T., Junaid, M., Yang, L., Ma, Y.-B., Cui, Z.-S., Wei, D.-P., Shi, H.-F., Pei, D.-S., 2019. Nanotoxicity of different sizes of graphene (G) and graphene oxide (GO) *in vitro* and *in vivo*. *Environ. Pollut.* 247, 595-606.
- Karami, A., Romano, N., Galloway, T., Hamzah, H., 2016. Virgin microplastics cause toxicity and modulate the impacts of phenanthrene on biomarker responses in African catfish (*Clarias gariepinus*). *Environ. Res.* 151, 58-70.

- Kim, K., Jeon, H., Choi, S., Tsang, D.C.W., Oleszczuk, P., Ok, Y.S., Lee, H., Lee, S., 2018. Combined toxicity of endosulfan and phenanthrene mixtures and induced molecular changes in adult zebrafish (*Danio rerio*). *Chemosphere* 194, 30-41.
- Koelmans, A.A., Besseling, E., Shim, W.J., 2015. Nanoplastics in the aquatic environment. In: Bergmann, M., Gutow, L., Klages, M. (Eds.), *Marine Anthropogenic Litter*. Springer, Berlin, pp. 329-344.
- Koelmans, A.A., Bakir, A., Burton, G.A., Janssen, C.R., 2016. Microplastic as a vector for chemicals in the aquatic environment. Critical review and model-supported re-interpretation of empirical studies. *Environ. Sci. Technol.* 50, 3315-3326
- Kong, W., Kum, H., Bae, S., Shim, J., Kim, H., Kong, L., Meng, Y., Wang, K., Kim, C., Kim, J., 2019. Path towards graphene commercialization from lab to market. *Nat. Nanotechnol.* 14, 927-938.
- Lei, L., Wu, S., Lu, S., Liu, M., Song, Y., Fu, Z., Shi, H., Raley-Susman, K.M., He, D., 2018. Microplastic particles cause intestinal damage and other adverse effects in zebrafish *Danio rerio* and nematode *Caenorhabditis elegans*. *Sci. Total Environ.* 619-620, 1-8.
- Li, J., Liu, H., Chen, J.P., 2018. Microplastics in freshwater systems: A review on occurrence, environmental effects, and methods for microplastics detection. *Water Res.* 137, 362-374.
- Lin, W., Jiang, R., Wu, J., Wei, S., Yin, L., Xiao, X., Hu, S., Shen, Y., Ouyang, G., 2019. Sorption properties of hydrophobic organic chemicals to micro-sized polystyrene particles. *Sci. Total Environ.* 690, 565-572.
- Linard, E.N., Apul, O.G., Karanfil, T., van den Hurk, P., Klaine, S.J., 2017. Bioavailability carbon nanomaterial-adsorbed polycyclic aromatic hydrocarbons to *Pimephales promelas*: influence of adsorbate molecular size and configuration. *Environ. Sci. Technol.* 51, 9288-9296.
- Liu, Y., Nie, Y., Wang, J., Wang, J., Wang, X., Chen, S., Zhao, G., Wu, L., Xu, A., 2018. Mechanisms involved in the impact of engineered nanomaterials on the joint toxicity with environmental pollutants. *Ecotoxicol. Environ. Saf.* 162, 92-102.
- Ma, Y., Huang, A., Cao, S., Sun, F., Wang, L., Guo, H., Ji, R., 2016. Effects of nanoplastics and microplastics on toxicity, bioaccumulation, and environmental fate of phenanthrene in fresh water. *Environ. Pollut.* 219, 166-173.
- Niu, Z., Liu, L., Zhang, L., Chen, X., 2014. Porous graphene materials for water remediation. *Small* 17, 3434-3441.
- Pei, Z., Li, L., Sun, L., Zhang, S., Shan, X., Yang, S., Wen, B., 2013. Adsorption characteristics of 1,2,4-trichlorobenzene, 2,4,6-trichlorophenol, 2-naphthol and naphthalene on graphene and graphene oxide. *Carbon* 51, 156-163.
- Perrichon, P., Le Menach, K., Akcha, F., Cachot, J., Budzinski, H., Bustamante, P., 2016. Toxicity assessment of water-accommodated fractions from two different oils using a zebrafish (*Danio rerio*) embryo-larval bioassay with a multilevel approach. *Sci. Total Environ.* 568, 952-966.
- Picó, Y., Barceló, D., 2019. Analysis and prevention of microplastics pollution in water: Current perspectives and future directions. *ACS Omega* 4, 6079-6179.

General discussion

- Pitt, J.A., Trevisan, R., Massarsky, A., Kozal, J.S., Levin, E.D., Di Giulio, R.T., 2018a. Maternal transfer of nanoplastics to offspring in zebrafish (*Danio rerio*): A case study with nanopolystyrene. *Sci. Total Environ.* 643, 324-334.
- Pitt, J.A., Trevisan, R., Massarsky, A., Kozal, J.S., Levin, E.D., Di Giulio, R.T., 2018b. Maternal transfer of nanoplastics to offspring in zebrafish (*Danio rerio*): A case study with nanopolystyrene. *Sci. Total Environ.* 643, 324-334.
- Qiao, R., Sheng, C., Lu, Y., Zhang, Y., Ren, H., Lemos, B., 2019. Microplastics induce intestinal inflammation, oxidative stress, and disorders of metabolome and microbiome in zebrafish. *Sci. Total Environ.* 662, 246-253.
- Rainieri, S., Conlledo, N., Larse, B.K., Granby, K., Barranco, A., 2018. Combined effects of microplastics and chemical contaminants on the organ toxicity of zebrafish (*Danio rerio*). *Environ. Res.* 162, 135-143.
- Ribeiro, F., O'Brien, J.W., Galloway, T., Thomas, K.V., 2019. Accumulation and fate of nano- and micro-plastics and associated contaminants in organisms. *Trends Anal. Chem.* 111, 139-147.
- Rochman, C.M., Hoh, E., Kurobe, T., Teh, S.J., 2013. Ingested plastic transfers hazardous chemicals to fish and induces hepatic stress. *Sci. Rep.* 3, 3263.
- Salazar-Coria, L., Rocha-Gómez, M.A., Matadamas-Martínez, F., Yépez-Mula, L., Vega-López, A., 2019. Proteomic analysis of oxidized proteins in the brain and liver of the Nile tilapia (*Oreochromis niloticus*) exposed to a water-accommodated fraction of Maya crude oil. *Ecotoxicol. Environ. Saf.* 171, 609-620.
- Sanchez, V.C., Jachak, A., Hurt, R.H., Kane, A.B., 2012. Biological interactions of graphene-family nanomaterials: An interdisciplinary review. *Chem. Res. Toxicol.* 25, 15-34.
- Shen, M., Zhang, Y., Zhu, Y., Song, B., Zeng, G., Hu, D., Wen, X., Ren, Z., 2019. Recent advances in toxicological research of nanoplastics in the environment: A review. *Environ. Pollut.* 252, 511-521.
- Skjolding, L.M., Ašmonaitė, G., Jølleck, R.I., Andresen, T.L., Selck, H., Baun, A., Sturve, J., 2017. An assessment of the importance of exposure routes to the uptake and internal localisation of fluorescent nanoparticles in zebrafish (*Danio rerio*), using light sheet microscopy. *Nanotoxicology* 11, 351-359.
- Sleight, V.A., Bakir, A., Thompson, R.C., Henry, T.B., 2017. Assessment of micropalstic-sorbed contaminant bioavailability through analysis of biomarker gene expression in larval zebrafish. *Mar. Pollut. Bull.* 116, 291-297.
- Souza, J.P., Mansano, A.S., Venturini, F.P., Santos, F., Zucolotto, V., 2019. Antioxidant metabolism of zebrafish after sub-lethal exposure to graphene oxide and recovery. *Fish. Physiol. Biochem.* 45, 1289-1297.
- Storer, N.Y., Zon, L.I., 2010. Zebrafish models of p53 functions. *Cold Spring Harb. Perspect. Med.* 2, a001123.
- Sun, Y., Yang, S., Zhao, G., Wang, Q., Wang, X., 2013. Adsorption of polycyclic aromatic hydrocarbons on graphene oxides and reduced graphene oxides. *Chem. Asian J.* 8, 2755-2761.
- Tabish, T.A., Memon, F.A., Gomez, D.E., Horsell, D.W., Zhang, S., 2018. A facile synthesis of porous graphene for efficient water and wastewater treatment. *Sci. Rep.* 8, 1817-1831.

- Thompson, E.D., Burwinkel, K.E., Chava, A.K., Notch, E.G., Mayer, G.D., 2010. Activity of Phase I and Phase II enzymes of the benzo[a]pyrene transformation pathway in zebrafish (*Danio rerio*) following waterborne exposure to arsenite. *Comp. Biochem. Physiol. Part C: Toxicol. Pharmacol.* 152, 371-378.
- van Pomeran, M., Brun, N.R., Peijnenburg, W.J.G.M., Vijver, M.G., 2017. Exploring uptake and biodistribution of polystyrene (nano)particles in zebrafish embryos at different developmental stages. *Aquat. Ecotoxicol.* 190, 40-45.
- Vestel, J., Caldwell, D.J., Constantine, L., D'Aco, V.J., Davison, T., Dolan, D.G., Millard, S.P., Murray-Smith, R., Parke, N.J., Ryan, J.J., Straub, J.O., Wilson, P., 2016. Use of acute and chronic ecotoxicity data in environmental risk assessment of pharmaceuticals. *Environ. Toxicol. Chem.* 35, 1201-1212.
- Vieira, L.R., Sousa, A., Frasco, M.F., Lima, L., Morgado, F., Guilhermino, L., 2008. Acute effects of benzo(a)pyrene, anthracene and a fuel oil on biomarkers of the common goby *Pomatoschistus microps* (Teleostei, Gobiidae). *Sci. Total Environ.* 395, 87-100.
- Vijver, M.G., Zhai, Y., Wang, Z., Peijnenburg, W.J.G.M., 2018. Emerging investigator series: the dynamics of particle size distributions need to be accounted for in bioavailability modelling of nanoparticles. *Environ. Sci. Nano* 5, 2473-2481.
- Wang, J., Chen, Z., Chen, B., 2014. Adsorption of polycyclic aromatic hydrocarbons by graphene and graphene oxide nanosheets. *Environ. Sci. Technol.* 48, 4817-4825.
- Wang, J., Liu, X., Liu, G., Zhang, Z., Wu, H., Cui, B., Bai, J., Zhang, W., 2019a. Size effect of polystyrene microplastics on sorption of phenanthrene and nitrobenzene. *Ecotoxicol. Environ. Saf.* 173, 331-338.
- Wirnkor, V.A., Ebere, E.C., Ngozi, V.E., Oharley, N.K., 2019. Microplastic-toxic chemical interaction: a review study on quantified levels, mechanism and implication. *SN Appl. Sci.* 1, 1400.
- Wolf, J.C., Wheeler, J.R., 2018. A critical review of histopathological findings associated with endocrine and non-endocrine hepatic toxicity in fish models. *Aquat. Toxicol.* 197, 60-78.
- Yang, J., Zhong, W., Chen, P., Zhang, Y., Sun, B., Liu, M., Zhu, Y., Zhu, L., 2019. Graphene oxide mitigates endocrine disruption effects of bisphenol A on zebrafish at an early development stage. *Sci. Total Environ.* 697, 134158.
- Yu, F., Yang, C., Zhu, Z., Bai, Z., Ma, J., 2019. Adsorption behavior of organic pollutants and metals on micro/nanoplastics in the aquatic environment. *Sci. Total Environ.* 694, 133643.
- Zhai, Y., Xia, X., Wang, H., Lin, H., 2020. Effect of suspended particles with different grain sizes on the bioaccumulation of PAHs by zebrafish (*Danio rerio*). *Chemosphere* 242, 125299.
- Zhang, J.-H., Sun, T., Niu, A., Tang, Y.-M., Deng, S., Luo, W., Xu, Q., Wei, D., Pei, D.-S., 2017a. Perturbation effect of reduced graphene oxide quantum dots (rGOQDs) on aryl hydrocarbon receptor (AhR) pathway in zebrafish. *Biomaterials* 133, 49-59.
- Zhang, X., Zhou, Q., Zou, W., Hu, X., 2017b. Molecular mechanisms of developmental toxicity induced by graphene oxide at predicted environmental concentrations. *Environ. Sci. Technol.* 51, 7861-7871.

General discussion

Zhao, J., Wang, Z., Zhao, Q., Xing, B., 2014. Adsorption of phenanthrene on multilayer graphene as affected by surfactant and exfoliation. *Environ. Sci. Technol.* 48, 331-339.

Ziccardi, L.M., Edgington, A., Hentz, K., Kulacki, K.J., Kane, D.S., 2016. Microplastics as vectors for bioaccumulation of hydrophobic organic chemicals in the marine environment: a state-of-the-science review. *Environ. Toxicol. Chem.* 35, 1667-1676.

Zou, W., Zhou, Q., Zhang, X., Mu, L., Hu, X., 2018. Characterization of the effects of trace concentrations of graphene oxide on zebrafish larvae through proteomic and standard methods. *Ecotoxicol. Environ. Saf.* 159, 221-231.

CONCLUSIONS AND THESIS

CONCLUSIONS

The results obtained in the present Thesis lead us to the following conclusions:

- I.** Polystyrene NPs and MPs alone did not cause acute effects in zebrafish embryos and brine shrimp larvae, even with the reported ingestion of these materials by both organisms. However, toxicity increased when MPs (4.5 μm and 0.5 μm) were contaminated with B(a)P. Exposure to MPs-B(a)P resulted into B(a)P accumulation in brine shrimp larvae and zebrafish embryos. The MP size played a significant role in explaining the toxicity of MPs with sorbed B(a)P, indicating that smaller MPs pose a greater potential risk for brine shrimps due to the increase of surface to volume ratio that results into a higher amount of B(a)P sorbed for potential transfer.
- II.** The methodology employed for the assessment of PAH sorption to MPs based on the analysis of both, aqueous and solid phases, provides information that helps to understand the interaction and mechanisms of sorption of PAHs to MPs of different sizes. The estimated amount of compounds sorbed to MPs is usually overestimated if based only on the analysis of the aqueous phase.
- III.** 0.5 μm MPs were found to sorb higher amount of B(a)P than 4.5 μm MPs indicating that size is a key parameter influencing the role of MPs as carriers of organic pollutants. At complex environmental conditions, as those reflected by the PAH mixture present in the WAF of a naphthenic crude oil, PAH sorption to 4.5 μm MPs was mainly driven by PAH hydrophobicity and initial PAH concentration. Moreover, competition among PAHs for binding sites of MPs results in complex interactions between PAHs and MPs.
- IV.** Pristine 4.5 μm PS MPs induced biotransformation metabolism in the liver of adult zebrafish, showing liver injury characterised by tissue vacuolisation, whereas 50 nm NPs mainly affected the antioxidant system.
- V.** 4.5 μm PS MPs did not act as a significant vector of PAHs (B(a)P and the mixture of the WAF of the naphthenic North Sea crude oil) to adult zebrafish. Analysis of the transcription levels showed an upregulation in biotransformation metabolism and oxidative stress in fish exposed to MPs WAF compared to fish exposed to MPs-B(a)P, which is linked to the observed bioavailability of PAHs from MPs-WAF exposure that was not observed in MPs-B(a)P exposure. Nevertheless, significant differences were not observed compared to control fish or to fish exposed to PAHs alone, suggesting that the PAH concentrations used were not enough to induce these parameters. Looking at tissue level, only PAHs from WAF alone caused injuries on liver fish at an early exposure time.

Conclusions and thesis

- VI.** GO showed a high sorption capacity for PAHs that was mainly driven by the hydrophobicity of each PAH. Thus, GO in the environment could play a potential role as carrier of organic pollutants to aquatic organisms.
- VII.** Tested concentrations (100-1000 µg/L) of GO and rGO(PVP) did not cause significant effects on zebrafish embryo development ($EC_{50} > 10$ mg/L), even when they were combined with PAHs. In adult zebrafish, oxidative stress was observed according to the results of catalase activity in the gills, but without further appearance of histopathological alterations. The inhibition of AChE activity in all fish treated for 21 days indicated a potential neurotoxic effect. Only dissolved B(a)P provoked changes in liver biotransformation biomarkers, and these effects were not observed when zebrafish were exposed to GO combined with PAHs. At tissue level, hepatic vacuolisation was observed in fish co-exposed to GO+WAF, which is possibly linked to the bioavailability of the PAHs from WAF when they are co-exposed with GO.

THESIS

Polystyrene nanoplastics (50 nm) are able to translocate and spread into the zebrafish embryo body and to affect the antioxidant system of adult zebrafish while microplastics (4.5 µm) do not internalise but affect biotransformation metabolism and increase liver vacuolisation. Microplastics and graphene oxide family nanomaterials are not acutely toxic, but sorb polycyclic aromatic hydrocarbons and act as carriers (Trojan horse effect) to brine shrimps and zebrafish, showing graphene oxide a greater capacity to transfer polycyclic aromatic hydrocarbons. The sorption capacity of microplastics was inversely related to their size and for both, microplastic and graphene oxide nanomaterials, depends on the hydrophobicity of each polycyclic aromatic hydrocarbon and on their initial concentration. Microplastics and graphene oxide family nanomaterials modulate the effects of polycyclic aromatic hydrocarbons. Graphene oxide alone and with sorbed polycyclic aromatic hydrocarbons causes neurotoxicity and liver tissue alteration in adult zebrafish.